UNIVERSITY OF SOUTHAMPTON

SCHOOL OF MEDICINE

The Melanocortin 1 Receptor and Cutaneous Biology

by

Claire Louise Jackson

Thesis for the degree of Doctor of Philosophy

October 2006

UNIVERSITY OF SOUTHAMPTON

ABSTRACT

SCHOOL OF MEDICINE

Doctor of Philosophy

THE MELANOCORTIN 1 RECEPTOR AND CUTANEOUS BIOLOGY

by Claire Louise Jackson

The melanocortin 1 receptor (MC1R) is a 7-pass transmembrane G protein-coupled receptor, which is expressed on the surface of various cell types including melanocytes and melanoma cells, and is a key component in the regulation of human pigmentation. Previous work has shown that the pro-opiomelanocortin cleavage enzymes (pro-hormone convertase 1 and 2) and αMSH (the ligand for MC1R) are located within the melanosome in melanocytes (Peters *et al.*, 2000). This could imply a role for αMSH acting independently of MC1R within the melanosome, but also raises the question of whether MC1R is also present at the melanosome. In order to investigate whether MC1R is located at the melanosome, human MC1R was tagged at the C-terminus with enhanced green fluorescent protein (eGFP) and transfected into *Mc1r* null B16G4F melanoma cells. The subcellular localisation of MC1R-eGFP was established by observing co-localisation with organelle specific probes labelled with red fluorescent markers and in particular αPEP-13 and αPEP-1 antibodies were employed to label Pmel-17 protein in early melanosomes and tyrosinase related protein-1 in late melanosomes respectively. Confocal microscopy and image analysis of the cell transfectants demonstrated evidence of co-localisation of MC1R-eGFP at the melanosome. In addition, co-localisation of MC1R with melanosomes along dendrites was also observed. Furthermore, melanoma cell transfectants containing eGFP C-terminally tagged Asp294His variant *MC1R* demonstrated similar co-localisation of variant MC1R and the melanosome. Isolation of melanosomes from B16 transfectants containing wild-type MC1R-eGFP also suggested that MC1R was present in these organelles. The results indicate that MC1R is present at the melanosome, and suggests that part of the function of MC1R may be mediated through its association with this organelle. It may be hypothesised that MC1R could become associated with the melanosome from other organelles such as the ER and transgolgi networks since this is were the receptor is made and the melanosome is thought to incorporate other melanosomal proteins from these sites. The presence of MC1R within endosomes and also the receptors ability to internalise has been debated, which also adds the possiblity that MC1R may be associated with melanosomes by the fusion of endosomes which have internalised from the plasma membrane containing activated MC1R. MC1R internalisation was investigated via three approaches which included eGFP tagging of MC1R, the use of a FITC-αMSH fusion protein, and also by radioligand binding and acetic acid removal of the surface associated ligand. The latter approach successfully demonstrated the internalisation of wild-type and Asp294His variant MC1R.

List of Contents

List of Figures and Tables

Acknowledgements

Firstly, I would like to acknowledge and thank my supervisors Professor Eugene Healy and Professor Peter Friedmann.

I would secondly like to acknowledge and thank Dr Sam Robinson and Dr Sandie Dixon whose work and assistance and support contributed to this thesis and proved invaluble in the success of generating results. I would also like to acknowledge and thank Dr Anton Page for his work and assistance in preparing melanosome samples for TEM and his general guidance with imaging techniques. Other members of the Biomedical Imaging Department of Southampton University also provided vital assistance, in particular Roger Alston who taught me the skills of successful confocal microscopy.

I would thirdly like to thank my friends within Dermatopharmacology for their support and friendship, and also to Luke, my father, my brother and friends in Yorkshire and in Southampton for their support and encouragement during this period. I dedicate this thesis to the loving memory of my mother Susan Avril Jackson (1948-2002) whose courage and caring will forever be an inspiration to me. I know that she would have been proud of me today.

List of Abbreviations

A_{550}	Absorbance 550 nanometres
ACTH	Adrenocorticotropin
AGRP	Agouti related peptide
ASIP	Agouti signalling protein
ASP	Agouti signalling protein
ATP	Adenosine triphosphate
B16G4F	Mouse melanoma cell line derived from the black 6 strain
BOCA	Brown oculocutaneous albinism
BRET	Bioluminescence resonance energy transfer
BSA	Bovine serum albumin
Ca^{++}	Calcium
cAMP	Cyclic adensosine monophosphate
cm	Centimetre
CREB	cAMP response-binding element
^{o}C	Degrees centigrade
DCT	DOPAchrome tautomerase
DHI	5, 6-dihydroxyindole
DHICA	5, 6-dihydroxyindole-2- carboxylic acid
dH_2O	Deionised water
DMEM	Dulbecos minimal essential medium
DMSO	Dimethyl sulphoxide
DNA	Deoxyribonucleic acid
DNase	Deoxyribonuclease
dNTP(s)	Deoxynucleosides(s)
ddNTP(s)	Dideoxyribonucleoside(s)
DOPA	3, 4- dihydroxyphenylalanine
EDTA	Ethylenediaminetetra-acetic acid
ELISA	Enzyme linked immunosorbant assay
ER	Endoplasmic reticulum
FACS	Fluorescence activated cell sorting / Flow cytometry
FBS	Foetal bovine serum
FISH	Fluorescence *in situ* hybridisation
FITC	Fluoroisothiocyanate
eGFP	Enhanced green fluorescent protein

GFP	Green fluorescent protein
GPCR	G-protein coupled receptor
HEK293A	Human embryonic kidney 293A
HPLC	High performance liquid chromatography
x g	x gravity
g	Gram
IMS	Industrial methylated spirit
kb(s)	Kilobase(s)
kDa	Kilodaltons
l	Litre
LB	Luria-bertani
MCR	Melanocortin receptor
MC1R	Melanocortin-1 receptor
MC2R	Melanocortin-2 receptor
MC3R	Melanocortin-3 receptor
MC4R	Melanocortin-4 receptor
MC5R	Melanocortin-5 receptor
MITF	Micro-opthalmia transcription factor
MSH	Melanocyte stimulating hormone
mRNA	Messenger ribonucleic acid
µg	Microgram
µl	Microlitre
µm	Micrometre
µM	Micromolar
mA	Milliamp
mg	Milligram
ml	Millilitre
mm	Millimetre
M	Molar
MW	Molecular weight
NDP-αMSH	Nle^4, D-Phe^7-α-melanocyte stimulating hormone
nm	Nanometre
nM	Nanomolar
NaOH	Sodium hydroxide
OA	Ocular albinism
OCA	Oculocutaneous albinism (types OCA1-4)
PAX3	Paired box gene 3

αPEP-1	TRP 1 antibody abbreviation
αPEP-13	Gp100 antibody abbreviation
PBS	Phosphate buffered saline
PCR	Polymerase chain reaction
PKA	Protein kinase A
POMC	Pro-opiomelanocortin
ROCA	Rufous oculocutaneous albinism
rpm	Revolutions per minute
SOX10	SRY-box gene 10
TBS	Tris buffered saline
TEM	Transmission electron microscopy
Tm	Melting temperature
Tris	Tris (hydroxymethyl)-methylamine
TRP	Tyrosinase related protein (Trp, TRP)
TTBS	Tween tris buffered saline
TYR	Tyrosinase
TYRP	Tyrosinase related protein (Tyrp, TYRP)
U	Unit
UHQ	Ultra high quality (water)
USF-1	Upstream stimulating factor-1
3'UTR	3 primed untranslated region
UV	Ultraviolet
UVR	Ultraviolet radiation
V	Volts
v/v	Volume per unit volume
w/v	Weight per unit volume
Z plane	Z slice / single plane

Chapter 1

Introduction

1.1 Biology and Histology of the Skin

The skin is the largest multifunctional organ of the human body covering an area of approximately 2 m^2, and comprises of three main layers including the epidermis, the dermis, and the hypodermis (otherwise known as the subcutaneous layer of adipose tissue) (figure 1.1a) (McGrath *et al.,* 2004; Chu *et al.,* 2003). The epidermis is a multilayered epithelium (figure 1.1b) consisting primarily of keratinocytes, which constitute about 95 percent of the epidermal cells and mature to form a *stratum corneum* layer of dead cells at the skin surface (Archer, 2004; Kimyai-Asadi *et al.,* 2003). As well as preventing the loss of water and other essential substances from the body, the *stratum corneum* functions as a protective barrier against damaging environmental chemicals, biologically infectious agents, and ultraviolet radiation (UVR) (Archer, 2004; Elias *et al.,* 2003). The *stratum granulosum* lies beneath the *stratum corneum*, consisting of flattened keratinocytes which contain keratohyalin granules giving rise to the granular appearance of these cells. In addition, these keratinocytes contain lamellar granules (also named Odland bodies) which are approximated to be 100-300 nm in size (McGrath *et al.,* 2004). According to Odland, these lamellar granules were particularly numerous within the upper cells of the *stratum spinosum* and they migrate towards the cells periphery as they entered the *stratum granulosum* (McGrath *et al.,* 2004). Lamellar granules release lipids into the intercellular space, which are important for intercellular cohesion and hence maintaining a protective barrier against the external environment and to prevent fluid loss from the body (Archer, 2004; Elias *et al.,* 2003). The *stratum spinosum* contains viable keratinocytes; keratin tonofilaments within the cytoplasm terminate at desmosome junctions at the surface of the keratinocyte, which gives rise to the spiny appearance.

Figure 1.1: Diagram of the Skin and the Epidermis

(a)

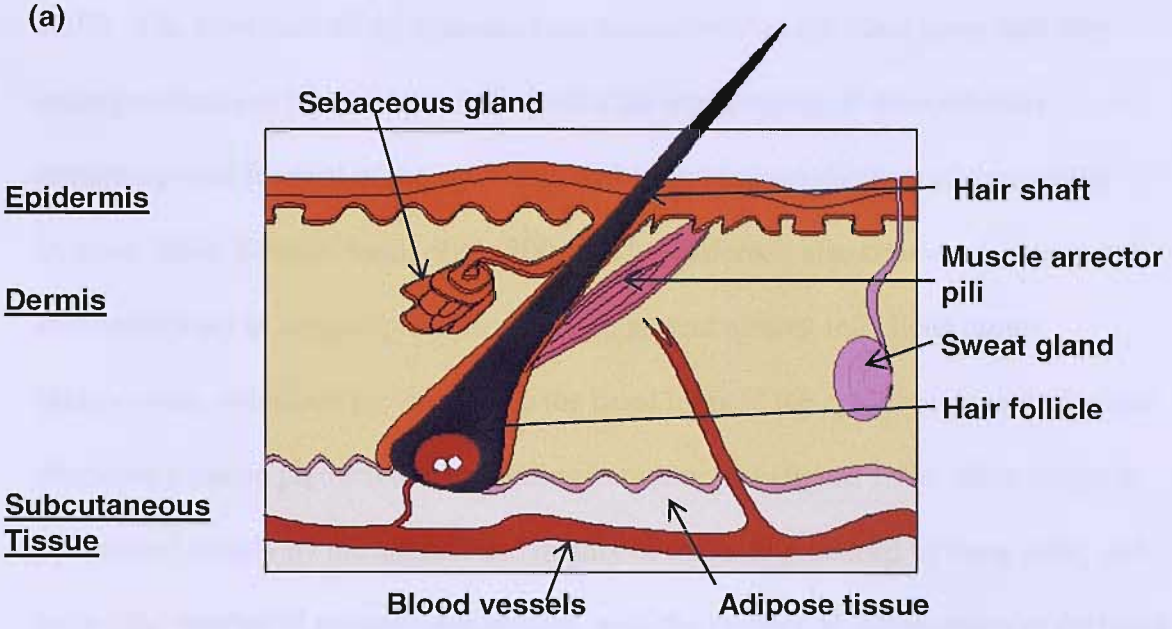

(b)

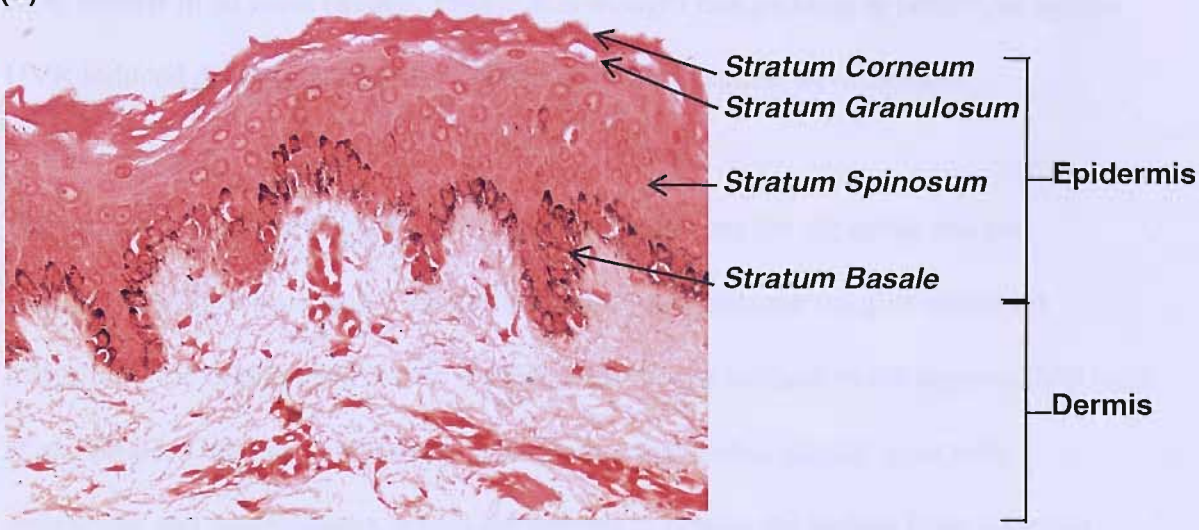

Legend for figure 1.1: (a) Cross-section of the skin demonstrating the epidermis, dermis and subcutaneous tissue. (b) The multilayered epidermis and underlying dermis (picture kindly donated by Dr S. Dixon, showing Mason Fontana staining of melanin in human skin).

The *stratum basale* is the deepest layer of the epidermis and consists of a single layer of columnar or cuboidal cells along the basement membrane (Archer, 2004; Elias *et al.*, 2003). The stem cells of the epidermis are situated within the basal layer, and they undergo mitosis to replenish the cells within the upper layers of the epidermis permitting total renewal of the epidermis within approximately three to four weeks (Archer, 2004; Kimyai-Asadi *et al.,* 2003). The epidermis also contains Langerhans' cells, which act as antigen presenting cells to protect against infectious agents. Melanocytes, which are present within the basal layer of the epidermis, synthesise and distribute melanin pigment to surrounding keratinocytes (figure 1.1b). Skin colour is determined mainly by the amount and quality of melanin produced by these cells, and not by the number of melanocytes present, with the number of melanocytes in the basal layer similar in all races (Szabo, 1954). It is thought that melanin is protective against UVR induced damage and against UVR induced skin cancer development.

The underlying dermis (figure 1.1) is a supporting matrix for the epidermis and incorporates fibroblasts which synthesise and release collagen (to give structural integrity to the dermis) and elastin, (which adds tensile strength to the dermis) (McGrath *et al.,* 2004). Other cells types contained within the dermis include mast cells, monocytes and macrophages, which are present to protect the dermis from infection (McGrath *et al.,* 2004). The dermis is rich in blood vessels, which supply the skin with oxygenated blood and remove cellular waste (Archer, 2004; McGrath *et al.,* 2004). Hair follicles and sebaceous glands are present in the dermis, although the relative numbers of hair follicles and sebaceous glands varies with body site. Glabrous (non-haired) skin lacks hair follicles and sebaceous glands (Archer, 2004; McGrath *et al.,* 2004). The presence of hairs at the skin surface, especially on the scalp, serves to trap heat at this site in response to external cold stimulus, whereas sweat glands permit body

cooling by the secretion and evaporation of sweat (containing mainly water, salt, and cellular waste products) (Archer, 2004; McGrath *et al.*, 2004). The purpose of sebum, which is deposited upon hair and secreted at the surface of the hair follicle, is to lubricate the skin and hair, maintain the skin barrier and in doing so protecting the skin from the external environment (Archer, 2004; Elias *et al.*, 2003; McGrath *et al.*, 2004).

1.2 The Role of the Melanocyte and Melanin Biosynthesis

Melanoblasts are melanocyte precursors derived from the neural crest (Rawles, 1947), which migrate during embryogenesis through the mesenchyme to the uveal tract of the eye, the inner ear, the medulla oblongata in the brain and the epidermis and the hair follicles (Mayer, 1973). The melanocyte synthesises melanin pigment within membrane bound organelles called melanosomes, and subsequently transfers this pigment contained within the melanosome to surrounding keratinocytes in the epidermis. Within the basal epidermis a melanocyte can transfer melanin-containing melanosomes to up to 40 surrounding keratinocytes via their dendrites, and this grouping is referred to as the epidermal melanin unit (Fitzpatrick and Breathnach, 1963). Melanin is a biopolymer of which there are two types, black / brown eumelanin and red / yellow phaeomelanin (Prota and Thomson, 1976). Eumelanin is synthesised within eumelanosomes and is thought to be photoprotective, whilst phaeomelanin is synthesised within phaeomelansomes, and differs structurally to eumelanin by containing a greater number of cysteine residues (Prota, 1992; Smit *et al.*, 1998). The photoprotective role of phaeomelanin is unclear in that phaeomelanin exhibits phototoxicity when irradiated with UV *in vitro* (Chedekel *et al.*, 1978; Takeuchi *et al.*, 2004).

Eumelanin and phaeomelanin are both generated from tyrosine and share a common synthetic pathway to form DOPAquinone (figure 1.2). The enzyme tyrosinase catalyses tyrosine hydroxylation to 3, 4- dihydroxyphenylalanine (DOPA), which subsequently

becomes oxidised to DOPAquinone (also by tyrosinase). In the eumelanin pathway, DOPAquinone is converted to DOPAchrome which becomes isomerised to 5, 6-dihydroxyindole-2- carboxylic acid (DHICA) via the enzyme DOPAchrome tautomerase (DCT) also known as tyrosinase related protein-2 (Korner and Gettins, 1985). DHICA is oxidised by DHICA-oxidase, also known as tyrosinase related protein-1 (TRP-1) (Jimenez-Cervantes *et al.,* 1994) with the assistance of the catalyst Pmel17 / silver protein to polymerise DHICA to brown eumelanin (Chakraborty *et al.,* 1996) (figure 1.2). Alternatively DOPAchrome is isomerised to 5, 6-dihydroxyindole (DHI) which is converted to black eumelanin via tyrosinase. Another enzyme, peroxidase, has also been implicated in the conversion of both DHICA and DHI to melanin (Shibata *et al.,* 1993). Phaeomelanin is generated from DOPAquinone via a separate pathway in which DOPAquinone incorporates cysteine residues to forms 5-S-cysteinylDOPA. The 5-S-cysteinylDOPA is further metabolised into alanyl-hydroxy-benzathiazine, which subsequently leads to the formation of phaeomelanin (figure 1.2).

Melanosomes, which are structurally similar to lysosomes, are discrete organelles, which are considered to be derived from vesicles budding from either the rough endoplasmic reticulum (ER) or golgi which fuse to form premelanosomes (Palumbo *et al.,* 1997). The melanosomal enzymes including tyrosinase, TRP-1, and DCT are synthesised at the rough ER and undergo post-translational modification (i.e. glycosylation) within the golgi prior to their incorporation into stage II melanosomes (Korner and Pawelek, 1982). On electron microscopy, eumelanosomes are elliptical and are approximately 0.9 x 0.3 μm^2 in size, whereas phaeomelanosomes appear spherical and are on average 0.7 μm in diameter (Zimmerman *et al.,* 1981). Both eumelanosomes and phaeomelanosomes undergo four stages of maturation, during

which the respective types of eumelanin or phaeomelanin are deposited along the internal matrix structure during the later stages of maturation.

Figure 1.2: The Melanogenesis Pathway

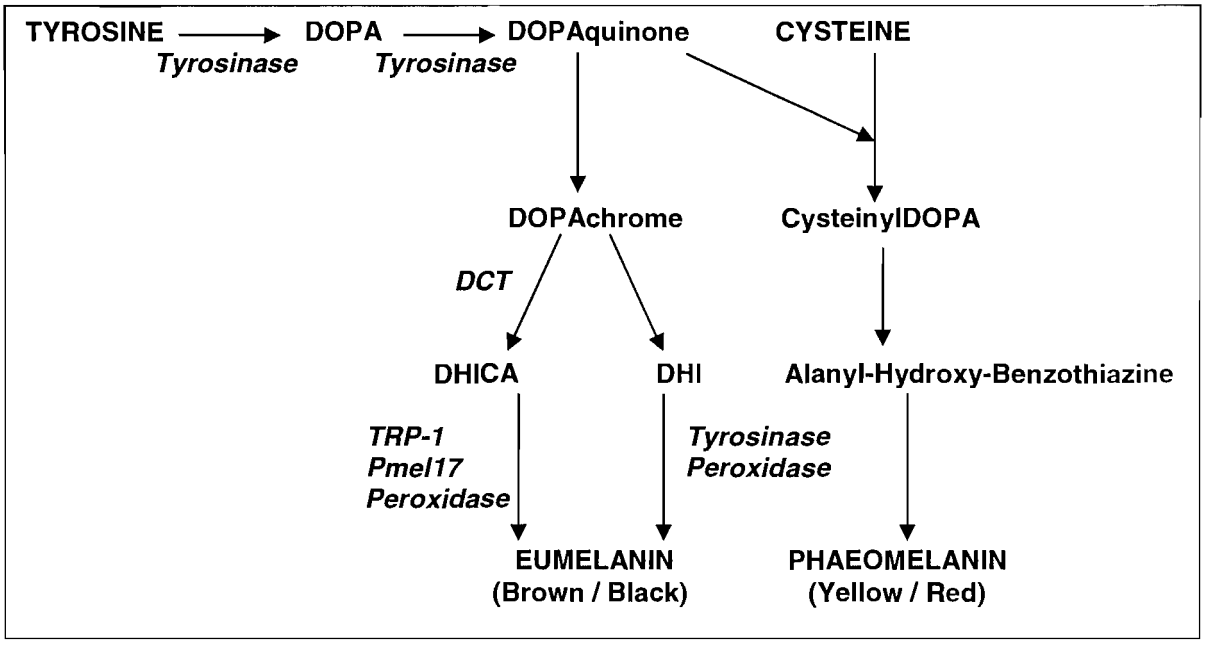

Legend for figure 1.2: A diagram of the melanogenesis pathway from Tyrosine to Eumelanin (the brown / black pigment) and to Phaeomelanin (the red / yellow pigment). The enzymes / catalysts Tyrosinase, TRP-1, DCT, and Pmel17 are shown in italics.

Stage I eumelanosomes and phaeomelanosomes appear common in their ultrastructure, and are premelanosomes derived by the fusion of budding vesicles from the ER and golgi (Zimmerman *et al.*, 1981). Stage II eumelanosomes go on to develop an ellipsoidal shape and contain a well organised glycoprotein matrix within the lumen of each organelle (Zimmerman *et al.*, 1981). However, the stage II phaeomelanosomes remain spherical in shape and appear less internally organised. Stage III eumelanosomes and phaeomelanosomes contain increasing deposits of eumelanin or phaeomelanin, and the stage IV eumelanosomes are heavily melanised with eumelanin along their matrices and appear completely black when viewed by transmission electron microscopy (TEM) (Zimmerman *et al.*, 1981). In contrast, stage IV phaeomelanosomes remain granular in appearance when fully mature as less phaeomelanin is deposited along their disorganised internal matrices (Zimmerman *et al.*, 1981) (figure 1.3b). Stage

I melanosomes collect within the perinuclear region within the melanocyte, however the mature melanosomes are localised at the cell periphery and along dendrites prior to their transfer into keratinocytes (Hoashi *et al.,* 2005). Rab27a is a member of the Rab protein family, and is a GTP-binding protein of the Ras superfamily and is involved in the fusion and trafficking of vesicles (Chen *et al.,* 1997). Rab27a and the motor protein myosinVa are present within later stage melanosomes, and are responsible for their movement from the perinuclear area to the outer melanocyte membrane, and subsequently along dendrites via actin filaments. In mouse melanocytes, the protein myosinVa is recruited onto the surface of melanosomes by complexes present at the melanosome surface containing Rab27a and melanophilin; interestingly the absence of any one of these three proteins causes the accumulation of melanosomes within the cell body cytoplasm of the melanocyte (Li *et al.,* 2005). The melanosomes are captured onto microtubules by the presence of myosinVa and move bidirectionally towards actin rich distal portions of dendrites which extend from the melanocyte body (Wu *et al.,* 2005). Once accumulated at the distal portions of the dendrites, the melanised melanosomes are transferred to surrounding keratinocytes within the epidermis and hair follicles. The transfer of melanosomes from melanocyte to keratinocytes in cell culture has been observed by use of time lapse cinematography and electron microscopy (Okazaki *et al.,* 1976). The dendrites, containing melanosomes, which were projecting from melanocytes became enveloped and phagocytosed by the adjacent keratinocytes (Okazaki *et al.,* 1976). Once enveloped, the dendrites were surrounded by another membrane, and this 'sac-dendrite complex' became degraded for dispersal of the larger single melanosomes and the smaller melanosomes which were in clusters (Okazaki *et al.,* 1976). Yamamoto and Bhawan, (1994) also described two other possible mechanisms of melanosome transfer including: membrane fusion of the melanocyte and keratinocyte to permit passage of melanosomes into the keratinocyte; and exocytosis of

melanosomes from the melanocyte followed by their endocytosis into keratinocytes through the formation of coated pits.

Figure 1.3: Melanosome Maturation within the Melanocyte and Transfer into Keratinocyte via Dendrites

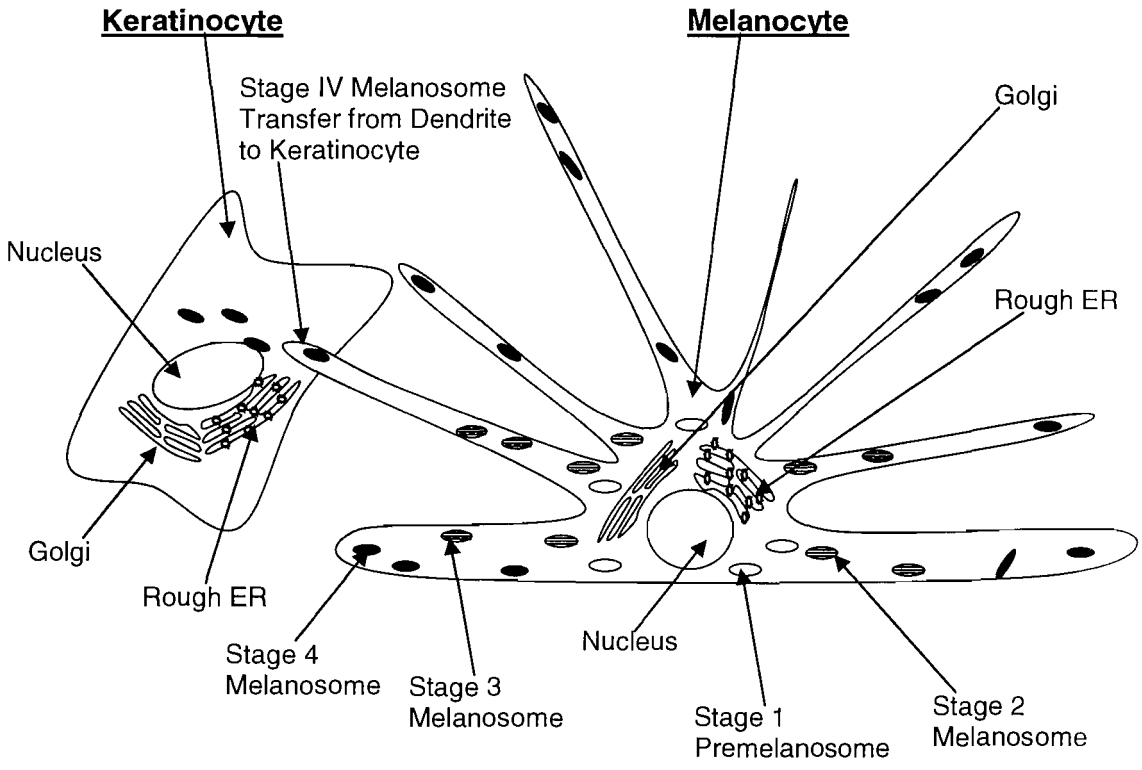

Legend for figure 1.3: The stage I melanosomes are thought to be derived from vesicles budding from the rough ER and golgi. Stage II melanosomes incorporate melanogenic enzymes such as tyrosinase, TRP-1, and DCT from the ER and golgi which enable the melanosomes to synthesise melanin. Melanin is deposited on organized matrices within the stage II melanosome. Stage III melanosomes become more heavily melanised, and fully melanised stage IV melanosomes travel to the cell periphery and along dendrites ready for transfer into surrounding keratinocytes.

1.3 Variation in Pigmentation of Skin and Hair

Normal variation in skin and hair colour within the human race is due to varying amounts of eumelanin and phaeomelanin in these tissues. Although the density of epidermal melanocytes varies over different areas of the human body, the difference in melanocyte number at similar body sites between individuals of different races is

negligible (Szabo, 1954). Black individuals produce higher concentrations of eumelanin and have an increased number of significantly larger eumelanosomes when compared to the populations with lighter skin (Szabo *et al.*, 1969). Hunt *et al.*, (1995) reported that, using HPLC, the epidermis of non-European subjects have the highest levels of eumelanin to phaeomelanin in contrast to European subjects who had higher phaeomelnin to eumelanin content. Similarly, Yoon *et al.*, (2003) measured melanin ratios in the skin of different racial groups, and determined that African-American skin contained proportionally the most eumelanin whilst Asian and Caucasian skin contained decreasing levels of eumelanin and higher levels of phaeomelanin respectively. Melanocytes and melanoma cells derived from human Caucasian and Negroid skin has demonstrated similar levels of tyrosinase at the mRNA and protein level (Jimenez *et al.*, 1988). In fact, the increased levels of melanin in Negroid skin is not dependent on an abundance of tyrosinase, but is determined by an increased level of tyrosinase activity (Fuller *et al.*, 1993). However, normal pigmentation in humans is a genetically complex trait, and regulation of pigmentation by other genes may be more relevant *in vivo*. Whilst polymorphisms in the *melanocortin 1 receptor* (*MC1R*) account for most variation in human pigmentation, other genes such as *golden* in zebrafish, which is very similar to the human ortholog gene and protein, is thought to encode for a cation exchanger called slc24a5 that is possibly located at the melanosome (Lamason *et al.*, 2005). It has been suggested that the human *SLC24A5* gene may play a key role in human pigmentation because evolutionary studies have indicated that this gene is highly conserved in African and East Asian populations, whilst a variant allele, which is found in European populations, is correlated with lighter skin pigmentation (Lamason *et al.*, 2005). The *P* gene (the human homologue of the murine *pink-eyed dilution* gene), and the *agouti signalling protein* (ASP) have been implicated as genes which may also play a role in pigmentation variation (Valverde *et al.*, 1995). It is possible that these other

genes may determine rarer pigmentation phenotypes, for example the Celts that have dark hair colour and fair skin, and some Australian Aboriginal children that have fair hair and dark skin (Holman and Armstrong, 1984). In addition, many monogenic pigmentation disorders exist in humans, resulting in a whole variety of pigmentation phenotypes across the globe. Fortunately, murine models have permitted and advanced the study of genes that directly influence mouse coat colour, and many of these coat colour mutations have been compared with the homologous human pigmentation phenotypes / pigment disorders leading to the identification of causative genes in humans (table 1.1).

Table 1.1: Genes Related to Human Pigmentation

Human gene / locus	Protein	Human mutation / polymorphism phenotype	Mouse coat colour phenotype
Melanosome associated proteins			
KIT 4q11-q12	cKIT (tyrosine kinase receptor)	Piebaldism	Dominant white spotting (W); causing a white spot on the head and ventral abdomen
LOC51151 5p14.3-q12.3	MATP / SLC45A2 (also AIM-1, a transporter protein)	Oculocutaneous albinism type 4 (OCA4)	Underwhite (uw); causes hypopigmentation of the eyes hair and skin, which may change with age
OA1 Xp22.3	OA1 (a GPCR)	Ocular albinism type 1 (OA1)	Oa1 (oa1) hypopigmentation of the ocular fundus in mutant animals compared with wild-type, and enlarged melanosomes in the retinal pigment epithelium
OCA2 15q11.2-q12.3	P protein (regulator of melanosome pH)	Oculocutaneous albinism type 2 (OCA2)	Pink-eyed dilute (p) causes the equivalent of human tyrosinase-positive albinism
Sl 12q14.3-qter	Steel factor (also Stem cell factor / Mast cell growth factor and ligand for cKIT)	Hypopigmentation	Steel (Sl); Mice homozygous for the viable Sl allele steel-Dickie (Sld) are sterile, severely anemic, and black eyes and white hair
SILV 12q13-q14	Gp100 / pMel17 / silver (DHICA-polymerisation)	Unknown	Silver (si) causes a 'diluted' lighter coat colour
SLC24A5 15q21.1	SLC24A5 (a cation exchanger)	SLC24A5 variants are associated with fair skin in European populations	*Slc24a5* null zebra fish have hypo-pigmented retina, and melanophores, however this gene has not been investigated in the mouse
TYR 11q14-q21	Tyrosinase (reduces tyrosine to DOPA)	Oculocutaneous albinism type 1 (OCA1)	Albino (c); causing a complete lack of pigment in the hair skin and eyes
TYRP1 / Gp75 9p23	Trp-1 / Gp75 (DHICA-oxidase and	Oculocutaneous albinism type 3	Brown (b); causing brown coat colour

	stabilises tyrosinase)	(OCA3)	
TYRP2 / DCT 13q32	Trp-2 / DCT (dopachrome tautomerase)	Unknown	Slaty (slt); Mutations in this melanocyte-specific protein gene cause coat color dilution
Melanosome trafficking proteins			
F2RL1 5q13	PAR2 (a GPCR)	Unknown	F2rl1 / PAR2 is an antiinflammatory receptor in the colon. PAR2 plays a key role in chronic joint inflammation. Using an adjuvant monoarthritis mouse model of chronic inflammation, they found that expression of PAR2 was substantially upregulated in inflamed tissues
MYO5A 15q21	Myosin Va (a motor protein)	Griscelli syndrome	Dilute (d) causes lightening of coat color, and severe neurological defects shortly after birth
RAB27A 15q21	Rab27a (member of the RAS protein family)	Griscelli syndrome	Ashen (ash) causes lightening of coat color because of defects in melanosome transport
Signalling proteins and ligands			
ASIP 20q11.2-q12	Agouti signal protein (inverse agonist of MC1R)	Unknown	Agouti (A); also a colour is used to describe yellow hair with a black tip giving rise to a brown looking coat colour, non-agouti (a) have black hair, and agouti overexpression lethal yellow (Ay) causes yellow hair
MC1R 16q24.3	MC1R (a GPCR)	Red Hair / fair skin	Extension (E); named because the pigment is extended along the hair shaft. Wild-type EE mouse is black,

			the recessive yellow (ee) is yellow, and the Tobacco (Etob) is hyperpigmented due to hyperactive MC1R
MITF 3p122.3-14.1	MITF (a transcription factor)	Waardenburg syndrome type 2	Micro-ophthalmia (mi) mutants lack MITF affecting melanocytes, mast cells, and osteoclasts development. This causes hypopigmentation in coat and eyes; other pathologies include deafness, bone resorption anomalies, mast cell deficiency and lethality
POMC 2p23.3	POMC (precursor of melanocortins i.e. the MC1R agonists ACTH and MSH)	Red Hair	Pomc1; the wild-type results in a black coat colour, whilst Pomc1 null mice have a yellow coat colour

Table adapted from Sturm *et al.,* 2001. Aberdam *et al.,* 1998; Brannan *et al.,* 1991; Chhajlani and Wikberg, 1992; Copeland *et al.,* 1990; Du and Fisher, 2002; Engle and Kennett, 1994; Ferrell *et al.,* 2003; Fleischman *et al.,* 1991; Halaban and Moellmann, 1990; Incerti et al., 2001; Jackson *et al.,* 1992; Jackson *et al.,* 1998; Kwon *et al.,* 1987; Kwon *et al.,* 1991; Kwon *et al.,* 1994; Kwon et al., 1995; Lamasson *et al.,* 2005; Lutz *et al.,* 1991; Lyon *et al.,* 1992; Mountjoy *et al.,* 1992; Newton *et al.,* 1996; Newton *et al.,* 2001; Nystedt *et al.,* 1994; Owerbach *et al.,* 1981; Robbins *et al.,* 1993; Tachibana *et al.,* 1994; Tolmachova *et al.,* 1999; Williams *et al.,* 1990; Wilson *et al.,* 2000.

1.4 Natural and Transgenic Mouse Models and Human Pigmentation Abnormalities

1.4.1 Melanoblast Survival

Naturally occurring coat colour mutations in mice have facilitated the study of melanocyte development. For example, the phenotypes of two mutant strains of mice, dominant white spotting (W) and steel (Sl), are similar in that both strains develop a white coat colour on the head and also on the ventral part of the abdomen, which is due

to impaired melanoblast survival, differentiation and migration during embryogenesis (Nocka *et al.,* 1989; Matsui *et al.,* 1990). The *dominant white spotting* (*W*) locus encodes for the proto-oncogene c-kit, a tyrosine kinase transmembrane receptor (Chabot *et al.,* 1988), which selectively binds kit ligand (also known as mast cell growth factor (MGF) / stem cell factor / steel factor) (Williams *et al.,* 1990) encoded by the *Steel* (*Sl*) locus (Copeland *et al.,* 1990). Two examples of defective melanoblast survival in humans include piebaldism and Waardenburg syndrome. Germline human c-kit gene mutations are responsible for piebaldism, which results in a white forelock and areas of skin hypopigmentation (Fleischman *et al,* 1991). Waardenburg syndrome is a hereditary group of four disorders that cause deafness and hypopigmentation, caused by different gene mutations. Waardenburg syndrome type 1 and type 3 are associated with paired-box gene-3 (*PAX3*) mutations (Tassabehji *et al.,* 1992), Waardenburg syndrome type 2 is caused by mutations in the micro-opthalmia transcription factor (*MITF*) gene mutations (Hughes *et al.,* 1994), and SRY-box gene 10 (*SOX10*) mutations result in Waardenburg syndrome type 4 (Pingault *et al.,* 1998). PAX3 and SOX10 are transcription factors expressed in stem cells migrating out of the neural crest (Chalepakis *et al.,* 1994; Kim *et al.,* 2003; Paratore *et al.,* 2001). The expression of MITF is critical for melanoblast development (Opdecamp *et al.,* 1997) and MITF expression is dependent on its transactivation by PAX3 and SOX10 (Bondurand *et al.,* 2000; Busca and Ballotti, 2000; Tchibana, 1999; Verastegui *et al.,* 2000).

1.4.2 Human Ocular Albinism Type One

Albinism incorporates a number of hypopigmentation diseases, which are divided into clinical disorders known as ocular albinism (OA) and oculocutaneous albinism (OCA). OA1 is an X-linked disorder which is characterized by the hypopigmentation of the eye and is thought to be a mild form of OCA (Bassi *et al.,* 1995; Bassi *et al.,* 1996; d'Addio

et al., 2000; Schiaffino *et al.*, 1995; Schiaffino *et al.*, 1999). Histology of affected tissues in this disorder has demonstrated the presence of large melanosomes in both skin and retinal pigment epithelium melanocytes, and this has implied that defective melanosome biogenesis may be responsible for the hypopigmented retina and photophobia (Garner and Jay, 1980). OA1 has been mapped to the *OA1* gene, which is regulated by MITF and encodes a G-protein-coupled receptor (GPCR) called OA1 normally found on the membranes of intracellular organelles such as lysosomes, late endosomes and melanosomes (Schiaffino *et al.*, 1995). The presence of this GPCR on the membrane of the melanosome has led some researchers to suggest that the OA1 receptor may regulate melanosome development via signalling from the lumen of this organelle and activation of G proteins on the cytoplasmic side of the membrane (Vetrini *et al.*, 2004). Evidence to support this has been provided by the observation that G protein subunits associate with melanosomes (using double immunofluorescence staining with melanosomal markers) and co-localise with OA1 (on double immunogold assays) (Schiaffino *et al.*, 1999). The murine homologue of the human *OA1* gene is *oa1*, and a murine *oa1* knockout model had hypopigmentation of the eye, misalignment of the optic nerve, and the presence of large melanosomes within the retinal epithelia, which is comparable to the disease traits of human OA1 (Incerti *et al.*, 2000). These authors deduced that loss of oa1 receptor function prevented the final maturation of melanosomes and failed to inhibit melanosome enlargement in the knockout mice, and suggested that this was also the case in the human OA type 1 disease.

1.4.3 Human Oculocutaneous Albinism Type One

Human OCA1 is caused by at least thirteen different tyrosinase (*TYR*) gene mutations, which result in a lack of pigment in the eyes, skin and hair as well as impaired vision due to optic nerve maldevelopment (Gimenez *et al.*, 2004). The underlying defect is

that of impaired tyrosinase enzyme activity or retention of this protein within the ER (Halaban *et al.*, 2000). OCA1 may be sub-divided into two types. OCA1A results from *TYR* mutations which produce either no tyrosinase or inactive tyrosinase, and this causes the absence of pigment from birth which continues throughout life (Tripathi *et al.*, 1992). OCA1B individuals are affected less severely and develop varied levels of ocular and cutaneous pigment dependant on the rate of partial activity of tyrosinase (Giebel *et al.*, 1991; King *et al.*, 1991). Transgenic albino mice (which were naturally defective at *Tyr*) which were made to express a functional *Tyr* transgene, consequently developed pigmented hair and a normal retina with the correct numbers of rod photoreceptors, and normal optic nerve connections to the brain indicating that the *Tyr* gene is important in optic nerve development as well as in cutaneous pigmentation (Gimenez *et al.*, 2004).

1.4.4 Human Oculocutaneous Albinism Type Two

OCA2 has been mapped to the *P* gene on chromosome 15q11.2-q12 (Ramsay *et al.*, 1992) and is the most common form of albinism in humans. In OCA2 there is partial tyrosinase enzyme activity and basal pigmentation can increase with age, including the darkening of hair colour and the appearance of pigmented naevi, freckles, or lentigenes in the skin, however these individuals do not tan (King and Witkop, Jr., 1976). In Prader-Willi and Angelman syndromes the incidence of OCA2 is 1%, and this incidence may be the result of hemizygosity for inherited mutant alleles of the P gene (Lee *et al.*, 1994). The P protein is associated with the melanosome membrane and its specific function has been debated. Some authors have proposed that the P protein is of structural importance and others have suggested a role for it in the regulation of intramelanosomal pH (Puri *et al.*, 2000). Melanosomes from *pink-eyed dilution* (*p*) null mice appear irregularly shaped, granular and less pigmented with a higher ratio of

phaeomelanin to eumelanin (Prota *et al.,* 1995). In addition, these melanosomes demonstrate a lack of p protein / tyrosinase / Tyrp1 complexes characteristic of immature melanosomes implicating the *p* gene as a regulator of normal melanosome biogenesis (Orlow *et al.,* 1993). Whereas the pH of wild-type melanosomes ranges from 3.0 to 4.6 (with pH inversely related to the degree of melanisation) (Bhatnagar *et al.,* 1993), melanosomes extracted from *p* deficient mice demonstrated a non acidic pH (Puri *et al.,* 2000) suggesting that *p* function is important for maintaining an acidic environment for successful melanin synthesis. However there is evidence to suggest that a neutral pH environment is in fact optimal for tyrosinase activity and melanogenesis. Ancans and Thody, (2000) reported that the neutralisation of an acidic pH in the melanosome induces melanogenesis *in vitro* within tyrosinase positive-amelanotic mouse and human melanoma cells. Subsequent work by the same group demonstrated that the use of proton pump inhibitors neutalised the acidic pH within the melanosomes of cultured human melanoma cell lines and also melanocytes from Caucasian skin, this neutralising effect correlated with a relative increase in melanin production (Ancans *et al.,* 2001). Not only were these effects greatest in cells that had low basal levels of melanogenesis, but melanocytes cultured from Negroid skin with high basal levels of melanogenesis appeared unresponsive to further melanin induction by proton pump inhibition / pH neutralisation (Ancans *et al.,* 2001). In 2003, King *et al.,* demonstrated for the first time that other genes could modify the OCA phenotype. Eight individuals with red hair colour at birth were confirmed to have OCA2 due to various *P* gene mutations. Six of the eight individuals who also had *MC1R* variants (known to be responsible for red hair colour) continued to have red hair into later life whereas the remaining two OCA2 patients who did not continued to have red hair in later life did not harbour *MC1R* variants, suggesting that the *MC1R* genotype altered the OCA2 phenotype (King *et al.,* 2003). Sturm *et al.,* (2003) proposed that *MC1R* variants

which predispose to the development of melanoma may interact with OCA2 polymorphisms (in non-OCA2 subjects) to influence the number of moles in skin and alter the predisposition to melanoma. Interestingly, of nine *MC1R* variants which are associated with red hair and fair skin, the high penetrance alleles such as Asp84Glu, Arg151Cys, Arg160Trp, and Asp294His in conjunction with either one of two OCA2 polymorphisms (Arg305Trp and Arg419Gln) resulted in an increase in mole number in individuals with brown eye colour (Sturm *et al.*, 2003).

1.4.5 Human Oculocutaneous Albinism Type Three

Brown OCA (BOCA) and rufous OCA (ROCA) are two rarer forms of OCA (Manga *et al.*, 1997). BOCA and ROCA are classified as OCA3 and are associated with mutations in *TRP-1* (Manga *et al.*, 1997). However, BOCA and ROCA are physically distinct, BOCA was initially found in Nigerian populations and subsequently in Black or Negroid populations of Africa and America (King *et al.*, 1980). ROCA was first described in the Black populations of Africa and Papua New Guinea (Walsh, 1971). Individuals with ROCA are described to have red / bronze skin colour and ginger / red coloured hair with blue or brown eyes, and either normal vision or mild nystagmus. Individuals with BOCA present with light brown / tan coloured skin, brown eyes and normal vision / mild nystagmus. Kidson *et al.*, (1993) demonstrated that there were normal numbers of melanosomes (in various stages of maturation) within skin and hair bulbs of Black individuals who had ROCA, and furthermore showed that in keratinocytes the mature melanosomes (in normal numbers) clustered together instead of being dispersed singly as seen in the keratinocytes from normally pigmented Black individuals. BOCA is the human homologue of the brown mouse (encoded at the *b* locus) where brown eumelanin is produced instead of black eumelanin. Boissy *et al.*, (1996) investigated dizygotic African-American twins who were discordant for OCA3. Melanocytes cultured from the OCA3 twin produced only brown melanin and not black

melanin, and this was thought to be due to a truncated form of TRP-1 encoded by a homozygous deletion within exon 6 of *TRP-1*. This prevented the production of TRP-1, however tyrosine hydroxylase activity of the OCA3 melanocytes were comparable to the non-OCA3 melanocytes from the normal twin. (Boissy *et al.*, 1996) suggested that this *TRP-1* mutation affected the interactions of TRP-1 with tyrosinase and dysregulated tyrosinase activity, hence causing predominant brown eumelanin synthesis instead of black eumelanin synthesis. Boissy and co-workers subsequently demonstrated that mutations in *TRP-1* cause the retention of TRP-1 within the ER, which prevented the stabilisation of tyrosinase by TRP-1 within the melanosome (Boissy *et al.*, 1998). Mutated *Tyr* and mutated *Tyrp1* demonstrated a prolonged association with calnexin and Bip, resulting in their abnormal retention within the ER of mouse melanocyte cell lines (melan-a, melan-b, and melan-c) (Boissy *et al.*, 1996). These authors suggested that some OCA1 and OCA3 cases could be ER retention diseases and that a mutation in one melanogenic protein could affect the maturation and stability of other proteins within the melanogenic pathway (Toyofuku *et al.*, 2001).

1.4.6 Human Oculocutaneous Albinism Type Four

OCA4 is an autosomal recessive hypopigmentary disorder encoded at the *LOC51151* locus (Newton *et al.*, 2001). The gene responsible for OCA4 is the human homologue of the mouse *underwhite* (*uw*) gene, which encodes the membrane associated transporter protein (MAPT) (Newton *et al.*, 2001). Mutations in the *uw* gene result in the significant reduction of melanin content in the skin and hair of underwhite mice, which display a characteristic white area of hair on their ventral abdomen, and this phenotype is similar in humans with OCA4 (Lehman *et al.*, 2000). To characterise OCA4, Costin *et al.*, (2003) cultured primary melanocytes from *uw / uw* and wild-type mice and investigated the processing and sorting of melanogenic proteins. The OCA4

melanocytes contained medium dark vesicles harbouring tyrosinase, Tyrp1, and Dct enzymes. Ultrastructural analysis showed that the vesicles secreted from OCA4 melanocytes contained mostly early stage melanosomes, and together these data suggested that disrupted tyrosinase trafficking and altered melanosome maturation are responsible for the OCA4 hypopigmentation phenotype (Costin *et al.*, 2003).

1.4.7 Human Hypopigmentation Disorders Caused by Mutated Melanosomal Proteins

Other disorders which cause hypopigmentation of skin and hair due to impaired trafficking of melanosomes have also been investigated with the use of naturally occurring and transgenic murine models. Griscelli syndrome is an autosomal recessive disorder in which patients display varying degrees of hypopigmented skin and silver / grey hair colour. These patients also suffer from immunological dysfunction with uncontrollable activation of T lymphocytes and macrophages (haemophagocytic syndrome) and sometimes have neurological impairments (Griscelli *et al.*, 1978). The corresponding mouse model named ashen ($Rab27a^{ash}$) exhibits a loss of function mutation in the *Rab27a* gene, which encodes the transporter protein Rab27a, responsible for melanosome transfer along actin filaments in dendrites of melanocytes. In contrast to normally distributed melanosomes, the melanosomes of these ashen mice tend to cluster around the perinuclear region of the melanocyte (Wilson *et al.*, 2000). A similar phenotype is observed in the dilute mouse in which the actin dependant motor protein Myosin Va is mutated, this prevents its association with the Rab27a protein which is required for normal melanosome trafficking (Au and Huang, 2002). The transgenic expression of Rab27a and separately Rab27b (a structural isoform of Rab27a) rescued the ashen mouse coat colour to produce a darker colour similar to that of the wild-type mouse (Barral *et al.*, 2002). Enhanced green fluorescent (eGFP) labelling of Rab27a permitted the visualization of Rab27a in melanocytes and

melanoma cell lines, and confirmed that eGFP-Rab27a co-localised with proteins that are present within melanosomes, lysosomes and endosomes (Hume *et al.*, 2001). The transfection of a dominant Rab27a mutant protein in pigment cells caused the redistribution of pigment granules, which clustered around the perinuclear area, similar to the clustering of pigment granules already described in melanocytes derived from *ashen* and *dilute* mice (Hume *et al.*, 2001). Therefore Hume *et al.*, (2001) suggested that the phenotype of Griscelli syndrome in humans occurs as a consequence of abnormal melanosome distribution.

1.5 Agonists and Inverse Agonists of MCIR

The melanocortin pathway has been implicated in the regulation of many physiological functions including pigmentation, obesity, inflammation, sexual function, and steroidogenesis. A receptor agonist may be described as a stimulatory ligand that promotes an increase in receptor activity, whilst an antagonist can directly inhibit agonist binding to prevent receptor activity. Alternatively an inverse agonist can compete with an agonist for the receptor's ligand binding site and cause an opposing response. The pro-opiomelanocortin (*POMC*) gene, positioned on human chromosome 2p23.3 (Zabel *et al.*, 1983; Satoh and Mori, 1997) encodes a large precursor molecule from which the melanocortin receptor agonists α-melanocyte stimulating hormone (αMSH), βMSH, and γMSH and adrenocorticotrophin (ACTH) 1-39 are derived by post-translational modification of POMC by the prohormone convertase (PC) enzymes (Eipper *et al.*, 1980; Smith *et al.*, 1988). PC1 cleaves the large POMC protein in acidic pH conditions to produce the ACTH 1-39, and PC2 subsequently cleaves the first 13 amino acids at the C-terminus of ACTH 1-39 to produce αMSH (Jackson *et al.*, 1997). Post-translation cleavage of the POMC protein also produces β-lipotropin (βLPH) and

corticotropin-like intermediate lobe peptide (CLIP) (Li, 1964; Scott *et al.*, 1976). βLPH cleavage gives rise to β-endorphin and γ-lipoprotein (γLPH) from which βMSH is also formed (Chretien and Li, 1967; Chretien Gilardeau, 1970; Chretien *et al.*, 1979). The peptides αMSH, NDP-αMSH, ACTH, ACTH 1-17, SHU9119, and MTII are all agonists of MC1R. ACTH 1-39, ACTH 1-17 and αMSH, are naturally occurring, whilst NDP-αMSH is a potent synthetic analogue of MSH, which has been utilised for MC1R ligand binding and signalling experiments (Schiöth *et al.*, 1995; Schiöth *et al.*, 1996). SHU9119 and melanotan II (MTII) are synthetic cyclic lactam MSH (4-10) analogues, which are potent melanotropins; SHU9119 is an agonist at MC1R and an antagonist at MC3R, and MTII is an agonist at both MC1R and MC3R and a potent antagonist at MC4R (Al-Obeidi *et al.*, 1989; Dorr *et al.*, 1996; Hruby *et al.*, 1995). Cooper *et al.*, (2005) demonstrated that αMSH, SHU9119, and MTII could suppress antigen-induced lymphocyte proliferation in monocyte-depleted and B lymphocyte-depleted assays, which suggested that αMSH, SHU9119, and MTII may have been exerting these immunosuppressive effects via MC1R on monocytes and B lymphocytes, and also possibly via MC3R expressed on B lymphocytes. MC4R is thought to play a role in sexual function, since MC4R is expressed in nerve fibers and mechanoreceptors in the glans of the penis, and MTII can act as an agonist of MC4R to induce penile erection (Van der Ploeg *et al.*, 2002).

Agouti and the agouti-related protein (Agrp) are inverse agonists of Mc1r, and bind to this receptor with a similar affinity as αMSH (Lu *et al.*, 1994; Siegrist *et al.*, 1997; Suzuki *et al.*, 1997; Ollman *et al.*, 1997). The *agouti* locus in mouse encodes for the 131 amino acid agouti protein, which regulates pigmentation in mammalian hair follicle melanocytes, and induces phaeomelanin synthesis (Bultman *et al.*, 1992; Miller *et al.*, 1993; Ozeki *et al.*, 1995). In mice with a natural agouti coat colour, the agouti protein

is synthesised in a pulse during early hair growth, which may be observed as a yellow phaeomelanin band of hair under the tip of black dorsal fur, however mutant mice that over-express agouti have a yellow coat colour (Jackson, 1997). Agouti over-expressing mice have normal tyrosinase activity; however, since they do not express Trp-1 or Dct these mice do not produce eumelanin (Koyabashi *et al.,* 1995). The agouti signalling protein (*ASP*) gene encodes for a 132 amino acid human homologue of the mouse agouti protein, and *ASP* mRNA is expressed in testis, ovary, heart, liver, kidney, and foreskin (Lu *et al.,* 1994; Millar *et al.,* 1995; Wilson *et al.,* 1995; Voisey *et al.,* 2001; Kanetsky *et al.,* 2002). Binding of mouse agouti and the human ASP to Mc1r and MC1R causes a reduction in cAMP signalling with a concomitant decrease in tyrosinase activity, melanogenesis and melanocyte cell growth (Lu *et al.,* 1994; Graham *et al.,* 1997; Sajai *et al.,* 1997; Siegrist *et al.,* 1997; Suzuki *et al.,* 1997). In order to evaluate the whether there is a role for ASP in human pigmentation, Voisey *et al.,* (2001) investigated for the presence of ASP polymorphisms in individuals who harboured *MC1R* variants (Voisey *et al.,* 2001). The group of African-American, Australian Aboriginal, Spanish Basque, Apache Indian, Hispanic, Asian, and Caucasian subjects where screened for polymorphisms in the *ASP* gene, and no non-synonymous polymorphisms were found in three coding exons and one non-coding exon (Voisey *et al.,* 2001). However a single polymorphism was detected within the 3'UTR region of exon four, in a small percentage of the group including the Spanish, Asian and African-American individuals, however because of the low frequency of this 3'UTR polymorphism no association with pigmentation outcome was found (Voisey *et al.,* 2001). Individuals with red and brown hair who were compound heterozygotes for Arg151Cys, Arg160Trp, Asp294His did not harbour ASP polymorphisms suggesting that ASP did not effect their pigmentation outcome (Voisey *et al.,* 2001). Kanetsky *et al.,* (2002) employed PCR and restriction fragment length polymorphism (RFLP)

analysis and in agreement with the work carried out by Voisey *et al.*, (2001) determined that there were no polymorphisms within the coding regions of ASP but identified the polymorphism (g.8818A→G) within the 3'UTR. In a group of Caucasians, the carriage of the G *ASP* allele was statistically associated with pigmentary traits such as brown hair and brown eye colour, and these authors suggested that there may be an '*ASP* allele dosage effect' whereby individuals that are homozygous for the G *ASP* allele are more likely to have brown hair and brown eye colour than those who are heterozygous for the G allele (Kanetsky *et al.*, 2002). Interestingly, transgenic mice over-expressing human ASP have a yellow coat colour, and murine melanocytes cultured in the presence of human ASP produced less cAMP *in vitro*, implying that the ASP promoted phaeomelanin production in these cells (Wilson *et al.*, 1995). Even though the human ASP protein shares 80% amino acid homology with the mouse agouti protein, and can cause a yellow coat colour when overexpressed in the mouse, ASP in humans appears not to function as a regulator of pigmentation in humans (Wilson *et al.*, 1995; Voisey *et al.*, 2001). It is perhaps possible that ASP may play a role in other systems such as with metabolic regulation, like the MC4R antagonist agouti-related protein (AGRP) which has been linked to obesity (Ollmann *et al.*, 1997).

1.6 The Melanocortin Receptor Family

Molecular cloning has identified five subtypes of the melanocortin receptor (MCR) family (Chhajlani and Wikberg, 1992a). These 7-pass transmembrane G-protein coupled receptors bind melanocortin peptide ligands. The MC1, MC3, MC4, and MC5 receptors have affinities for αMSH, βMSH, γMSH and ACTH (Schioth et al., 1995) however, MC2R does not naturally associate with the MSH peptides and binds ACTH alone (Schiöth *et al.*, 1996a). The MCRs share approximately 40-60% protein homology, and the use of bioluminescence resonance energy transfer (BRET)

demonstrated that the closely related MC1R and MC3R, formed homodimers and heterodimers, which occurred independently of agonist binding (Mandrika *et al.*, 2005). Human *MC2R* positioned on chromosome 18p11.2 encodes for a 297 amino acid ACTH receptor, which is primarily expressed in the adrenal gland and is important in stimulating steroidogenesis (Gantz *et al.*, 1993c; Mountjoy *et al.*, 1992). Transfection studies have shown that the MC2R signals through the cyclic adenosine monophosphate (cAMP) pathway upon binding ACTH (Weber *et al.*, 1993). Mutations in the *MC2R* gene have been found to be associated with familial glucocorticoid deficiency (FGD) type 1, which is a rare autosomal recessive syndrome caused by a deficient response to ACTH. In FGD type 1, patients have a characteristic diminished level of plasma cortisol and an excess of ACTH, which leads to severe hypoglycaemia and hyperpigmentation of the skin (Shepard *et al.*, 1959).

The *MC3R* gene is located on chromosome 20q13.2-q13.3 and encodes a 361 amino acid protein (Gantz *et al.*, 1993a; Gantz *et al.*, 1993c). Roselli-Rehfuss *et al.*, (1993) reported that MC3R is expressed in regions of the hypothalamus and the limbic system, especially the arcuate and posterior periventricular hypothalamic nuclei which are important for the control of cardiovascular neuroendocrine processes and thermoregulation. MC3R is also expressed in the placenta, gut, and in heart (Chhajlani, 1996; Gantz *et al.*, 1993a). MC3R preferentially binds γMSH (Schiöth *et al.*, 1998), but also binds αMSH and ACTH and couples to the cAMP and inositol phospholipid / Ca^{2+} signalling pathways (Konda *et al.*, 1994). *MC3R* is thought to play a role in energy homeostasis; for example *Mc3r*$^{-/-}$ null mice exhibited a lower rate of metabolism with a 50 – 60% increased adipose mass and a concomitant 50% decrease in running activity on a wheel test when compared to the *Mc3r* wild-type controls (Butler *et al.*, 2000).

On chromosome band 18q22 *MC4R* encodes a protein of 333 amino acids in length and is expressed mainly in the hypothalamic paraventricular nuclei in the brain (Gantz *et al.*, 1993b; Sundaramurthy *et al.*, 1998). MC4R can bind ACTH, βMSH, γMSH and agouti related protein (AGRP) as well as αMSH and NDP-αMSH, resulting in production of intracellular cAMP (Chhajlani, 1996; Grieco *et al.*, 2002; Haskell-Luevano *et al.*, 1997; Ho and Mackenzie, 1999; Hruby *et al.*, 2003; Yang *et al.*, 1999). *MC4R* is thought to be responsible for the regulation of appetite through binding of αMSH to this receptor and linkage-analysis has identified an association between human obesity and *MC4R* polymorphisms (Ollmann *et al.*, 1997). Interestingly a similar association between obesity and *POMC* gene alterations has been observed (Krude *et al.*, 1998; Marsh *et al.*, 1999). Mutations that impair the function of leptin, the leptin receptor, αMSH and Mc4r, or polymorphism which increase the melanocortin receptor antagonists agouti (as in Ay/a mice) or agouti-related protein (Agrp) are causal of an increased apetite and obesity in mammals (Huszar *et al.*, 1997). Leptin, encoded by the *obese* (*ob*) gene, is secreted from adipose tissue and is thought to regulate food intake and body weight (Mistry *et al.*, 1997). (Seeley *et al.*, 1996) proposed that αMSH binding to Mc4r may mediate leptin effects in the brain to inhibit appetite and reduce weight gain. Marsh *et al.*, (1999) demonstrated MTII, which is an MSH-like agonist, could not inhibit the feeding habits of obese Mc4r deficient mice, furthermore, obese $Mc4r^{-/-}$ mice were resistant to the inhibitory effects of leptin on feeding suggesting that the effects of leptin weremediated via Mc4r. However, non-obese $Mc4r^{-/-}$ mice did respond to the leptin, suggesting also that Mc4r was not the only mechanism of leptin action (Marsh *et al.*, 1999). In humans, subjects with specific *POMC* gene polymorphisms that result in defective POMC protein synthesis are subsequently deficient in the POMC peptide derivatives ACTH and αMSH, and develop early onset obesity, adrenal insufficiency, and some are reported to have red hair (Krude *et al.*, 1998). In humans, obesity is

associated with polymorphisms in the coding region of *MC4R*, obese individuals are usually heterozygous for *MC4R* polymorphisms, suggesting that obesity may occur as a result of a dominant *MC4R* variant (Vaisse *et al.,* 1998; Yeo *et al.,* 1998). However, because some GPCRs have the ability to form dimers and oligomers, some authors have hypothesised that dominant negative MC4R variants may dimerise with the wild type MC4R to inactivate wild-type receptor signalling (Ho and Mackenzie, 1999).

Human *MC5R* positioned on chromosome 18p11.2 encodes for a protein of 325 amino acids (Chowdhary *et al.,* 1995; Fathi *et al.,* 1995; Gantz *et al.,* 1994a). MC5R is expressed at low levels within the hypothalamic paraventricular nuclei in the brain and throughout peripheral tissues including the pancreas, thymus, adrenal and prostate glands (Chhajlani, 1996). Furthermore, MC5R is expressed in sebaceous glands in the skin (Thiboutot *et al.,* 2000) and αMSH, βMSH, γMSH and ACTH have been shown to play a role in regulating human sebum secretion (Thody and Shuster, 1973a; Thody and Shuster, 1973b; Thody and Shuster, 1975). Knockout mouse experiments have shown that Mc5r disruption results in the widespread dysfunction of the exocrine glands and a marked reduction in sebum (Chen *et al.,* 1997). Murine Mc5r binds αMSH, ACTH including ACTH 1-10, ACTH1-17 and the full length ACTH 1-39, all of which result in cAMP signalling and transient Ca^{2+} production in HEK293 cells (Hoogduijn *et al.,* 2002). The concentration of αMSH and ACTH for IP_3 signalling exceeded that required to transiently increase $Ca2^{+}$ production, suggesting that IP_3 signalling did not mediate Ca^{2+} production (Hoogduijn *et al.,* 2002). Ryanodine receptors are endogenously expressed in HEK293A cells, and caffeine induced agonism of these receptors stimulated the transient production of Ca^{2+} (Hoogduijn *et al.,* 2002). Ryanodine receptor inhibitors in combination were able to reduce the ACTH 1-10 induction of Ca^{2+} in a time dependant manner, which suggested that the Ca^{2+} signalling presumably

through MC5R may be modulated via ryanodine receptor interaction (Hoogduijn *et al.*, 2002).

1.7 The Melanocortin-1-Receptor

MC1R is a 7-pass transmembrane GPCR belonging to the subfamily of five melanocortin receptors (figure 1.4). The murine Mc1r and human MC1R were originally cloned and sequenced by (Mountjoy *et al.*, 1992) and simultaneously the human MC1R was also cloned by (Chhajlani and Wikberg, 1992). Subsequently, (Gantz *et al.*, 1994b) used fluorescence *in situ* hybridisation (FISH) to locate the *MC1R* gene to human chromosome 16q24.3. The *MC1R* gene contains an open reading frame of 954 base pairs which encodes a protein of 317 amino acids (figure 1.4). MC1R / Mc1r is a central control point in the regulation of melanin production and in determining the relative proportion of eumelanin and phaeomelanin in mammals (including humans) (Rees, 2000; Robbins *et al.*, 1993; Valverde *et al.*, 1995). As well being present on melanoma cells, melanocytes and keratinocytes in skin, human MC1R is expressed on several other cell types including, fibroblasts, endothelial cells, leucocyte sub-populations (monocytes, B and some T-lymphocytes) and in the periaquaductal grey matter in the brain (Becher *et al.*, 1999; Bhardwaj *et al.*, 1997; Chhajlani, 1996; Chhajlani and Wikberg, 1992; Cooper *et al.*, 2005; Neumann *et al.*, 2001; Varga *et al.*, 1976; Xia *et al.*, 1995). An isoform / splice variant of MC1R described as MC1RB has been identified, encoding for a receptor with an additional 65 amino acids at the C-terminus but pharmacologically similar to the non-spliced MC1R (Tan *et al.*, 1999). MC1RB is expressed in testicular cells, in fetal heart and in melanoma cells (Tan *et al.*, 1999). Tan *et al.*, (1999) demonstrated that the MC1RB splice variant retained its ability to bind ACTH, αMSH, γMSH and the melanocortin analogues NDH-αMSH, MT-II and SHU-9119 and produced specific increases in

Figure 1.4: The MC1R Protein

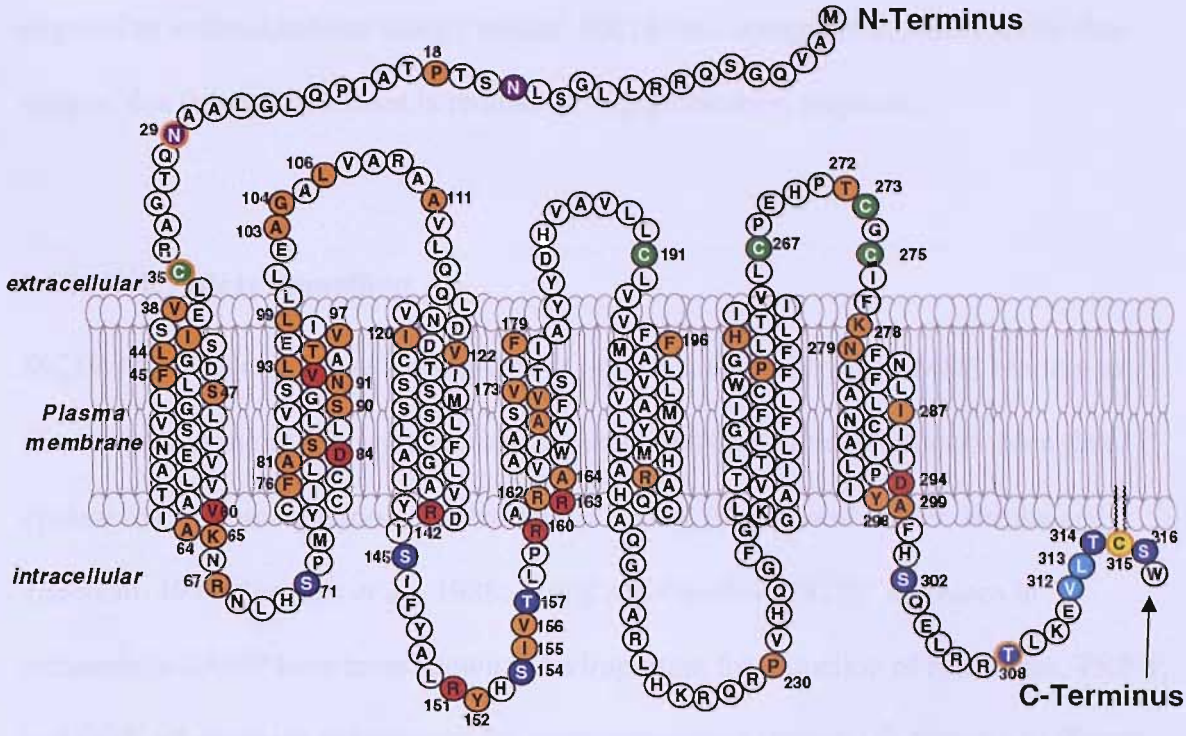

Legend for figure 1.4: Taken from Garcia-Barron *et al.,* (2005) and the MC1R structure is based on the model by Ringholm *et al.,* (2004). The wild-type consensus amino acid sequence (Genbank AF326275) are represented by their letter codes and sequence variants and post-translational modification sites are depicted in different coloured circles. Key: Red = red hair colour vartiant; Orange = natural mutation; Purple = potential N-glycosylation site; Dark Blue = potential phosphorylation site; Green = potential disulphide bond site; Light blue = dileucine-like motif; Yellow = potential acylation site.

cAMP levels *in vitro* when transiently transfected into COS-7 cells and stably expressed in CHO cell lines, and suggested that this splice variant receptor may have a role in pigmentation. However, there is a lack of subsequent evidence to show the frequency of the MC1RB isoform and whether this elongated receptor has any influence on human pigmentation. However, recently, Rouzaud *et al.,* (2006) identified and characterised another splice variant of MC1R, named MC1R350, and suggested that this isoform may act as a negative regulator of melanin synthesis by significantly decreasing the expression of MITF and tyrosinase in response to αMSH. In addition, they indicated that the number of MC1R350 receptors was inversely correlated with melanin content

within melanocytes (Rouzaud *et al.*, 2006). However UVR did not induce MC1R350 expression in the skin even though normal MC1R was upregulated, which could also suggest that this splice variant is redundant in pigmentation responses.

1.8 MC1R / Mc1r Signalling

MC1R / Mc1r is coupled to a stimulatory G-protein, and following αMSH binding to this receptor at the melanocyte surface, the activated Gαs subunit activates adenylate cyclase to cause upregulation of intracellular cAMP (Fuller *et al.*, 1979; Hirobe and Takeuchi, 1977; Jimenez *et al.*, 1988; Wong and Pawelek, 1973). Increases in intracellular cAMP have been shown to be important for induction of tyrosinase, TRP-1, and DCT, all of which are required for eumelanogenesis (figure 1.5, figure 1.6) (Busca *et al.*, 1996; Kobayashi *et al.*, 1995; Prota, 1992). The cAMP binds to the regulatory subunits of serine / threonine protein kinase A (PKA), which causes release of the catalytic subunits of this usually inactive tetramer (Kim *et al.*, 1993). Increased cAMP and activation of PKA subsequently allows cAMP-responsive element-binding protein (CREB) to bind to the *MITF* promoter to induce the transcription of *MITF* resulting in the production of MITF protein (Ao *et al.*, 1998; Bertolotto *et al.*, 1996; Bertolotto *et al.*, 1998). MITF binding to the M box (GTCATGTGCT) within the promoter regions of *tyrosinase*, *TRP-1*, and *TRP-2* results in their transactivation and their subsequent upregulation (Bertolotto *et al.*, 1998). *TRP-1* promoter activity is also thought to be regulated via MITF binding to an E box, whilst the *DCT* promoter is likely controlled by MITF binding to an E box and a CRE-like motif (Bertolotto *et al.*, 1996; Bertolotto *et al.*, 1998). Hence, activation of these promoters increases melanogenesis within the melanocyte. In mice, ASP has been shown to induce a switch from eumelanin to phaeomelanin synthesis by down-regulating *tyrosinase* and *Dct*, whilst increasing expression of a ubiquitinous transcription factor known as ITF2. The addition of αMSH

caused down-regulation of ITF2 expression, and ASP induced upregulation of ITF2 caused a reduction in *MITF* expression and function (Furumura *et al.,* 2001).

The induction of pigmentation in human skin by the injection of αMSH has been demonstrated (Lerner and McGuire, 1964; Levine *et al.,* 1991). Similarly, UVR can also induce pigmentation in human skin, and this is through a number of mechanisms which can cause the upregulation of both MSH and MC1R from keratinocytes and melanocytes, with a concomitant decrease in neprlysin, which is an endopeptidase expressed on melanocytes and is thought to control the breakdown of melanocortins *in vivo* (Abdel-Malek *et al.,* 1999; Aberdam *et al.,* 2000; Scott *et al.,* 2002). PI3-kinase has been shown to cause cell proliferation, differentiation, and neurite formation in a neuronal PC12 cell model (Kimura *et al.,* 1994). UVR and αMSH induction of cAMP via MC1R causes the formation of dendrites in melanocytes and melanoma cells, and in B16 melanoma cells the inhibition of PI3-kinase stimulated both dendrite formation and melanogenesis (Busca *et al.,* 1996). Busca *et al.,* (1996) demonstrated that forskolin induction of cAMP could inhibit PI3-kinase, and downstream activation of small GTPase binding proteins of the Rho family (Rho and Rac). Busca *et al.,* (1998) demonstrated that inhibition of Rho and Rac was required for cAMP-induced dendrite formation in B16 melanoma cells. The induction of cAMP has also been shown to activate the MAPkinase (ERK-1 and ERK-2, which are serine-threonine kinases) signalling pathway in human melanocytes and in B16 melanoma cells (Busca *et al.,* 2000; Englaro *et al.,* 1998). Busca *et al.,* (2000) found that cAMP could activate the MAPkinase pathway via the activation of small GTPase p21 Ras and subsequent phosphorylation of Raf-1 or βRaf kinase (Raf isoform expressed neural crest derived cells) and phosphorylation of MEK MAPkinase. MEK phosphorylation mediates ERK-1 and ERK-2 activation, and the activated ERK-1 and ERK-2 then translocate to the

nucleus to phosphorylate and activate transcription factors such as *MITF* to promote *tyrosinase* expression and melanin synthesis (Busca *et al.*, 2000; Englaro *et al.*, 1998). Some investigations lead to a hypothesis that UVR may induce membrane phospholipids to activate the phospholipase C pathway, and diacylglycerol (DAG) release to induce the phosphorylation of protein kinase C (PKC) (Gilchrest *et al.*, 1996; Nishizuka, 1986), and Park *et al.*, (1999) found that over-expression of PKCβ in non-pigmented B16G4F melanoma cells could induce tyrosinase activation. However there is evidence which demonstrated that inhibition of the PKC did not affect melanogenesis suggesting that PKC signalling is not crucial for melanin synthesis (Friedmann *et al.*, 1990; Bertolloto *et al.*, 1998). UVR can also induce nitric oxide (NO), causing erythema by increasing the blood flow in skin. NO activation of guanylate cyclase promotes the production of intracellular cyclic guanosine monophosphate (cGMP), and cGMP-dependent protein kinase activation can promote melanogenesis, which can be blocked by inhibition of NO synthase and guanylate cyclase (Romero-Graillet *et al.*, 1996). Romero-Graillet *et al.*, (1997) showed that keratinocytes could produce NO following UV irradiation, suggesting that keratinocytes may produce NO to have a paracrine effect on melanoctyes to induce melanogenesis. Keratinocytes also produce prostaglandin E2 (PGE2), αMSH, ACTH, and endothelin-1, which all induce melanocyte activation, melanogenesis and dendricity (Abdel-Malek *et al.*, 1989; Hunt *et al.*, 1994; Yohn *et al.*, 1993). Conversely, keratinocytes also can act to inhibit melanogenesis by secreting interleukin 1-α (IL-1α), tumour necrosis factor-α (TNFα), interferons (IFN), and β-fibroblast growth factor (βFGF) following UV irradiation (Halaban *et al.*, 1988; Köck *et al.*, 1991; Kameyama *et al.*, 1989; Swope *et al.*, 1989).

Transfection studies have enabled the functions of MC1R and some MC1R variants to be investigated. HEK293 cells transfected with MC1R demonstrated that MC1R can

immobilise intracellular Ca^{2+} as well as cAMP suggesting an alternative signalling pathway from this receptor (Mountjoy *et al.*, 2001). The Val60Leu, Arg151Cys, Arg160Trp, and Asp294His variants were stably transfected into HEK293 and melanoma cell lines, and demonstrated that these variants had diminished CREB phosphorylation but retained some cAMP signalling in response to αMSH (the Asp294His variant having the least CREB phosphorylation and cAMP response) (Newton *et al.*, 2005). Corre *et al.*, (2004) demonstrated that UV-induced activation of the *POMC* and *MC1R* promoters was mediated via the stress activated kinase p38, suggesting that p38 may be an alternative signalling pathway from MC1R following αMSH binding. Down stream targets of p38 include the transcription factors MITF and the upstream stimulating factor-1 (USF-1) (Galibert *et al.*, 2001; Mansky *et al.*, 2002). MITF and USF-1 contain the same E-box motifs (CANNTG) (Aksan and Goding, 1998). Melanocytes derived from USF-1-null mice failed to demonstrate *POMC* and *MC1R* expression in response to UV irradiation, which indicated that the USF-1 transcription was crucial for UV induced p38 mediated upregulation of *POMC* and *MC1R* (Corre *et al.*, 2004). MITF-null mice are known to lack all pigment cells (Steingrimsson *et al.*, 1994), however USF-1-null mice exhibit normal levels of pigmentation (Vallet *et al.*, 1998), indicating that USF-1 is unlikely to play a major role in melanocyte development.

Figure 1.5: Relationship between MC1R / Mc1r and Melanin Type

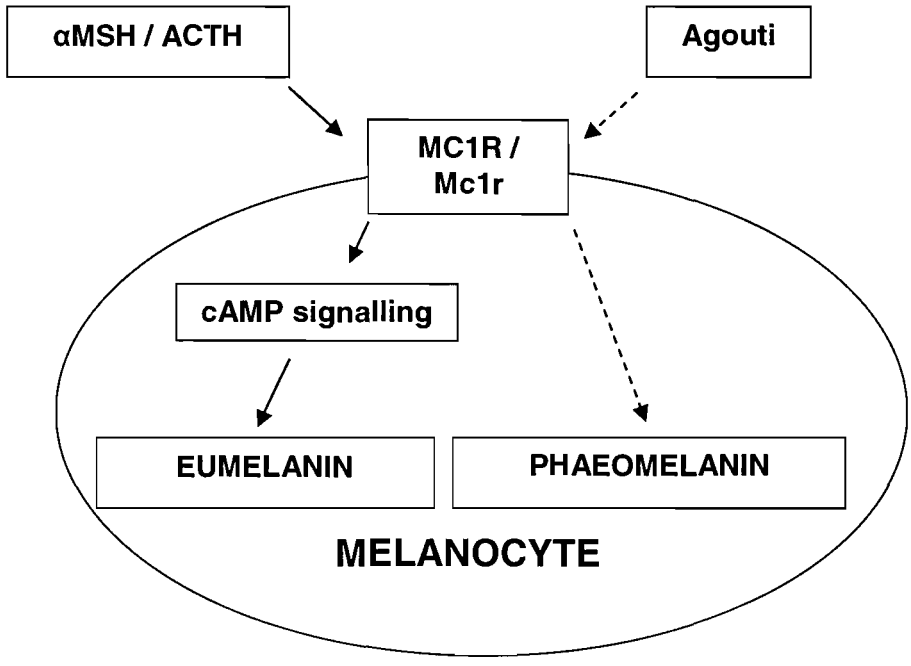

Legend for figure 1.5: Control signals for the production of eumelanin and phaeomelanin. αMSH binds to wild-type Mc1r and signals through cAMP to produce eumelanin. Agouti is the inverse agonist which competes with αMSH to bind to Mc1r and preferentially causes the production of phaeomelanin within the melanocyte.

Figure 1.6: MC1R / Mc1r Signalling Pathway

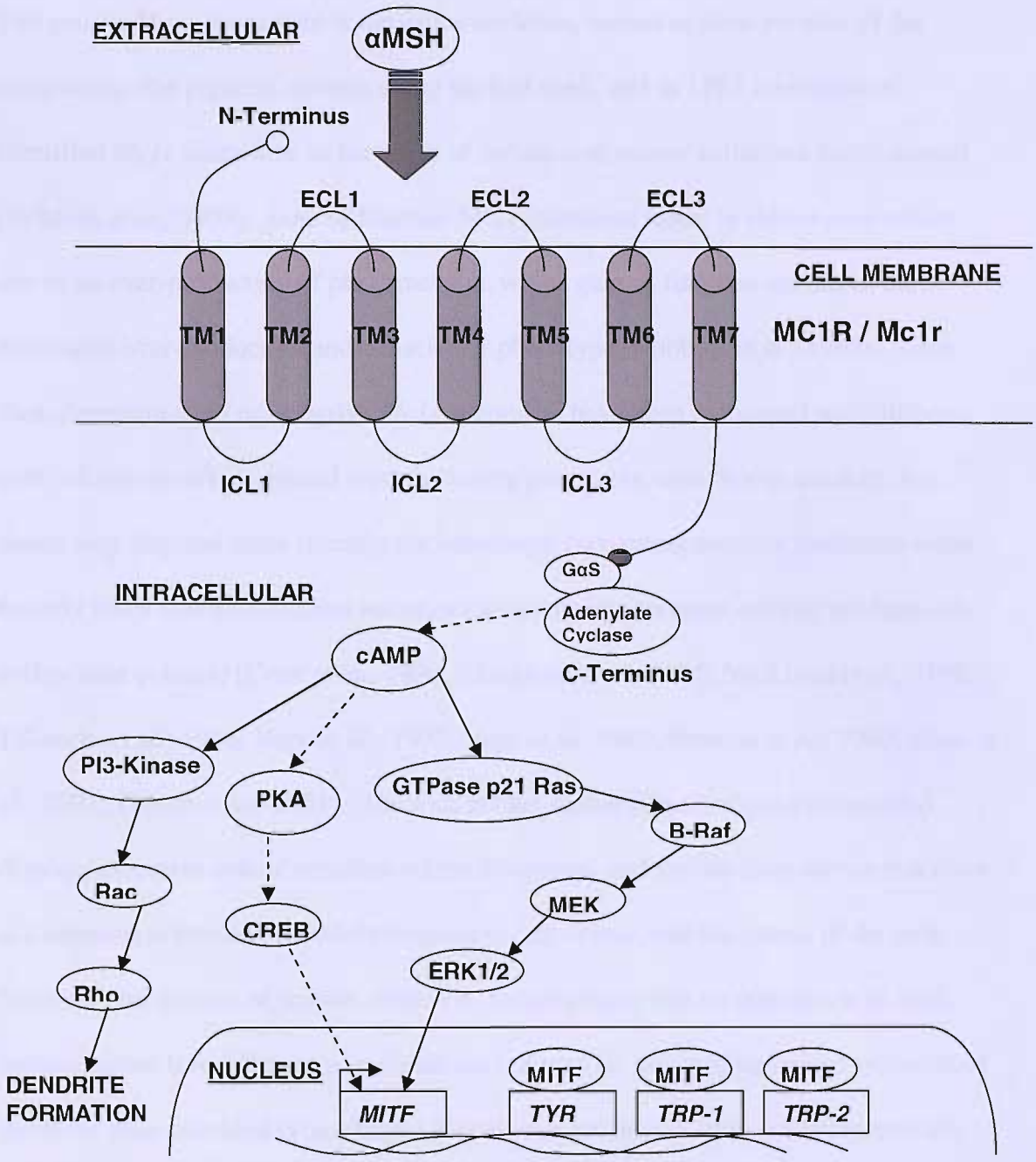

Legend for figure 1.6: αMSH binding to MC1R / Mc1r causes stimulatory G-protein (GαS) activation, and adenylate cyclase induction of cAMP. Upregulation of intracellular cAMP causes PI3-kinase, PKA and MAPkinase signalling, which initiates actin fiber rearrangement to promote dendrite formation and *MITF* expression. MITF subsequently binds to the promoters of *tyrosinase*, *TRP-1*, and *DCT* permitting the expression of these melanogenic proteins. (TM = transmembrane domain; ICL = intracellular domain; ECL = extracellular domain).

1.9 Mc1r Genotype and Pigmentation

The murine *Mc1r* is encoded at the *extension* locus, named as such because of the observation that pigment extends along the hair shaft, and in 1993 investigators identified *Mc1r* alterations as the cause of certain coat colour variations in this animal (Robbins *et al.,* 1993). Loss of function *Mc1r* mutations result in yellow coat colour due to an over-production of phaeomelanin, whilst gain of function mutations cause eumelanin over-production and a black hair phenotype (Robbins *et al.,* 1993). Since then, dominant and / or recessive *Mc1r* alterations have been associated with different coat colours in various animal types including guinea pig, cow, horse, chicken, fox, sheep, dog, pig, and more recently the bananaquit (activating receptor mutations cause brown / black coat colours, and mutations which reduce receptor activity produce red / yellow coat colours) (Cone et *al.,* 1996; Klungland *et al., 1*995; Marklund *et al.,* 1996; Takeuchi *et al.,* 1996; Vage *et al.,* 1997; Vage *et al.,* 1999; Newton *et al.,* 2000; Kijas *et al.,* 2001; Theron *et al.,* 2001). The rock pocket mouse (*Chaeotdipus intermedius*) displays extensive colour variation within its species, and studies have shown that there is a correlation between the Mc1r frequency, coat colour, and the colour of the rock habitat in this species of mouse, moreover, because there was no correlation of coat colours across five different geographic sites, it may be assumed that rapid evolution of the *Mc1r* gene provided camouflaged pocket mice protection from predatory animals (Hoekstra *et al.,* 2004; Hoekstra *et al.,* 2005). Similarly the beach mouse has a light coat colouration to camouflage itself. Interestingly, Hoekstra *et al.,* (2006) identified a charge-changing amino acid mutation in the *Mc1r* in beach mice, which causes diminished Mc1r function, presumably because the altered charge of the protein may alter conformation and prevent the access of αMSH to its N-terminal binding site. Recently, the Mc1r gene sequence was also amplified from the extinct woolly mammoth, and interestingly two alleles were found to encode for one functional

receptor, and one receptor with dramatically reduced activity, suggesting that the woolly mammoth had variation in its coat colour, and perhaps better adapting this animal to its environment (Rompler *et al.,* 2006).

1.10 MC1R Genotype and Pigmentation

Human studies have demonstrated that *MC1R* variants are also responsible for variation in human skin and hair pigmentation, and over 75 variants have been reported, but only a few have been functionally characterised to date (Reviewed by Wong and Rees, 2005). The frequency of *MC1R* variants is increased in blonde and red haired individuals than in those with natural darker hair tones, and several non-synonymous *MC1R* variants have been linked with UV light-sensitive phenotypes including red hair, fair skin, freckles, and an increased risk of skin cancer in Caucasians (Valverde *et al.,* 1995; Box *et al.,* 1997; Smith *et al.,* 1998; Flanagan *et al.,* 2000; Healy *et al.,* 2000; Palmer *et al.,* 2000; Bastiaens *et al.,* 2001; Naysmith *et al.,* 2004). Valverde *et al.,* (1995) reported that *MC1R* variants were most prevalent in individuals with red hair in contrast to those with blonde, brown or black hair within British / Irish Caucasians, and found that approximately 55-75% of individuals with skin types I-II harboured at least one MC1R variant, whilst less than 5% of subjects with skin types III and IV contained *MC1R* variants. The same group later investigated a cohort of Irish subjects, many of whom had fair skin type, and demonstrated that 75% contained *MC1R* variants, and of this group 30% were compound heterozygous for two variants or homozygous for one MC1R variant (Smith *et al.,* 1998). Interestingly, the Arg151Cys *MC1R* variant in combination with any other variant was significantly more common in individuals with a poor tanning response, and both the Arg151Cys and Asp294His variants were associated with more freckling following repeated exposure to natural UVR (Smith *et al.,* 1998). Smith *et al.,* (1998) also found that the Asp294His *MC1R* variant was over-

represented in British patients with non-melanoma skin cancer. Box *et al.,* (1997) also found that MC1R variants were associated with red hair colour and fair skin type in a group of Caucasian monozygotic and dizygotic twins, however some of the dizygotic twins who harboured the same *MC1R* variants were discordant for red hair colour suggesting that the MC1R variants were not soley responsible for the red hair and fair skin phenotype (Box *et al.,* 1997). Flanagan *et al.,* (2000) conducted a familial study, and demonstrated that homozygous Arg151Cys, Arg160Trp, Asp294His *MC1R* variant alleles were almost always responsible for red hair colour in one hundred and seventy four individuals from eleven large families with a preponderance of red hair compared with ninety nine unrelated red haired people. The most frequent *MC1R* variant was Val60Leu allele and these researchers suggested that this variant was perhaps a low penetrance allele for red hair when homozygous or in combination with Arg151Cys, Arg160Trp or Asp294His (Flanagan *et al.,* 2000). The 537insC variant was found in one family who all had red hair, suggesting that this allele may be a dominant red hair allele (Flanagan *et al.,* 2000). Flanagan *et al.,* (2000) correlated *MC1R* variants with pale skin, and a variant osage effect on beard colour, and freckling, however there was no evidence to show that *MC1R* variants affected eye colour within this study. *MC1R* variants are associated with increased freckling and a lower eumelanin to phaeomelanin ratio in hair (Bastiaens *et al.,* 2001; Naysmith *et al.,* 2004). Healy *et al.,* (2000) examined one hundred and eleven Irish and English individuals randomly collected irrespective of skin and hair colour, and the frequency of the functionally impaired Arg142His, Arg151Cys, Arg160Trp, Asp294His variants and the 179ins causing a prematre stop codon and truncated MC1R protein was investigated. Healy *et al.,* (2000) found that individuals who tanned well following exposure to UVR harboured less MC1R variants. Over one quarter of the group were heterozygous for the Arg142His, Arg151Cys, Arg160Trp, or Asp294His variants and were most sensitive to UVR (Healy

et al., 2000). Since MC1R heterozygotes are common within Caucasion populations Healy *et al.*, (2000) suggested that *MC1R* is an important susceptibility gene for sunburn, photoaging and skin cancer. Hence, Healy *et al.*, (2000) hypothesised that the number of variants might determine sun-sensitivity in people irrespective of red hair colour.

Transfection studies have enabled the investigation of MC1R variants *in vitro*, and have helped to clarify their functional relevance. Frandberg *et al.*, (1998) first reported that the Arg151Cys variant had impaired cAMP signalling despite demonstrating sufficient binding to a radiolabelled αMSH analogue. Schiöth *et al.*, (1999) also carried out functional analysis on the Val60Leu, Arg142His, Arg151Cys, Arg160Trp, and the Asp294His *MC1R* variants which were separately transfected into COS-1 cells. They demonstrated that these variant receptors were not able to produce cAMP to the same degree as the wild-type receptor, despite displaying a similar binding affinity for NPD-αMSH (Schiöth *et al.*, 1999). In addition, other transfection studies have shown that the Val60Leu, Arg142His, Arg151Cys, Arg160Trp, Pro162Arg, and Asp294His *MC1R* variants are functionally impaired in their coupling to adenylyl cyclase and have a reduced ability to signal via cAMP yet they bind ligand with similar affinity to the wild-type MC1R (Jimenez-Cervantes *et al.*, 2001; Robinson and Healy, 2002; Sanchez *et al.*, 2002). HEK293 and melanoma cell lines stably transfected with the Val60Leu, Arg151Cys, Arg160Trp, and Asp294His variants demonstrated some CREB phosphorylation and diminished cAMP signalling in response to αMSH (Newton *et al.*, 2005). Other variants, less commonly observed in the population such as Ile40Thr and Val122Met have also been reported in transfection studies to be partial loss of function variants (Jimenez-Cervantes *et al.*, 2001b). Transfection experiments have also demonstrated that the human MC1R is more sensitive to αMSH and ACTH than the

mouse Mc1r when cAMP production was compared (Abdel-Malek *et al.,* 1999; Mountjoy, 1994; Suzuki *et al.,* 1996).

Transgenic mouse experiments have enabled the investigation of the effects of wild-type and variant MC1R on mouse skin and hair colour (Healy *et al.,* 2001). Mouse bacterial artificial chromosomes (BAC) containing wild-type *Mc1r* could efficiently rescue the loss of *Mc1r* function in recessive yellow mice, resulting in a darker coat colour with pigmentation of the ears and tail, demonstrating that Mc1r controls interfollicular and follicular pigmentation (Healy *et al.,* 2001). Similarly, human wild-type *MC1R* resulted in black coat hair, ears, and tail with no evidence of phaeomelanin production, suggesting that human MC1R may be insensitive to agouti, and implying that agouti may not have a significant role in human hair colour. The human Arg151Cys and Arg160Trp variant *MC1Rs* partially rescued the loss of murine *Mc1r*, whereas the human Asp294His *MC1R* were even less efficient in rescuing loss of *Mc1r* (Healy *et al.,* 2001).

1.11 MC1R Genotype, Sun Sensitivity, and Skin Cancer Risk

A lack of pigmentation, red hair and fair skin, increased sensitivity to the sun, an inability to tan, increased numbers of nevi, freckles, CDKN2A and CDK4 mutations are all risk factors associated with the development of melanoma and non-melanoma skin cancers (Rees *et al.,* 2006). Since *MC1R* variants were shown to be associated with red hair, and fair skin (Valverde *et al.,* 1995), it was proposed that *MC1R* variants may also be a risk factor for melanoma and non-melanoma skin cancers. Valverde *et al.,* (1996) and determined that *MC1R* variants were a risk factor for the development of melanoma, and that the Asp84Glu was not a major risk factor variant. In contrast Ichii-Jones *et al.,* (1998) found no association between *MC1R* variants and skin cancer.

Polymorphisms in *ASP* gene have been associated with dark pigmentation, however, Landi *et al.,* (2005) found no association between *ASP* with pigmentation or with melanoma risk in a case control study involving a Mediterranian cohort of 267 melanoma patients and 382 controls. These researchers did however find that *MC1R* variants conferred a 2-4 fold increased risk of sporadic and familial melanoma (Landi *et al.,* 2005). Over the years numerous case-control studies have identified strong associations between *MC1R* variants and an increased risk UVR photodamage to the skin, familial and sporadic melanoma, and non-melanoma skin cancers such as basal cell carcinoma and squamous cell carcinoma. An association was found between *MC1R* variants and development of pigmentation lesions such as ephelides (which appear in early childhood) and solar lentigines (which appear as photodamage with increasing age) (Bastiaens *et al.,* 2001b). Bastiaens *et al.,* (2001b) observed that individuals with one or two MC1R variants had a 3-11 fold increased risk of developing severe lentigines, and this association remained independently of skin type and hair colour. Recently Landi *et al.,* (2006) associated *MC1R* variants along with *BRAF* oncogene mutations, and suggested that BRAF mutations were a high risk factor for melanoma in Caucasians without chronic sun damaged skin. However, since these researchers only compared young Caucasians (without chronic sun damage) with older Caucasian subjects (who had chronic sun damage), it would be expected that older subjects with chronic sun damage are more likely to develop melanoma regardless of *BRAF* mutations. Therefore in order to show that *BRAF* mutations are causal of melanoma irrespective of sun damage, an age matched study including patients with and without chronic sun damage could be conducted. Moreover, there is evivence to suggest that *BRAF* is not a susceptibility gene candidate for melanoma according to the MeLiM swine model of hereditary melanoma (Geffrotin *et al.,* 2004). This model did however implicate three melanoma risk regions of the swine chromosomes 1, 6, and 7, which

could be matched with human chromosomes 9p, 16q, and 6p, which strengthens the hypothesis that *CDKN2A* on human chromosome 9p, and *MC1R* on human chromosome 16q are likely candidates as susceptibility genes for melanoma (Geffrotin *et al.*, 2004). CDKN2A is also known as the cell cycle regulator p16, and mutations in the *CDKN2A* gene are linked with familial melanoma (van der Velden *et al.*, 2001). A *CDKN2A* gene mutation causing the p16-Leiden deletion in Dutch families causes familial atypical multiple-mole melanoma, however those individuals also habouring *MC1R* variants and in particular the Arg151Cys variant are at an increased risk of developing melanomas (van der Velden *et al.*, 2001). More recently, 395 American subjects from 16 American CDKN2A families with a prevalence of familial melanoma, were found to be at a higher risk of melanoma if they also harboured multiple *MC1R* variants, and this association remained after accounting for other risk factors such as nevi count, fair skin, freckling and germ line mutations for *CDKN2A* and *CDK4* (Goldstein *et al.*, 2005). Other case-control studies have aimed to identify the *MC1R* variants that confer the most risk for the development of melanoma and non-melanoma skin cancers. Kennedy *et al.*, (2001) investigated the *MC1R* genotypes of 123 patients with cutaneous melanoma, compared with 385 control subjects and 453 patients with non-melanoma skin cancer. The presence of *MC1R* variants increased the risk of melanoma independently of skin type and hair colour, and those who harboured homozygous or heterozygous compounds of the Val60Leu, Val92Met, Arg142His, Arg151Cys, Arg160Trp, Arg163Gln, and the His260Pro variants were at double the risk of skin cancer than those individuals who carried only one variant; interestingly the Asp84Glu conferred the highest risk for skin cancer development (Kennedy *et al.*, 2001). Palmer *et al.*, (2000) also found an association between *MC1R* variants and development of sporadic and familial cutaneous malignant melanoma in a cohort of 460 Australian melanoma patients and 399 control subjects. The Arg151Cys, Arg160Trp,

and Asp294 variants were found to double the risk of skin cancer development, however, in contrast to the findings of Kennedy *et al.*, (2001), Palmer found no association between melanoma risk and the carriage of the Val60Leu or Asp84Glu variants (Palmer *et al.*, 2000). Box *et al.*, (2001) also found that Arg151Cys, Arg160Trp, and Asp294 variants increased the risk of fair skin, development of solar lesions, BCC and SCC, and no increased risk when individuals harboured the Val60Leu, Val92Met, or the Arg163Gln. When human melanocytes containing *MC1R* variants were UV irradiated in the presence of αMSH, melanocytes that were homozygous for Arg160Trp, compound heterozygous for Arg160Trp and Asp294His, or heterozygous for Arg151Cys and Asp294His, but not cells that were homozygous for Val92Met variants, had reduced cAMP signalling compared to the wild type MC1R consistent with work carried out in house by Robinson and Healy (2002), and a concomitant increase in UVR induced cell death (Scott *et al.*, 2002).

1.12 Evolution of MC1R

It has been predicted that *MC1R* mutations originated over 20-40,000 years ago (Harding *et al.*, 2000). Contrastingly, haplotype analysis has shown linkage disequilibrium between a variable tandem repeat and the *MC1R* coding region, and assuming a mean VNTR mutation rate of 1%, it has been estimated that *MC1R* variants associated with red hair (such as Arg151Cys) may have arisen at least 7500 years ago, suggesting that these polymorphisms existed far more recently in the Caucasian population than first predicted (Smith *et al.*, 2001). The variation in MC1R was also investigated within African, Indian and Chinese populations, whilst variants were discovered in the Chinese subjects, there were no variants found in the African group (Rana *et al.*, 1999). *MC1R* was cloned and sequenced from gorilla, pygmy-chimpanzee, orangutan, and baboon to study the evolutionary history of MC1R and to investigate the

role of selection on genetic variation in human pigmentation (Rana *et al.*, 1999). One hundred and twenty one subjects were genotyped, and Rana *et al.*, (1999) found that the human consensus sequence was found to be different to the sequences originally published with Arg164Ala, Thr90Ser and Arg163Glu (Chhajlani and Wikberg 1992, Mountjoy *et al.*, 1992, Gantz *et al.*, 1993). Rana *et al.*, (1999) next studied MC1R variation in a cohort of Indians, Chinese, Southeast Asians, Japanese, Mongolian, Yakut and American Indians (to determine whether alleles associated with Asians existed before the split between American Indians and Asian populations. Seventy percent of the group harboured the Arg163Gln variant, and interestingly the Val92Met and the A942G substitution always appeared together (Rana *et al.*, 1999). Rana *et al.*, (1999) found that the Arg163Gln *MC1R* mutation was most associated with the darker skinned Indians and Africans than the East and Southeast Asians, the Yakut, and American Indians. The neutral theory of evolution predicts that less functionally important regions of a gene should evolve faster than functional areas, whereas the selection theory predicts that less deleterious synonymous mutations can evolve at a faster rate than the non-synonymous mutations. Rana *et al.*, (1999) compared primate *MC1R* sequences with horse, fox, cow, and horse, and found that five non-synonymous polymorphisms were conserved except within baboon that had a Val92Met substitution equal to that observed within humans (Rana *et al.*, 1999). A parsimony tree was used to map amino acid changes along primate lineages, and the ancestral human MC1R was found to be identical to the human consensus sequence; furthermore the parsimony tree indicated that the MC1R sequences of gorilla, chimpanzee and human had evolved faster than the baboon and orangutan sequences (Rana *et al.*, 1999). Ohta (1995) calculated the ratio of non-synonymous to synonymous amino acid changes at forty nine gene loci in primates, and found that the ratio was <1 for *MC1R* indicating that MC1R is not subject to strong selective control, unless the positive selection is underway

(Ohta, 1995). Highly melanised skin is known to be protective against UV-induced photolysis of folate (Branda and Eaton, 1978), and folate is required for normal embryonic neural tube development and spermatogenesis (Bower and Stanley, 1989; Lee *et al.,* 2006), which suggests that having highly melanised skin is a selection advantage in the Southern-hemisphere in order to protect folate for reproductive success. Another selection advantage in high UVR conditions is to protect against extreme sun burning and blistering of the skin, since broken skin could permit the entry of pathogens, equally the excessive loss of body fluids could be fatal. Conversely, in the Northern-hemisphere it may have been a selection advantage not to produce high levels of melanin, to permit maximal UVR absorption for vitamin D synthesis, which is crucial for bone development and preventing diseases such as osteoporosis (Holick, 2006).

1.13 MC1R Structure and Functional Consequences of Variant MC1Rs

GPCRs share common structural features consisting of an extracellular portion of variable length at the N-terminus, and a heptahelical transmembrane (TM) domains and an intracellular cytosolic carboxyl terminal, which tends to be post-translationally modified by the acylation (addition of acetyl groups) of conserved Cys residues (Probst *et al.,* 1992). Many GPCRs contain conserved Cys residues located in the extracellular loops of the receptor and it is suggested that intramolecular disulfide bridges may form at these positions that stabilise the receptors tertiary structure (Probst *et al.,* 1992). Other conserved Cys residues are found in the cytosolic tail of many GPCRs which may play a functional role in enabling G-protein interactions following ligand binding and activation of the receptor (Liu *et al.,* 1995; Wess *et al.,* 1991). The cytosolic tail region may also be involved in other functions including trafficking to the cell membrane, intracellular signalling and receptor desensitisation / internalisation, as the acylation

(palmitoylation or myristoylation) of conserved C-terminal Cys residues and acyl chain integration into the lipid bilayer can mediate these processes (Qanbar *et al.*, 2003). Conserved Cys residues act to secure the tertiary structure of MC1R and play a vital role in permitting the binding of ligand, and cAMP signalling because these are disrupted when Cys residues are mutated to Gly within MC1R at positions 35, 267, 273 and 275 (positioned within extracellular loops of the TM domain) (Frandberg *et al.*, 2001b). Previously Frandberg *et al.*, (1998) demonstrated that a region of four amino acids, K226-R227-Q228-R229 in second half of third intracellular loop of MC1R were essential for coupling to the stimulatory G-protein and almost all cAMP function could be ablated by mutating eleven polar and basic amino acids to alanine / glycine / cysteine within the third intracellular loop of MC1R. C-terminal domains of GPCRs can vary in length and MC1R possesses a short C-terminal region containing 14 amino acids (Prusis *et al.*, 1997). Some GPCRs have the ability to form homo- and hetero-dimers is known, and until recently it was assumed that MC1R could also dimerise. Sanchez-Laorden *et al.*, (2006) demonstrated that HA (hemagglutinin peptide) and FLAG (a small hydrophilic peptide) tagged MC1R formed constitutive homodimers and heterodimeric complexes in human HBL melanoma cells and HEK293T cells. MC1R dimers are thought to be held together by disulphide bonds, because the addition of the reducing agent 2-mercaptoethanol prevented dimerisation (Sanchez-Laorden *et al.*, 2006). These researchers found dimerisation of the unglycosylated 30 KDa and the glycosylated 36 KDa forms of MC1R, which suggests that MC1R can dimerise within the ER and golgi apparatus (Sanchez-Laorden *et al.*, 2006). The Arg151Cys, Arg160Trp, and Asp294His variants also dimerised with wild-type MC1R, and these authors suggested that dimerisation may be a novel mechanism by which variant MC1Rs may exert a dominant-negative effect on the wild-type MC1R (Sanchez-Laorden *et al.*, 2006).

1.14 The Role of MC1R in Non Pigmentary Systems

The POMC derived peptides αMSH, βMSH, γMSH, and ACTH1–39 are known to display many anti-inflammatory effects involving different inflammatory cells such as macrophages, mast cells, B cells and T cells. These peptides have inhibitory effects on NFκB activation, thought to be through the degradation of IκBα, and hence inhibition of pro-inflammatory cytokines such as TNFα, IL-1β, and IL-6 and adhesion molecule expression such as the intracellular adhesion molecule-1 (ICAM-1) (Hiltz *et al.*, 1992; Ichiyama *et al.*, 1999; Taherzadeh *et al.*, 1999; Wikberg *et al.*, 2000) and have been shown to modulate chronic inflammatory diseases including inflammatory bowel disease, allergy (allergic airway inflammation), joint arthritis, contact hypersensitivity, and systemic inflammation (endotoxemia) (Catania *et al.*, 1995; Ceriani *et al.*, 1994; Getting *et al.*, 2002; Grabbe *et al.*, 1996; Rajora *et al.*, 1997; Raap *et al.*, 2003). Getting *et al.*, (2003) suggested that MC1R is redundant and that MC3R was responsible for modulating the anti-inflammatory effects of the melanocortin pepides. However, there is evidence that MC1R activation reduces CD86 expression and interleukin-10 (IL-10) production from monocytes (Bhardwaj *et al.*, 1996; Gantz *et al.*, 2003; Luger *et al.*, 1997). Further work by Cooper *et al.*, (2005) demonstrated suppression of antigen-induced lymphocyte proliferation in the presence of αMSH and hypothesised that these immunosuppressive effects in humans were modulated in some way via MC1R signalling, but not by cAMP, because there was no difference between individuals with wild-type MC1R and those with non-functional MC1R variants (Cooper *et al.*, 2005). Alternatively, or in addition to the pigmentary effects, non-pigmentary effects of *MC1R* on proliferation and binding to extracellular matrix proteins may be important in the promotion of skin carcinogenesis (Robinson and Healy 2002). The wild-type MC1R demonstrated a decrease in cell proliferation, but non-functional MC1R variants continued to proliferate in the presence of αMSH (Robinson and Healy 2002). The

presence of the wild-type MC1R inhibited melanoma cell binding to fibronectin (an extracellular matrix protein) upon stimulation with αMSH, whereas this effect was not seen in the MC1R variant transfected B16G4F cells.

1.15 Intracellular MC1R

There is evidence to suggest that wild-type MC1R can internalise. Based on ligand binding data, Orlow *et al.,* (1990) demonstrated internal ^{125}I-βMSH binding sites in Cloudman S91 cells assumed to contain wild-type or variant MSH receptors according to their ability to respond to βMSH. Both cell types had similar cell surface binding sites, whereas the cells containing the variant receptors had a reduced number of intracellular βMSH binding sites, which suggested that the wild-type receptor internalised more efficiently than the 'mutated' MSH receptors. Further evidence for MC1R internalisation comes from studies by Siegrist *et al.,* (1988) and Siegrist *et al.,* (1989), which showed that ^{125}I-βMSH binding sites decreased at the cell surface by 60% in B16-F1 and Cloudman S91 melanoma cell lines after 2 hours of ligand binding. However, some cell lines (e.g. human D10 and 205 melanoma cell lines) show an increase in βMSH binding sites at the cell surface after 24 hours of ligand binding (Eberle *et al.,* 1993; Siegrist and Eberle 1993). Researchers have also suggested wild-type MC1R internalises based on their observations of a granular intracellular staining pattern of FITC labelled anti-MC1R (Böhm *et al.,* 1999). Furthermore, MC1R has been observed within intracellular endosomes in skin sebocytes by use of immunogold TEM, which suggested the possibility of wild-type MC1R recycling back to the cell surface within intracellular endosomes (Stander *et al.,* 2002). Although this may be correct, these interpretations assume that the anti-MC1R antibody is specific, which may not be the case. Based on the fact that MC1R plays a crucial role in pigmentation, and that the site of melanin synthesis occurs in the melanosome, it is possible that some of the

intracellular MC1R may in fact be located at this organelle. There is evidence demonstrating the presence of the enzymes PC1, PC2 and 7B2, and MSH and ACTH peptides in the melanosome (Peters *et al.*, 2000). These researchers hypothesised that the αMSH and ACTH peptides could have pigmentary effects acting independently of MC1R at the melanosome, however, they never investigated for the presence of MC1R at this site.

1.16 Aims

Although MC1R is known to be located at the cell surface, recent work demonstrating the presence of αMSH within the melanosome (Peters *et al.*, 2000), raising the question as to whether αMSH may act independently of a melanocortin receptor within this organelle, or MC1R may also be within or close to the melanosome to enable αMSH to have its action. Whereas some investigators have used MC1R antibodies for immunohistochemical detection of the receptor in tissue sections, the specificity of these antibodies in an intracellular environment is unclear (Böhm *et al.*, 2002; Salazar-Onfray *et al.*, 2002). Therefore the aim of this study was to generate melanoma cell lines stably transfected with eGFP tagged human wild-type MC1R and separately human variant MC1R in order to look at the subcellular localisation of the receptor. In addition, investigations for differences between wild-type and variant MC1R In terms of intracellular localisation would be carried out. Furthermore, comparison of internalisation of wild-type MC1R and variant MC1R would be undertaken to determine whether MC1R variants, which are functionally compromised in terms of cAMP signalling, can internalise with similar efficiency to the wild-type MC1R.

Chapter 2

Materials and Methods

2.1 Chemicals and Solutions

Chemicals were purchased as VWR-Merck grade Anala R®, or equivalent unless otherwise stated. Solutions were prepared using deionised water (dH_2O) produced by reverse osmosis using the Barnstead water purification system. Solutions for nucleic acid manipulations were prepared using Ultra High Quality water (UHQ H_2O), which is produced from dH_2O and further purified by reverse osmosis to a resistance of 18 mega-Ohms (Barnstead) and subsequently autoclaved at 15 psi for 15 minutes. Disposable polypropylene 1.5 ml and 0.5 ml tubes and tips were autoclaved at 18 psi for 30 minutes. Glassware was sterilised by heating to 160°C for a minimum of 1 hour. All sterile plastics including universals, bijoux and Petri dishes were acquired from Bibby Sterilin. DNA modifying enzymes were purchased from (Promega, Southampton, UK). All chemicals and enzymes were stored and handled as recommended by the manufacturer. Bacterial growth medium and solutions (appendix 1.1) were sterilised by autoclaving at 15 psi for 15 minutes. Antibiotics (appendix 1.1.5) and other heat sensitive solutions were sterilised by filtration through a 0.22 μm Millipore filter.

2.2 Plasmids and Bacteria

The pEGFP vectors (Clontech-BD BioScience, Royston, UK) encode for an enhanced green fluorescent protein (eGFP) and are designed to permit the labelling of Proteins at the C- or N-terminals depending on the orientation of the vector. The multiple cloning site (MCS) of the pEGFP-C1 and pEGFP-N3 vectors contain unique restriction sites for the incorporation of the DNA of interest. The *eGFP* is upstream of the MCS in the pEGFP-C1 plasmid for labelling of Protein at the N-terminus, and downstream of the

MCS in the pEGFP-N3 plasmid for labelling of Protein at the C-terminus. The pEGFP-C1 and pEGFP-N3 vectors also contain restriction sites that flank the eGFP in order to excise this DNA (Clontech-BD BioScience, Royston, UK). The pEGFP-C1 and pEGFP-N3 plasmids contain a unique Ase I / Not I restriction site to allow linearisation of the vector without disruption of the DNA insert (within the MCS), the *eGFP*, or any other feature. The SV40 polyadenylation signals downstream of the MCS in the pEGFP-C1 and downstream of *eGFP* within the pEGFP-N3 vector enables processing of the 3' end of the eGFP mRNA, and the sequence flanking *eGFP* contains a Kozak consensus translation initiation site, which increases protein translation efficiency (Kozak, 1987). The presence of a neomycin-resistance cassette (neo^r), consisting of the SV40 early promoter, the neomycin / kanamycin resistance gene of Tn5, and polyadenylation signals from the Herpes simplex thymidine kinase gene (HSV TK poly A), allows selection of stably transfected cells with geneticin (G418, appendix 1.7.3). These vectors also contain a CMV promoter and an SV40 origin for replication in mammalian cells expressing the SV40 T-antigen. The presence of a pUC origin of replication permits propagation of the vector within *E. coli* and the kan^r confers kanamycin resistance in these bacteria.

2.2.1 Growth and Storage of E. coli TOP 10

The *Escherichia coli TOP 10* bacteria (Grant *et al., 1*990) was grown in LB broth (appendix 1.1.1) for 16 hours at 37°C on an orbital shaker at 180 rpm. For long term storage, a suspension was stored at -70°C in LB broth containing 10% glycerol (appendix 1.1.3).

2.2.2 Preparation of Competent E. coli TOP 10

A static culture of *TOP 10* bacteria in 10ml of LB broth was grown overnight at 37°C. An aliquot (1 ml) of the starter culture was used to inoculate 25 ml of LB broth (sufficient for 10 transformations) and incubated on an orbital shaker at 180 rpm at 37°C until the cells were of sufficient density in the log phase of growth, this was measured by observing the optical density at an absorbance wavelength of 550nm (A_{550}). The required density was between 0.4-0.5, which was reached after approximately 2 hours of bacterial cell growth. The culture was then placed on ice for 20 minutes and all following procedures were performed at 4°C in order to maximise transformation efficiency. All reagents and materials including tips were therefore pre-cooled and this procedure was carried out at 4°C in the cold room. Cells were harvested by centrifugation at 2,000xg (MSE Minor) for 10 minutes and the supernatant discarded. The bacterial pellet was then immediately resuspended in 10 ml of ice-cold sterile 0.1 M $MgCl_2$ and re-centrifuged as above. The supernatant was discarded and the bacterial pellet resuspended in 1 ml of ice-cold sterile 0.1 M $CaCl_2$. The *E. coli* were allowed to stand on ice for a minimum of 1 hour before use as competent cells.

2.2.3 Transformation of Competent Cells

100µl of competent cells (2.2.2) were aliquoted into ice cold eppendorf tubes for each transformation. Ice-cold DNA was added to each tube of competent cells and left on ice for 30 minutes with occasional shaking. The competent cells were heat shocked at 42°C for 2 minutes in order to promote entry of the DNA into the cells. Cells were allowed to recover on ice for 30 minutes prior to spreading on LB agar plates (appendix 1.1.2) containing kanamycin (appendix 1.1.5), and incubated overnight at 37°C in an inverted position.

2.3 Isolation and Purification of Nucleic Acids

2.3.1 Miniprep

A spin miniprep kit (Qiagen, W. Sussex, UK) was used for small-scale purification of plasmid DNA from bacterial cells. All centrifugation was carried out using a bench top eppendorf microfuge 5417R. An overnight culture of bacteria (4.5 ml) was pelleted by centrifugation at 14,000 rpm for 5 minutes and the cell pellet completely resuspended in 250 µl resuspension solution P1 containing RNase A (appendix 1.3.1) ensuring all cell clumps were removed. The bacterial cells were lysed by the addition of 250 µl cell lysis solution P2 (appendix 1.3.2) and gentle mixing to avoid the shearing of genomic DNA. In order to precipitate genomic DNA, 350 µl of buffer N3 (content unknown, Qiagen, W. Sussex, UK) was added and the solution gently mixed immediately. Following centrifugation at 14,000 rpm for 10 minutes at room temperature the supernatant containing precipitated genomic DNA was separated from the compact white pellet containing proteins and cell debris, and transferred to a minicolumn (supplied) and centrifuged at 14,000 rpm for 1 minute (at room temperature) to bind the DNA to the column. The column was washed by the addition of 750 µl buffer PE (content unknown, Qiagen, W. Sussex, UK) and centrifuged for 1 minute at 14,000 rpm at room temperature (Eppendorf centrifuge 5417R). Residual wash buffer was removed by a further 1 minute of centrifugation before transfer of the column to a clean eppendorf and vacuum drying for 1 minute. The purified DNA was eluted from the column in 50 µl buffer EB (appendix 1.3.3), the buffer was added to the column and incubated for 1 minute at room temperature before centrifugation for 1 minute at 14,000 rpm. The yield of DNA was determined by electrophoresis of the DNA product on an agarose gel.

2.3.2 Midiprep

Large scale purification of plasmid DNA from bacterial cells was performed using a Midiprep kit (Qiagen, W. Sussex, UK). Bacteria from 25 ml of an overnight culture in LB broth containing kanamycin (appendix 1.1.5) were pelleted by centrifugation at 2,000xg (MSE Mistral 3000i) for 30 minutes at 4°C. The bacterial pellet was resuspended in 4 ml resuspension buffer P1 (appendix 1.3.1) containing RNaseA. Bacterial cells were lysed by addition of 4 ml lysis buffer P2 (appendix 1.3.2) the lysis reaction was mixed gently by inverting the tube 4 times to avoid shearing of genomic DNA and incubated for 5 minutes at room temperature. The precipitation of genomic DNA, proteins, cell debris was achieved by addition of 4 ml neutralisation buffer P3 (appendix 1.3.7) and mixed immediately (by inverting the tube 4 times) the solution was poured into a supplied QIAfilter cartridge and allowed to incubate at room temperature for 10 minutes. A Qiagen-tip 100 was equilibrated by the addition of 4 ml of buffer QBT (appendix 1.3.4) which emptied by gravity flow. The bacterial lysate was then filtered through the QIAfilter cartridge and the supernatant was ejected into the Qiagen-tip and allowed to enter the resin by gravity flow. The resin was washed with 2 x 10 ml buffer QC (appendix 1.3.5) and the DNA eluted in 5 ml of the buffer QF (appendix 1.3.6). The DNA was precipitated by the addition of 0.7 volumes of room temperature isopropanol and centrifugation at 2,000xg (MSE Mistral 3000i) for 1 hour at 4°C. The supernatant was removed and the pellet washed with 2 ml of 70% ethanol and recentrifuged at 14,000 rpm (Eppendorf centrifuge 5417R) for 5 minutes. The supernatant was removed and the resultant pellet vacuum dried for 5 minutes prior to resuspension in 75 µl of buffer EB (appendix 1.3.3). For high copy plasmids, expected DNA yields of 75-100 µg could be achieved, which was determined by agarose gel electrophoresis of the DNA product.

2.4 Agarose Gel Electrophoresis of DNA

DNA was separated and quantified by agarose gel electrophoresis, using high strength ultrapure analytical grade agarose (Bio-Rad, Hemel Hempstead, UK). The agarose gels were prepared in a Bio-Rad perspex tray and the ends were sealed with tape. A working dilution of 1 x TAE solution was prepared from a 50 x TAE stock solution (Thistle, Glasgow, UK, appendix 1.2.1) and used as electrophoresis buffer. The agarose was dissolved in 1 x TAE by heating in a microwave and molten agarose was cooled to approximately 50°C prior to the addition of 0.4 µg/ml ethidium bromide, and poured into the tray on a level surface. Whilst molten, a comb was inserted into the gel approximately 1 cm from the top. Once set, the gel was placed into an electrophoresis gel tank and DNA samples were prepared with 2 µl orange G solution (appendix 1.2.2) and sterile water to a total volume of 10 µl, and loaded into wells along side a 1 Kb plus DNA molecular weight marker (Gibco-Invitrogen, Paisley, UK). The 1 Kb Plus DNA ladder consists of 12 bands ranging in size from 1,000 to 12,000 bp in exact 1,000 bp increments as well as 7 bands from 100 to 850 bp, which enabled the approximation of size and quantity of the DNA sample according to the position and intensity of the sample DNA to ladder DNA respectively. The DNA was electrophoresed by applying a current at 70 volts across the gel and visualised using a UV dual intensity transilluminator (UVP, Cambridge, UK), and a photographic image was obtained using a digital camera with an orange filter.

2.5 Purification of DNA from Cultured Cells

The purification of DNA from cultured B16G4F cell transfectants was carried out using a DNeasy purification kit (Qiagen, W. Sussex, UK). The bench top eppendorf microfuge 5417R was used for every centrifugation step within this protocol, which was carried out at room temperature. Cells were cultured and 5 x 10^5 cells pelleted by

centrifugation at 1100 rpm for 5 minutes in an eppendorf. Cell pellets were resuspended in 200 µl PBS. The cells were lysed by addition of 200 µl lysis buffer AL (unknown content, Qiagen, W. Sussex, UK) and 20µl of 20mg / ml proteinase K prior to vortexing for 5 seconds, followed by incubation for 10 minutes at 70°C to yield a homogeneous solution. 200 µl of 100% ethanol was added to the sample and mixed by vortexing, the solution including any precipitate was transferred into a DNeasy spin column in a 2 ml collection tube (supplied) and centrifuged for 1 minute at 8,000 rpm. The flow through was discarded and the column transferred to a new collection tube (supplied). The bound DNA was washed by the addition of 500 µl wash buffer AW1 (content unknown, Qiagen, W.Sussex, UK) and centrifugation for 1 minute at 8,000 rpm. The flow through was again discarded and the sample washed again by addition of 500µl wash buffer AW2 (content unknown, Qiagen, W. Sussex, UK) and centrifuged for 3 minutes at 14,000 rpm. The column was transferred to a fresh eppendorf and vacuum dried for 2 minutes to ensure removal of residual ethanol as this may interfere with subsequent reactions. The sample was eluted by the addition of 100 µl of buffer AE (content unknown, Qiagen, W. Sussex, UK) to the column and incubation for 1 minute at room temperature before centrifugation at 8,000 rpm.

2.6 DNA Cutting and Modification

Restriction enzymes and buffers (10 x concentration) (Promega, Southampton, UK) were stored at -20°C. The restriction enzymes produced overhang end digest in preference to blunt end digests in order to ensure tight ligations (see 2.7.2). Restriction enzyme digest reactions contained approximately 1-2 µg of DNA and 5-10 units of enzyme per µg DNA in a total reaction volume of 10-50 µl. Reactions were incubated at 37°C (unless otherwise indicated by the manufacturer) overnight to ensure maximum digestion.

2.7 Linearisation of Circular DNA

Circular vector DNA was linearised by restriction digestion (2.6) at a unique point within the plasmid (without disruption of the insert of genes within the vector). The digested plasmid DNA was then dephosphorylated before ligation in order to prevent re-circularisation.

2.7.1 Dephosphorylation of Plasmid DNA

Calf intestinal alkaline phosphatase (CIAP, Promega, Southampton, UK) was added to the digested DNA (1U CIAP/μg DNA) and incubated at 37°C for 30 minutes, the incubation was repeated with the further addition of 1U CIAP/μg DNA at 37°C for 30 minutes in order to maintain enzymic activity. The reaction was heated at 50°C for 10 minutes to finally inactivate the alkaline phosphatase. Purification of the plasmid DNA was performed using a Qiaquick PCR purification kit (2.9.1) prior to usage in cloning.

2.7.2 Ligation of Linearised DNA

Covalent joining of DNA molecules was performed using T4 DNA ligase (Promega, Southampton, UK). A typical ligation reaction contained 10 ng vector and 3-5 molar excess of insert DNA, 1μl acetylated BSA (1 mg/ml), 1μl 10 x ligase buffer (appendix 1.4.1) and 1μl T4 DNA ligase. Vector and insert DNA were originally digested with the same restriction enzymes that produced complementary overhang ends and permitted insertion of the DNA at a specific site within the digested vector. Ligation reactions were incubated at 4°C overnight and subsequently used for transformation into competent bacterial cells (2.2.3).

2.8 Amplification of DNA by Polymerase Chain Reaction (PCR)

DNA was amplified in a GeneAmp PCR System 9700 thermal cycler (Applied Biosystems, Warrington, UK). Template DNA was amplified by denaturing for 5 minutes at 94°C, followed by 35 cycles of 94°C for 1 minute, T_m°C for 1 minute and extension at 72°C for 2 minutes, with a final cycle of 72°C for 7 minutes. The annealing temperature was selected on the basis of each primer T_m°C -5°C [where T_m°C = 4(G+C) + 2(A+T)]. A 50 µl PCR reaction contained: 1 mM MgCl, 1 x reaction buffer (Bioline, London, UK, appendix 1.5.1), 0.2 mM of each deoxynucleotide, 250 ng of each primer, 100 ng of template DNA and 2.5U Bio*Taq* polymerase (Bioline, London, UK).

2.9 Purification of DNA

DNA fragments were purified prior to sequencing or cloning in order to remove contaminating enzymes, primers or nucleotides. Purification of PCR products was carried out using a Qiaquick PCR purification kit Qiagen, W. Sussex, UK) or by gel extraction and purification using a Qiaquick gel purification kit Qiagen, W. Sussex, UK).

2.9.1 Qiaquick PCR Purification Kit (Qiagen, W. Sussex, UK)

Five volumes of buffer PB (content unknown, Qiagen, W. Sussex, UK) were added to the DNA to be purified and mixed before addition to a Qiaquick spin column (supplied). The DNA was bound to the column by centrifugation for 1 minute at 14,000 rpm at room temperature (Eppendorf centrifuge 5417R, used for each centrifugation step). 750 µl of wash buffer PE (content unknown, Qiagen, W. Sussex, UK) was added to the column prior to centrifugation for 1 minute at 14,000 rpm at room temperature. Residual wash buffer (containing ethanol) was removed from the column by further centrifugation for 1 minute at 14,000 rpm at room temperature and vacuum dried for 1

minute. The purified DNA was eluted from the column by addition of 30 µl buffer EB (appendix 1.3.3) and incubation for 1 minute at room temperature and centrifugation for 1 minute at 14,000 rpm.

2.9.2 Qiaquick Gel Extraction Kit (Qiagen, W. Sussex, UK)

All centrifugation steps were carried out using a bench top eppendorf microfuge 5417R at room temperature. Prior to DNA extraction the DNA was visualised and a clean scalpel blade was used to excise the specific DNA band from the agarose gel (2.4). 3 volumes of buffer QG (unknown, Qiagen, W. Sussex, UK) were added to a sterile eppendorf prior to the addition of the gel extract and incubated at 50°C to completely dissolve the gel slice. One gel volume of isopropanol was added to the sample and mixed by inversion prior to decanting onto a Qiaquick spin column (supplied). The DNA was bound to the column by centrifugation for 1 minute at 14,000 rpm, excess agarose was removed by the addition of 0.5 ml buffer QG before repeating the centrifugation step as above. The column was washed by the addition of 750 µl buffer PE (content unknown, Qiagen, W. Sussex, UK) and centrifuged for 1 minute at 14,000 rpm. Residual ethanol was removed by a further centrifugation step (as above) and vacuum drying for 1 minute. The purified product was eluted from the column into a clean eppendorf by addition of 30 µl buffer EB (appendix 1.3.3) to the membrane. The column was incubated with buffer EB for 1 minute before centrifugation for 1 minute at 14,000 rpm.

2.10 Rapid PCR Screening of Recombinant *E. coli TOP 10* Clones

Colonies were picked using a sterile loop and suspended in 10 µl ultra high quality H_2O (UHQ), the loop was then used to streak an LB agar plate containing (30 µg/ml) kanamycin to maintain the colony. 10 µl of 0.25 M KOH was added to the 10 µl

suspension and the solution boiled for 5 minutes at 100°C to lyse the bacteria. 10 µl 0.5 M Tris-HCl was added to neutralise the reaction and the volume made up to 300 µl with UHQ H_2O. 1 µl of this template was used in a 10 µl PCR reaction (2.8) using primers within the insert to screen the bacterial clone for the presence of the *MC1R* construct.

2.11 Automated DNA Sequencing

Automated DNA sequencing was performed using an Applied Biosystems (ABI) model 377 DNA Sequencing system using a Thermosequenase dye terminator cycle sequencing kit (Amersham Biosciences, Little Chalfont, UK). This technique uses four fluorescent dye-labelled dideoxynucleotide terminators and employs a thermostable DNA polymerase (Thermosequenase, Amersham Biosciences, Little Chalfont, UK) to determine DNA sequences by the chain termination method. This method involves three steps: 1) Primer annealing to the DNA template, 2) DNA extension incorporating unlabelled deoxynucleoside triphosphates (dNTPs), and 3) termination of extension following the incorporation of a fluorescent dye labelled dideoxynucleotide triphosphate (ddNTP) specific to A, C, G or T. Each sequence determination is carried out as a single reaction, containing all four dNTPs and all four ddNTPs. The ddNTP lacks the necessary 3'-OH group required for chain elongation, therefore the oligonucleotide chain is terminated at different nucleotides (A, C, G, or T) along the extension product, and each product may be separated according to size by high resolution denaturing gel electrophoresis. Each ddNTP (A, C, G, or T) is detected by the laser scanning across the gel during electrophoresis, causing the labelled DNA to fluoresce.

2.11.1 Sequencing Reactions

Sequencing reactions were performed using a GeneAmp PCR System 9700 (Applied Biosystems, Warrington, UK). High quality template DNA is essential for sequencing.

Generally, 1 μg of double stranded DNA was used per 1kb template length in a sequencing reaction. The reaction tube contained 4 μl of the premix (supplied by Amersham Biosciences, Little Chalfont, UK) and 50 ng of primer in a total volume of 10 μl. The tubes were placed in the thermal cycler and preheated to 96°C for 1 minute to reduce false priming before 60 cycles of denaturation at 96°C for 20 seconds, annealing at 46°C for 20 seconds and extention at 60°C for 4 minutes. The reactions were held at 4°C after thermocycling was complete. The extension products were purified by ethanol precipitation with the addition of 34 μl of ice cold 100% ethanol + 3.5 μl 7.5 M ammonium acetate (supplied), and left on ice for at least 15 minutes before centrifugation at 14,000 rpm (Eppendorf centrifuge 5417R) for 15 minutes. The DNA pellet was vacuum dried for 5 minutes to remove residual ethanol and subsequently resuspended in 4 μl formamide loading dye (Amersham Biosciences, Little Chalfont, UK) and kept on ice prior to sequencing.

2.11.2 Gel Preparation

The acrylamide-urea gel was cast between two glass plates separated by spacers of 0.2 mm thickness. To avoid fluorescent contamination along the laser scanning areas of the glass plates, the plates were washed thoroughly with the strong detergent Alconox (VWR, Poole, UK), rinsed with hot water followed by dH_2O, and then dried by spraying with 100% industrial methylated spirit (IMS) and air drying. Once completely dry the bottom glass plate was laid horizontal and two spacers placed at each edge and the front plate laid carefully on top. The plates were positioned using a spirit level to ensure that the gel would distribute evenly between the plates. The gel was prepared using 25 ml 4.8% acrylamide, 6M urea Gene PAGE plus gel solution (Amresco, Anachem, Luton, UK, appendix 1.6.1) with the addition of 150 μl 10% ammonium persulphate (Sigma, Poole, UK) and 15 μl TEMED (Sigma, Poole, UK) to initiate

polymerisation. Once the gel had been poured, a flat spacer was inserted into the top of the gel to create a space for a sharks tooth comb, and left for 2 hours to allow polymerisation of the gel solution. Once the gel was set, the flat spacer was carefully removed and the large well washed out with dH_2O. Subsequently, a 36 well disposable sharks tooth comb was positioned carefully into the large well between the plates so that the teeth were inserted to a depth of 0.2 mm and this created individual wells.

2.11.3 Gel Electrophoresis

The plates containing gel and the lower buffer reservoir were placed into the electrophoresis chamber and secured before fitting the upper buffer reservoir. The laser scanning region of the gel at the base of the plates was scanned prior to the placement of the upper buffer chamber, this permitted the cleaning of the scanning region (if required) with UHQ / drying with IMS to ensure the absence of background fluorescence. The buffer chambers were filled with 1 x TBE (prepared by dilution of 50 x TBE with dH_2O, appendix 1.6.2). The resuspended sample pellets were denatured by heating at 95°C for 2 minutes and placed back on ice prior to loading. Before loading, each well was prewashed with 1 x TBE to remove air bubbles, remaining unpolymerised gel and urea (as this may affect the electrophoresis step). 2 µl of sample was loaded into each well, and electrophoresis carried out for 7 hours at 2,500 volts, the sequencer maintained constant current, wattage and temperature at 40 mAmps, 30 watts and 52°C respectively. The sequence data was automatically collected and analysed by computer software (ABI prism: Sequencing analysis 3.4), and chromatograms were checked manually checking each base against a known target sequence.

2.12 Cell culture

Cell lines were maintained in DMEM (Invitrogen, Paisley, UK) media supplemented with 10% heat inactivated foetal bovine serum (Invitrogen, Paisley, UK), 2mM L-Glutamine (Invitrogen, Paisley, UK) and 2 μg/ml Ciprofloxacin (Bayer, Berkshire, UK) at 37°C in 5% CO_2 (DMEM supplemented with the above solutions will be referred to as complete media, appendix 1.7.1). The cell lines were maintained free of mycoplasma contamination as per the Stratagene PCR test (Stratagene, Amsterdam, The Netherlands). All cell lines were passaged at 60-70% confluence. Cells were stored at –80°C or in liquid nitrogen in storage media (appendix 1.7.4).

2.12.1 Cell Passage

Cells were passaged by firstly removing the media and washing with room temperature sterile PBS to remove any residual media. Cell dissociation solution (appendix 1.7.2) was added to the cells, and incubated at 37°C to allow detachment of the cells from the base of the flask. Complete media was added to resuspend the cells before transfer of the suspension to a sterile universal. The cells were pelleted by centrifugation at 1,100 rpm for 5 minutes at 4°C (MSE Mistral 3000i) and finally resuspended in 1ml of complete media prior to counting on a haemocytometer. 10 μl of the 1ml cell suspension was placed on a haemocytometer and cells were counted on a 4 x 4 square grid. The number of cells counted on the haemocytometer was used to calculate the approximate total number of cells per ml and an appropriate number of cells were replaced into a fresh culture flask containing fresh complete DMEM (e.g. 2 x 10^5 cells in 12ml complete DMEM per T75 flask).

2.13 Production of Stable Transfectants

Cells were transfectanted with circular or linear DNA by electroporation. Electroporation causes the cells to become porous when a voltage is applied and thus incorporation of the circular / linear DNA occurs, the circular DNA is only transiently incorporated for approximately 48 hours. The linearised DNA may be stably incorporated into the cells genome indefinitely provided that the appropriate selection conditions within the cell growth media are present.

2.13.1 Preparation of Cells for Electroporation

Cells must be growing at a rapid rate in the log phase of growth to ensure successful electroporation of DNA and survival of the cells during the electroporation process. The cells were grown to 60-70% confluence in a T175 cm^2 flask (and observed to be healthy) and passaged into two T175 cm^2 flasks the day before the electroporation. The engineered pEGFP plasmid constructs containing the DNA of choice were previously sequenced (2.11) to ensure no deletions, insertions or mutations were present before purification of each plasmid using Qiagen midipreps (2.3.2). 10 µl of linearised plasmid DNA (2.7) was placed at the base of a pre-sterilised 4 mm electroporation cuvette (Molecular Bioproducts, supplied by VWR, Poole, UK), and kept on ice prior to the electroporation step. 4 x 10^6 cells in 400 µl complete media were added to the cuvette and maintained on ice for 10 minutes prior to electroporation. Cells were transfected by electroporation using a Bio-Rad Gene Pulser II set at 176 volts and a capacitance of 2,500 µFd (method optimised in the same laboratory by Dr S. Robinson). Following electroporation the cells were immediately transferred to a volume of complete media and dispensed 200µl per well in 96-well culture plates. This ensured that the transfected cells were diluted sufficiently to allow for single clones to grow within each well of the 96 well plate. 48 hours post transfection, 1.5 mg/ml geneticin (G418) (appendix 1.7.3,

Invitrogen, Paisley, UK) was added into the culture media to select for cells expressing the plasmid (note that this was the selection antibiotic specific to the pEGFP Clontech vectors, Clontech-BD BioScience, Royston, UK). The media was replaced twice a week until clones could be seen within 96 well plate. Individual clones were expanded and analysed for successful transfection. In the case of the pEGFP plasmid transfected cells, the emission of green fluorescence was observed by fluorescence microscopy.

2.14 Fluorescence Microscopy of Transfectants

Cells were seeded on 16 mm diameter glass coverslips within 12 well culture plates at a density of 1 x 10^5 cells per well and grown in complete media overnight at 37°C. The cell containing coverslips were washed with PBS prior to fixation with 500 µl paraformaldehyde (4%) for 7 minutes at room temperature. Fixation was stopped by removing the paraformaldehyde and incubating the cells with 500 µl of 50 mM ammonium chloride solution for 10 minutes at room temperature. In order to remove traces of all solutions, the coverslips were washed twice with PBS. Coverslips containing fixed cells were mounted onto glass slides with a small volume (approximately 5 µl) of vectashield (Vector Laboratories, Peterborough, UK), a transparent non-fluorescent mountant with fluorophore protective action, to protects the sample from some photo bleaching caused by exposure to a light source. Each coverslip was sealed to the glass slide using nail varnish, this prevented sample drying, as the formation of crystals prevents clear microscopy images.

2.15 Immunofluorescent Labelling of Cells

Cells (seeded at 1x10^5 cells per well) were cultured in complete media onto glass coverslips, in the wells of a 12-well culture plate. Cells on coverslips were grown

overnight in order to ensure a sufficient monolayer of cells for optimal immunolabelling. Prior to immunolabelling, cells on coverslips were fixed for 7 minutes with 4% paraformaldehyde. Fixation was stopped by placing the cells on coverslips in 50 mM ammonium chloride for 10 minutes (at room temperature), and subsequently permeabilised for 6 minutes using ice cold 100% methanol. Coverslips containing fixed and permeable cells were inverted onto 100 µl of primary antibody (diluted appropriately in PBS) on a sheet of parafilm and incubated at room temperature for 1 hour. The coverslips containing the fixed cells were then washed (cell side up) in clean wells of a 12 well tray containing PBS before inversion onto 100 µl of fluorochrome conjugated secondary antibody (diluted appropriately in PBS) on a clean sheet of parafilm, and left in the dark for 30 minutes at room temperature. Following this, the coverslips were mounted on glass slides using vectashield (Vector Laboratories, Peterborough, UK, UK), and the edge of the coverslip sealed to the slide using nail varnish to prevent sample drying.

2.15.1 Labelling of Golgi with BODIPY Texas Red Ceramide

The BODIPY Texas Red (TR) Ceramide BSA conjugate (Molecular Probes-Invitrogen, Paisley, UK) is a lipid monomer which is specifically incorporated into the golgi (and also newly synthesised lipids) of live cells, and emits a red fluorescence at 617 nm when excited by green light at 589 nm. $1x10^5$ cells were grown overnight on coverslips within 12 well culture plates prior to labelling. The cells were initially washed with 1 x HBSS media (Invitrogen, Paisley, UK) at 37°C, and subsequently incubation for 30 minutes at 4°C with 5 µM BODIPY TR Ceramide BSA complex in 1 x HBSS. The cells were then rinsed 3 times with ice cold complete DMEM media prior to incubating for a further 30 minutes with fresh DMEM at 37°C. The cells were then fixed with 4%

paraformaldehyde as previously described (above) and observed by fluorescence microscopy.

2.16 Confocal Microscopy of Transfectants

Cells were prepared on coverslips as previously described in 2.15 and analysed by use of a Leica SP2 laser scanning confocal microscopy. Confocal settings were as follows: Laser λ488, resolution 1024 x 1024 pixels, laser speed 400 Hz. All images were captured at 100 x magnification and each voxel was 150 nm in size. 3D images were generated by capturing individual cross sections every 1μm throughout the Z plane of the sample, before reconstructing a maximum projection utilising the Leica software.

2.17 Flow Cytometry

Flow cytometry was carried out on a Becton Dickinson FACScan flow cytometer. The presence of green fluorescence was investigated in approximately 10,000 events per transfected cell line. Cells were passaged and $2x10^5$ cells transferred into FACS tubes and pelleted by centrifugation for 5 minutes at room temperature at 1,500 rpm (MSE Mistral 3000i). Cell pellets were resuspended in 500μl FACS buffer (appendix 1.8.1) prior to analysing. Subsequent FACS data was analysed using Win MDI5.8 computer software (Verity House Software, inc.).

2.18 Ligand Binding

Cells were seeded at $4x10^4$ cells per well in 96-well culture plates, and allowed to grow overnight. Prior to radioactive labelling, cells were washed once with ice cold binding buffer (appendix 1.9.1) and residual buffer removed by pipetting before the addition of radioactive ligand. In order to perform a competition binding assay, cells were

incubated for 2 hours at room temperature with 0.001 nM to 3000 nM concentrations of unlabelled Nle^4, D-Phe^7-α-melanocyte stimulating hormone (NDP-MSH, Bachem, St. Helens, UK) in 0.05 ml binding buffer containing 15,000 counts per minute (cpm) of [^{125}I] NDP-MSH (Amersham Biosciences, Little Chalfont, UK). Following the incubation step, cells were then washed twice with 0.2 ml of ice cold binding buffer, which was completely removed before lysis of the cells. 0.1 ml of 0.1 M NaOH was added to lyse the cells and the lysate transferred to a tube containing 900 µl of 0.1 M NaOH. Radioactivity (representing ligand binding) was measured using a Packard auto-Gamma Counter (Packard Bioscience LtD), and the data was analysed using a software package for radioligand binding analyses (GraphPad Software, Inc San Diego, USA). Non-specific binding of radiolabelled NDP-MSH was determined in the presence of non radioactive 3 µM NDP-MSH.

2.19 Investigation of Internalisation using ^{125}I NDP-αMSH

Cells transfected with an untagged MC1R construct were seeded at $4x10^4$ cells per well in 96-well culture plates, and allowed to grow overnight. (Note that the cells were seeded in the central area of the plate, and wells surrounding the cells were also filled with binding buffer to create a humid environment to prevent liquid evaporation from the wells during the 37°C incubation of the experiment). Prior to radioactive labelling, cells were washed once with ice cold binding buffer (appendix 1.9.1) and residual buffer removed before the addition of radioactive ligand. In order to perform an internalisation ligand binding assay, cells were incubated for 0, 30, 60 and 120 minutes at 37°C with the lowest competition binding assay concentration of 10^{-12} M Nle^4, D-Phe^7-α-melanocyte stimulating hormone (NDP-MSH, Bachem, St. Helens, UK) in 0.05 ml binding buffer containing 15,000 counts per minute (cpm) of [^{125}I] NDP-MSH (Amersham Biosciences, Little Chalfont, UK Pharmacia Biotech). The 96-well plate

containing cells and radioactivity was attached to buoyant polystyrene blocks, secured with elastic bands, and floated in a water bath at 37°C (the plate was sealed using parafilm to ensure that no water could enter the wells). Following the incubation step, cells were then washed twice with 0.2 ml of ice cold binding buffer, which was completely removed (to reduce background radiation) before the addition of 0.1 ml of 0.1 M NaOH to lyse the cells from the plates and the lysate was transferred to a tube containing 900 µl of 0.1 M NaOH. Radioactivity was measured as described in 2.19.

2.20 MC1R-eGFP Internalisation

Cells transfected with the pEGFP-N3 vector containing *MC1R* were used to investigate receptor internalisation. $1x10^5$ cells were seeded onto 16 mm diameter glass coverslips in 12 well plates and cultured in 1 ml complete media at 37°C overnight. The transfectants containing eGFP tagged MC1R were subsequently incubated with 10^{-6} M αMSH or 10^{-6} M NDP-αMSH (a concentration know to increase cAMP production via MC1R signaling and promote pigmentation in melanogenic murine B16 and S91 melanoma cells) for up to 45 minutes at 37°C to induce receptor-ligand internalisation. Cells were fixed and mounted as previously described (2.14).

2.20.1 Sucrose Inhibition of Internalisation

The presence of sucrose actively inhibits receptor / ligand internalisation by inhibiting the formation of clathrin coated pits. Therefore, prior to the addition of 10^{-6} M αMSH / 10^{-6} M NDP-αMSH, the cells were pre-incubated with 1 ml of 0.5 M hypertonic sucrose in media for 30 minutes at 37°C. The cellular distribution of MC1R-eGFP was then examined by confocal microscopy. This method was adapted from Gao *et al.*, (2003).

2.21 cAMP Assay

The second messenger cyclic AMP (cAMP) is an important regulator of cell proliferation and differentiation because of its ability to act as a mediator of a variety of growth factors and hormones. Several hormones and neuropeptides have been known to activate the cAMP pathway through the enzyme adenlyl cyclase. The conventional method of measuring cAMP is by radioimmunoassay (RIA) - whereby the succinyl ester derivative of cAMP is radioiodinated. However, it is difficult to get a pure and labelled radioiodiated cAMP, and this can give rise to high background radiation counts. Therefore a non radioactive cAMP Assay Kit by R&D Systems was used. This assay is based on the competitive binding technique in which cAMP present in a sample competes with a fixed amount of alkaline phosphatase-labeled cAMP for binding of a rabbit polyclonal antibody. During the incubation, the polyclonal antibody becomes bound to the goat anti-rabbit antibody coated onto the microplate. Following a wash to remove excess conjugate and unbound sample, a substrate solution is added to the wells to determine the bound enzyme activity. The color development is stopped and the absorbance is read at 405 nm. The intensity of the color is inversely proportional to the concentration of cAMP in the sample (R&D Systems, Abingdon, UK).

The cells were seeded at $2x10^5$ cells per well and cultured overnight in 24-well plates. The cells were then treated with fresh media alone (for basal cAMP production) or with fresh media containing additives (eg. αMSH and forskolin at various concentrations) and incubated at 37°C for a further 30 minutes. The media was removed, and 200 µl 0.1 M HCl was added for 10 minutes to lyse the cells. Lysed cells were centrifuged in a bench top microfuge at 600xg for 5 minutes at 4°C (Eppendorf centrifuge 5417R) and the cell supernatants removed and diluted 1:5 in assay buffer ED2 (R&D Systems, Abingdon, UK). The cAMP standards were prepared as outlined in the manufacturer

protocol (R&D Systems, Abingdon, UK) and ranged from 0.78 pmol/ml to 200 pmol/ml. Samples and standards were transferred to a 96-well ELISA plate and reagents were added (as per manufacturer protocol, R&D Systems, Abingdon, UK). The presence of cAMP was detected and quantified by the presence of a colour product. A Beckman Optical Density plate reader (Beckman Coulter, High Wycombe, UK) was utilised to quantify the colour change within each well, and software calculated the concentration of cAMP per well using the standard curve generated from the cAMP standards.

2.22 Isolation of Melanosomes from Melanoma Cell Lines

Melanosomes were extracted from the transfected melanoma cell lines containing MC1R tagged with eGFP. The melanosome isolation method was adapted from Seiji M *et al., 1*961. An eight-layered sucrose gradient was created 18 hours prior to the melanosome extraction, sucrose solutions were pipetted (500 µl volumes) starting with the least dense 1.50, 1.55, 1.60, 1.80, 2.00, 2.20, 2.40, and 2.60 M into a clear 5 ml ultracentrifuge tube (Beckman Coulter, High Wycombe, UK) through a glass Pasteur pipette. Each layer produces a clear visible interface and this technique avoids the mixing of the solutions. When carried out at room temperature the solutions increase in viscosity yet remain fluid and easily pass down the glass pipette. The gradient is left to stand at 4°C for 18 hours exactly. Cells were grown in T175 culture flasks to yield approximately $6x10^7$ cells. The cells were grown to at least 70% confluence dissociated from the flask and resuspended in complete media before centrifugation at 700xg for 10 minutes at 4°C (MSE Mistral 3000i). The supernatant was discarded and the pellet resuspended in 1 ml of ice cold Dounce buffer (appendix 1.11.1) and incubated for 10 minutes on ice in order to lyse the cells. The cell suspension was transferred to a pre-chilled Dounce Homogeniser on ice and the cells thoroughly lysed by 40 strokes of the

pestle. The homogenised cell suspension was then centrifuged at 700xg for 10 minutes at 4°C (MSE Mistral 3000i) and the supernatant retained as this contained the melanosome fractions. In order to maximise the recovery of melanosomes the remaining pellet was then resuspended in 1 ml of ice cold Dounce buffer (appendix 1.11.1) and incubated for a further 10 minutes on ice prior to re-homogenisation in a pre-chilled Dounce Homogeniser on ice (40 strokes of the pestle). This product was then centrifuged at 700xg for 10 minutes at 4°C (MSE Mistral 3000i) and the supernatant decanted. The supernatants from the Dounce Homogeniser steps were pooled and centrifuged at 11,000 g for 10 minutes at 4°C (Eppendorf centrifuge 5417R), the supernatant was decanted and the sediment retained, and resuspended in a 0.3 M sucrose solution before centrifugation at 15,000xg for 10 minutes (Eppendorf centrifuge 5417R). The supernatant was discarded and the sediment was resuspended in a 0.3 M sucrose solution to produce the 'large granule suspension'. The melanosomes were then extracted from the melanoma cell transfectants by ultracentrifugation. The 'large granule suspension' was floated on the top of the sucrose gradient by careful pipetting to avoid mixing of the gradient. The gradient plus cells was centrifuged in an ultracentrifuge (Beckman Coulter Optima L-80 X P Ultracentrifuge, Beckman Coulter, High Wycombe, UK) using a pre-chilled swing-out rotor (Beckman SW50.1) at 103,000xg for 1 hour and 10 minutes at 4°C. Following ultracentrifugation the upper fractions, which included mitochondria were discarded whilst the lower fractions were kept. Melanotic cells produce a dense brown / black pellet at the base of the centrifuge tube whilst amelanotic cells produce a less dense floating white fraction enriched with melanosomes. The quality of the melanosome enriched fraction was assessed by TEM (2.23).

2.23 Transmission Electron Microscopy

In order to observe cells and organelles at a higher magnification than the ordinary light microscope level, cells and organelles were fixed and observed by transmission electron microscopy (TEM). Electron microscopy is a method where electrons are passed either through the sample in non-coated areas or is reflected by the presence of dense metals (labelling nucleic acids, proteins, and lipids). The image created is 2D and in great detail at 100,000 x magnification.

2.23.1Preparation of Melanosomes for TEM

(The following protocol was supplied by Dr. A. Page, Biomedical Imaging Dept. Southampton University). The preparation of the melanosome fraction for TEM involved adding 0.25 volumes of primary fixative comprising of 3% glutaraldehyde and 4% formaldehyde in a 0.1 M PIPES buffer (pH 7.2) (appendix 1.12.3) and incubated at 4°C for at least 1 hour. The fixed melanosome fraction was then centrifuged at 11,000xg for 10 minutes at 4°C (Eppendorf centrifuge 5471R) in order to remove the sucrose / fixative solution. This pellet was then resuspended in a small volume of primary fixative prior to post fixation, dehydration and embedding in resin. The specimens are rinsed twice by the addition of 0.1 M PIPES buffer (at pH 7.2) for 10 minutes at room temperature and centrifuged at 11,000xg for 10 minutes (Eppendorf centrifuge 5471R). The melanosome pellet is post fixed for 1 hour in 1% osmium tetroxide buffered in 0.1 M PIPES (pH 7.2) followed by rinsing twice in 0.1 M PIPES buffer (at pH 7.2) for 10 minutes at room temperature and centrifugation at 11,000xg for 10 minutes (Eppendorf centrifuge 5471R). The melanosome pellet is dehydrated stepwise by washing for 10 minutes each with 30% ethanol, 50% ethanol, 70% ethanol and 95% ethanol. Once the sample is totally dehydrated in absolute ethanol for 20 minutes (repeated twice), the specimen is washed in acetonitrile for 10 minutes and is

subsequently saturated in 50:50 acetonitrile:resin overnight. The melanosome pellet is then set in Spurr resin (appendix 1.12.2) for 6 hours prior to embedding in fresh resin, which is polymerised at 60°C for 20-24 hours. Silver sections are cut using a Leica OMU3 ultramicrotome and mounted on to copper grids, which are subsequently stained with uranyl acetate followed by Reynolds lead stain (appendix 1.12.3). The sections are then viewed using a Philips 201 transmission electron microscope.

2.24 Immunofluorescent Labelling and Confocal Microscopy of Melanosomes

Each centrifugation step was carried out using an Eppendorf centrifuge 5417R. Melanosome enriched fractions were fixed by adding 0.25 volumes of 4% paraformaldehyde and centrifuged at 11,000xg for 5 minutes at 4°C. The melanosome pellets were washed in 100 µl PBS and centrifuged at 11,000xg for 5 minutes at 4°C. The melanosome pellet was resuspended in 100 µl of primary antibody (diluted appropriately in PBS) and incubated for 30 minutes at room temperature. The labelled melanosomes were then centrifuged at 11,000xg for 5 minutes at 4°C and the supernatant containing excess antibody removed, and the pellet washed with PBS, prior to re-centrifugation at 11,000xg for 5 minutes at 4°C. The melanosome pellet was then resuspended in 100 µl of fluorescently labelled secondary antibody and incubated in the dark for a further 30 minutes. The melanosomes were then centrifuged at 11,000xg for 5 minutes at 4°C, washed with PBS and centrifuged at 11,000xg for 5 minutes at 4°C. The fluorescently labelled melanosomes were finally resuspended in 10 µl PBS. 5 µl of the melanosome suspension was placed onto a glass microscope slide with 5 µl of vectashield (mountant) and a coverslip placed on top and sealed on the glass slide with nail varnish. The immunofluorescent labelled melanosomes were observed by fluorescence microscope or by laser scanning confocal fluorescence microscopy (Leica SP2 microscope). The melanosomes were also observed under transmitted light and

phase contrast to observe the melanised granules prior to observing fluorescence emissions in the same focal plane.

Chapter 3

Generation of eGFP Tagged MC1 Receptors

3.1 Introduction

MC1R is expressed at the surface membrane of pigment cells, which allows the receptor to bind hormone agonists such as αMSH and other POMC derived peptides. Evidence for MC1R at the cell surface has been demonstrated in melanoma cells by the use of binding of radio-labelled MC1R specific peptides (Tatro *et al.*, 1990; Varga *et al.*, 1976; Varga *et al.*, 1976b). However, Orlow *et al.*, (1990) performed ligand binding studies, which also showed the presence of internal binding sites for ^{125}I-βMSH within Cloudman S91 mouse melanoma cell fractions. The function of internal MSH binding sites has not been elucidated, however other work carried out by Chakraborty *et al.*, (1991) showed a relationship between the distribution of internal and external ^{125}I-βMSH binding sites following ultraviolet B radiation (UVB) induction of melanogenesis in Cloudman S91 murine melanoma cells. They observed that UVB irradiation caused an increase in the number of external ^{125}I-βMSH binding sites with a concurrent decrease in intracellular sites (Chakraborty *et al.*, 1991). These authors hypothesised that UVB induced the redistribution of βMSH receptors which in turn increased cellular responsiveness to βMSH. This could suggest that MSH receptors are stored within the cell, ready for presentation at the membrane surface in order to enhance responses to MSH. However, where exactly do these internal MC1Rs reside? There are a number of possibilities for the location of internal MC1R, including the ER and trans golgi network, however an intriguing possibility is that they could be in the melanosome.

Proteomic analysis of the melanosome, and the use of mass spectrometry and subcellular fractionation has enabled the identification of 12 melanosome specific

proteins and 56 other proteins in the melanosome that are shared with other organelles (Basrur *et al.*, 2003). As well as important pigmentary proteins and enzymes there are a number of receptors that have been found within this organelle. The receptor for activated C-kinase-1 (RACK-1) is present in the melanosome and is important for the anchorage of protein kinase C-β (PKC-β) to this organelle (Park *et al.*, 2004). Another example is the kinectin transmembrane receptor, which has been shown to associate with the melanosome surface. Its role is to mediate the formation of links between the melanosome and microtubules via the enzyme known as kinesin, relevant for functions in melanosome movement (Vancoillie *et al.*, 2000). The *ocular albinism type 1 (OA1)* gene encodes a GPCR which is expressed by different pigment cells and has been shown to be present within the melanosome (Basrur *et al.*, 2003). Ocular albinism type 1 (OA1) is a human X-linked disorder in which vision is impaired and components of the eye are hypopigmented. Most OA1 patients have mutations in *OA1* rendering them genetically null at this locus. However, proteomic analysis has failed to detect the presence of MC1R within the melanosome (Basrur *et al.*, 2003).

It is of interest that the presence of POMC and some of its hormone derivatives, including αMSH and ACTH, have been demonstrated within the melanosomes of cultured human skin melanocytes (Peters *et al.*, 2000). Also present within this organelle are the enzymes known as prohormone convertase 1 (PC1) and PC2, which are responsible for the processing of POMC into biologically active fragments (Peters *et al.*, 2000). These researchers suggested that αMSH and ACTH peptides may have pigmentary effects within the melanosome that somehow act independently of MC1R (although they did not look for MC1R at this site). However it may also be hypothesised that MC1R could be present close to or at the melanosome in order to

mediate the pigmentary effects of these peptides (based on the evidence for internal MC1R above).

Currently the available antibodies against human MC1R are considered inadequate for the purpose of investigating the intracellular localisation of MC1R. Therefore, in order to investigate whether MC1R is present inside the cell, and in particular at the melanosome, it was decided that the best approach was tagging of human MC1R with enhanced green fluorescent protein (eGFP). The benefit of using this method is that it allows subcellular localisation of MC1R without the requirement for antibodies. However the addition of a 276 amino acid eGFP at the N- or C- terminus of human MC1R (317 amino acid) could compromise or alter the function of the receptor. Previous research employing eGFP tagging of 7-pass transmembrane GPCRs, including MC4R, has generally used a C-terminal tag, which permits ligand binding and subsequent signalling (Barak *et al.,* 1997; Blondet *et al.,* 2004; Ivic *et al.,* 2002; Rached *et al.,* 2003; Tarasova *et al.,* 1997). In this chapter, constructs were made of wild-type MC1R tagged at the N-terminus and the C-terminus with eGFP. These constructs were transfected into mouse melanoma cells, and stable transfectants were derived. The B16G4F mouse melanoma cell line was used because it does not constitutively express Mc1r and therefore provides a useful model system for transfection studies to facilitate the *in vitro* analysis of human MC1R in the absence of endogenous murine Mc1r (Solca *et al.,* 1993). Investigations then focussed on examining whether eGFP tagging of MC1R at the N-terminus and separately at the C-terminus compromises MC1R function in terms of ligand binding and signalling through cAMP. In addition, eGFP C-terminally tagged Asp294His MC1R cell transfectants were generated in order to compare the intracellular localisation of variant and wild-type MC1 receptors in this system.

3.2 Materials and Methods

3.2.1 Expression Vectors

The pEGFP-C1 and pEGFP-N3 (figure 3.1) plasmid vectors (Clontech) were utilized to tag MC1R with enhanced green fluorescent protein (eGFP) at the N- and C-terminus of MC1R respectively. The eGFP is acquired from the jelly fish *Aequorea victoria* (Prasher *et al.*, 1992) and has widely been utilised successfully as a gene expression marker (Chalfie *et al.*, 1994; Inouye and Tsuji, 1994). The pEGFP vectors encode a red-shifted variant (GFPmut1) of wild-type GFP, which has brighter green fluorescence for improved visualization (Cormack *et al.*, 1996). The eGFP is excited at a wavelength of 488nm and emits fluorescence at 507nm and can be visualized using conventional fluorescence microscopy as well as scanning fluorescence confocal microscopy.

Figure 3.1: pEGFP-C1 and pEGFP-N3 Clontech Expression Vectors

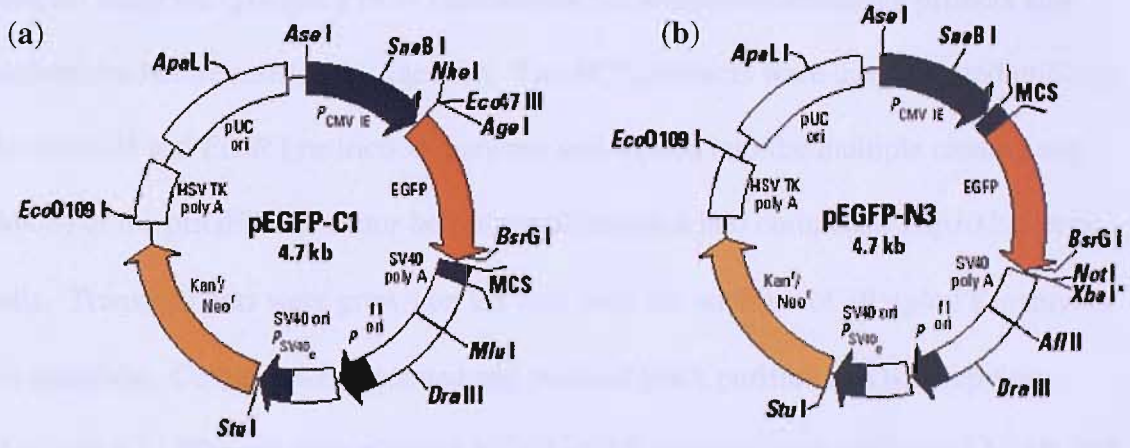

Legend for figure 3.1: (a) The pEGFP-C1 vector and (b) The pEGFP-N3 vector contain a CMV promoter sequence (black arrow), an eGFP gene (red arrow). The C and N in the nomenclature of each vector refers to the end of the gene of interest (insert) that the eGFP is attached. The Kanamycin / Neomycin resistance cassette is shown in orange (arrow). Each vector contains various restriction enzyme sites for directional cloning of gene into the MCS. The VSP I restriction site is positioned before the CMV which was used to linearise the plasmid for stable transfection into mammalian cells.

3.2.2 Generation of Wild-type MC1R Tagged at the C-terminus with eGFP

The coding region of human wild-type *MC1R* was amplified by PCR from previously sequenced pCR3.1 constructs (Schiöth *et al.*, 1999). Denaturation was carried out for 5 minutes at 94°C followed by 35 cycles of denaturation for 1 minute at 94°C, annealing at 55°C for 1 minute and extension at 72°C for 2 minutes. Further extension was carried out at 72°C for 7 minutes during the final cycle. The primers (Table 3.1) were specific for *MC1R* and included *Hind* III and *EcoR* I restriction sites respectively (MC1FW and MC1RVN3) to allow directional cloning into the pEGFP-N3 expression vector (for labelling the MC1 receptor at the C-terminus) and were designed to ensure that *MC1R* remained in frame with the *eGFP*. The reverse 3' MC1RVN3 primer was designed to remove the *MC1R* stop codon in order to allow the full translation of the *MC1R-eGFP* construct. Prior to purification, agarose gel electrophoresis was used to confirm the presence of a single PCR product of correct molecular size. The PCR products were purified using the QIAquick PCR Purification Kit to remove remaining primers and nucleotides before restriction digestion. The PCR products were then digested utilizing the *Hind* III and *EcoR* I restriction enzymes and ligated into the multiple cloning site (MCS) of the pEGFP-N3 vector before transformation into competent *Top10* bacterial cells. Transformants were grown on LB agar with the addition of 10 μg/ml kanamycin for selection. Colonies were isolated and plasmid DNA purified by QIAprep Spin Miniprep Kit. The resulting plasmid *MC1R-eGFP* construct was designated N3MCWT (figure 3.2) for the eGFP C-terminally labeled wild-type human MC1R.

Table 3.1: Primers for Amplification of MC1R with Restriction Sites

Primer Name	Direction	Sequence and restriction site
MC1FW	Forward	5′ *Hind* III 3′ ggcctgaagcttactatggctgtgcaggga
MC1RVN3	Reverse	5′ *EcoR* I 3′ cgcgaattcgctccccaggagcatgtcagcac

Figure 3.2: Diagrammatic Representation of the N3MCWT Construct

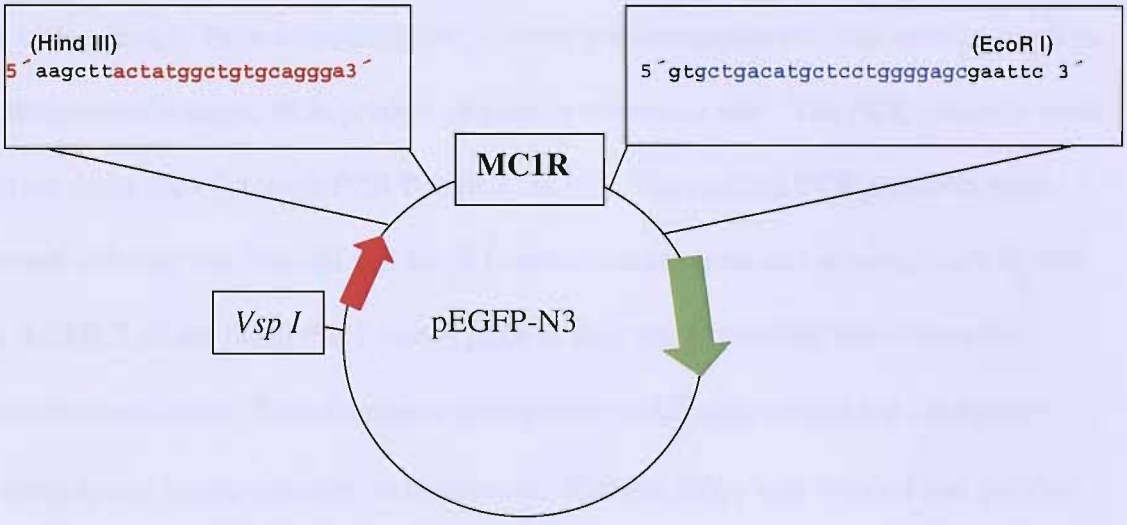

Legend for figure 3.2: The construct N3MCWT, containing wild-type MC1R in the pEGFP-N3 vector. The forward and reverse (antisense) sequences containing the Hind III and EcoR I restriction sites (in black) flanking the wild-type MC1R are highlighted in red and blue respectively. The eGFP sequence (green arrow) positioned at the C-terminus of the MC1R insert and the CMV promoter (red arrow) are shown. The Vsp I enzyme site, which was used to linearise the engineered vector for transfection purposes without disruption of the promoter/ MC1R / eGFP sequences is also highlighted.

3.2.3 Generation of Wild-type MC1R Tagged at the N-terminus with eGFP

The previously sequenced pCR3.1 constructs were used to amplify the coding regions of human wild-type *MC1R* by PCR (Schiöth *et al.,* 1999). The PCR conditions are as described within 3.2.2, however the primers MC1FWC1 and MC1RVC1 (see table 3.2) were designed to include *Hind* III and *EcoR* I restriction sites before and after *MC1R* to allow directional cloning into the pEGFP-C1 expression vector. This ensured that *MC1R* remained in frame with the antecedent *eGFP* for the labelling of MC1R at the N-terminus with eGFP. The reverse 3'MC1RVC1 primer was designed to keep the *MC1R* stop codon intact. Prior to purification, agarose gel electrophoresis was used to confirm the presence of a single PCR product of correct molecular size. The PCR products were purified using the QIAquick PCR Purification Kit. The purified PCR products were digested utilizing the *Hind* III and *EcoR* I restriction enzymes and subsequently ligated into the MCS of the pEGFP-C1 vector prior to their transformation into competent *Top10* bacterial cells. Transformants were grown on LB agar containing 10 µg/ml kanamycin and single colonies were selected. Plasmid DNA was isolated and purified using a QIAprep Spin Miniprep Kit. The resulting plasmid construct containing the wild-type MC1R tagged at the N-terminus with eGFP was designated as C1MCWT (figure 3.3).

Table 3.2: Primers for Amplification of MC1R with Restriction Sites

Primer Name	Direction	Sequence and restriction site
MC1FWC1	Forward	5′ *Hind* III 3′ cgagctcaagcttcgatggctgtgcagggatcc
MC1RVC1	Reverse	5′ *EcoR* I 3′ gcggcgaattctcaccaggagcatgtcagcacc

Figure 3.3: Diagrammatic Representation of the C1MCWT Construct

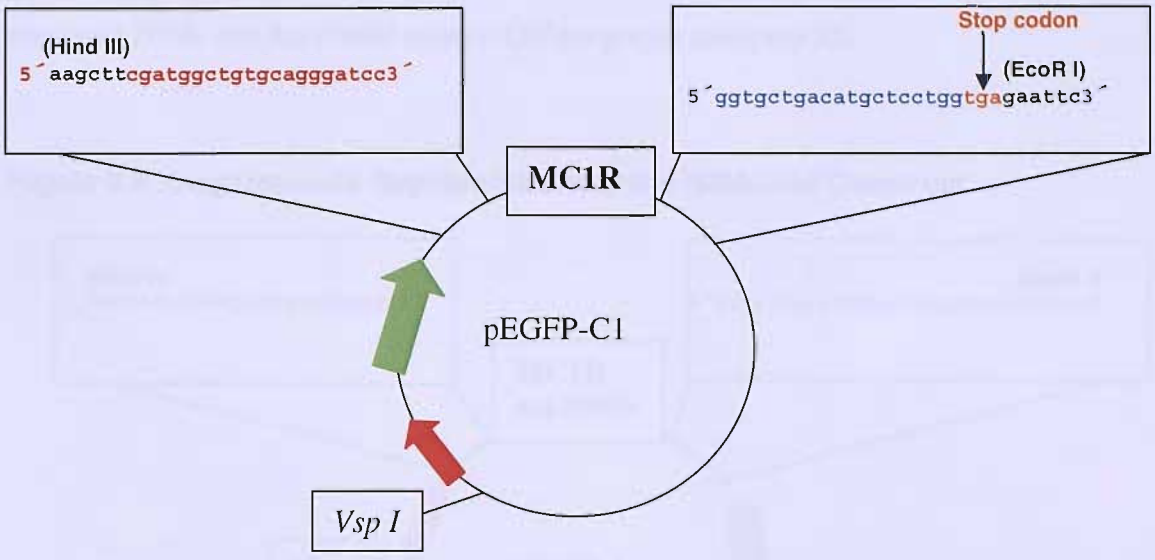

Legend for figure 3.3: The C1MCWT construct containing wild-type MC1R tagged at the N-terminus with eGFP. The forward and reverse (antisense) sequences with Hind II and EcoR I (black), flanking the wild-type MC1R are highlighted in red and blue respectively and the stop codon in orange. The eGFP sequence (green arrow) positioned before the MC1R insert and the CMV promoter (red arrow) are depicted. The Vsp I enzyme site used to linearise the engineered vector for transfection into mammalian cells without disruption of the CMV promoter/ eGFP/ MC1R sequences is also shown.

3.2.4 Generation of Asp294His MC1R Variant Tagged at the C-terminus with eGFP

A construct was generated for the C-terminal tagging of the Asp294His MC1R variant with eGFP. The 1415bp fragment was PCR amplified using the MC1FW and MC1RVN3 primers (see table 3.1) which contained the *Hind* III and *EcoR* I restriction enzyme sites respectively. These restriction enzyme sites permitted the directional cloning of human *Asp294His MC1R* into pEGFP-N3 (method as described above). The reverse 3'MC1RVN3 primer removed the *Asp294His MC1R* stop codon to allow the full translation of the Asp294His MC1R-eGFP chimera named N3MC294 (figure 3.4). The 5.7Kb N3MC294 plasmid construct was verified by agarose gel electrophoresis and was subsequently transformed into competent *Top10* bacterial cells. The transformed bacteria were cultured on LB agar with added 10μg/ml kanamycin for selection

purposes. Single bacterial colonies containing N3MC294 were selected, and plasmid construct DNA was harvested using a QIAprep spin miniprep kit.

Figure 3.4: Diagrammatic Representation of the N3MC294 Construct

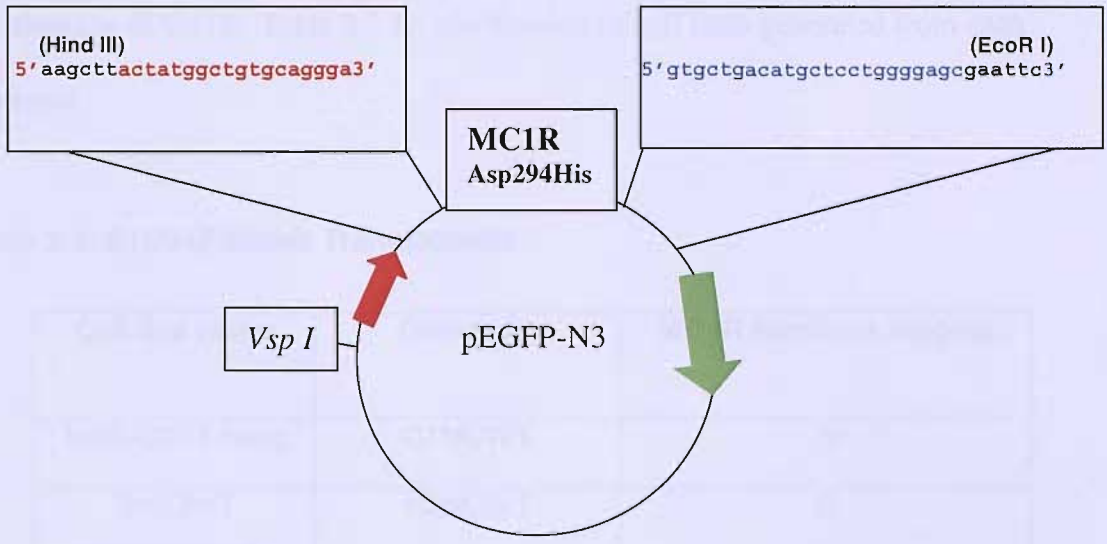

Legend for figure 3.4: The construct N3MC294 contained the Asp294His MC1R variant. The 5 prime and 3 prime (antisense) sequences flanking the wild-type MC1R are highlighted in red and blue respectively contained Hind III and EcoR I restriction enzyme sites (highlighted in black) for ligation into the pEGFP-N3 vector. The eGFP sequence (green arrow) at the C-terminus of the Asp294His MC1R insert, and the CMV promoter (red arrow) positioned before the MCS within the vector are indicated. The Vsp I enzyme site used to linearise the vector for stable transfection into the B16G4F cells is shown.

3.2.5 Stable Transfection of B16G4F Mouse Melanoma Cells

The constructs were sequenced to ensure no deletions, insertions or mutations were present before purification of each plasmid using QIAGEN midipreps. Stable transfection of the B16G4F mouse melanoma cells was carried out by electroporation using the Biorad Gene Pulser II. Cells were transfected separately with the plasmid constructs C1MCWT, N3MCWT, N3MC294, (figures 3.2, 3.3, 3.4 respectively), which had been linearised using the restriction enzyme *Vsp* I (also known as *Ase* I). The single *Vsp* I site allowed linearisation without disruption of *MC1R*, *eGFP*, CMV promoter or

neomycin resistance sequences. As a control, B16G4F cells were separately transfected with the linearised pEGFP-N3 vector alone in order to observe the eGFP fluorescence and localisation without the influence of the MC1 receptor. After 48 hours, G418 was added to the medium and stable transfectants were generated by culturing long term in the presence of G418. Table 3.3 for clarification of cell lines generated from each construct.

Table 3.3: B16G4F Stable Transfectants

Cell line name	Construct	MC1R terminus tagging
B16MCWT-Ntag	C1MCWT	N
B16GWT (generation 1)	N3MCWT	C
B16MCWT-Ctag* (generation 2)	N3MCWT2	C
B16MC294-Ctag	N3MC294	C
B16GFP	pEGFP-N3	No MC1R

* The eGFP C-terminally tagged human wild-type MC1R transfected B16G4F cell lines were regenerated due to the presence of contaminating empty pEGFPN3 vector within the B16GWT cell lines.

3.2.6 Flow Cytometry

Cells were analysed by flow cytometry in order to quantify green fluorescence intensity of the B16G4F transfectants. This was done as per methods 2.13.

3.2.7 Fluorescence Microscopy

Fluorescence microscopy was performed on the B16G4F transfectants using a Leica fluorescence microscope. See methods 2.12 for further description.

3.2.8 Ligand Binding

Competition ligand binding assays were performed as described within methods 2.14, for the purpose of investigating the presence of surface membrane MC1 receptors on the B16G4F transfectants.

3.2.9 cAMP Analysis of Transfectants

Intracellular cAMP levels were quantified by use of a cAMP immunoassay kit (R&D systems) as per manufacture's instructions (see methods 2.15).

3.2.10 Confocal Microscopy of Transfectants

Confocal microscopy was used to characterise the B16G4F transfectants for observing intracellular patterns of MC1R-eGFP at a higher power of magnification. The SP2 laser scanning confocal fluorescence microscope permitted the scanning of 3D images and the analysis of z planes through these 3D images (see methods 2.10 and 2.12 for details).

3.3 Results

3.3.1 Generation of Stably Transfected B16G4F Melanoma Cell Lines Containing Human Wild-type MC1R Tagged at the C-terminus with eGFP

The B16G4F mouse melanoma cells were stably transfected with the N3MCWT plasmid construct, which contained human wild-type MC1R tagged at the C-terminus with eGFP (figure 3.2). Cell lines were obtained by dilution of the cells to 0.3 cells per well within a 96 well culture plate. After 48 hours successful stably transfected clones were expanded with G418 selection. Forty one cell lines were generated and identified as B16GWT, the individual clones were numbered from 1 - 41.

3.3.2 Characterisation of B16GWT Cell Lines by Flow Cytometry and Fluorescence Microscopy

All B16GWT cell lines were analysed by flow cytometry in order to observe and characterise the cell lines that emitted the brightest green fluorescence. The B16G4F untransfected cell line was used as an eGFP negative control, due to minimal green autofluorescence. Of the 41 B16GWT transfectants analysed the mean fluorescence intensity (MFI) of green fluorescence varied between $10^{0.1}$ and 10^{2} (figure 3.5) and the combined median MFI of green fluorescence was 10^{1} (see figure 3.5). The B16G4F non transfected control cells exhibited MFIs between $10^{0.1}$ and $10^{0.25}$, and 11 of the B16GWT clones exhibited similar levels of autofluorescence which implied that these clones were not efficiently transfected with the MC1R-eGFP construct. However, 30 of the B16GWT cell lines exhibited green fluorescence, which was above the cut off MFI of $10^{0.5}$ (this MFI was chosen as an appropriate threshold for indication of green fluorescence due to the presence of eGFP).

Figure 3.5: Analysis of the Median Fluorescence Intensity of Green Fluorescence Exhibited by the B16GWT Transfectants Examined by Flow Cytometry

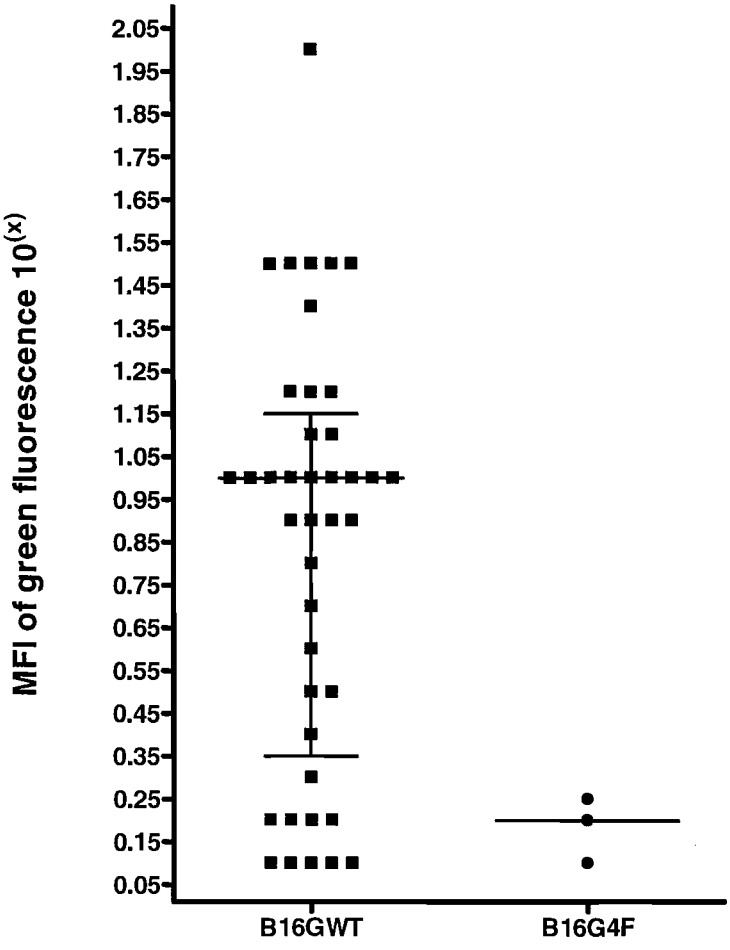

Legend for figure 3.5: A scatter plot to show the distribution of peak values representing the MFI of each cell line emitting green fluorescence by eGFP. The median and interquartile range of all MFI values is displayed.

In a sample of 11 B16GWT cell lines originally observed by fluorescence microscopy, the percentage of cells emitting eGFP fluorescence was scored by eye. At least 10 fields of cells were observed for each transfectant. Importantly, there were varying levels of green fluorescence emitted between cell lines. Moreover, any one cell line demonstrated further variation in eGFP fluorescence between single cells. The group of 11 B16GWT transfectants exhibited a high level of green fluorescence (scored as +++) within approximately 5-20% of the cells. Approximately 60-85% of cells emitted a low to medium green fluorescence, scored as + and ++ respectively, and some remaining cells were noted to have no fluorescence. Under a fluorescence microscope the MC1R-

eGFP fusion protein was seen as a pattern of punctate dots that were distributed throughout the cytoplasm, which appeared to be excluded from the nucleus. The green fluorescence was also accentuated at the plasma membrane in some cells. When compared with the flow cytometry data, the microscopy observations appeared to be more useful as a screening tool for the presence of MC1R-eGFP and allowed for a more detailed characterisation of the transfectants (figure 3.6). Therefore for all future experiments microscopy was used in preference to flow cytometry to examine for the presence of green fluorescence, and for selection of cell lines for further characterisation (on the basis of at least 5% of the cells emitting +++ green fluorescence and above). This decision was also influenced by the fact that visualisation of brightly fluorescent cells under fluorescence microscopy was likely to be a pre-requisite for investigation of co-localisation of MC1R at the melanosome using confocal microscopy.

At the same time as screening for green fluorescence of the B16GWT cell lines, screening of the B16GWT transfectants by PCR confirmed the presence of MC1R. However, gel electrophoresis also demonstrated the presence of empty pEGFP-N3 vector contamination within some of the B16GWT cell lines. It was therefore necessary to regenerate the eGFP C-terminally tagged human wild-type MC1R transfectants, in order to ensure that cell lines containing the MC1R-eGFP construct alone were available for the future investigations.

Figure 3.6: A Comparison of FACs Analysis with Fluorescence Microscopy

(a) B16GWT36

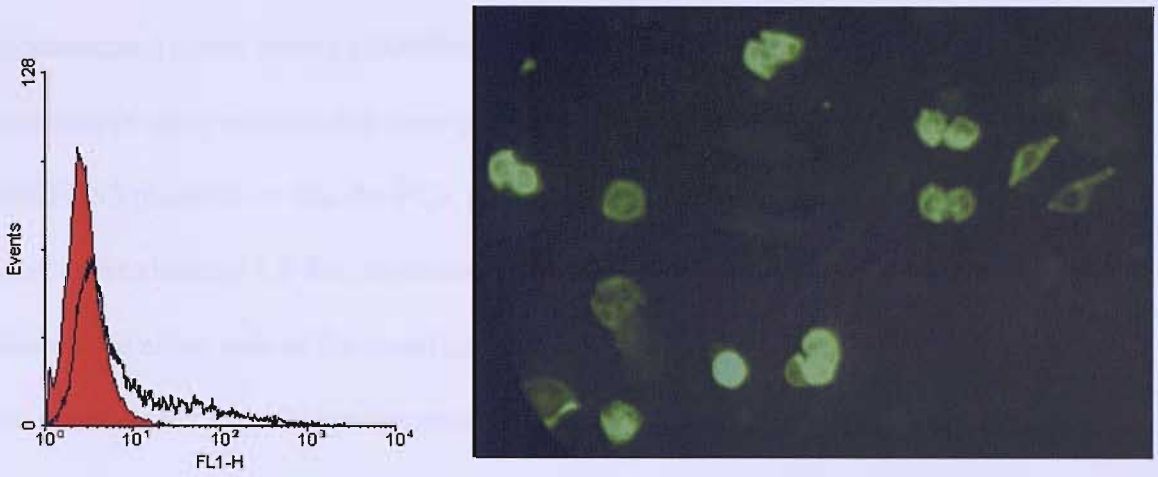

(b) B16GWT47

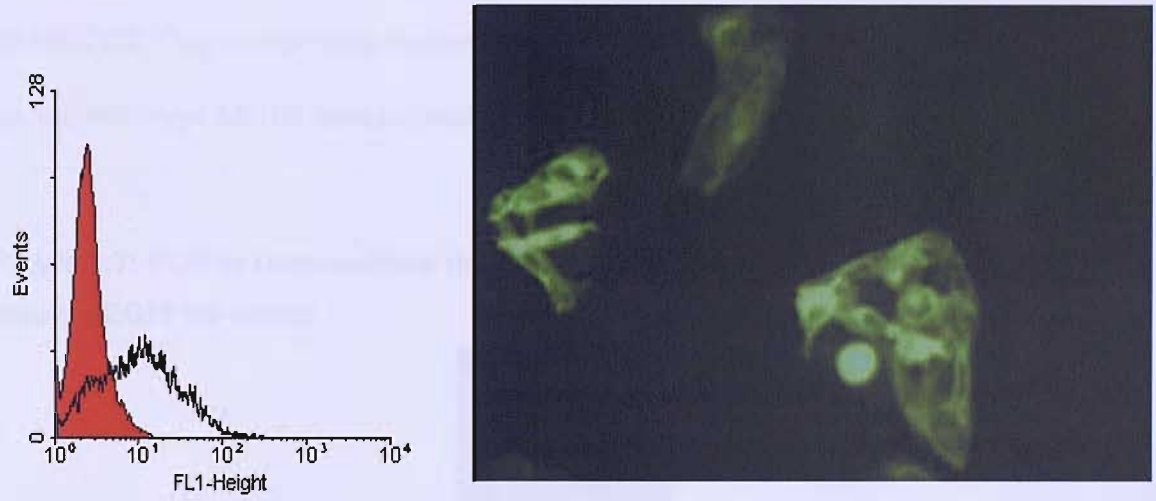

Legend for figure 3.6: The flow cytometry histograms shown in (a) and (b) demonstrated the distribution of 10,000 events (B16G4F cells) along the Y axis and emission eGFP green fluorescence along the X axis. The red peaks indicate the untransfected B16G4F cells and the open peaks shifted to the right along the X axis demonstrate the increasing green fluorescence emitted, however the histograms were less informative when compared with observing the MC1R-eGFP transfected cell lines using a fluorescence microscope. Representative cell lines include (a) B16GWT36 and (b) B16GWT47 demonstrating variation in eGFP green fluorescence by flow cytometry and fluorescence microscopy.

3.3.3 Regeneration of B16G4F Melanoma Cell Lines Stably Transfected with Human Wild-type MC1R Tagged at the C-terminus with eGFP

The B16G4F cells were re-transfected with a new N3MCWT construct which was not contaminated by the empty pEGFP-N3 vector. This was proven by carrying out a PCR experiment using primers that were positioned outside of the insert (within the pEGFPN3 plasmid) so that the PCR product would demonstrate the presence of a single band approximately 1.6 Kb (representing the full length of the insert plus sections of the plasmid on either side of the insert), or two bands of approximately 1 Kb (representing the insert alone) and 600 bps (representing a length of the multiple cloning site within the plasmid void of the insert) (figure 3.7). Twenty eight new stably transfected cell lines were expanded from a 96 well culture plate. These cell lines were designated as B16MCWT-Ctag to represent the second generation of eGFP C-terminally tagged human wild-type MC1R transfectants and were numbered individually from 1 - 28.

Figure 3.7: PCR to Demonstrate that the N3MCWT2 Construct did not contain empty pEGFPN3 vector

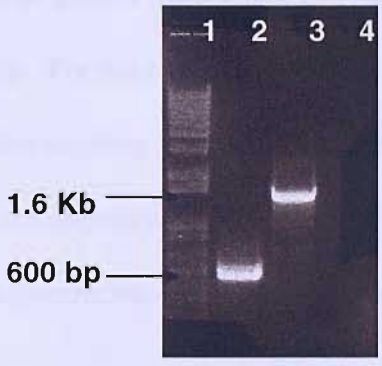

Legend for figure 3.7: A PCR gel image to show: Lane 1: 1 Kb DNA Plus Ladder (Unvitrogen, UK), Lane 2: The 600 bp PCR product from the empty pEGFPN3 plasmid, Lane 3: The 1.6 Kb PCR product from the regenerated N3MCWT2 construct, Lane 4: Negative control. The primers were positioned within the pEGFPN3 plasmid flanking the 1 Kb wild-type MC1R insert. This proved that there was no contaminating empty pEGFPN3 vector within the purified construct preparation.

3.3.4 Generation of Stably Transfected B16G4F Melanoma Cell Lines with Human Wild-type MC1R Tagged at the N-terminus with eGFP

The B16G4F mouse melanoma cells were separately stably transfected with the C1MCWT plasmid construct, which contained human wild-type MC1R with an eGFP tag at the N-terminus (figure 3.2). Individual clones were reared from a 96 well culture plate and were expanded with G418 selection. Fifty seven individual cell lines were generated from single colonies, these B16G4F transfectants were identified by the name B16MCWT-Ntag, and individual cell lines were numbered from 1 - 57.

3.3.5 Characterisation of B16MCWT-Ctag and B16MCWT-Ntag Cell Lines by Fluorescence Microscopy and PCR

The B16MCWT-Ctag cell lines were initially characterised by fluorescence microscopy (based on the previous decision that this was the most suitable method of screening). All 28 B16MCWT-Ctag cell lines were observed at 40 x magnification looking at 10 fields of view per line and this was carried out on two separate occasions (Table 3.4). Fluorescence intensity was graded from + to ++++, indicating low to high green fluorescence respectively. For the purpose of further investigations, it was deemed that ≥ 5% of cells in a cell line emitting green fluorescence with an intensity of +++ and above was acceptable. An overview of the B16MCWT-Ctag cells included 1 - 20% of all cells emitted a green fluorescence of +++ and ++++, whilst the remainder exhibited less than ++.

Fluorescence microscopy was performed on all 57 B16MCWT-Ntag cell lines, which contained the eGFP tag at the N-terminus of human wild-type MC1R. Ten fields of view were examined at 40 x magnification for each cell line on one occasion. Approximately 1-10% of the B16MCWT-Ntag cell lines emitted a medium level of

green fluorescence (scored as ++) and the remaining 80-90% of cells emitted a low level of green fluorescence (scored as +), with a small proportion of cells showing negligible green fluorescence. The presence of the *MC1R* gene insert in the B16MCWT-Ntag lines was subsequently confirmed by PCR amplification utilising MC1FWC1 and MC1RVC1 primers that were specific to the pEGFP-C1 vector flanking the MC1R insert, this demonstrated a single 1475bp PCR product consistent with the presence of MC1R in those transfectants. These results suggested that despite the presence of MC1R-eGFP in these lines the B16MCWT-Ntag cells did not emit a sufficient intensity of green fluorescence for further investigations into the intracellular localisation of MC1R within these lines.

Table 3.4: B16MCWT-Ctag Cell Lines

Clone No.	Microscopy 1	Microscopy 2	Suitability for studies YES / NO
1	5% +++, 80% ++, 15% NF	5% ++++, 80% ++, 15% NF	YES
2	90% +, 10% NF	98% +, 2% NF	NO
3	5% ++, 80% +, 15% NF	10% ++++, 80% ++, 10% NF	YES
4	2% ++, 90% +, 8% NF	2% ++++, 85% ++, 13% NF	YES
5	90% +, 10% NF	2% ++, 90% +, 8% NF	NO
6	1% ++, 90% +, 9% NF	1% +++, 85% +, 14% NF	NO
7	1% +++, 90% +, 9% NF	2% ++++, 85% +, 13% NF	YES
8	**7% +++, 80% ++, 13% NF**	**5% +++, 85% ++, 10% NF**	**YES**
9	90% +, 10% NF	2% ++, 90% +, 8% NF	NO
10	1% ++, 90% +, 9% NF	1-2% ++, 90% +, 8% NF	NO
11	2% ++++, 85% +, 13% NF	15% +++, 80% ++, 5% NF	YES
12	5% ++, 90% +, 5% NF	98% +, 2% NF	NO
13	1% +++, 85% +, 14% NF	1% ++, 90% +, 9% NF	NO
14	90% +, 10% NF	80% +, 20% NF	NO
15	10% ++, 80% +, 10% NF	1% ++, 90% +, 9% NF	NO
16	90% +, 10% NF	2% +++, 90% +, 8% NF	NO
17	90% +, 10% NF	2% +++, 90% +, 8% NF	NO
18	90% +, 10% NF	95% +, 5% NF	NO
19	5% ++, 80% +, 15% NF	5% +++, 80% ++, 15% NF	YES
20	10% ++, 60% +, 30% NF	10-20% +++, 70% ++, 10% NF	YES
21	95% +, 5% NF	90% +, 10% NF	NO
22	2% ++, 90% +, 8% NF	90% +, 10% NF	NO
23	90% +, 10% NF	1% +++, 95% +, 4% NF	NO
24	**20% +++, 70% ++, 10% NF**	**20% ++++, 75% ++, 5% NF**	**YES**
25	2% ++, 90% +, 8% NF	10% +++, 80% +, 10% NF	YES
26	2% ++, 90% +, 8% NF	2% +++, 80% +, 18% NF	NO

27	**5% +++, 80% ++, 15% NF**	**5% +++, 80% +, 15% NF**	**YES**
28	1% ++, 90% +, 9% NF	2% ++, 95% +, 3% NF	NO

Cell lines highlighted in bold were used in ligand binding and cAMP experiments. NF refers to negligible fluorescence.

Table 3.5: B16MCWT-Ntag Cell Lines

Clone No.	Microscopy 1	Suitability for studies YES / NO
1	5% ++, 80% +, 15% NF	NO
2	5% ++, 80% +, 15% NF	NO
3	80% +, 20% NF	NO
4	5% ++, 80% +, 15% NF	NO
5	5% ++, 80% +, 15% NF	NO
6	5% ++, 80% +, 15% NF	NO
7	5% ++, 80% +, 15% NF	NO
8	5% ++, 80% +, 15% NF	NO
9	5% ++, 80% +, 15% NF	NO
10	5% ++, 80% +, 15% NF	NO
11	80% +, 20% NF	NO
12	5% ++, 80% +, 15% NF	NO
13	5% ++, 80% +, 15% NF	NO
14	80% +, 20% NF	NO
15	5% ++, 80% +, 15% NF	NO
16	5% ++, 80% +, 15% NF	NO
17	80% +, 20% NF	NO
18	5% ++, 80% +, 15% NF	NO
19	5% ++, 80% +, 15% NF	NO
20	5% ++, 80% +, 15% NF	NO
21	5% ++, 80% +, 15% NF	NO

22	5% ++, 80% +, 15% NF	NO
23	80% +, 20% NF	NO
24	5% ++, 80% +, 15% NF	NO
25	5% ++, 80% +, 15% NF	NO
26	5% ++, 80% +, 15% NF	NO
27	80% +, 20% NF	NO
28	80% +, 20% NF	NO
29	5% ++, 80% +, 15% NF	NO
30	80% +, 20% NF	NO
31	5% ++, 80% +, 15% NF	NO
32	5% ++, 80% +, 15% NF	NO
33	90% +, 10% NF	NO
34	1% +++, 85% +	NO
35	80% +, 20% NF	NO
36	5% ++, 80% +, 15% NF	NO
37	5% ++, 80% +, 15% NF	NO
38	5% ++, 80% +, 15% NF	NO
39	5% ++, 80% +, 15% NF	NO
40	5% ++, 80% +, 15% NF	NO
41	80% ++, 20% NF	NO
42	10% ++, 80% +, 10% NF	NO
43	2% ++, 90% +, 8% NF	NO
44	10% ++, 80% +, 10% NF	NO
45	5%++, 80% +, 15% NF	NO
46	5%++, 80% +, 15% NF	NO
47	95% +, 5% NF	NO
48	5% ++, 80% +, 15% NF	NO
49	5% ++, 80% +, 15% NF	NO
50	5% ++, 80% +, 15% NF	NO
51	80% +, 20% NF	NO

52	5% ++, 80% +, 15% NF	NO
53	5% ++, 80% +, 15% NF	NO
54	80% +, 20% NF	NO
55	1% ++, 90% +, 9% NF	NO
56	5% ++, 80% +, 15% NF	NO

NF refers to negligible fluorescence.

3.3.6 Derivation of Single Cell Clones from the B16MCWT-Ctag Cell Lines

The B16MCWT-Ctag transfectants, which had been previously characterised by fluorescence microscopy exhibited varying levels of eGFP fluorescence. The variation in MC1R-eGFP expression in the transfectants may have occurred due to: differences in eGFP expression throughout the cell cycle, differences in degradation of MC1R-eGFP (perhaps also related to the cell cycle), or the presence of more than one clone per cell line. In order to further investigate whether the cell lines might contain multiple clones, single cells from B16MCWT-Ctag-8 and B16MCWT-Ctag-24 were grown in 96 well culture plates and expanded. In order to ensure the presence of a single cells in 30% of the wells, the transfected cell lines were diluted in DMEM (complete media) to a concentration of 0.3 cells per well. The single cell clones were expanded with G418 selection, and 10 clones were examined by fluorescence microscopy from each of the lines. Each clone was observed at 40 x magnification and at least twice examining 10 fields of view. All 20 single cell clones exhibited levels of eGFP green fluorescence similar to that of their parental lines B16MCWT-Ctag-8 and B16MCWT-Ctag-24 respectively (as shown in figure 3.8). The B16MCWT-Ctag-8 parental cell line and single cell clones all incorporated three main populations of cells: 1) approximately 5-10% of cells with +++ high intensity green fluorescence, 2) approximately 85% with ++ low / medium intensity green fluorescence, 3) and approximately 10-15% exhibited

negligible fluorescence. In each clone the brighter green fluorescent cells had a punctate pattern of green fluorescence distributed throughout the cytoplasm which was excluded from the nucleus. The B16MCWT-Ctag-24 parental cell line and single cell clones also demonstrated three main populations of cells: 1) approximately 20% of cells emitting ++++ strong green fluorescence, 2) 75% with ++ medium fluorescence, 3) and 5% with negligible fluorescence. Again, the punctate pattern of green fluorescence in these clones was similar to that observed in all of the previously examined cell lines.

Figure 3.8: Single Cell Clones

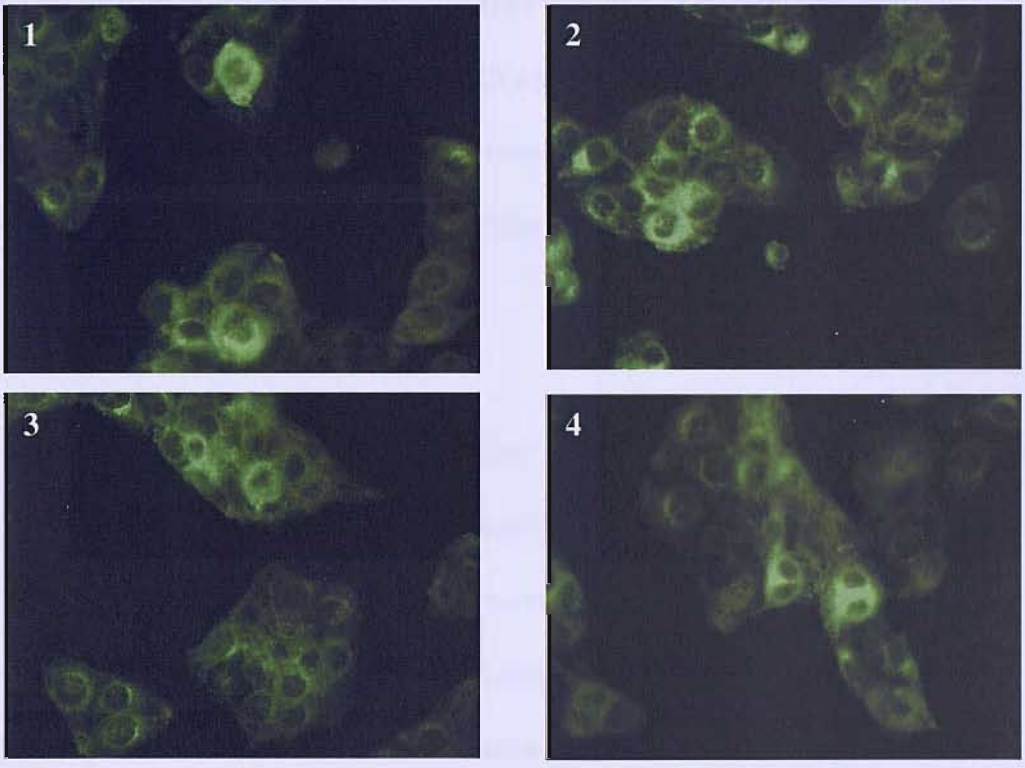

Legend for Figure 3.8: (1) B16MCWT-Ctag-24 parental cell line, and three separate single cell clones (2 – 4) derived from this cell line. Note that the single cell clones emitted similar eGFP green fluorescence as the parental cell line.

3.3.7 Generation of Stably Transfected B16G4F Melanoma Cell Lines with Human Asp294His MC1R Variant Receptor Tagged at the C-Terminus with eGFP

In order to carry out a comparative study, a human Asp294His MC1R variant was tagged at the C-terminus with eGFP. This variant has been associated with the red hair / fair skin phenotype and an increased risk of skin cancer in humans (Box *et al.*, 1997). The Asp294His polymorphism occurs within the intracellular portion of the seventh transmembrane domain of the receptor which somehow prevents the receptor from signalling via cAMP despite retaining αMSH binding properties (Schiöth *et al.*, 1999). It is possible that this non-functional MC1 receptor variant could have a different subcellular distribution to that of the wild-type receptor. The B16G4F mouse melanoma cells were stably transfected with a plasmid which contained the human Asp294His MC1R variant tagged at the C-terminus with eGFP (figure 3.4). Twenty seven individual cell lines were generated, labelled as B16MC294-Ctag with individual clones numbered from 1 - 27.

3.3.8 Characterisation of the B16MC294-Ctag Cell Lines by Fluorescence Microscopy

The B16MC294-Ctag cell lines were characterised once by observing at least 10 fields of view at 40 x magnification using a fluorescence microscope. Cell were scored as before, noting the percentages of cells exhibiting low to high green fluorescence intensity (represented as + to ++++). Nineteen of 27 cell lines emitted a fluorescence of +++ and ++++ in at least 25% of cells (Table 3.6).

Table 3.6: B16MC294-Ctag Cell Lines

Clone No.	Microscopy 1	Suitability for studies YES / NO
1	1% +++, 90% +, 9% NF	NO
2	**20% +++, 60% ++, 20% NF**	**YES**
3	15% +++, 60% ++, 25% NF	YES
4	5% +++, 80% +, 15% NF	YES
5	10% +++, 80% +, 10% NF	YES
6	20% +++, 60% ++, 20% NF	YES
7	5% +++, 80% +, 15% NF	YES
8	5% +++, 80% +, 15% NF	YES
9	5% ++, 80% +, 15% NF	NO
10	1% +++, 90% +, 9% NF	NO
11	**5% +++, 80% + 15% NF**	**YES**
12	2% +++, 85% +, 13% NF	NO
13	2% +++, 85% +, 13% NF	NO
14	20% ++++, 70% +++, 10% +	YES
15	**25% +++, 60% ++, 15% NF**	**YES**
16	10% +++, 85% +, 5% NF	YES
17	5% +++, 80% +, 15% NF	YES
18	1% +++, 90% +, 9% NF	NO
19	5% +++, 80% +, 15% NF	YES
20	90% +, 10% NF	NO
21	2% ++, 80% +, 18% NF	NO
22	2% ++, 80% +, 18% NF	NO
23	2%+++, 80% +, 18% NF	NO
24	1% +, 90% +, 9% NF	NO
25	90% +, 10% NF	NO
26	90% +, 10% NF	NO
27	1% +++, 90% +, 9% NF	NO

Cell lines highlighted in bold were used in ligand binding and cAMP experiments. NF refers to negligible fluorescence.

3.3.9 Ligand Binding Analysis of the B16MCWT-Ctag and B16MCWT-Ntag Cell Lines

In order to investigate whether the MC1R-eGFP fusion protein could bind ligand at the membrane surface, three B16MCWT-Ctag cell lines including B16MCWT-Ctag-8, B16MCWT-Ctag-24, and B16MCWT-Ctag-27 were analysed by ^{125}I NDP-MSH radio-

ligand binding assay (carried out on 2 separate occasions). All three transfectants showed significant radioligand binding compared to that of the B16G4F untransfected parental cell line, which did not express any receptor binding sites (figure 3.9 a). The binding affinity of ^{125}I NDP-MSH to MC1R appeared to be similar in all three transfectants (figure 3.9 b). By contrast when wild-type MC1R was tagged at the N-terminus with eGFP, the ligand binding capacity appeared to be obstructed in 11 of the B16MCWT-Ntag cell lines. None of the cell lines tested showed ligand binding. Taken in conjunction with the fluorescence data, this result raised questions about the usefulness of the B16MCWT-Ntag lines (see discussion for further studies).

3.3.10 Ligand Binding Analysis of the B16MC294-Ctag Cell Lines

The B16MC294-Ctag cell lines, transfected with a C-terminally tagged human Asp294His variant MC1R-eGFP fusion protein exhibited green fluorescence when observed by fluorescence microscopy. The Asp294His *MC1R* gene was amplified by PCR and DNA sequencing confirmed the correct variant Asp294His MC1R sequence. In order to investigate the presence of the Asp294His variant MC1R-eGFP at the membrane surface, three representative B16MC294-Ctag cell lines were analysed by radio-ligand binding. The three cell lines named B16MC294-Ctag-2, B16MC294-Ctag-11, and B16MC294-Ctag-15 each demonstrated the cell surface expression of Asp294His variant MC1R-eGFP, by retaining their ability to bind ^{125}I NDP-MSH on two separate occasions. All three transfectants showed significant radio-ligand binding compared to that of the B16G4F untransfected parental cell line, which had no ligand binding capacity (figure 3.10 a). The binding affinity of MC1R to the ^{125}I NDP-MSH radio-ligand was similar in all three transfectants investigated (figure 3.10 b) which was comparable to that of the wild-type receptor demonstrated in figures 3.9 (a) and (b).

Figure 3.9: ^{125}I NDP-MSH Radioligand Binding Analysis of the B16MCWT-Ctag Transfectants

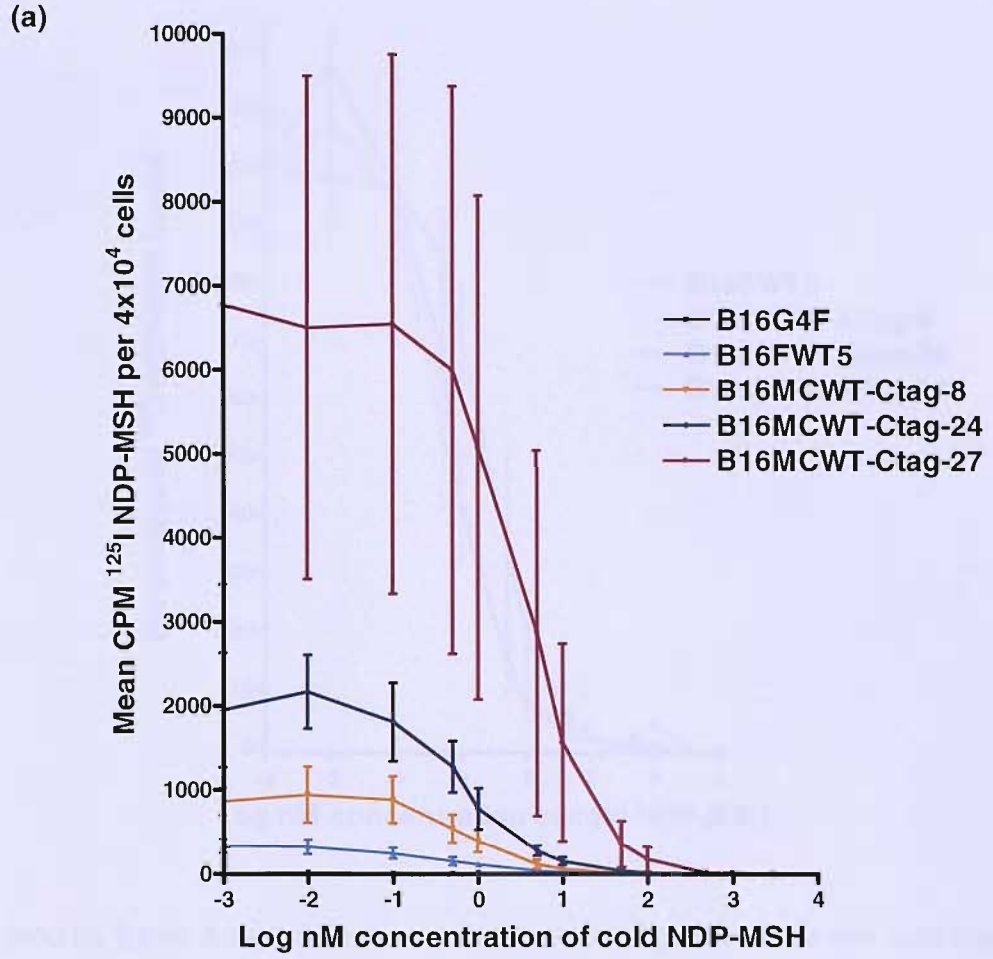

Legend for figure 3.9 (a): Competitive radioligand binding data was obtained using a fixed concentration of ^{125}I NDP-MSH and varying concentrations of cold NDP-MSH. This graph demonstrates ligand binding curves of three B16MCWT-Ctag transfectants (containing human wild-type MC1R-eGFP), a B16FWT5 transfectant (containing human wild-type MC1R tagged with a FLAG epitope) know to bind ligand, and the untransfected B16G4F parental melanoma cells (negative control). The data represents the mean and standard deviation of two separate experiments.

(b)

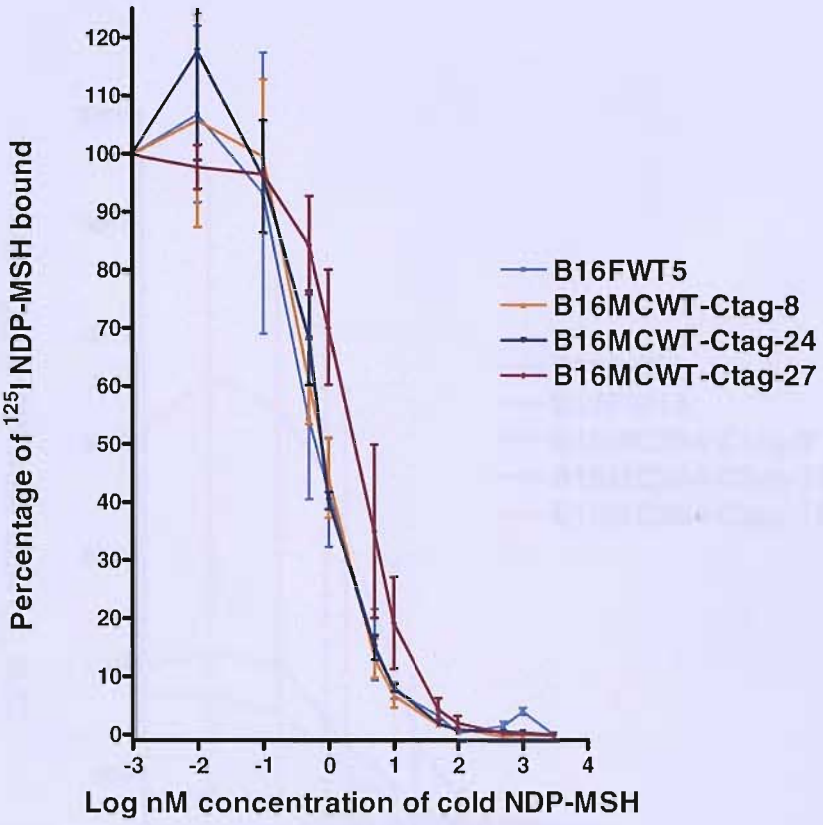

Legend for figure 3.9 (b): The data presented in this graph have been normalised to show the percentage of ^{125}I NDP-αMSH binding at varying concentrations of cold NDP-αMSH in the same three B16MCWT-Ctag transfectants and the positive control B16FWT5 cells (normalised to binding at 10^{-12} M cold NDP-αMSH). The data represents the mean and standard deviation of 2 separate experiments.

Figure 3.10: ^{125}I NDP-MSH Radioligand Binding Analysis of the B16MC294-Ctag Transfectants

(a)

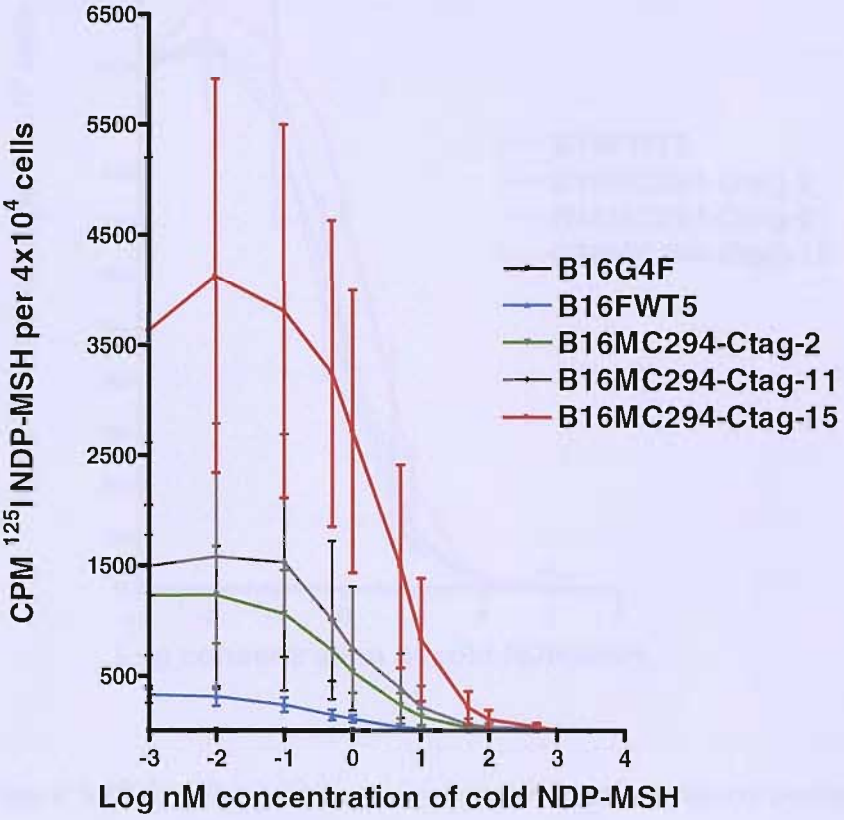

Legend for figure 3.10 (a): Radio-ligand binding data for the Asp294His variant MC1R-eGFP transfected B16MC294-Ctag cell lines, and the positive control B16FWT5 cells (containing human wild-type MC1R-FLAG), by using a fixed concentration of ^{125}I NDP-MSH and varying concentrations of cold NDP-MSH. The B16G4F untransfected parental cell line did not have receptor binding sites. The data represents the mean and standard deviation of 2 separate experiments.

(b)

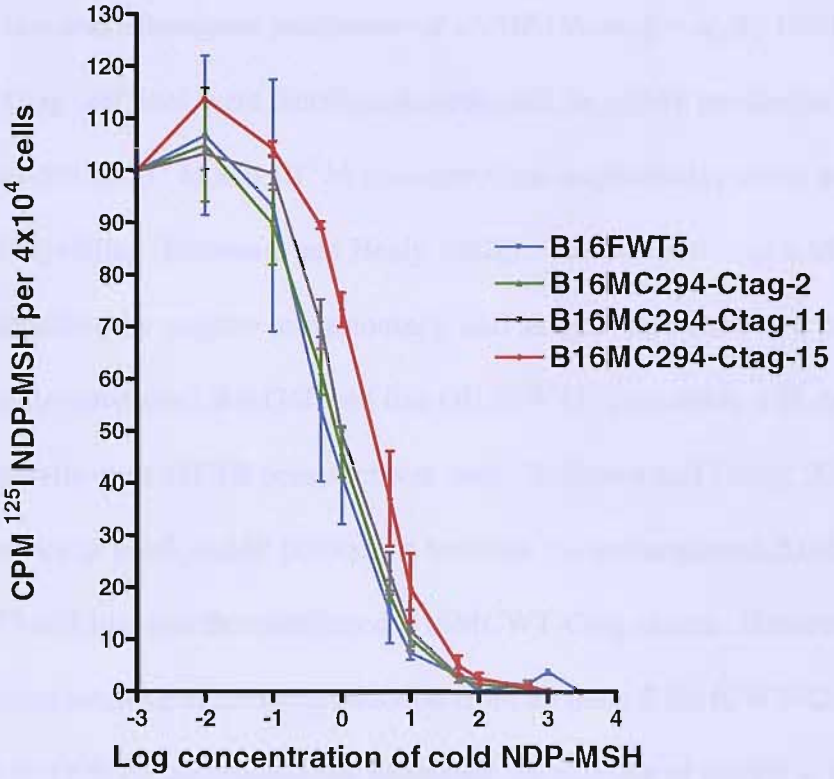

Legend for figure 3.10 (b): The graph demonstrates normalised ligand binding data showing the percentage of ^{125}I NDP-αMSH binding at varying concentrations of cold αMSH in three B16MC294-Ctag transfectants containing human Asp294His MC1R variant tagged at the C-terminus with eGFP, and the positive control B16FWT5 cells. The B16G4F untransfected parental cell line did not have receptor binding sites. The data represents the mean and standard deviation from 2 separate experiments.

3.3.11 Signalling via cAMP in the B16MCWT-Ctag Transfectants

The binding of αMSH to MC1R causes intracellular signalling via the activation of adenylyl cyclase and subsequent production of cAMP (Mountjoy *et al.*, 1992). The B16MCWT-Ctag cell lines were therefore investigated for cAMP production in response to αMSH at 10^{-8} M and 10^{-6} M concentrations respectively, which are known to cause MC1R signalling (Robinson and Healy, 2002). The production of cAMP by these cells was determined by enzyme immunoassay, and as a positive control, a previously-generated stably transfected B16G4F cell line (B16FWT5) containing a FLAG epitope tagged human wild-type MC1R construct was used (Robinson and Healy, 2002). There was no difference in basal cAMP production between the untransfected B16G4F cells, the B16FWT5 cell line and the transfected B16MCWT-Ctag clones. However, there was a significant increase in cAMP production from all three B16MCWT-Ctag cell lines and the B16FWT5 control cell line following the addition of αMSH at 10^{-8}M and 10^{-6}M respectively (figure 3.11 a). In order to ensure that the untransfected B16G4F cells could signal via cAMP, and that the reason for the absence of a response to αMSH by these cells was due to the lack of MC1R, the B16G4F cells were also examined for cAMP signalling in the presence of 10^{-3} M IBMX. An increase in cAMP signalling was observed following addition of IBMX, although it did not reach the same levels as that following addition of αMSH in the other cell lines. The data in figure 3.11 (a) was also plotted following correction for the receptor numbers per cell based on the absolute counts per minute obtained at 10^{-12} M cold NDP-αMSH in the ligand binding experiments (figure 3.11 b). Figure 3.11 (b) demonstrates that the B16MCWT-Ctag cell transfectants produced approximately one third of the cAMP, which was produced in the B16FWT5 cells. The difference being the addition of a small FLAG peptide at the N-terminus (B16FWT) opposed to the large eGFP molecule at the C-terminus (B16MCWT-Ctag) of wild-type MC1R respectively.

Figure 3.11: cAMP Analysis of the B16MCWT-Ctag Transfectants

(a)

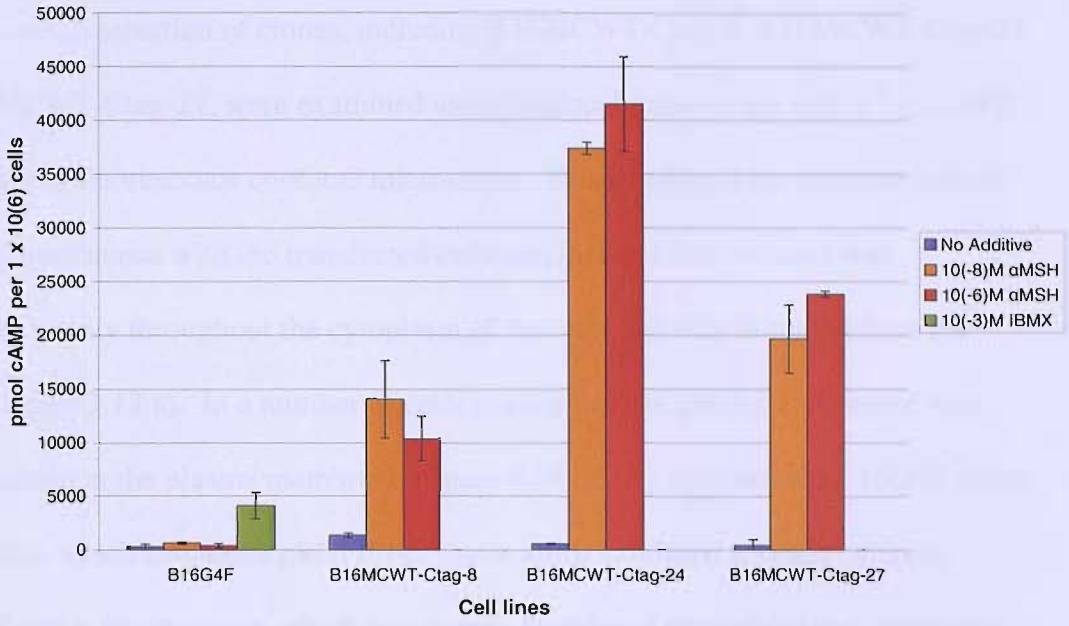

(b)

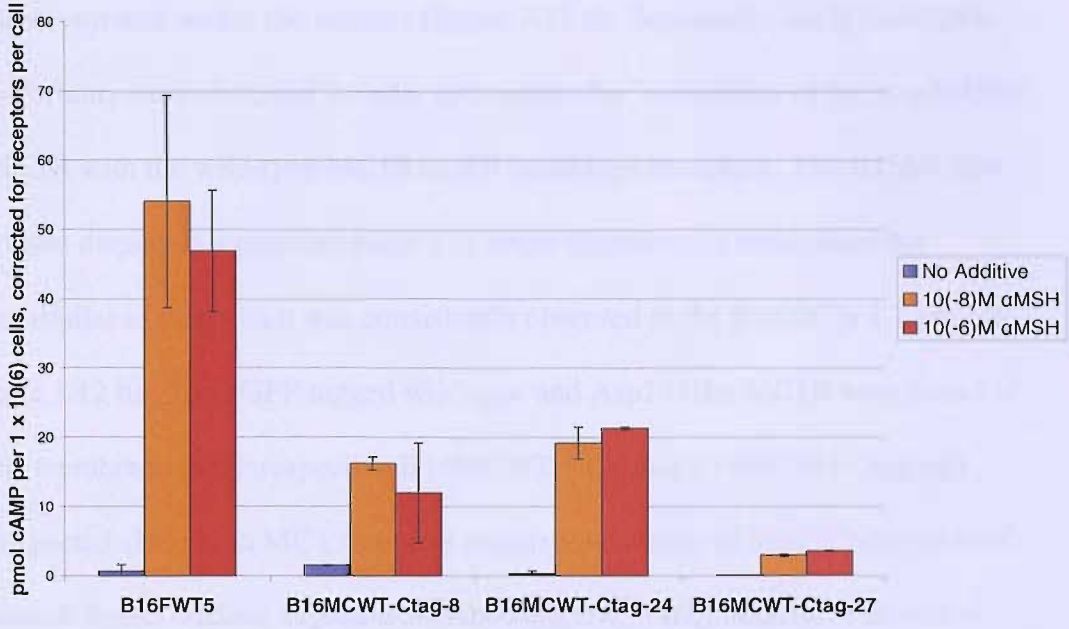

Legend for figure 3.11: (a) The intracellular level of cAMP in the untransfected B16G4F cells, and the B16MCWT-Ctag transfectants are shown. (b) The cAMP response of the B16G4F, B16FWT5 (flag tagged human wild-type MC1R) positive control cells, and the B16MCWT-Ctag transfectants following correction for number of MC1 receptors based on the ligand binding results at 10^{-12} M cold NDP-αMSH. The data represents the mean and SD from 2 separate experiments.

3.3.12 Confocal Microscopy Observations of B16MCWT-Ctag Cell Lines

Following the initial characterisation by fluorescence microscopy, ligand binding and cAMP assays, a selection of clones, including B16MCWT-Ctag-8, B16MCWT-Ctag-24 and B16MCWT-Ctag-27, were examined using confocal microscopy with a Leica SP2 laser scanning fluorescence confocal microscope. This confirmed the punctate pattern of green fluorescence with the transfected cells and that this fluorescence was distributed mainly throughout the cytoplasm of the cells and was excluded from the nucleus (figure 3.12 a). In a number of cells in each line the green fluorescence was also prominent at the plasma membrane (figure 3.12 b). By contrast, the B16G4F stable transfectants which contained pEGFP-N3 vector alone exhibited a totally different pattern of green fluorescence, which was evenly distributed throughout the cytoplasm and also concentrated within the nucleus (figure 3.12 a). Separately, the B16MC294-Ctag transfectants were observed in order to compare the localisation of the Asp294His variant MC1R with the wild-type MC1R-eGFP (wild-type receptor). The B16MC294-Ctag cell lines displayed a punctate pattern of green fluorescence throughout the cytoplasm similar to that which was consistently observed in the B16MCWT-Ctag cell lines (figure 3.12 b). The eGFP tagged wild-type and Asp294His MC1R were found at the plasma membrane in the respective B16MCWT-Ctag and B16MC294-Ctag cell lines, as expected since both MC1 receptors retained the ability to bind ^{125}NDP-αMSH in competition ligand binding experiments (shown above). Importantly, cells within each cell line examined by confocal microscopy presented differing amounts of green fluorescence at the surface membrane. However, overall the B16MCWT-Ctag cell lines were similar in appearance to the B16MC294-Ctag transfectants when images were compared (figure 3.12 b).

Figure 3.12: MC1R-eGFP Localisation within the B16G4F Transfectants in Comparison to the B16GFP (pEGFP-N3 Only) Transfectants

(a)

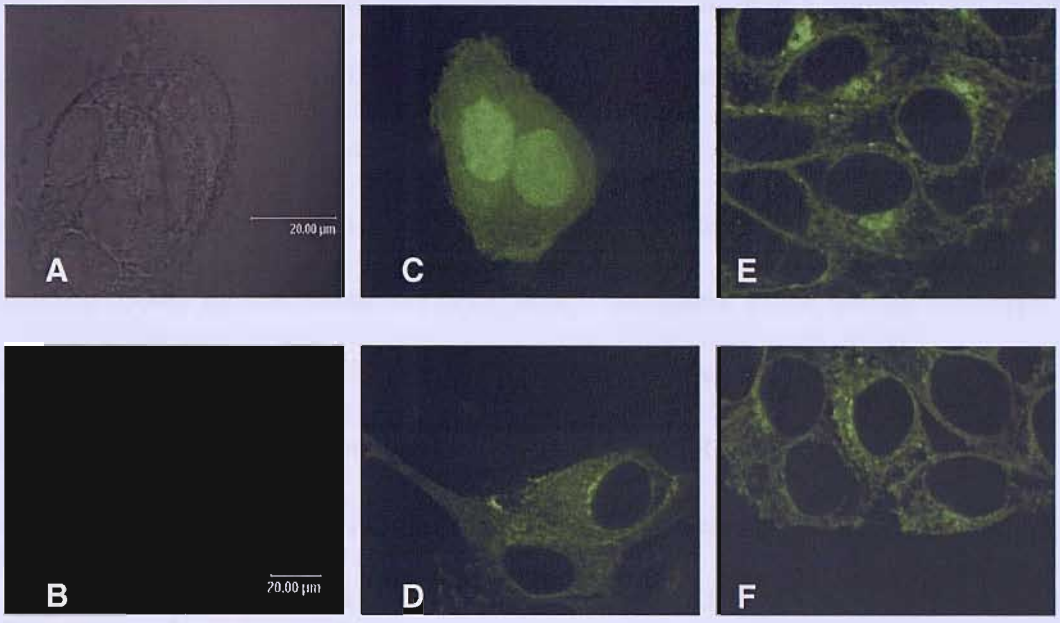

Legend for figure 3.12 (a): (A) B16G4F non transfected cells, observed by transmitted light, (B) Same B16G4F cells were observed by confocal microscope under blue light and demonstrated a lack of green auto fluorescence, (C) B16G4F cells stably transfected with the pEGFP-N3 clontech vector alone, (D, E, F) 3 separate B16MCWT-Ctag cell lines stably transfected with eGFP tagged human wild-type MC1R displaying a punctate pattern of green fluorescence which is throughout the cytoplasm and excluded from the nucleus. Some MC1R-eGFP is accentuated at the plasma membrane.

(b)

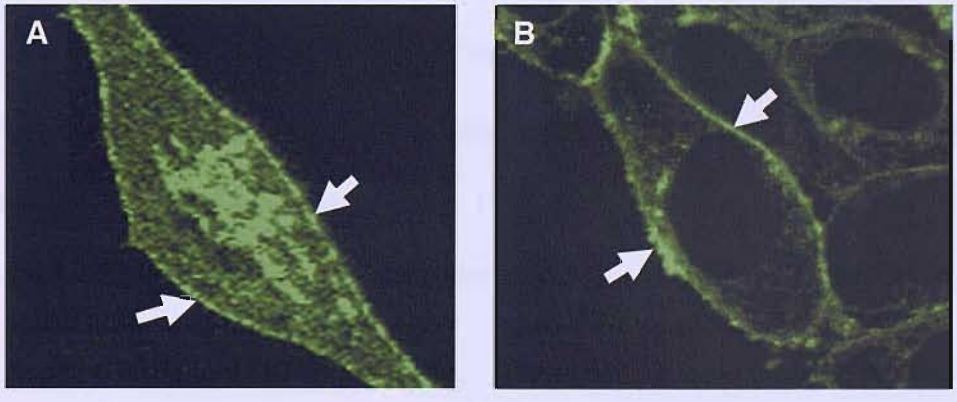

Legend for Figure 3.12 (b): Confocal microscopy of (A) the B16MCWT-Ctag and (B) the B16MC294-Ctag transfectants containing eGFP tagged human wild-type MC1R and Asp294His variant MC1R respectively. The green fluorescence at the plasma membrane is shown by white arrows.

3.4 Discussion

The work presented within this chapter relates to the generation of a pigment cell model using eGFP-labelled MC1R for the purpose of exploring the cellular distribution of both the wild-type MC1R and Asp294His variant MC1R. Work described within this chapter has been concerned with the generation and characterisation of stably transfected B16G4F mouse melanoma cells, which contained: 1) the human wild-type MC1R tagged at the C-terminus with eGFP, 2) the human wild-type MC1R tagged at the N-terminus with eGFP, 3) the human Asp294His MC1R variant tagged at the C-terminus with eGFP, 4) and pEGFP-N3 vector alone transfected cells. These cell lines were named as: 1) B16MCWT-Ctag, 2) B16MCWT-Ntag, 3) B16MC294-Ctag, and 4) B16GFP respectively, and were created in order to investigate the presence of intracellular MC1R without the use of MC1R antibodies, which have previously been unable to sufficiently label intracellular MC1R. The B16G4F cells were used since this cell line has been successfully cultured and utilised for other studies within the lab, also this amelanotic cell type permitted the visualisation of fluorescent eGFP without a high melanin content resulting in the quenching of the fluorescent emission. Importantly the B16G4F cells lack endogenous murine Mc1r and this allowed the investigation of transfected human MC1R. The use of eGFP has been widely used for labelling GPCRs and has proved to permit normal receptor ligand interactions and subsequent signalling in a number of *in vitro* systems (Barak *et al.,* 1997; Blondet *et al.,* 2004; Ivic *et al.,* 2002; Rached *et al.,* 2003; Tarasova *et al.,* 1997).

The B16MCWT-Ctag cell lines were successfully generated and characterisation of these transfectants was done by fluorescence microscopy. The B16MCWT-Ctag cell lines exhibited strong green fluorescence due to the presence of the C-terminally tagged wild-type MC1R-eGFP construct. However the B16MCWT-Ntag transfectants emitted

a low level of green fluorescence, suggesting that the N-terminally tagged wild-type MC1R-eGFP construct was not successfully being synthesised or perhaps was even broken down rapidly. The lack of ligand binding at the plasma membrane suggested that the presence of the eGFP molecule at the N-terminus may have impeded the receptor in some way, such as to cause the intracellular retention or physical blockage of the ligand binding sites. It may also be speculated that the lack of green fluorescence exhibited by these transfectants was due to a reduced rate of production of the N-terminally tagged MC1R-eGFP chimeric protein, hence resulting in a low record of ^{125}I NDP-αMSH counts per minute. The quantification of MC1R-eGFP mRNA from the B16MCWT-Ntag cells was not required since the main focus of work was not to compare N-terminal and C-terminal tagging of MC1R with eGFP, it was decided that the B16MCWT-Ctag cells were appropriate for investigating the presence of intracellular receptor.

The B16MCWT-Ctag cell lines exhibited varying levels of green fluorescence, which could have been due to differences in the expression rate of the MC1R-eGFP fusion protein in each cell. It was also possible that multiple clones were present within individual cell lines. Therefore in order to elucidate this, single cells were obtained from two B16MCWT-Ctag cell lines and were diluted in order to produce single cell clones within 96 well culture plates. Ten single cell clones were expanded from each cell line and were observed by fluorescence microscopy. When compared with their respective parental cell lines, the sub-clones exhibited a similar variation in green fluorescence and retained a similar morphology. This suggested that the original B16MCWT-Ctag cell lines were derived from single cells. The variation in green fluorescence may therefore be attributed to non-synchronised cell cycling with continual synthesis and break down of MC1R-eGFP protein occurring at different rates.

In order to investigate whether MC1R ligand binding was disrupted by the presence of an eGFP tag at the C-terminus, a competitive ligand binding study was done. Results showed that the B16MCWT-Ctag transfectants retained the ability to bind NDP-αMSH ligand, and each cell line exhibited a similar level of binding affinity for the NDP-αMSH ligand. Further work was done to characterise whether αMSH could initiate cAMP signalling within these transfectants. By means of a positive control a B16FWT clone, which was stably transfected with human wild-type MC1R tagged with a FLAG epitope, was used since it had been previously characterised for ligand binding and cAMP production (Robinson and Healy, 2002). It has been reported that the addition of a FLAG tag does not alter cAMP synthesis following receptor activation (unpublished data, Garcia-Borron, Pigment Cell Research conference 2003). The B16MCWT-Ctag cell lines produced a cAMP signal following the addition of αMSH, however once corrected for receptor numbers per cell (equivalent to maximum ligand binding values) the B16MCWT-Ctag clones produced only a partial cAMP signal, which was approximately a third of that produced by the B16FWT control. Therefore the presence of an eGFP tag at the C-terminus appeared to disrupt but not totally obliterate MC1R signalling via cAMP.

Further work within this chapter was concerned with the B16MC294-Ctag transfectants and the localisation of the Asp294His MC1R variant also tagged at the C-terminus with eGFP. The Asp294His MC1R variant is one of the polymorphisms responsible for the red hair and fair skin phenotype in humans, which is also associated with an increased risk of skin cancer. Importantly this variant is not capable of cAMP signalling and activation of this receptor by αMSH binding induces the production of phaeomelanin rather than eumelanin. Therefore, this variant was investigated to look for possible

differences in receptor localisation. The B16MC294-Ctag cell lines were initially characterised by fluorescence microscopy, and the majority of clones exhibited a strong green fluorescence. Similar to that seen in the B16MCWT-Ctag cell lines the levels of green fluorescence intensity varied between cell lines and also between cells within individual cell lines. In order to examine receptor ligand interactions, competitive ligand binding analysis was done on the B16MC294-Ctag transfectants. The Asp294His MC1R variant retained the ability to bind NDP-αMSH despite the presence of eGFP. The ligand binding affinity curves were similar when compared with the ligand binding results from the B16MCWT-Ctag transfectants.

The cells were finally characterised by laser scanning fluorescence confocal microscopy, which permitted a higher resolution inspection of the punctate pattern of green fluorescence. The control B16GFP cell lines transfected with the pEGFP-N3 vector alone displayed a mottled and diffuse pattern of green fluorescence, which was throughout the cytoplasm and also within the nucleus of cells. It was also noticed that these control B16GFP cells did not display green fluorescence accentuation at the plasma membrane. The green fluorescence was not arranged in a punctuated pattern in the absence of MC1R, which suggested that the punctate pattern of green fluorescence from the MC1R-eGFP chimera in the B16MCWT-Ctag and B16MC294-Ctag cells was due to the MC1R trafficking normally with the attached eGFP molecule and not merely adhering together. Each eGFP construct was driven by a CMV promoter, which permitted the high production rate of eGFP (in the B16GFP transfectants) and MC1R-eGFP (in the B16MCWT-Ctag and B16MC294-Ctag transfectants), this allowed for clear visualisation of the receptor. Importantly the absence of intranuclear green fluorescence in the B16MCWT-Ctag and B16MC294-Ctag transfectants demonstrated that the MC1R-eGFP was trafficking appropriately throughout the cell and was not

forced into the nucleus. The green fluorescence was accentuated at the membrane surface in some of the B16MCWT-Ctag and B16MC294-Ctag cells, which was expected as ligand binding studies have already demonstrated the presence of MSH binding sites at the cell surface (Tatro *et al.*, 1990; Varga *et al.*, 1976; Varga *et al.*, 1976b,). The punctate pattern of green fluorescence distributed throughout the cytoplasm was possibly due to the presence of MC1R-eGFP within intracellular organelles. Also, the B16MC294-Ctag transfectants displayed comparable ligand binding properties and exhibited a similar pattern of green fluorescence irrespective of the non-functional nature of this variant MC1R receptor. The further investigation of this intracellular localisation of MC1R-eGFP will be considered within chapter 4.

Chapter 4

Subcellular Localisation of eGFP Tagged MC1 Receptors

4.1 Introduction

Human wild-type MC1R-eGFP and separately human Asp294His MC1R-eGFP were stably transfected into B16G4F melanoma cells (as outlined in chapter 3). This consequently produced a punctate pattern of green fluorescence throughout the cytoplasm, consistent with the presence of intracellular MC1R. These findings are in accordance with previous research that has demonstrated intracellular αMSH binding sites within melanoma cells, however, the specific subcellular location of MC1Rs has not been determined (Orlow *et al.,* 1990). The presence of intracellular MC1R is not surprising since protein synthesis and processing occurs within the endoplasmic reticulum (ER) and golgi apparatus, thus, wild-type MC1R may be expected to be present at the ER and golgi. Similarly, variant MC1R may be present in these organelles, but based on the fact that retention of mutated tyrosinase occurs within the ER (and is associated with oculocutaneous albinism type 1) it is possible that variant MC1R could also be retained within the ER (Halaban *et al.,* 2000; Toyofuku *et al.,* 2001). In addition, some frame shift mutations in *MC4R* (another member of the melanocortin receptor family), which have been associated with child-hood obesity, have been reported to result in the intracellular retention of the receptor, and a decrease in cell surface expression (Lubrano-Berthelier *et al.,* 2003). However, a number of MC1R variants have been shown to bind ligand, and are therefore presumably located at the cell surface (Robinson and Healy, 2002) suggesting that retention of variant MC1R in the ER would be partial rather than complete.

In addition to the ER and golgi, there are a number of other intracellular organelles in which MC1R may possibly be located. Endosomes are responsible for the

internalisation and subsequent processing of GPCRs from the cell membrane (reviewed in Seachrist and Ferguson, 2003). Immunogold labelling of MC1R (utilising an antibody directed against amino acids 2-18 of human MC1R) has suggested the presence of human MC1R along the intracellular side of the cell surface of basal and differentiating sebocytes, and also within cytoplasmic tubular endosomes in these cells (Stander *et al.,* 2002). However, it is unknown whether the antibody used in that study cross-reacts with other proteins or other melanocortin receptors (such as MC5R which has been shown to have a broad distribution of mRNA in skin) (Thiboutot *et al.,* 2000). If MC1R is truly situated in endosomes in sebocytes, then its presence in melanosomes would also be a possibility based on the 'sharing' of proteins between endosomes and melanosomes. For example, endosomes and early stage I-II melanosomes both contain the lysosomal / late endosomal marker proteins LAMP-1 and LAMP-2 (Orlow *et al.,* 1993; Zhou *et al.,* 1993), and melanosomes and lysosomes also share common structural and functional characteristics such as acid phosphatase activity (Otaki, 1970; Seiji and Kikuchi 1969). Proteomic analysis has demonstrated the presence of another GPCR encoded by *Oa1* in purified early stage melanosomes (Basrur *et al.,* 2003). Leading up to that publication, previous work had utilised GFP tagging of murine Oa1 to permit visualization of the wild-type and variant Oa1 receptor within a transfected COS cell expression system, which does not contain melanosomes. In that study, wild-type Oa1 was localised to the late endolysosomal compartment, whereas mutated forms of Oa1 were found to be retained within the ER (Shen *et al.,* 2001). Proteomic analysis was carried out on early melanosomes since this type of analysis could not be carried out on melanin containing late melanosomes (personal communication with Professor V. Hearing). Therefore since MC1R was not detected within early melanosomes, it is still possible that MC1R may be present or incorporated into the later stage melanosomes. Further support for the hypothesis that MC1R might be situated in the

melanosome comes from the fact that immunocytochemistry of cultured melanocytes using antibodies against ACTH 17-39, ACTH 1-10, αMSH, PC1, PC2 and 7B2 has demonstrated a granular pattern of staining distributed throughout the cell body and in granular structures around the nuclei and the distal tips of the melanocytes (Peters *et al.*, 2000). PC1 is a prohormone convertase which cleaves ACTH from the precursor POMC, and PC2 prohormone convertase, with its co-enzyme 7B2, is responsible for the subsequent cleavage of αMSH from ACTH in low pH environments. Immuno-electronmicroscopy was used to further demonstrate the presence of PC1, PC2 and 7B2 within melanosomes (Peters *et al.*, 2000) and previously co-workers had also demonstrated the existence of αMSH within the melanosomes of cultured melanocytes (Schallreuter *et al.*, 1999). These researchers hypothesised that αMSH and ACTH peptides could have pigmentary effects within the melanosome, which do not involve the MC1R. Although this is feasible, the question arises as to how αMSH could have intramelanosome effects in the absence of a receptor such as MC1R at that site. It is possible that αMSH could act via another melanocortin receptor (MC2R, MC3R, MC4R or MC5R) but there is no evidence to show that any of these melanocortin receptors are present at the melanosome. Indeed, evidence for the relatively greater importance of MC1R rather than αMSH in pigmentation comes from knock out mouse studies, in which Mc1r null mice produce a significantly lighter coat colour than POMC null mice (Robbins *et al.*, 1993; Yaswen *et al.*, 1999). Thus, it is hypothesised that the presence of intracellular MC1R close to or at the melanosome could be important for mediating the pigmentary effects of αMSH in melanocytes and melanoma cells. Thus the aim of the work undertaken within this chapter was to investigate whether MC1R is present within the melanosomes of melanoma cells stably transfected with MC1R-eGFP.

4.2 Materials and Methods

4.2.1 Immunofluorescence

In order to determine the subcellular localisation of eGFP-labelled wild-type and variant MC1Rs, and in particular whether it is in the melanosome, a co-localisation study was performed using the B16G4F transfectants previously generated in chapter 3. An array of antibodies / markers for labelling the ER, golgi apparatus, and early / late stage melanosomes were employed for this purpose. Calnexin is a molecular chaperone which resides in the membrane of the ER, and an anti-calnexin antibody was used (at a dilution of 1:200) for labelling fixed and methanol permeabilised cells to identify the ER. The anti-calnexin antibody (Stressgen) is a rabbit polyclonal antibody raised against a synthetic peptide derived from the carboxyl terminus of canine calnexin, which is identical in its amino acid sequence to the carboxyl terminus of the mouse, human and rat calnexins (Ou *et al.*, 1993). This primary antibody (and the αPEP-1 and αPEP-13 antibodies, see below) was labelled with a goat anti-rabbit IgG secondary antibody (working concentration 5 μg / ml) which was conjugated to an alexa fluor 633 (A633). The A633 was employed because it was excited by the 633 nm laser under fluorescence microscopy and emitted fluorescence at 647 nm (far-red range of the spectrum), thus preventing crossover with eGFP which was excited by the 488 nm laser and emitted between 480-550 nm. A bodipy-texas red-ceramide conjugate was used to delineate the golgi apparatus within live cells. Ceramides are derived from sphingolipids during lipid synthesis and degradation, and are present in abundance within the golgi apparatus. The N-((4-(4,4-difluoro-5- (2-thienyl)-4-bora-3a, 4a-diaza-s-indacene-3-yl)phenoxy)acetyl)sphingosine (BODIPY Texas Red Ceramide BSA complex, Molecular Probes) was excited at 589 nm and exhibited red fluorescence at 617 nm. In order to determine whether MC1R-eGFP was present within the melanosome, antibodies that were specific for the melanosomal proteins gp100 and Trp-

1 were employed for the visualisation of this organelle. The αPEP-1 is a rabbit polyclonal antibody directed against a synthetic peptide [KLHCEDYEELPNPNHSMV-COOH] corresponding to the C-terminus of murine Trp-1, which is present in stage II – IV (late stage) melanosomes (Jimenez *et al.,* 1988, Jimenez *et al.,* 1989). The αPEP-13 is a rabbit polyclonal antibody raised against the synthetic peptide [BSACGLGENSPLLSGQQV-COOH] specific for the murine Pmel17 protein (silver protein or gp100 in humans), which is abundant in stage I / II melanosomes (Kobayashi *et al.,* 1994; Zhou *et al.,* 1994). The αPEP-1 and αPEP-13 antibodies were a kind gift from Professor V. Hearing (NIH, Bethesda, USA) and were diluted 1:200 for labelling melanosomes in fixed and permeable cells. The fluorescence microscopy of the MC1R-eGFP transfected cells in chapter 3 suggested that MC1R was not present in the nucleus, and TO-PRO-3 (Molecular Probes), which detects double stranded nucleic acids in non-permeabilised cells fixed cells and fluoresces at 633 nm, was used at a dilution of 1:2000 in PBS (0.5 nM) to counter stain the nucleus to confirm this

4.2.2 Confocal Microscopy and Analysis by Leica Computer Software

Three wild-type MC1R-eGFP transfectants and two Asp294His variant MC1R-eGFP cell lines were immunofluorescently labelled for ER, golgi and melanosome, on at least two separate occasions. Successful immunofluorescent labelling of each cell line was confirmed using fluorescence light microscopy, and co-localisation analysis was subsequently carried out using a Leica SP2 laser scanning fluorescence confocal microscope. Two dimensional images were scanned at multiple points distanced every 1 μm through the Z plane of the cell, and 3D images were constructed from a series of Z sections. Single Z sections were extracted from the mid point of the 3D image and were subsequently analysed by Leica computer software. Figure 4.1 shows the fluorescence emitted from a single Z section extrapolated from a 3D image. In figure 4.1D, the X

axis represents increasing green fluorescence in all pixels with a green fluorescence signal and the Y axis represents increasing red fluorescence in all pixels with a red fluorescence signal. Pixels that had strong and approximately equal red and green fluorescence, consistent with significant co-localisation are depicted in blue on the graph. The pixels contained within this blue area on the graph are shown as white pixels on the composite images (figure 4.1E), consisting of red and green fluorescent images obtained from a single Z plane through the centre of a 3D cluster of cells, identifying where significant co-localisation is present.

Figure 4.1: Co-localisation of Red and Green Fluorescent Images

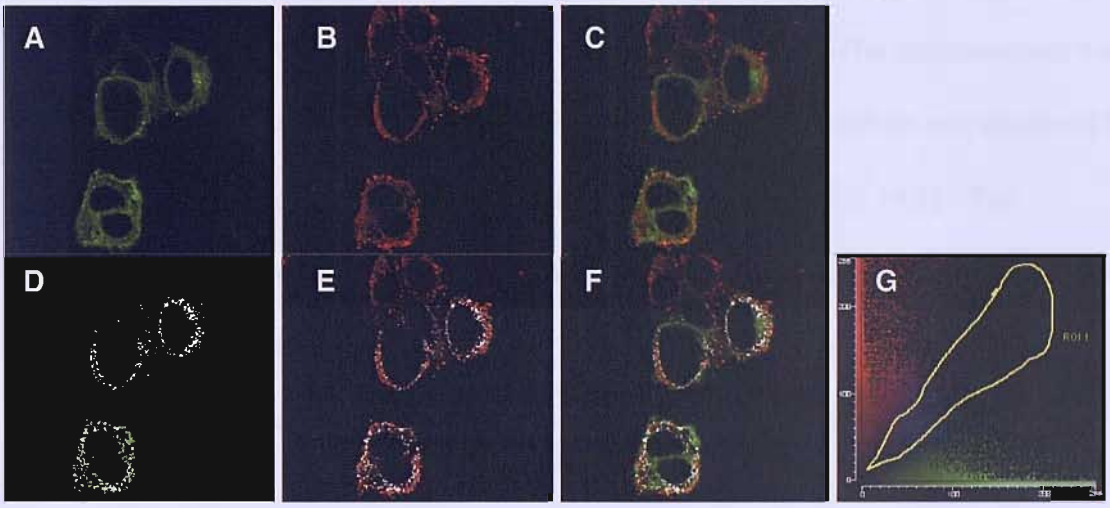

Legend for figure 4.1: A Z plane of B16G4F transfected cells was analyses for co-localisation: (A) demonstrates green fluorescence emitted by melanoma cells containing MC1R-eGFP, (B) shows red fluorescence due to A633 labelling, (C) demonstrates the same cells under transmitted light, merging green / red fluorescence respectively, (G) represents the two separate fluorescent outputs graphically with increasing green fluorescence on the X axis and increasing red fluorescence on the Y axis, and co-localised pixels are shown by the central blue. The most co-localised pixels were selected (by hand drawing within the blue area) and highlighted as a white mask, (D-F) demonstrates the white mask overlaid onto the green, red, and merged images (A-C) respectively.

4.2.3 Induction of Dendrites in Transfected Cells

In order to induce dendrites in the transfectants, cells were cultured for 96 hours separately with 10^{-5} M and 10^{-7} M forskolin (FORSK), 10^{-3} M 3-isobutyl-1-methylxanthine (IBMX), and 10^{-7} M 12-0-tetradecanoylphorbol 13-acetate (TPA) respectively. These concentrations were used since they have all been previously reported to induce the formation of dendrites within various pigment cells.

4.2.4 Melanosome Isolation

The melanosomes were isolated from melanoma cell lines as described within chapter 2 section 2.19. TEM was performed on the enriched melanosome fractions in order to observe and verify the purity of melanosomes (section 2.19.3). The melanosomes were fixed in 4% paraformaldehyde and the emission of green fluorescence was observed by fluorescence light microscopy and confocal microscopy (section 2.19.1). The melanosome-enriched fraction was immunofluorescently labelled with αPEP-1 with an A633 secondary antibody subsequently to look for co-localisation between Trp-1 protein and MC1R-eGFP.

4.3 Results

4.3.1 Cell Lines Used to Permit the Localisation of Intracellular MC1R-eGFP

Three B16MCWT-Ctag cell lines containing human wild-type MC1R tagged at the C terminus with eGFP, denoted as B16MCWT-Ctag-8, B16MCWT-Ctag-24, B16MCWT-Ctag-27 respectively, were selected for co-localisation studies. In order to compare the co-localisation of the eGFP tagged wild-type MC1R with that of the eGFP-labelled Asp294His variant MC1R, two B16MC294-Ctag transfectants (B16MC294-Ctag-11 and B16MC294-Ctag-15) were also investigated. As previously described all five cell lines exhibited a strong level of green fluorescence, which was present in a punctate pattern throughout the cytoplasm, with some accentuation. at the cell membrane.

4.3.2 Evidence for eGFP Tagged MC1R at the Endoplasmic Reticulum

The three B16MCWT-Ctag cell lines and two B16MC294-Ctag cell lines were observed by fluorescence microscopy following immunofluorescent labelling of calnexin / ER. All cells demonstrated a reticular pattern of red fluorescence throughout the cytoplasm and around the nucleus. However, a number of the cells that exhibited red fluorescence did not emit strong green fluorescence due to variability in green fluorescence between cells (as previously discussed in chapter 3). Using confocal microscopy and image analysis, each of the three B16MCWT-Ctag cell lines demonstrated co-localisation between the wild-type MC1R-eGFP and the ER in approximately 5 % of cells (i.e. those which emitted high intensity green fluorescence) (figure 4.2 a). The two B16MC294-Ctag cell lines demonstrated a similar pattern of co-localisation to that observed in the B16MCWT-Ctag transfectants (figure 4.2).

Figure 4.2: MC1R-eGFP Localisation at the Endoplasmic Reticulum

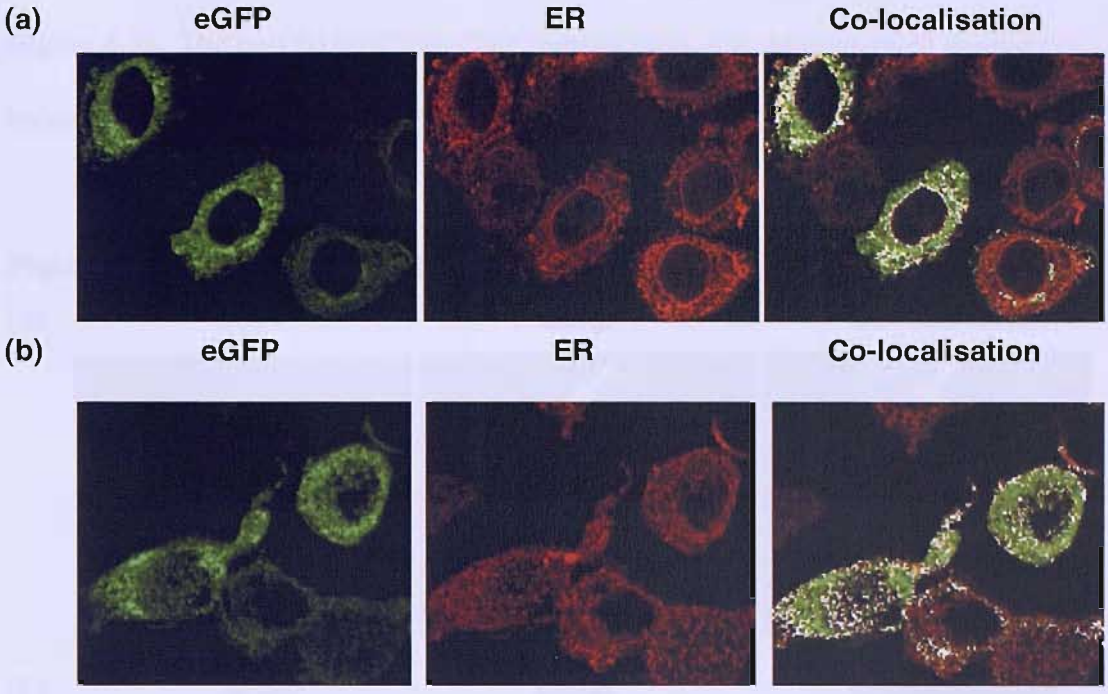

Legend for figure 4.2: Z sections from 3D images of (a) B16MCWT-Ctag transfectants and (b) B16MC294-Ctag transfectants. Left panels show green fluorescence from eGFP tagged human (a) wild-type MC1R and (b) Asp294His variant MC1R respectively. Centre panels show red fluorescence emitted by calnexin / ER immunofluorescent labelling. Right panels depict an overlaid composite image with co-localisation between MC1R-eGFP and the ER represented by the white pixels.

4.3.3 MC1R-eGFP at the Golgi Apparatus

The three B16MCWT-Ctag and two B16MC294-Ctag cell lines were investigated for the presence of MC1R-eGFP at the golgi. A bodipy-texas red conjugated ceramide (B-TR-ceramide) was used to label the golgi apparatus. The B-TR-ceramide was also incorporated into newly synthesised lipids at other sites of the cells, and this was taken into consideration during fluorescence microscopy and subsequent confocal microscopy and image analysis. All cells demonstrated a bright red fluorescence throughout the cytoplasm but the brightest red fluorescent signals were observed in close proximity to the nucleus, and this bright area of red fluorescence was assumed to represent the golgi apparatus (as suggested in the Molecular Probes user manual) and as per previous reports (Thieblemont and Wright, 1999). Confocal microscopy confirmed that all three

B16MCWT-Ctag cells lines contained eGFP-labelled wild-type MC1R at the golgi (figure 4.3). The two B16MC294-Ctag transfectants also demonstrated similar co-localisation of the Asp294His MC1R-eGFP with the golgi (figure 4.3).

Figure 4.3: MC1R-eGFP Localisation at the Golgi Apparatus

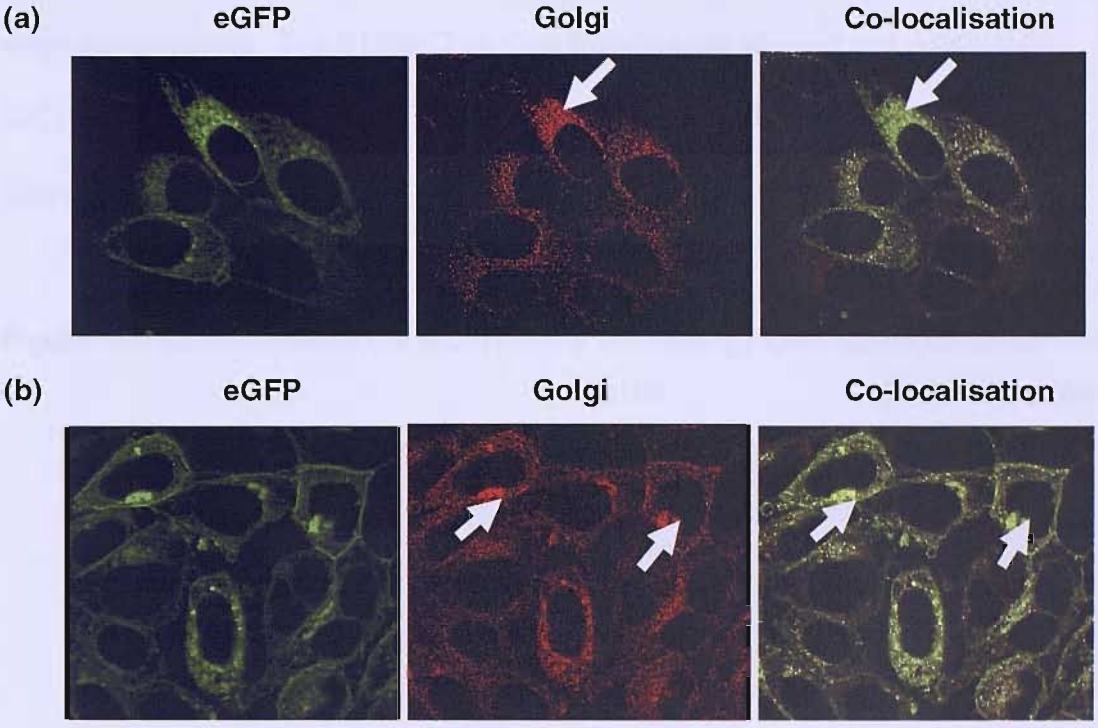

Legend for figure 4.3: Z sections from 3D images of (a) B16MCWT-Ctag transfectants and (b) B16MC294-Ctag transfectants. The left panels represent (a) wild-type and (b) Asp294His variant MC1R-eGFP, the centre panels show red fluorescence emitted by the B-TR-ceramide for golgi, and co-localisation images (right panels) demonstrate co-localisation between MC1R-eGFP and the golgi as represented by the white pixels (the golgi is depicted by the white arrows).

4.3.4 Co-localisation of MC1R-eGFP with Early and Late Stage Melanosomes

Further investigations aimed to examine whether the MC1R localised to the melanosome. The three B16MCWT-Ctag and two B16MC294-Ctag transfectants were labelled separately with two different antibodies αPEP-13 and αPEP-1, which targeted gp100 and Trp-1 proteins typically present in stage I-II and stage II-IV melanosomes respectively. Fluorescence microscopy of the cell lines revealed a punctate pattern of high intensity red fluorescence labelling for gp100 and Trp-1 throughout the cytoplasm

of all transfectants. Confocal microscopy subsequently confirmed that in all three B16MCWT-Ctag transfectants, the wild-type MC1R-eGFP co-localised with both early and late stage melanosomes (figures 4.4 and 4.5). However, there was more co-localisation of Trp-1 and MC1R-eGFP than gp100 and MC1R-eGFP (figure 4.4a, figure 4.4b). This suggested that the eGFP tagged wild-type MC1R was more abundant in late stage melanosomes. The B16MC294-Ctag transfectants showed that Asp294His MC1R-eGFP similarly co-localised to a greater extent with Trp-1 than with gp100 (figure 4.5 b).

Figure 4.4: Co-localisation of MC1R-eGFP with Early / Late Stage Melanosomes

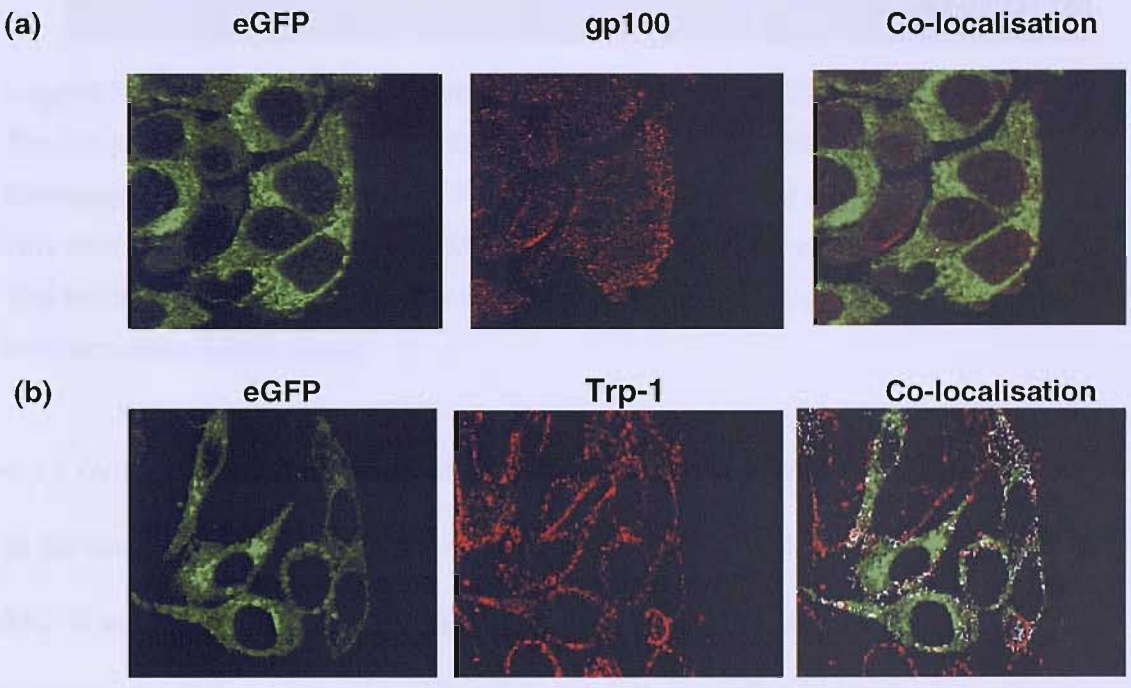

Legend for figure 4.4: Z sections from 3D images of B16MCWT-Ctag transfectants exhibiting green fluorescence due to presence of eGFP tagged human wild-type MC1R (left panels). The centre panels show (a) gp100 and (b) Trp-1 labelling in red respectively. The right panels depict composite images showing: little co-localisation between MC1R-eGFP and the gp100 / early stage I–II melanosomes (a), and greater co-localisation (white pixels) between MC1R-eGFP and Trp-1 / late stage II–IV melanosomes (b).

Figure 4.5: Co-localisation of Asp294His MC1R-eGFP with Early / Late Stage Melanosomes

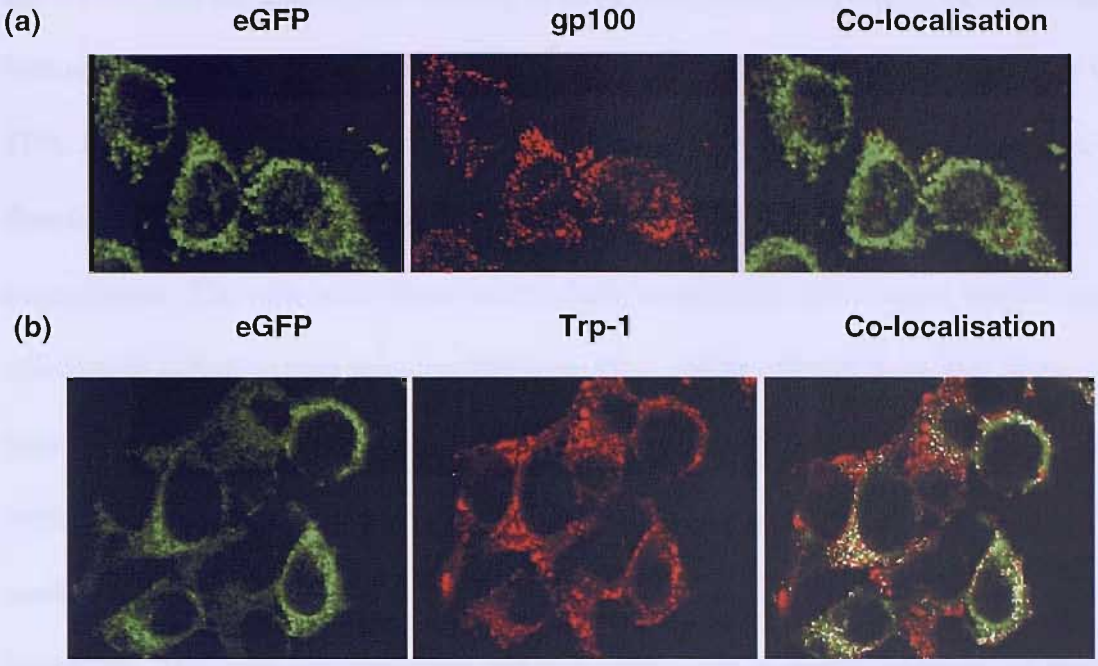

Legend for figure 4.5: Z sections from 3D images of B16MC294-Ctag transfectants. The left panels show the Asp294His MC1R-eGFP. The centre panels show red fluorescence of (a) gp100 and (b) Trp-1. The top right panel (a) shows that there was very little co-localisation between MC1R-eGFP and gp100 / stage I-II melanosomes. The bottom right panel shows that the MC1R-eGFP co-localised with Trp-1 / stage II-IV melanosomes (white pixels).

4.3.5 Generation of Dendrites in the eGFP Tagged MC1R Transfectants

In the above experiments that showed co-localisation of wild-type and Asp294His MC1R within ER, golgi, and mainly stage II-IV melanosomes, it was not possible to conclusively demonstrate co-localisation with full separation between organelles that were in close proximity, and this was due to resolution constraints of the confocal microscope. Therefore it is conceivable that MC1R-eGFP co-localisation at the melanosome could be correct or due to chance co-localisation of melanosomes adjacent to MC1R in the ER and golgi. In order to address this, the co-localisation of MC1R-eGFP with the melanosomal markers gp100 and Trp-1 was investigated within dendrites, since this is the site of melanosome migration during their maturation process, and ER and golgi are mostly excluded from dendrites. The B16MCWT-Ctag

transfectants were cultured separately in the presence of three different substances known to cause morphological changes in these melanoma cells, which included the formation of dendrites. Three B16MCWT-Ctag cell lines were cultured separately with TPA, IBMX, and forskolin. All three agents caused a decrease in cell proliferation, therefore this was considered when deciding how many cells to seed for these experiments. The cells were observed regularly to ascertain which agent was the most effective in initiating long thin dendrite formation, and in order to show that these additives were solely responsible for dendrite formation, controls for this experiment included culturing the cells in complete DMEM medium and in complete DMEM medium containing 1% DMSO (as DMSO was present in the working solution of forskolin). The cells were observed and characterised at 24 hours, 48 hours, 72 hours and 96 hours by light microscopy at 20 x magnification. There was no dendrite formation at 24 hours following the addition of 10^{-7} M TPA, 10^{-3} M IBMX, 10^{-5} M forskolin and 10^{-7} M forskolin and the control cells and DMSO only treated cells grew in monolayers and appeared characteristically bipolar with no dendrite formation. At 48 hours the cells treated with 10^{-3} M IBMX developed short dendrites, whilst the cells treated with 10^{-7} M and 10^{-5} M forskolin remained bipolar, however some did become tripolar and elongated (figure 4.6). At 72 hours the cells remained similar in appearance to the cells observed at 48 hours (data not shown). The cells were finally characterised at 96 hours by light microscopy, and dendricity was observed in the B16MCWT-Ctag transfectants treated with 10^{-7} M TPA, 10^{-3} M IBMX, and 10^{-5} M forskolin respectively (figure 4.7). Despite the fact that all three additives were capable of inducing dendrites, the most effective and potent inducer of dendrites was 10^{-3} M IBMX. The IBMX was subsequently used to produce dendritic cells in the proceeding experiments.

Figure 4.6: Dendrite Formation in a B16MCWT-Ctag Cell Line at 48 Hours

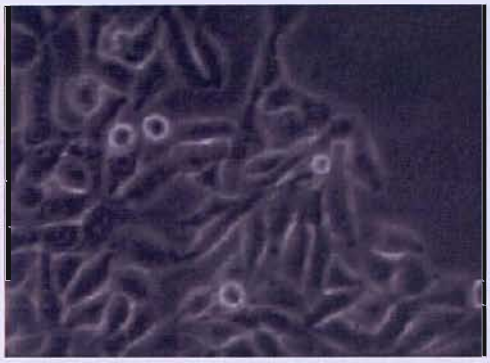

A) Control / complete DMEM

D) Complete DMEM + 10^{-5} M Forskolin

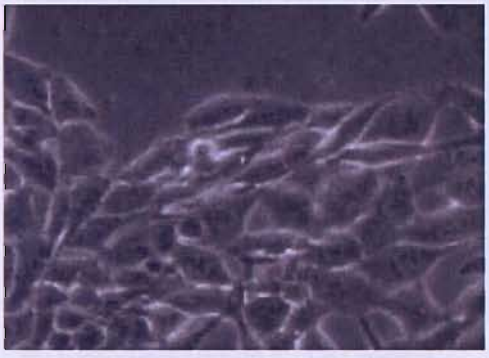

B) Complete DMEM + (1%) DMSO

E) Complete DMEM + 10^{-7} M TPA

C) Complete DMEM + 10^{-7} M Forskolin

F) Complete DMEM + 10^{-3} M IBMX

Figure 4.7: Dendrite Formation in a B16MCWT-Ctag Cell Line at 96 Hours

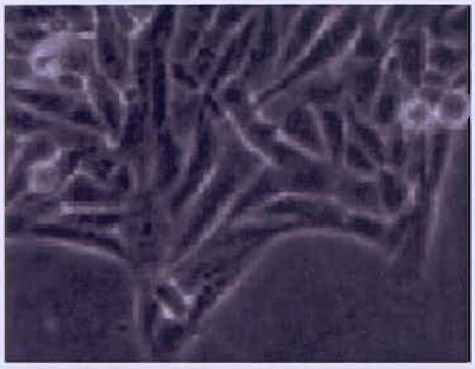

A) Control / complete DMEM

D) Complete DMEM + 10^{-5} M Forskolin

B) Complete DMEM + (1%) DMSO

E) Complete DMEM + 10^{-7} M TPA

C) Complete DMEM + 10^{-7} M Forskolin

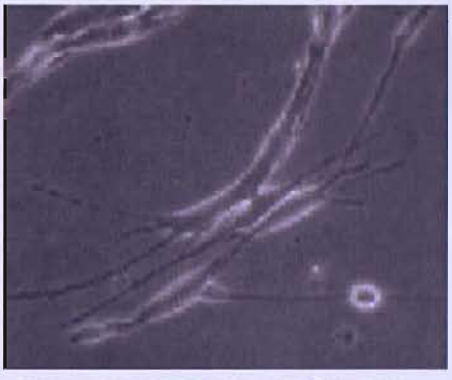

F) Complete DMEM + 10^{-3} M IBMX

4.3.6 Investigating the Presence of Green Fluorescence within Dendrites

Dendrites were induced in three B16MCWT-Ctag cell lines by 10^{-3} M IBMX and cells were observed by fluorescence microscopy at 96 hours. The nuclei of cells were immunofluorescently labelled using a To-pro-3 fluorophore, which emitted red fluorescence (figure 4.8). There was no co-localisation between the To-pro-3 and the MC1R-eGFP green fluorescence.

Figure 4.8: Green Fluorescence along Dendrites in B16MCWT-Ctag Cells

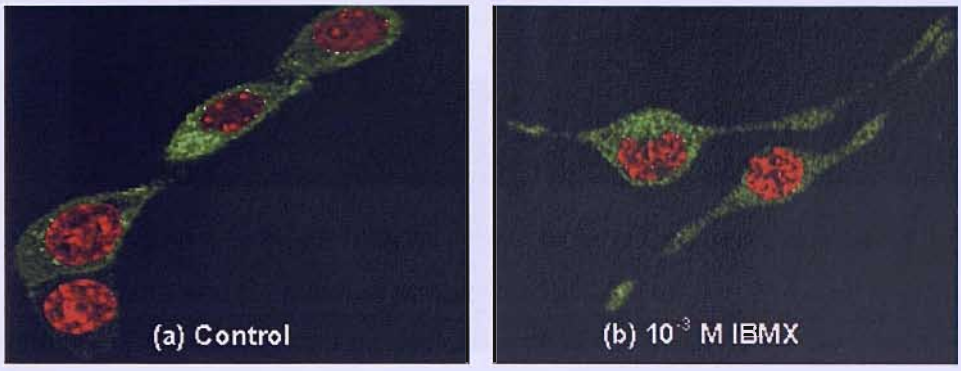

Legend for figure 4.8: The B16MCWT-Ctag transfectants were cultured in (a) complete DMEM medium and (b) medium containing 10^{-3} M IBMX for 96 hours to induce dendrite formation. The cells emitted a punctuate pattern of green fluorescence within the cytoplasm and throughout the dendrites (b), green fluorescence was excluded from the nucleus (red).

4.3.7 Co-localisation of eGFP Tagged MC1R with ER along Dendrites in the Cell Transfectants

Three B16MCWT-Ctag transfectants and two B16MC294-Ctag cell lines were investigated, and 10^{-3} M IBMX induced the formation of dendrites in each cell line. Immunofluorescent labelling of calnexin permitted the visualisation of ER within the dendritic cells by fluorescence microscopy. The B16MCWT-Ctag transfectants emitted the characteristic punctate pattern of green fluorescence throughout the cytoplasm, which also was present along the dendrites. As previously discussed this could be due to the fact that calnexin is also a component of melanosomes as well as ER. Confocal microscopy of the B16MCWT-Ctag transfectants confirmed that wild-type MC1R-eGFP co-localised with ER within the cell body and also along dendrites (figure 4.9 a). However, the majority of co-localisation occurred within the cell body. There was also an amount of green fluorescence which did not co-localise within the dendrites and remained separate to the ER labelling (figure 4.9 a). The two B16MC294-Ctag transfectants were observed by fluorescence microscopy and subsequently demonstrated a similar reticular pattern of calnexin labelling (ER). Both B16MC294-Ctag cell lines

Figure 4.9: MC1R-eGFP Localisation with Endoplasmic Reticulum within Dendritic Cell Transfectants

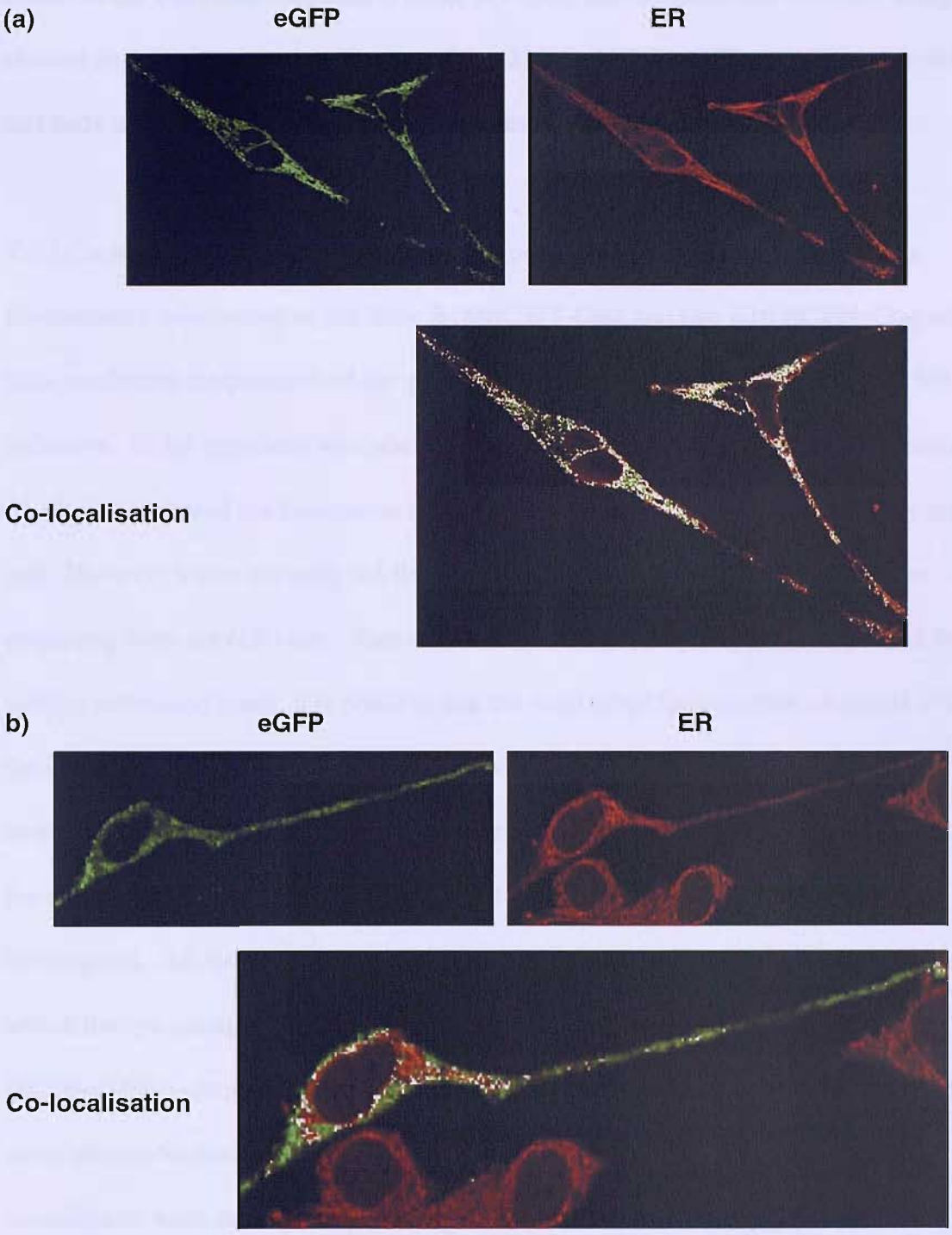

Legend for figure 4.9: Two Z section from 3D images of a) B16MCWT-Ctag transfectants and b) B16MC294-Ctag transfectants. The panels labelled 'eGFP' demonstrate dendritic cells exhibiting green fluorescence due to presence of eGFP tagged human (a) wild-type MC1R and (b) Asp294His variant MC1R respectively. The panels denoted as 'ER' show the red fluorescence emitted by calnexin / ER immunofluorescent labelling, using an A633 conjugated secondary antibody. The 'Co-localisation' panel depict an overlaid composite image with co-localisation between MC1R-eGFP and the ER represented by the white mask.

showed the same pattern of green fluorescence throughout the cell and within the dendrites (as was observed in the B16MCWT-Ctag transfectants) and confocal analysis showed that there was co-localisation of Asp294His MC1R-eGFP with ER within the cell body and to a lesser extent along dendrites (figure 4.9b).

4.3.8 Co-localisation of MC1R-eGFP with Golgi in Dendritic Cells Transfectants

Fluorescence microscopy of the three B16MCWT-Ctag and two B16MC294-Ctag cell lines confirmed the presence of the green fluorescence along dendrites following IBMX induction. Golgi apparatus was labelled (as described previously) with B-TR-ceramide, which demonstrated red fluorescence close to the nucleus within the cytoplasm of the cell. However lower intensity red fluorescence was also observed within dendrites projecting from the cell body. Since the B-TR-ceramide may also be incorporated into newly synthesised lipids, it is possible that the weaker red fluorescence observed within the dendrites corresponded to newly synthesised lipids rather than golgi apparatus. The dendritic B16MCWT-Ctag transfectants were examined by confocal microscopy, and the co-localisation pattern of wild-type MC1R-eGFP with B-TR-Ceramide was investigated. All three transfectants demonstrated the presence of green fluorescence within the cytoplasm and also along dendrites. The green fluorescence of wild-type MC1R-eGFP co-localised with B-TR-Ceramide mostly within the cell body however some also co-localised along dendrites (figure 4.10 a). Two B16MC294-Ctag transfectants were subsequently investigated by confocal microscopy and each demonstrated a similar punctate pattern of green fluorescence within the cytoplasm and along dendrites consistent with previous observations. The golgi staining demonstrated focal red fluorescence close to the nucleus, similar to that observed within the B16MCWT-Ctag cells. Co-localisation was observed between the green fluorescence of the Asp294His MC1R-eGFP and the focal higher intensity red fluorescence of golgi

labelling close to the nucleus (figure 4.10 b). Interestingly red fluorescence was observed at the junctions where the dendrites project out of the cell body and also along dendrites (figure 4.10 b). These areas co-localised occasionally with the green fluorescence suggesting that MC1R-eGFP co-localised with membrane lipids along the plasma membrane and within dendrites. It is possible that golgi apparatus was present within dendrites, however since not all the green fluorescence co-localised with B-TR-Ceramide, it may be assumed that the remaining green fluorescence represented MC1R-eGFP within other structures such as melanosomes.

Figure 4.10: MC1R-eGFP Localisation at the Golgi within Dendritic Cell Transfectants

(a)

eGFP

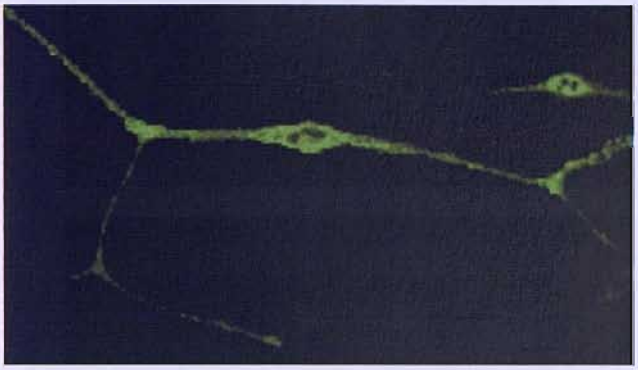

Golgi

Co-localisation

(b)

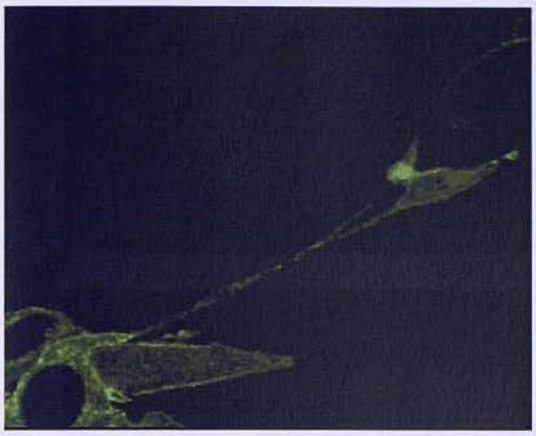

eGFP

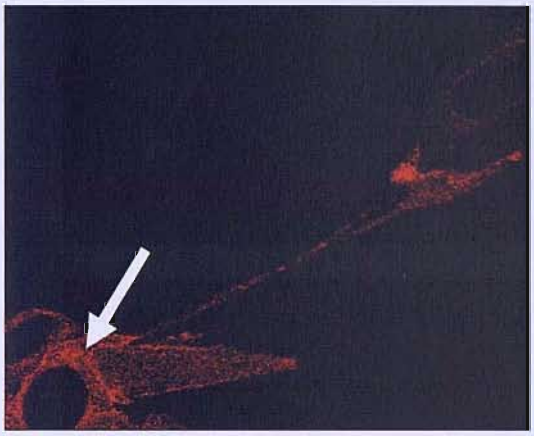

Golgi

Co-localisation

Legend for figure 4.10: Confocal images of (a) B16MCWT-Ctag transfectants and (b) B16MC294-Ctag transfectants. The panels labelled 'eGFP' demonstrate green fluorescence due to presence of wild-type MC1R-eGFP / Asp294His variant MC1R-eGFP respectively. The 'Golgi' images show red fluorescence emitted by B-TR-Ceramide, where the brightest fluorescence is golgi specific. The 'Co-localisation' panels represent overlaid composite images and the white pixels demonstrate areas of MC1R-eGFP co-localisation with golgi (white arrows) and newly synthesised lipids.

4.3.9 Co-localisation of MC1R-eGFP with Early and Late Stage Melanosomes in Dendritic Cell Transfectants

The final stage of the work examining co-localisation aimed to investigate the co-localisation of MC1R-eGFP with melanosome markers along dendrites. Immunofluorescent labelling of gp100 and of Trp-1 was demonstrated in three B16MCWT-Ctag and two B16MC294-Ctag transfectants respectively following the induction of dendrites. Cells were initially characterised by fluorescence microscopy. The labelling of gp100 exhibited red immunofluorescent labelling in the cell body and along the dendrites as can be seen in figure 4.11 (a). Separately, the Trp-1 labelling showed similar levels of red fluorescence and a similar pattern of punctuate labelling in the cell body and also in the dendrites (figure 4.11 b). However more of the Trp-1 labelling was present at the periphery of the cell, indicating that the late melanosomes may associate with the plasma membrane prior to trafficking along dendrite extensions. Confocal microscopy showed that in all three B16MCWT-Ctag transfectants there was extensive co-localisation of wild-type MC1R-eGFP with both gp100 and Trp-1, which contradicted the original finding that MC1R-eGFP co-localised less with gp100 than with Trp-1 in the non dendritic B16MCWT-Ctag transfectants. Contrastingly the two B16MC294-Ctag transfectants demonstrated less co-localisation of Asp294His MC1R-eGFP with gp100 along the dendrites (4.12 a). However confocal microscopy of Trp-1 labelling within the B16MC294-Ctag cell lines revealed a punctate pattern of red fluorescence similar to that observed within the B16MCWT-Ctag cells, and this strongly co-localised with the green fluorescence of Asp294His MC1R-eGFP within the cell body and also along dendrites (figure 4.12 b).

Figure 4.11: Co-localisation of Wild-type MC1R-eGFP with Melanosomes along Dendrites

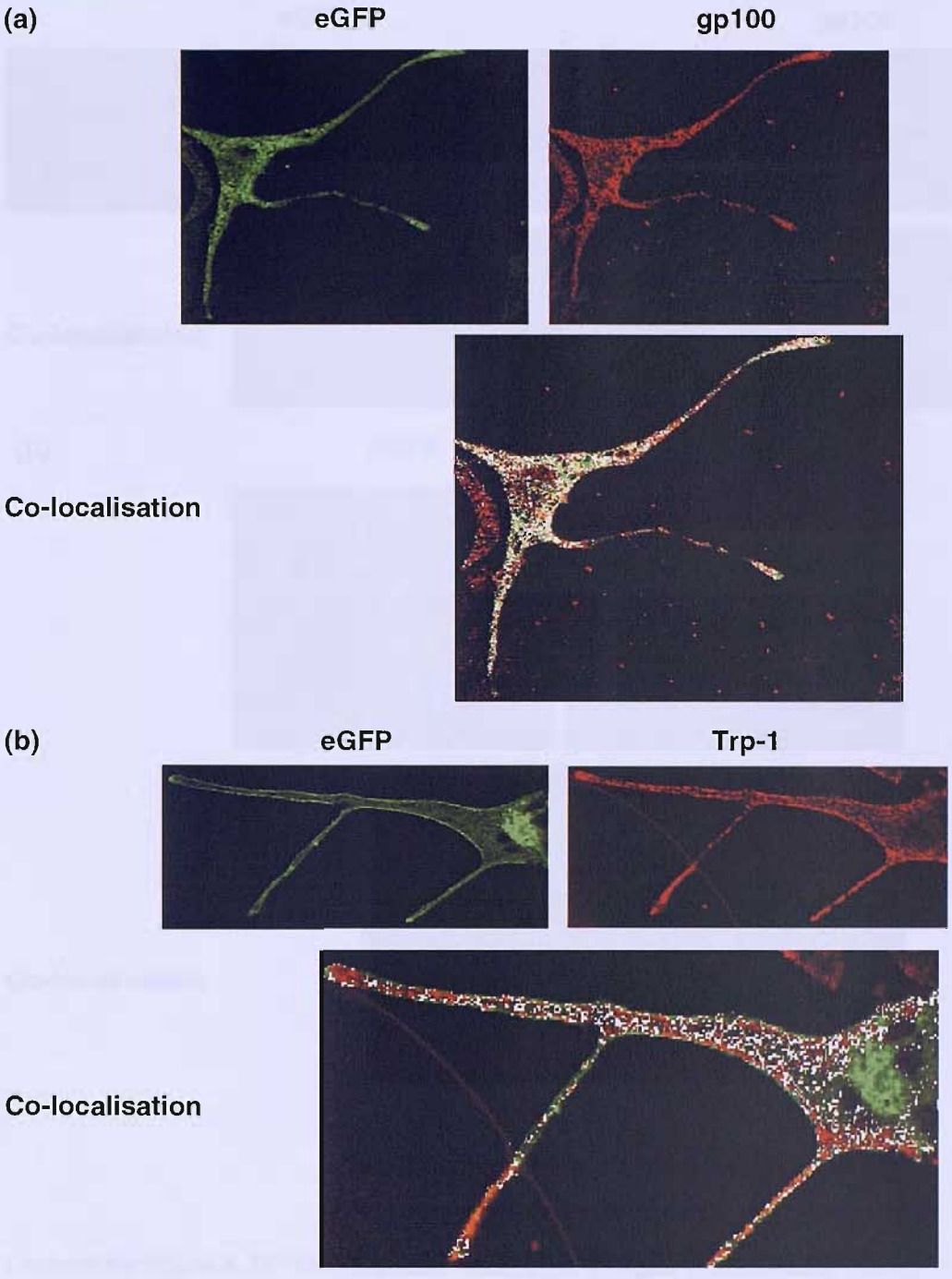

Legend for figure 4.11: Two Z sections from 3D images depicting B16MCWT-Ctag transfectants immunofluorescently labelled with a) αPEP-13 (gp100), b) αPEP-1 (Trp-1) respectively. The 'eGFP' panels show cells exhibiting green fluorescence due to presence of human wild-type MC1R-eGFP. The 'gp100' and 'Trp-1' panels show red fluorescence emitted by gp100 / A633 and Trp-1 / A633 respectively. The 'Co-localisation' composite images depict the co-localisation (white) of wild-type MC1R-eGFP and melanosomes.

Figure 4.12: Co-localisation of Asp294His MC1R-eGFP with Melanosomes along Dendrites

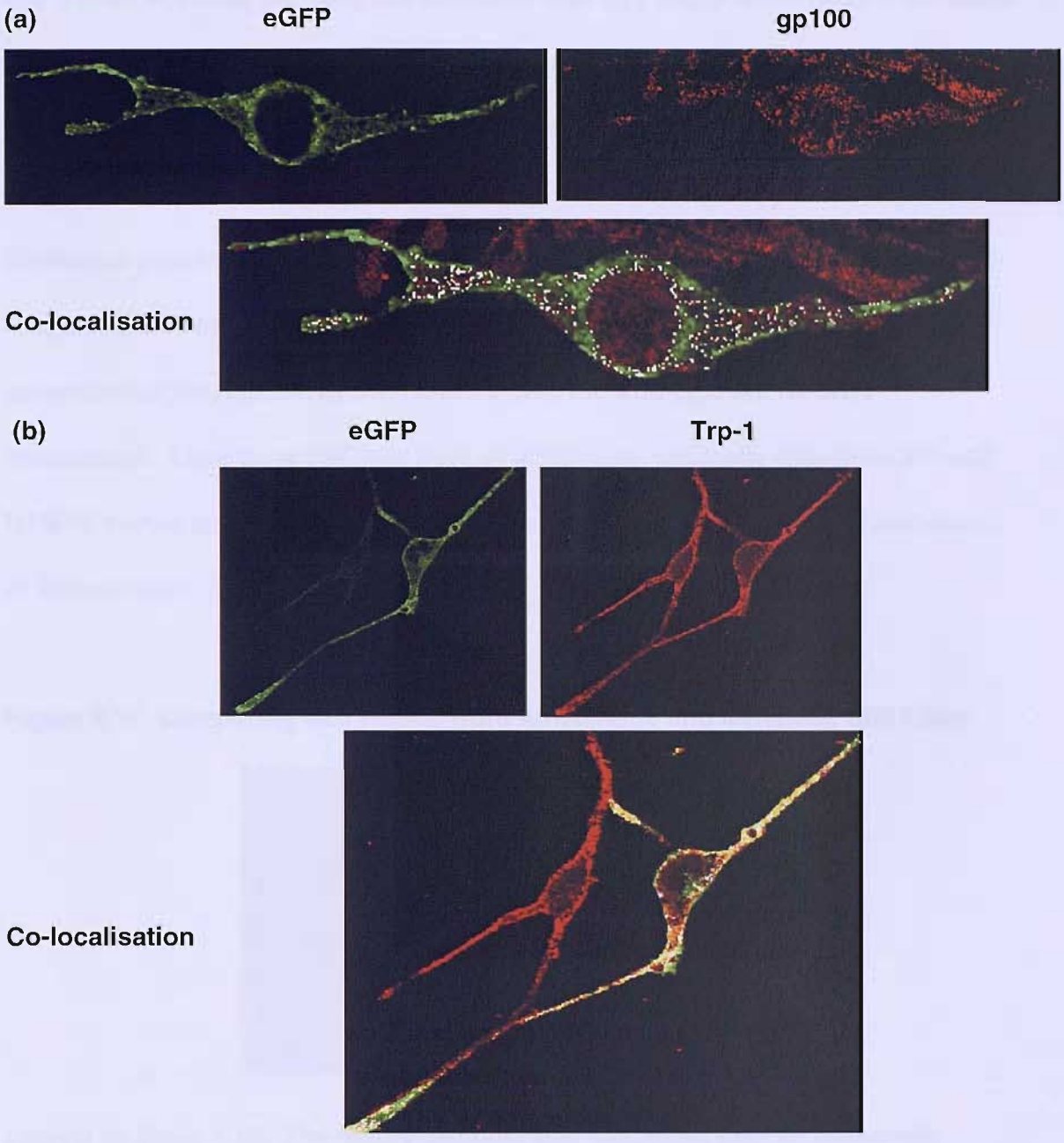

Legend for figure 4.12: Two Z sections from 3D images of B16MC294-Ctag transfectants were immunofluorescently labelled with a) αPEP-13 (gp100) and b) αPEP-1 (Trp-1) respectively. The 'eGFP' panels show cells exhibiting green fluorescence due to presence of eGFP tagged human wild-type MC1R. The 'gp100' and 'Trp-1' panels show the red fluorescence emitted by the respective gp100 / A633 and the Trp-1 / A633 immunofluorescent labelling. The 'Co-localisation' panels depict composite images showing co-localisation (white pixels) of Asp294His MC1R-eGFP with early and late melanosomes.

4.3.10 Evidence for MC1R-eGFP at the Melanosome

The B16MCWT-Ctag cell lines that contained wild-type MC1R-eGFP were fractionated by use of a sucrose density gradient and ultra centrifugation, with the aim of purifying melanosomes for the verification of green fluorescence by confocal analysis. Cells were grown to yield at least 6 x 10^7 cells which were cultured to approximately 80% confluence prior to extraction of melanosomes (as per methods 2.22) Two B16MCWT-Ctag cell lines were fractionated and one B16MC294-Ctag cell line was done for comparison of the Asp294His MC1R-eGFP with the wild-type MC1R-eGFP transfectants. Since these cell lines were all amelanotic, melanotic Cloudman S91 and B16F10 murine melanomas were used as controls to confirm the successful extraction of melanosomes (figure 4.13).

Figure 4.13: Comparing Cell Pellets from Amelanotic and Melanotic Cell Lines

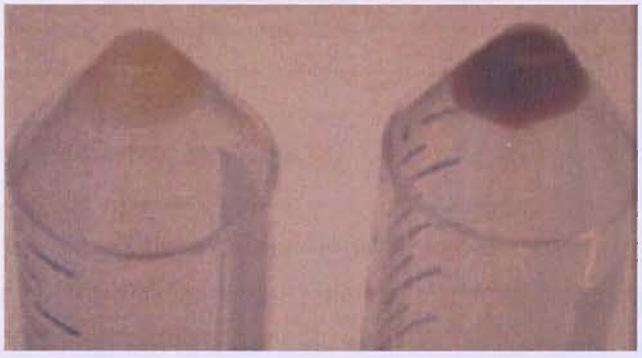

Legend for figure 4.13: The picture demonstrates cell pellets from an amelanotic B16MCWT-Ctag cell line (left), and melanotic B16F10 cells (right).

The cell pellets were homogenised using a Dounce homogeniser (with Teflon plunger), and the 'large granule suspension' was layered onto a sucrose density gradient ranging from 1.55 M to 2.6 M sucrose (methods 2.22). Following ultracentrifugation it was found that the melanotic B16F10 cells yielded a brown / black melanosome-enriched pellet at the base of the centrifuge tube (figure 4.14). However, the amelanotic B16MCWT-Ctag and B16MC294-Ctag cell lines produced a suspended white material

close to the base of the centrifuge tube (figure 4.14). This showed that the presence of melanin altered the density as well as the colour of the of the melanosome fraction. Each fraction obtained was assessed by light microscopy and by fluorescence confocal microscopy, whilst purity of the melanosome fraction was ascertained by TEM.

Figure 4.14: Cells Fractions Extracted from Amelanotic / Melanotic Cell Lines

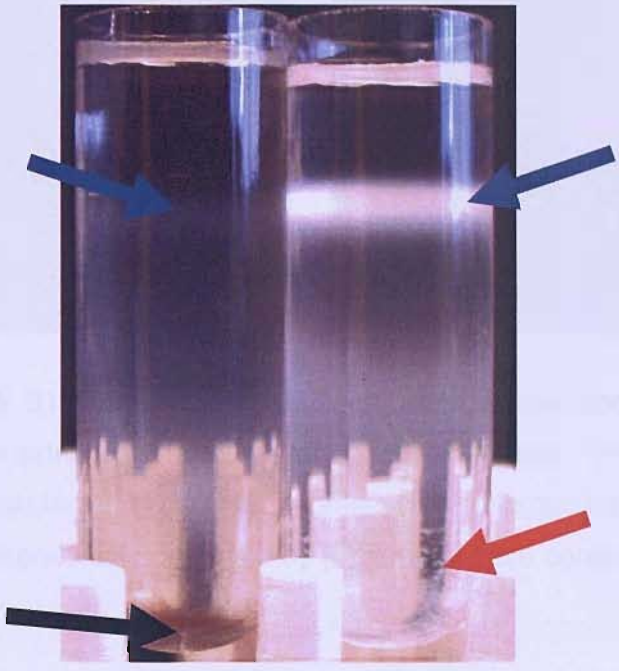

Legend for figure 4.14: The picture demonstrates sucrose density gradient ultracentrifugation of the B16F10 cells (left), and a B16MCWT-Ctag cell line (right). The strong white band at the top of each tube represents separated mitochondria (blue arrow). The B16F10 cells yielded a brown / black pellet at the base of the tube (black arrow), whilst the B16MCWT-Ctag cells produced a diffuse band near to the base of the tube with white particles in suspension (red arrow).

The melanosome-enriched cell extracts obtained from the two B16MCWT-Ctag and B16MC294-Ctag transfectants were observed by fluorescence microscopy, and each contained small clusters of green fluorescent particles. This suggested the presence of MC1R-eGFP within the melanosome-enriched suspension. The melanosomes from these cell lines were extracted and examined on four separate occasions (figure 4.15).

In contrast, the untransfected B16F10 and the Cloudman S91 cells did not exhibit green fluorescence when observed by fluorescence microscopy (data not shown) which was expected due to the absence of MC1R-eGFP.

Figure 4.15: Presence of MC1R-eGFP within Melanosomes Purified from B16MCWT-Ctag Transfectants

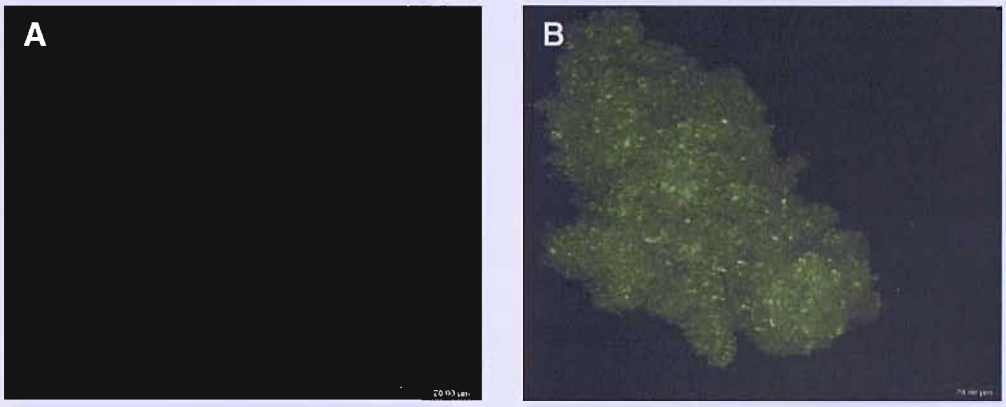

Legend for figure 4.15: B16MCWT-Ctag cells were homogenised and melanosomes were purified from cell extracts by sucrose density centrifugation. Enriched melanosomes were visualised by (a) phase contrast light microscopy and MC1R-eGFP emitting green fluorescence was observed by (b) fluorescence confocal microscopy.

Immunofluorescent labelling of Trp-1 (using αPEP-1 / A633) was then carried out on each melanosome-enriched fraction obtained from the control B16F10 cells, and the two B16MCWT-Ctag and B16MC294-Ctag cell lines. This was done to investigate co-localisation of red fluorescence from Trp-1 labelling of melanosomes with the green fluorescence of MC1R-eGFP. It was also necessary to demonstrate the presence of Trp-1 and the absence of co-localisation in the untransfected B16F10 cells, which was due to the absence of green fluorescence in these melanosome-enriched fractions. Fluoresence microscopy and confocal microscopy showed that the melanosome extracts obtained from the B16F10 cells produce high intensity red fluorescent labelling of Trp-1, similar to that observed in the two B16MCWT-Ctag and B16MC294-Ctag transfectants. The B16MCWT-Ctag and B16MC294-Ctag cell lines each demonstrated

co-localisation between the green (MC1R-eGFP) and red (Trp-1) fluorescence (figure 4.16).

Figure 4.16: Immunofluorescent Labelling of Trp-1 in Melanosome Fractions Exhibiting Green Fluorescence

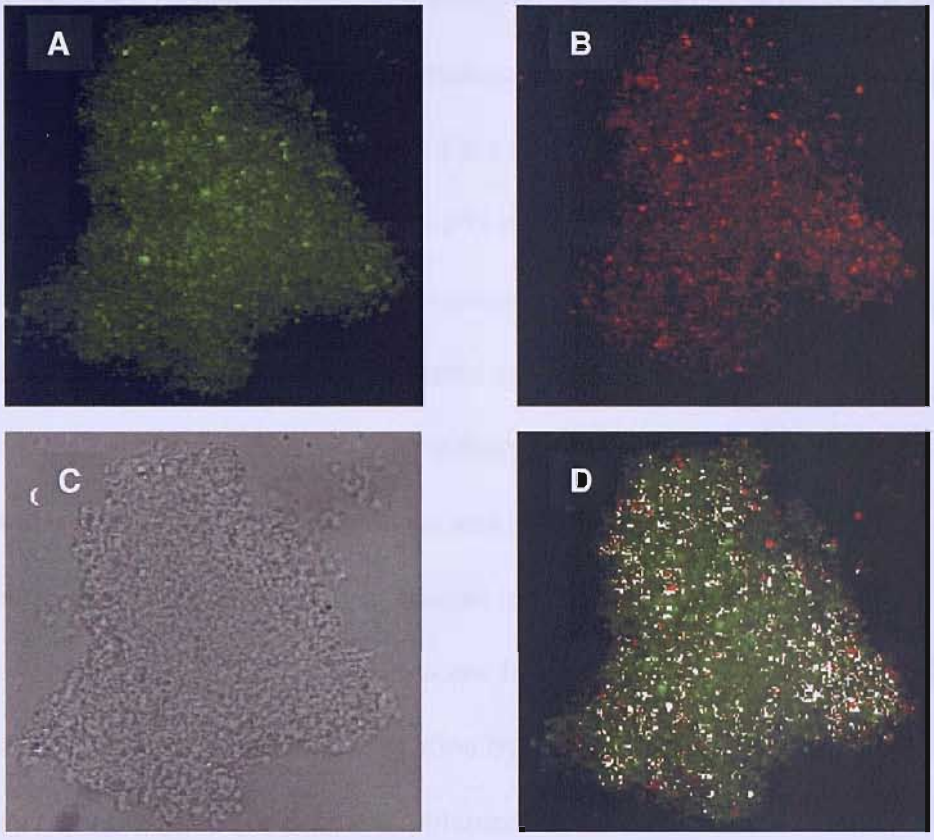

Legend for figure 4.16: The melanosome-enriched fractions exhibited (A) green fluorescence and (B) Trp-1 labelling (in red). (C) A transmitted light image was captured to show the same cell extract containing melanosomes. (D) Represents a composite 3D image of the A and B together. Areas of co-localisation are represented by the white pixels (determined by Leica confocal microscopy software). Notably some areas of green fluorescence did not co-localise with the Trp-1 labelling which indicated the presence of other cellular debris.

TEM was used to assess the purity of each melanosome fraction. This confirmed the presence of melanosomes in each cell extract however it identified the presence of cell debris. Further to a personal communication with Professor V. Hearing, melanotic cells were utilised in order to extract a better yield of melanosomes. Therefore B16F10 cells were stably transfected with the same wild-type MC1R-eGFP construct as previously

used for the B16MCWT-Ctag cell lines (the new B16F10 / wild-type MC1R-eGFP transfectants were generated in collaboration with Dr S. Robinson). The melanosomes were extracted from these B16F10 / wild-type MC1R-eGFP on three separate occasions using the same melanosome extraction method as before, however the addition of 10^{-6} M αMSH increased melanin production (observed as blacker cell pellets) and aimed to increase the yield of melanosomes. The melanosome-enriched pellet was brown / black in colour, and was positioned at the base of the ultracentrifuge tube as previously observed with the B16F10 and Cloudman S91 melanosome extractions. The TEM demonstrated an improved yield of melanosomes as can been seen in figure 4.17. However, some intracellular debris was noted amongst the melanosomes despite efforts to improve the purification process. The melanosome-enriched cell extracts were observed under a fluorescence microscope and this confirmed the presence of green fluorescence, however notably with a reduced level of fluorescence intensity compared to the previous B16MCWT-Ctag melanosome fractions (see figures 4.15 and 4.16). This was believed to be due to the absorption by melanin of excitatory visible light. The melanosome-enriched cell extracts obtained from the B16F10 cell lines (stably transfected with wild-type MC1R-eGFP) were observed by fluorescence confocal microscopy, which also confirmed the presence of green fluorescence (figure 4.18). The purified melanosomes stained strongly positive for the melanosome marker Trp-1, and significant co-localisation of MC1R-eGFP with Trp-1 was observed, confirming the presence of MC1R at the melanosome (figure 4.19). Concomitant staining for stage II – IV melanosomes (Trp-1) demonstrated co-localisation of wild-type MC1R-eGFP with melanosomes along dendrites within the transfected B16F10 lines (figure 4.19).

Figure 4.17: Purification of Melanosomes from Melanotic B16F10 Transfectants Containing Wild-type MC1R-eGFP

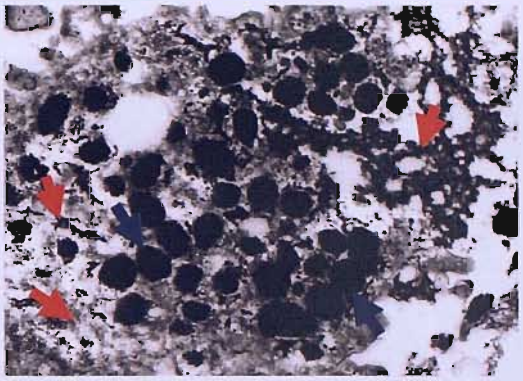

Legend for figure 4.17: TEM of heavily melanised stage IV melanosomes (blue arrows) derived from melanotic B16F10 melanoma cells stably transfected with wild-type MC1R-eGFP. Closer inspection of the TEM image showed that some other cell debris was present including rough ER (red arrows).

Figure 4.18: Green Fluorescence Observed within Melanosome Extracts from the B16F10 Transfectants Containing Wild-type MC1R-eGFP

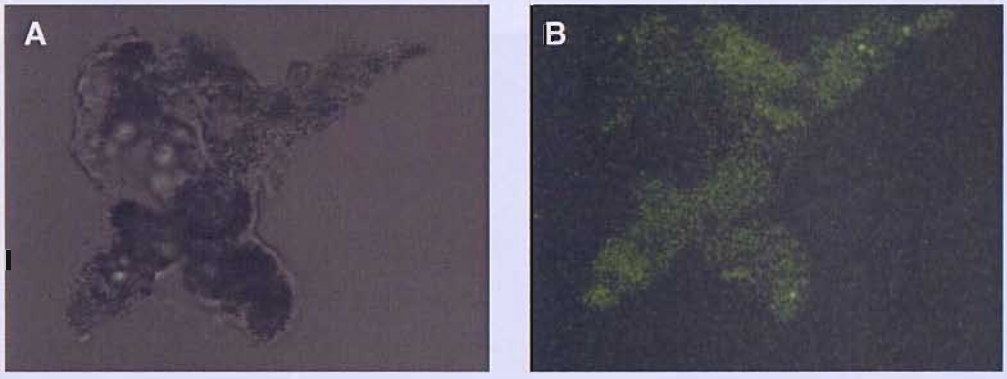

Legend for figure 4.18: B16F10 cell, stably transfected with wild-type MC1R-eGFP were homogenised and melanosomes were purified from cell extracts by sucrose density centrifugation. Enriched melanosomes were visualised by confocal microscopy (A) represents a transmitted light 3D image, (B) demonstrates green fluorescence emitted by the same cluster of cell extract containing an enriched population of melanosomes.

Figure 4.19: Co-localisation between MC1R and Stage II – IV Melanosome along Dendrites within B16F10 Transfectants Containing Wild-type MC1R-eGFP and in Melanosome Enriched Extracts

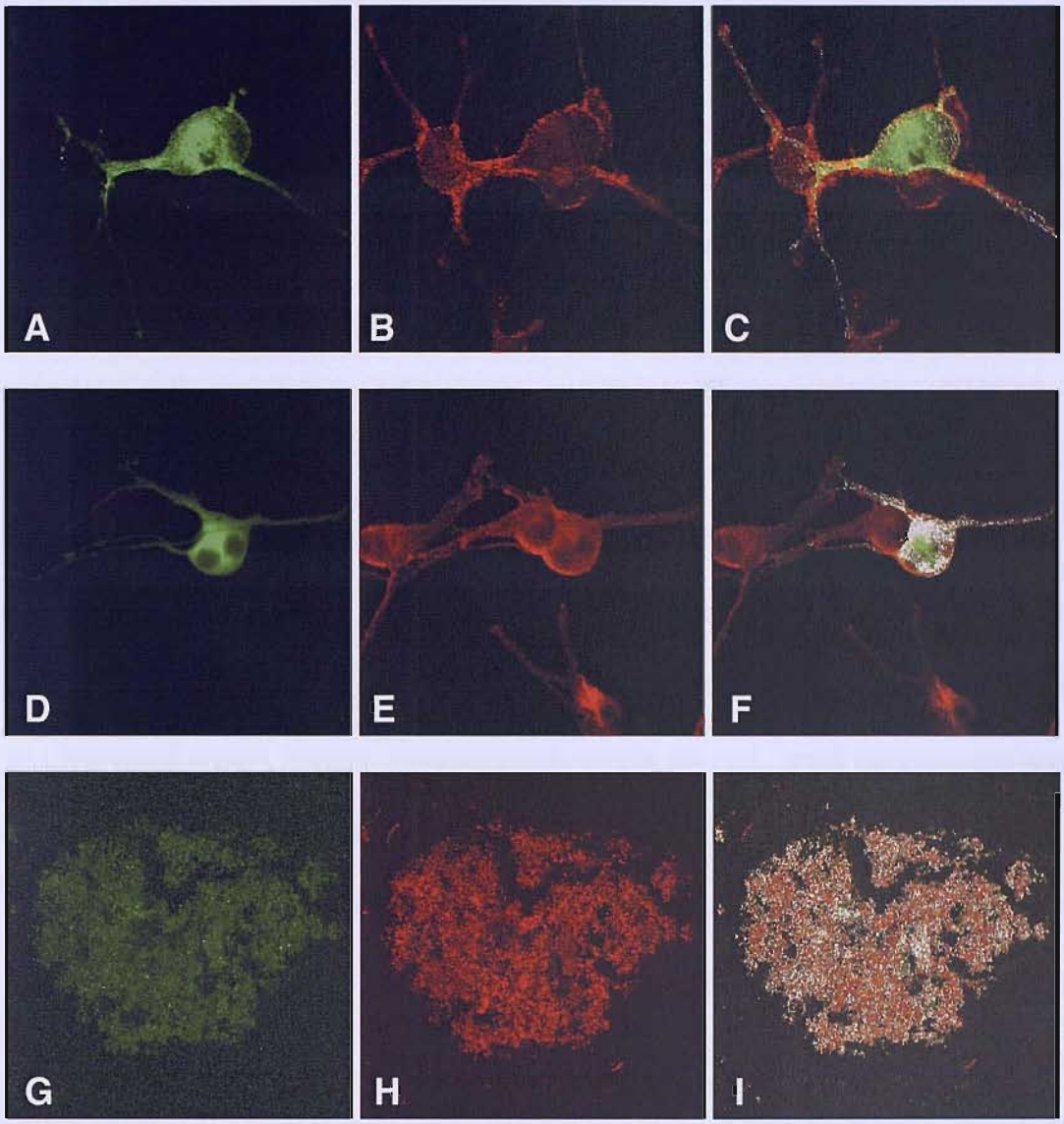

Legend for figure 4.19: Wild type MC1R is present in melanosomes in B16F10 transfected cells. Co-localisation of wild-type MC1R-eGFP with Trp-1 / A633 along dendrites (A – C and D – F) on confocal microscopy as depicted by white pixels in panels C and F respectively. Melanosomes isolated by sucrose density gradient show presence of MC1R-eGFP (G) and Trp-1 (H) on confocal microscopy with significant co-localisation (white pixels in I), indicating that MC1R-eGFP localises to the melanosome.

4.4 Discussion

The subcellular localisation of eGFP tagged human wild-type and Asp294His variant MC1R were investigated separately in stably transfected B16G4F cell lines. A fluorescence confocal microscope was utilised in order to visualise the green fluorescence emitted by the B16MCWT-Ctag and B16MC294-Ctag transfectants, which demonstrated that the eGFP-labelled wild-type and Asp294His variant MC1R were similarly distributed in a punctate pattern of green fluorescent particles within the cytoplasm with prominence at the plasma membrane. This organisation of MC1R-eGFP was notably different to that observed within the control cells transfected with the eGFP vector alone (shown within chapter 3), which exhibited green fluorescence throughout the entire cytoplasm and nucleus. The presence of a punctuate pattern of green fluorescence within the cytoplasm demonstrated that the eGFP-labelled MC1R was contained within specific compartments within the cell, green fluorescence was also accentuated at the plasma membrane indicating that the MC1R-eGFP could also successfully traffic to the outer cell membrane. The exclusion of MC1R-eGFP from the nucleus was not unexpected since there have been no previous reports describing the presence MC1R at this site. Evidence for ligand binding by the receptor (contained within chapter 3) complemented the confocal microscope finding of green fluorescence accentuation at the plasma membrane. Furthermore, an ELISA for the detection of cAMP was used to demonstrate that the B16G4F transfectants retaining at least partial cAMP signalling, following the addition of αMSH, despite the presence of eGFP at the C-terminus of MC1R.

Co-localisation experiments aimed to locate the position of MC1R-eGFP in cells that emitted a sufficient level of green fluorescence. The B16MCWT-Ctag transfectants demonstrated the co-localisation of green fluorescence with a number of intracellular

organelles including ER and golgi apparatus. This was predictable as it was expected that during the synthesis of MC1R-eGFP, the receptor would process through the ER and golgi network. More interestingly, both the wild-type and variant Asp294His MC1R demonstrated co-localisation with gp100 and Trp-1, which are proteins that are abundant in early and late stage melanosomes respectively. Authors have previously described how melanosomes arise from coated vesicles derived from the golgi apparatus which associate with lysosomes to share a common biosynthetic pathway (Diment *et al.*, 1995; Maul and Brumbaugh, 1971; Zhou *et al.*, 1993). Furthermore, the immature melanosome incorporates gp100 and Trp-1 proteins from the ER and the trans-golgi network during their maturation. Proteomic analysis of purified melanosomes determined that many proteins typically found within the ER, lysosome and golgi are also present within these organelles (Basrur *et al.*, 2003). It is conceivable that since the MC1R-eGFP co-localises with ER and golgi proteins, the receptor may be taken into melanosomes during the maturation process of the organelle. To add strength to the argument for MC1R at the melanosome, the MC1R ligand αMSH is present within early melanosomes as shown by proteomics (Basrur *et al.*, 2003) and immunohistochemistry (Peters *et al.*, 2000). The Trp-1 labelling co-localised more strongly with MC1R-eGFP and suggested that late melanosomes contain higher levels of the receptor. The conflicting proteomic analysis that did not show evidence for MC1R within the melanosome was done on early melanosomes (Basrur *et al.*, 2003) therefore MC1R may not be present in early melanosomes. Due to the limited resolution of the confocal microscope, the induction of dendrites in the transfectants permitted visualisation of melanosomes along the dendrites with separation from other organelles normally present within the cell body. Interestingly, following the induction of dendrites using IBMX, the early melanosomes that were immunofluorescently labeled with gp100 co-localised more with both wild-type and Asp294His MC1R-eGFP in the B16G4F

transfectants than that previously observed in the same cells which were not stimulated with IBMX. The IBMX may have promoted the association of MC1R-eGFP with the early melanosomes, which is perhaps part of the melanosome maturation process. MC1R-eGFP co-localised to a greater extent with the late stage II – IV melanosomal marker Trp-1 which concurs with the hypothesis that MC1R may be more abundant in late melanosomes.

As an alternative approach, melanosomes were purified from the B16MCWT-Ctag and B16MC294-Ctag cell lines in order to ascertain whether clusters of melanosomes emitted green fluorescence due to the presence of MC1R-eGFP. Melanosomes enriched cell extracts were visualised by TEM in conjunction with confocal microscopy to investigate the presence of green fluorescence. The melanosome enriched extracts were observed and demonstrated green fluorescence, furthermore co-localisation was observed between MC1R-eGFP and Trp-1. However, the amelanotic B16G4F transfectants proved to be impractical since the melanosome yield was relatively low and contaminating cell debris prevented the clear visualisation of 'green melanosomes', and when observing co-localisation between MC1R-eGFP and the Trp-1, some of the contaminating organelle debris may have also been labeled with Trp-1 / A633.

In order to improve the yield of melanosomes, another murine melanoma cell line was employed. Melanotic B16F10 melanoma cells were stably transfected with the same MC1R-eGFP construct as used for the B16MCWT-Ctag cell lines (done in collaboration with Dr S. Robinson). The subcellular fractionation of these melanotic B16F10 transfectants enabled the more efficient purification and a greater yield of melanosomes. The purity of the melanosomes was verified by TEM, and fluorescence confocal microscopy confirmed the presence of a green fluorescent signal. The green

fluorescence of the melanosomal extract of the melanotic B16F10 transfectants was notably less intense than the green fluorescence observed from the melanosomes extracted from the amelanotic B16G4F transfectants, which suggested that the presence of melanin in the B16F10 transfectants absorbed visible light and reduced the green fluorescence emission observed. However, the green fluorescence emitted by the B16F10 melanosome extracts was sufficient to observe co-localisation between MC1R-eGFP and the Trp-1 labelled stage II – IV melanosomes. Similarly, when the B16F10 cells were made dendritic by the addition of IBMX, there was co-localisation between the MC1R-eGFP and the Trp-1 along the dendrites. Immunogold labelling of MC1R-eGFP, was carried out on a number of occasions in house (by Dr A. Page) utilising anti-eGFP and anti-MC1R antibodies, however this failed to demonstrate the presence of MC1R at melanosomes within fixed cell preparations containing the B16F10 transfectants, and due to time and cost restrictions this route of investigation was not continued. However, without the Immunogold labelling of MC1R at the melanosome there is strong evidence to suggest that MC1R is present at or within melanosome organelles. The previous work by (Peters *et al.*, 2000) in conjunction with my results suggest that αMSH may signal through MC1R at the melanosome rather independently of the melanocortin receptors at this organelle. Further work is required to address the exact role of MC1R at the melanosome. However the hypothesis that MC1R is present at the melanosome suggests that MC1R receptors may control the morphology of the melanosome, and in conjunction with cAMP signalling from MC1R at cell surface, may play a different role in orchestrating the synthesis of eumelanin and phaeomelanin within pigment cells.

Chapter 5

Investigating MC1R internalisation

5.1 Introduction

Receptor internalisation is an endocytosis mediated mechanism that regulates the cell surface expression of many GPCRs. Following internalisation, the receptor bound agonist is either separated from the active receptor, which permits the recycling of receptors back to the plasma membrane via endosomes, or the receptor remains bound to ligand and is desensitised, or alternatively the receptor becomes down regulated from the cell surface to be broken down by lysosomes. These mechanisms have been documented in a number of 7-pass transmembrane GPCRs. The binding of agonist to the GPCR initiates phosphorylation of the G protein via GPCR kinases. Hence the G protein is uncoupled and the subsequent transient binding of arrestin proteins sterically obstructs G protein re-coupling to the receptor, which initiates internalisation of the GPCR via endocytotic vesicles (McArdle *et al.,* 2002). The internalisation of the thyrotropin-releasing hormone receptor (TRHR) has been documented in a number of studies, although these are based on the assumption that the ligand remains bound to the receptor. For example, one study utilised fluorescently labelled ligand to demonstrate ligand-TRHR internalisation and separately radio-ligand binding studies have suggested that the receptor can recycle to the cell surface in various murine cell models (Ashworth *et al.,* 1995; Petrou *et al.,* 1997; Yu *et al.,* 1998). The beta-2-adrenergic receptor (β_2AR) and the gonadotropic hormone receptor (GnRH-R) are thought to be desensitised via internalisation following sustained ligand binding, which has been shown by a decrease in cAMP signalling in both cases (Pitcher *et al.,* 1992; Su *et al.,* 1979). More recently, the internalisation of GnRH-R was observed by direct tagging of the receptor at the C-terminus with eGFP, which also confirmed that despite the presence of eGFP at the C-terminus, receptor functional and rate of internalisation was

not compromised (Hashizume *et al.*, 2001; Nelson *et al.*, 1999; Horvat *et al.*, 2001). Studies have demonstrated the rapid internalisation and desensitisation of the cysteinyl leukotriene type 1 receptor (CysLT1R), which is thought to involve the production of a Ca^{2+} signal by the receptor. Naik *et al.*, (2005) have suggested that CysLT1R internalisation is somehow controlled by a PKC-dependent system rather than the arrestin binding mechanism. However, the study of receptors such as type I Angiotensin II, and endothelial differentiation gene-1, has caused other researchers to suggest that the PKC plays a role in agonist induced receptor phosphorylation, but does not directly cause receptor internalisation (Vinson *et al.*, 1995; Watterson *et al.*, 2002).

The melanocortin receptors MC2R and MC4R have been shown to possess internalisation, desensitisation and recycling capabilities (Baig *et al.*, 2002; Gao *et al.*, 2003). The internalisation and desensitisation of MC2R has been demonstrated in adrenocortical Y1 cells following ACTH binding, with evidence to suggest that this receptor's internalisation mechanism is caused by the phosphorylation of a GPCR kinase (Baig *et al.*, 2002). Interestingly, an *MC2R* mutation was reported that resulted in the constitutive activation of this receptor and impaired receptor desensitisation following internalisation, this has lead these researchers to suggest that impaired desensitisation with enhanced basal activity of the receptor may be involved in the pathology of Cushing's syndrome (Swords *et al.*, 2002). The internalisation and recycling of human MC4R has been demonstrated in HEK293A transfectants by directly tagging the wild-type and mutant MC4R with eGFP. This has permitted visualisation of agonist induced receptor endocytosis by use of confocal microscopy (Blondet *et al.*, 2004; Gao *et al.*, 2003; Shinyama *et al.*, 2003). Gao *et al.*, (2003) initially demonstrated the presence of MC4R-eGFP green fluorescence at the plasma membrane of these HEK293A transfectants, with a 'chicken wire' like appearance, and its subsequent internalisation

upon receptor activation via the addition of agonist at 37°C over a 45 minute period. It was hypothesised that prolonged exposure to the agonist resulted in receptor degradation at the lysosome rather than recycling back to the plasma membrane via endosomes (Gao *et al.*, 2003). Subsequent investigations have demonstrated a lack of variant MC4R recycling to the cell membrane following ligand induced internalisation, and eGFP tagged MC4R variants containing either a CTCT-deletion, or a base change of Cys271Ala are retained intracellularly in HEK293A transfectants (Blondet *et al.*, 2004).

Some previous publications have suggested that MC1R can internalise, however these studies employed ligand binding experimental approaches, utilising either ^{125}I-βMSH or FITC tagged βMSH. Initial studies carried out on Cloudman S91 melanoma cells, demonstrated that ^{125}I-βMSH bound to the cell surface consistent with the presence of MC1R at the plasma membrane (Varga *et al.*, 1974). Subsequently, autoradiographical analysis of this melanoma cell line following exposure to ^{125}I-βMSH demonstrated the presence of discrete clusters of ligand arranged along the cell surface, which implied that the MSH receptors were spatially organised at this site (Varga and *et al.*, 1976a). The same group used FITC labelled βMSH to examine for ligand internalisation in Cloudman S91 cells, and showed co-localisation with fluorescently labelled TPPase, which is an enzyme abundant in golgi. This led these authors to suggest that βMSH exerted its effects in close proximity to the golgi, and since premelanosomes are derived from the golgi, further assumptions were made that this hormone may also in fact exert other effects in the locality of premelanosomes (Varga *et al.*, 1976b). Later work demonstrated that ferritin-labelled βMSH co-localised at premelanosomes suggesting that this hormone translocated to these sites (Lerner *et al.*, 1979). In a more recent study, Cloudman S91 cells that were incubated with ^{125}I-βMSH and subsequent

fractionation of the cells determined that ^{125}I-βMSH was present within lysosome enriched fractions, althought the ^{125}I-βMSH was absent from endosome enriched fractions (Wong and Minchin, 1996). It was therefore proposed that MC1R did not recycle back to the cell surface via these organelles, however this is based on an assumption that ^{125}I-βMSH remained bound to MC1R, and also assumes appropriate purity of fractions.

Evidence for MSH receptor internalisation also comes from the fact that B16-F1 and Cloudman S91 melanoma cell lines reduced the numbers of membrane ^{125}I-βMSH binding sites by approximately 60% after 2 hours of ligand binding and 85-90% after 10-20 hours of ligand binding (Siegrist *et al.*, 1988; Siegrist *et al.*, 1989). By contrast, in other experiments MSH peptides have also been shown to cause an increase or up-regulation of MSH binding sites at the cell surface. For example the human D10 and 205 melanoma cell lines both demonstrated increased ^{125}I-αMSH binding at 37°C after 24 hours of incubation of ^{125}I-αMSH (Eberle *et al.*, 1993; Siegrist and Eberle 1993). Indeed, other work has shown that UVB irradiation of Cloudman S91 cells (possessing wild-type MC1R) resulted in a decrease in intracellular ^{125}I-βMSH binding sites with a concomitant increase in external ^{125}I-βMSH binding sites, suggestive of receptor redistribution to the plasma membrane (perhaps to increase the cellular responsiveness to the MSH hormones) (Chakraborty *et al.*, 1991). Other researchers have suggested that MC1R may internalise based on their observations using an in house anti-MC1R antibody. In that study, the intracellular presence of MC1R in normal sebaceous glands and hair follicles, and also in various malformations / neoplasms of the skin, was detected with a FITC labelled anti-MC1R antibody (Böhm *et al.*, 1999; Stander *et al.*, 2002). These authors considered the intracellular granulated staining pattern of MC1R to represent receptor trafficking up to the cell surface or MC1R internalisation. MC1R

was also found to be present within intracellular endosomes of skin sebocytes using TEM, which suggested the possibility of MC1R recycling (Stander *et al.*, 2002). However these assumptions are based on the antibody staining pattern being specific for MC1R.

Whilst the evidence presented to date suggests that the wild-type MC1R may internalise, it would be preferable to visualise internalisation based on evidence from direct tagging of this receptor with eGFP. It is also unknown whether the MC1R variants, especially the Arg151Cys, Arg160Trp and Asp294His MC1R variants, which have reduced function can internalise. Orlow *et al.*, (1990) compared Cloudman S91 cells (expressing wild-type MSH receptors) and Cloudman S91 cells that had an impaired response to βMSH (assumed to be variant MSH receptors), and demonstrated both cell types had similar ^{125}I-βMSH binding sites at the cell surface, whereas the cells containing the variant receptors had a reduced number of intracellular MSH binding sites. Further investigation showed that there were reduced numbers of intracellular binding sites in the Cloudman S91 cells that possessed the less responsive MSH receptors, which suggested that the wild-type receptors may internalise to a greater extent than the variant MSH receptors. Therefore, in the current study the ability of wild-type and variant MC1Rs to internalise was investigated using an experimental approach which improved upon previous investigations on this topic.

5.2 Materials and Methods

The internalisation of MC1R was investigated using three separate approaches including: 1) the use of eGFP direct tagging of receptors, 2) the generation of cell lines containing untagged MC1R for the purpose of observing the internalisation of a FITC-αMSH fusion protein, and 3) the use of ligand binding experimental techniques to demonstrate cell surface and intracellular binding sites. As well as investigating wild-type MC1R internalisation using each of these approaches this study compared the internalisation wild-type and Asp294His variant MC1R transfected.

5.2.1 Generation of Stable HEK293A Transfectants Containing Human Wild-type and Asp294His MC1R-eGFP

Human embryonic stem cells (HEK293A) were stably transfected with human wild-type MC1R-eGFP and separately with human Asp294His variant MC1R-eGFP in order to permit the visualisation / internalisation of these receptors. The purified constructs named N3MCWT and N3MC294 respectively (described within chapter 3, figures 3.2 and 3.4) were linearised with *Vsp* I (also known as *Ase* I) prior to their separate transfections into the HEK293A cells by electroporation using a Biorad Gene Pulser II (2.13). Stable transfectants were cultured long term in the presence of G418 antibiotic, which selected for the transfected cells containing the construct. These cell transfectants were referred to as HEKMCWT-Ctag and HEKMC294-Ctag, and ten individual clones from each transfected line used to investigate internalisation.

5.2.2 Construction of Non-Tagged Human Wild-type MC1R, Stable Transfection of the B16G4F Melanoma Cells

The pEGFP-N3 vector (described within chapter 3) was used to create an untagged *MC1R* construct. The *eGFP* was excised from the pEGFP-N3 vector using the restriction enzymes *Hind* III and *Not* I which cut the *Hind* III and *Not* I restriction sites that flanked the eGFP sequence within the vector. The pEGFP-N3 vector (without eGFP) was visualised by gel electrophoresis using visible light / SYBR green system (free of ultraviolet irradiation and ethidium bromide to prevent vector mutation). PCR amplification (2.8) of human wild-type *MC1R* permitted the incorporation of *Hind* III and *Not* I restriction enzyme sites (using the MC1FW forward primer and MC1*Not*RVN3 reverse primer (table 5.1) respectively) to allow ligation of this insert into engineered pEGFP-N3 vector (eGFP removed). Competent *Top10* cells (2.2.2) were transformed with the untagged pEGFP-N3 / MC1R construct and grown on LB agar in the presence of 10 μg/ml kanamycin (appendix 1.1). Single colonies were selected and expanded for further experiments and this untagged wild-type *MC1R* construct was designated as N3-MCWT.

Table 5.1: Primers for Amplification of MC1R with Restriction Sites

Primer Name	Direction	Sequence and restriction site
MC1FW	Forward	5′ *Hind* III 3′ ggcctgaagcttactatggctgtgcaggga
MC1NotRVN3	Reverse	5′ *Not* I 3′ ttttccttttgcggccgctcaccaggagcatgtcagcacc

The N3-MCWT construct containing untagged human wild-type *MC1R* was sequenced to ensure that no deletions, insertions or mutations were present, and then purified using Qiagen midipreps (2.3.2) for stable transfection into B16G4F melanoma cells. The N3-MCWT construct (figure 5.1) was linearised using the restriction enzyme *Vsp* I for stable transfection into the B16G4F cells (by electroporation using the Biorad Gene Pulser II). Cell transfectants were cultured long term in the presence of G418 antibiotic, to ensure that the transfectants retained the *MC1R* gene.

Figure 5.1: Diagrammatic Representation of the Untagged MC1R Construct

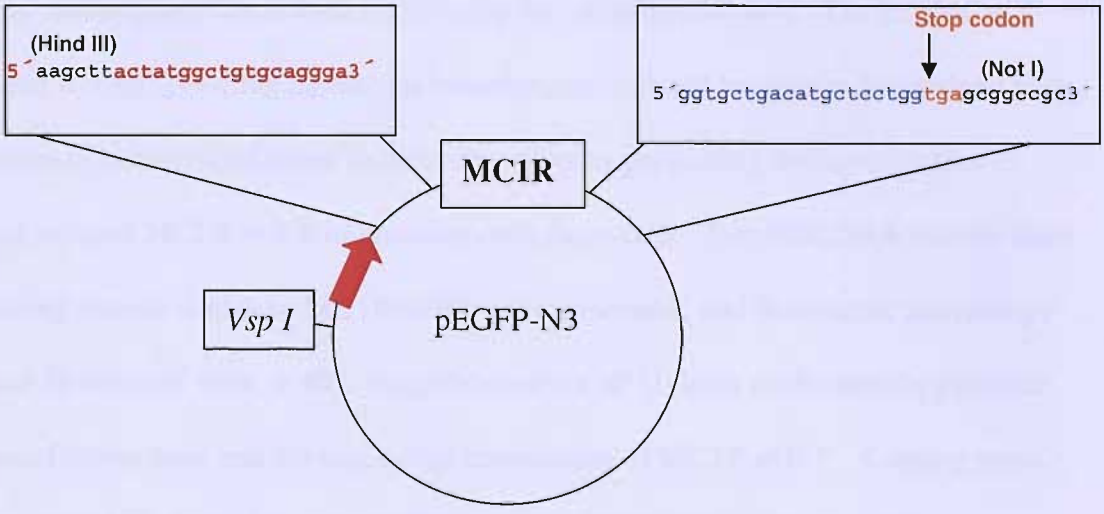

Legend for figure 5.1: Human wild-type *MC1R* was ligated into the pEGFP-N3 vector between restriction enzyme sites Hind III and Not I (shown in black). The eGFP sequence of the parent vector had been previously excised at these flanking Hind III and Not I restriction enzyme sites. The sequences flanking the *MC1R* insert are highlighted in red / blue, and the 3 prime sequence contained a stop codon (shown in orange). Other features include the CMV promoter (red arrow), and the Vsp I enzyme site which was utilised to linearise the vector for stable transfection experiments.

5.3 Results

5.3.1 Stable Transfection and Characterisation of HEK293A Cells with Human Wild-type and Asp294His MC1R-eGFP

The human embryonic kidney (HEK293A) cell line was stably transfected with wild-type and separately the Asp294His variant *MC1R*, tagged at the C-terminus with eGFP for the purpose of investigating the internalisation of these receptors. This approach had previously been implemented by Gao *et al.*, (2003) who reported on MC4R-eGFP internalisation in HEK293A cell transfectants, which was observed as a punctate pattern of intracellular green fluorescence following the addition of ligand. The B16MCWT-Ctag and B16MC294-Ctag melanoma transfectants outlined in chapter 3 contained high quantities of intracellular green fluorescence thereby preventing the investigation of agonist induced MC1R-eGFP internalisationin those cells. Ten HEK293A transfectants containing human wild-type MC1R-eGFP were generated, and fluorescent microscopy (at least 10 fields of view at 40 x magnification) of all 10 lines confirmed the presence of green fluorescence and the successful transfection of MC1R-eGFP. A strong green fluorescence was emitted in at least 20% of cells. Confocal microscopy of two HEKMCWT-Ctag cell lines (HEKMCWT-Ctag-1 and HEKMCWT-Ctag-9) confirmed the punctate pattern of green fluorescence throughout the cytoplasm. These HEKMCWT-Ctag transfectants displayed strong green fluorescence at the plasma membrane, and the punctate pattern of intracellular green fluorescence was also seen throughout the cytoplasm. Similarly, ten HEK293A cell lines containing human Asp294His variant MC1R-eGFP were generated (in collaboration with Dr S. Robinson) and fluorescence microscopy confirmed a similar pattern of green fluorescence with membrane accentuation and an intracellular punctate pattern. These HEKMC294-Ctag cell lines commonly exhibited strong green fluorescence within approximately 20% of the cells. Confocal microscopy of two HEKMC294-Ctag cell lines (HEKMC294-Ctag-

4 and HEKMC294-Ctag-9) confirmed exaggerated cell membrane accentuation of green fluorescence and the punctate pattern of fluorescent particles throughout the cytoplasm (figure 5.2).

Figure 5.2: Confocal microscopy of the HEKMCWT-Ctag and HEKMC294-Ctag transfectants.

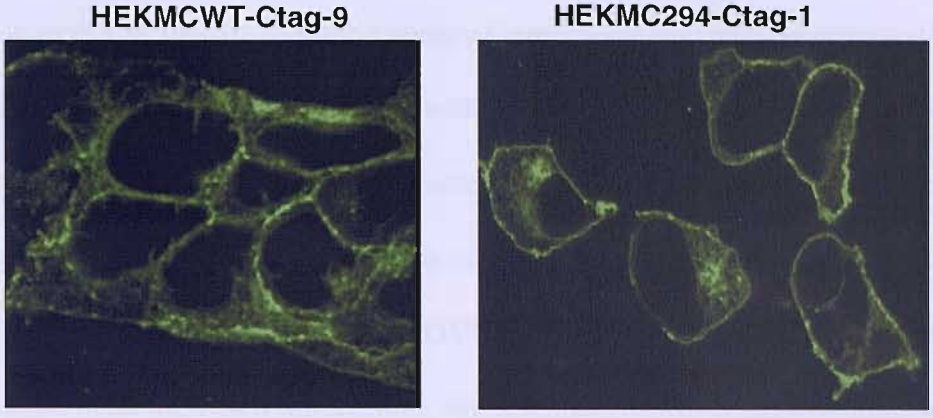

Legend for figure 5.2: Confocal microscope images of HEKMCWT-Ctag and HEKMC294-Ctag transfectants. Each line exhibited bright green fluorescence at the cell surface, but some also emitted intracellular fluorescence.

5.3.2 Internalisation of FITC-αMSH in Untagged MC1R Transfectants

The HEKMCWT and HEKMC294 cell lines were utilised to internalise green fluorescence upon the addition of ligand. Both cell lines were incubated at 37°C with and without αMSH (10^{-6} M) and observed at 5, 10, 15, 30 and 45 minutes by fluorescence microscopy (figure 5.3). No definite increase in fluorescence within the cytoplasm was seen in the wild-type *MC1R* transfected and variant *MC1R* transfected HEK293A cells. Confocal microscopy was also employed to look for evidence of internalisation, but following the addition of αMSH (10^{-6} M) for 30 and 45 minutes there was no evidence of a definite increase in internalisation. Although following αMSH treatment some cells contained brighter green particles, these bright green fluorescent particles were also apparent within other unstimulated clones. In case the intracellular fluorescence had arisen as a result of earlier internalisation, due to the

presence of αMSH in the FBS during cell culture, the HEKMCWT-Ctag-9 and HEKMC294-Ctag-4 cell lines were cultured separately with 0%, 1%, 5%, and 10% FBS to see whether the pattern of green fluorescence remained consistent. The cells failed to thrive in the total absence of FBS, however in the presence of 1% and 5% FBS the cells looked similar to those cultured in 10% FBS and continued to display intracellular green fluorescence. As an alternative approach, the HEKMCWT-Ctag-9 cells were pre-treated with 0.3 M sucrose to inhibit receptor internalisation (method obtained from Gao *et al.*, 2003). Following pre-treatment with 0.3 M sucrose in two separate experiments, the HEKMCWT-Ctag-9 cells appeared similar in appearance to the untreated controls and continued to demonstrate high levels of intracellular fluorescence. In addition, the super potent analogue of αMSH, NDP-αMSH, was substituted for αMSH to see whether this resulted in an increased intracellular fluorescence, however the appearance of the cells remained unchanged on two separate occasions when NDP-αMSH (10^{-6} M) was added for 45 minutes (figure 5.4). Therefore this experimental approach was not continued and the use of a synthetic FITC labelled αMSH fusion protein was employed to further investigate the internalisation characteristics of MC1R.

Figure 5.3: Distribution of MC1R-eGFP in the HEK293A Transfectants Following the Addition of αMSH

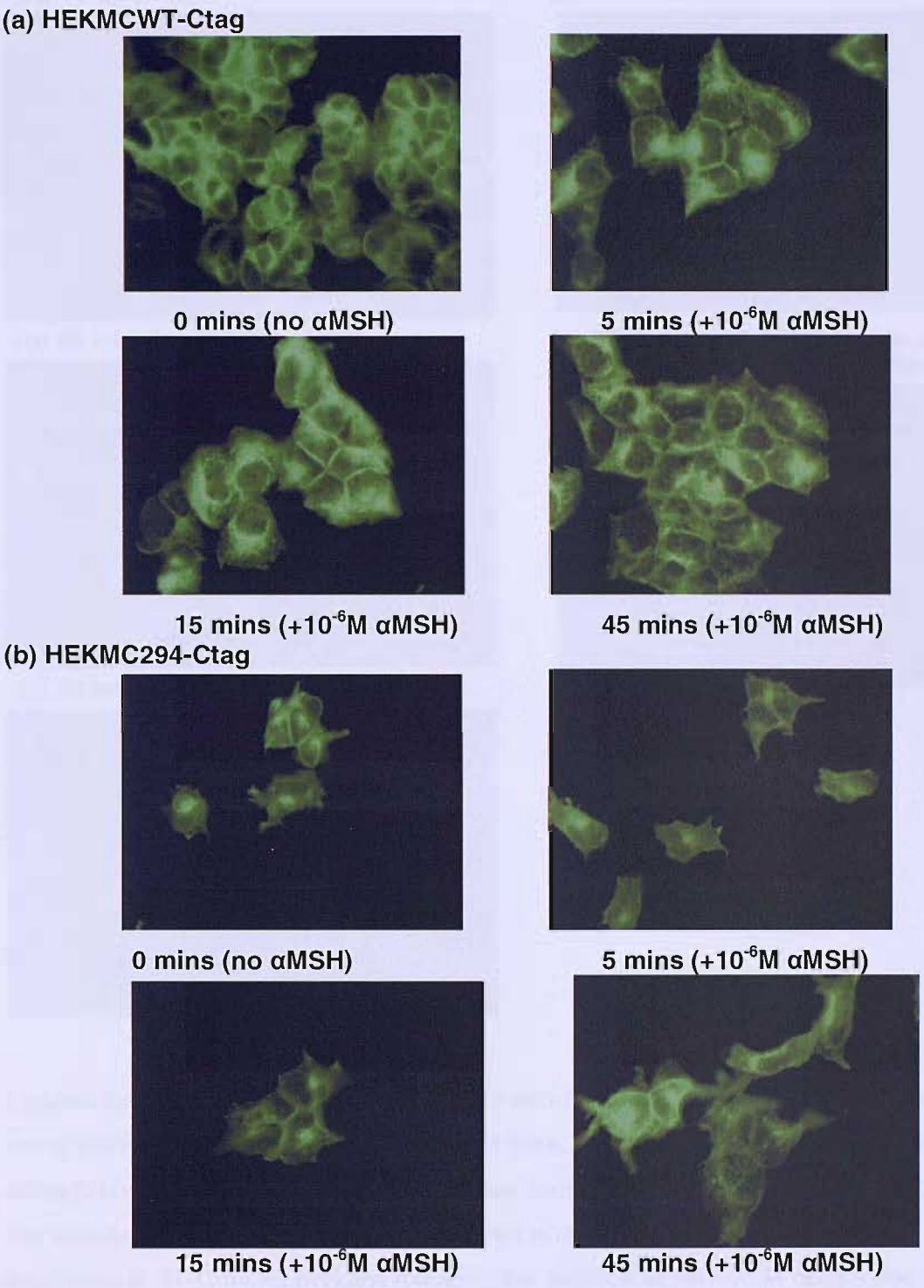

Legend for figure 5.3: Investigation of internalisation of MC1R-eGFP following the addition of 10^{-6} M αMSH in (a) wild-type MC1R-eGFP and (b) Asp294His MC1R-eGFP transfected HEK293A cells. No significant increase in intracellular wild-type or Asp294His variant MC1R-eGFP was observed following the addition of αMSH between 0 and 45 minutes.

Figure 5.4: Distribution of MC1R-eGFP in HEKMCWT-Ctag Transfectants Following the Addition of Ligand (αMSH / NDP-αMSH)

(a) No additive

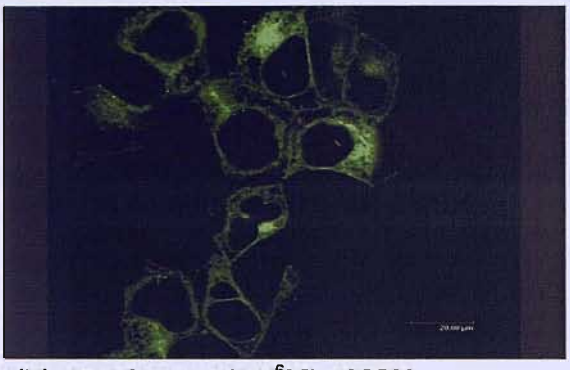

(d) 30 minutes 0.3 M Sucrose

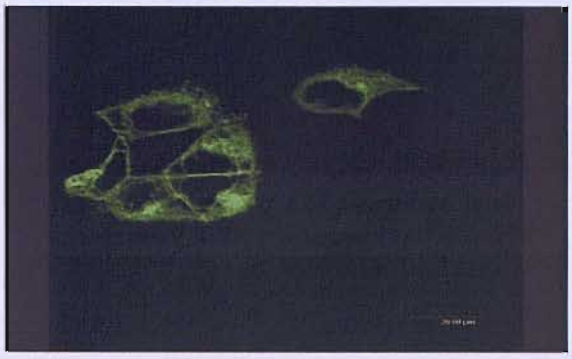

(b) 45 minutes (10^{-6}M) αMSH

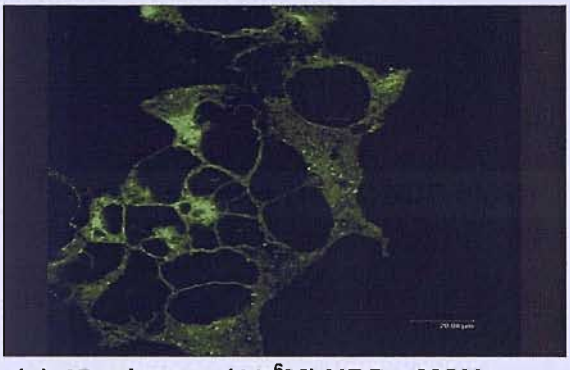

(e) 30 minutes 0.3 M Sucrose pre-treatment + 45 minutes (10^{-6}M) NDP-αMSH

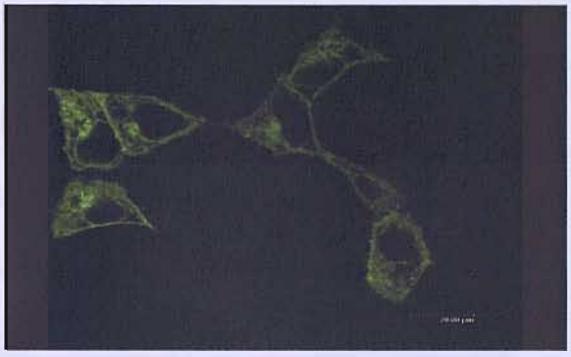

(c) 45 minutes (10^{-6}M) NDP-αMSH

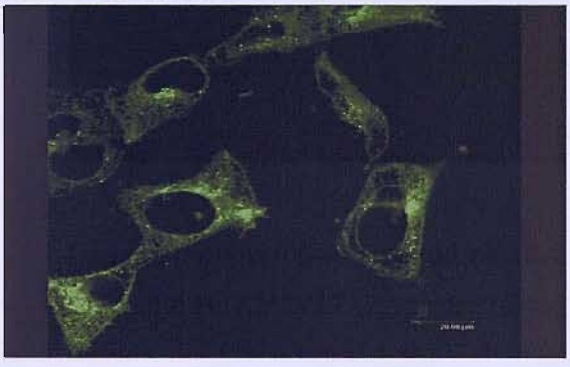

Legend for figure 5.4: The internalisation of wild-type MC1R-eGFP was investigated using the HEKMCWT-Ctag transfected cell lines. (a) Depicts untreated cells, which already contain a high level of internal green fluorescence. Further internalisation of the wild-type MC1R-eGFP was not observed when these cells were separately incubated at 37°C for 45 minutes following the addition of (b) 10^{-6} M αMSH and (c) 10^{-6} M NDP-αMSH. (d) Pre-incubation of the cells for 30 minutes with 0.3 M sucrose failed to inhibit the internalisation of wild-type MC1R-eGFP and similarly (e) following 30 minutes treatment with 0.3 M sucrose, followed by the addition of 10^{-6} M NDP-αMSH for 45 minutes.

5.3.3 Generation of Stably Transfected B16G4F Cells Containing Untagged Human Wild-type MC1R

The experiments carried out using the eGFP tagged MC1R transfected HEK293A cells did not clarify whether the wild-type and variant MC1R could internalise, therefore another experimental approach was undertaken. B16G4F melanoma cells were transfected with 'untagged' human wild-type *MC1R* to investigate MC1R internalisation in this line using FITC labelled αMSH. The B16G4F cells that were stably transfected with untagged human wild-type *MC1R* were named as B16MCWT-Untag, and thirty three clones were generated and hence given a number from 1-33. MC1R was PCR amplified and sequenced from fourteen cell lines, which confirmed the correct wild-type *MC1R* sequence in each of these lines. Three of these cell lines were characterised by ligand binding on two separate occasions (using the untransfected B16G4F and a previously transfected wild-type MC1R line, B16FWT5, as negative and positive controls respectively) (figure 5.5). Although the SD of both experiments was high, the results confirmed the presence of cell surface MC1R in these B16MCWT-Untag lines.

Figure 5.5: Competition Ligand Binding of B16MCWT-Untag Cell Lines

(a)

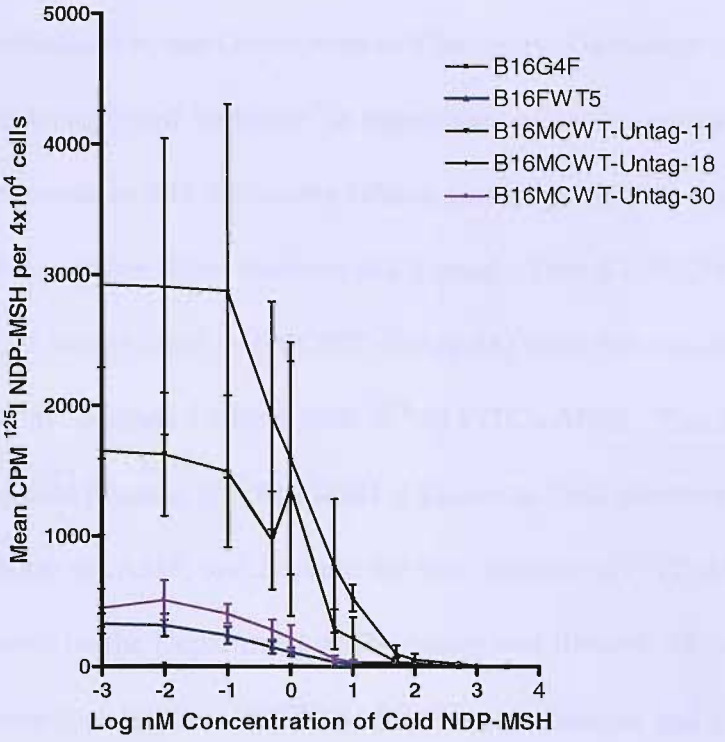

(b)

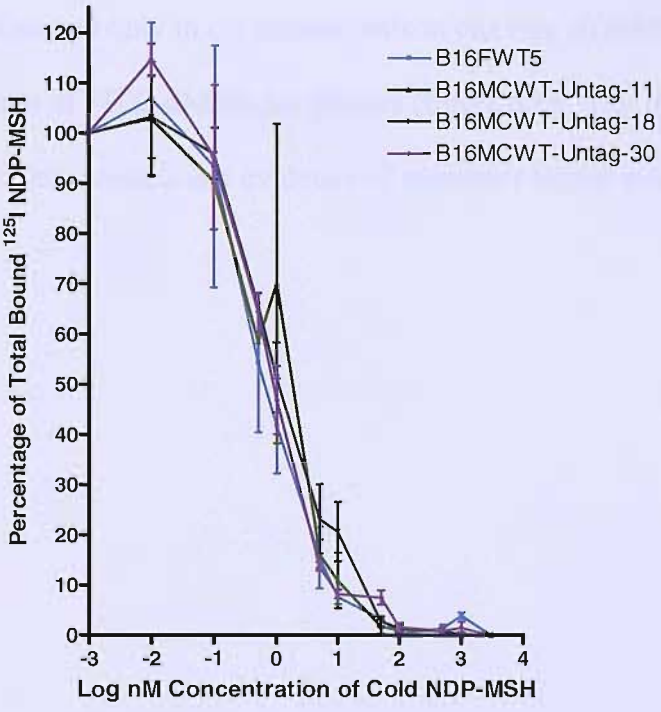

Legend for figure 5.5: Competitive radioligand binding in three B16MCWT-Untag cell lines showing ^{125}I NDP-MSH binding to MC1R in the presence of competing concentrations of cold NDP-MSH. The graphs demonstrate: a) the mean gamma counts per minute (CPM) from bound ^{125}I NDP-MSH per 4x10^4 cells, and b) The percentage of total ^{125}I NDP-αMSH bound at each concentration of cold NDP-αMSH (normalised to binding at 10^{-12} M cold NDP-αMSH). Means and standard deviations of 2 separate experiments.

5.3.4 Investigation of FITC-αMSH Internalisation in B16MCWT-Untag Cell Lines

FITC-αMSH (synthesised by the Department of Chemistry, University of Southampton) had previously been employed 'in house' in pigmentation assays, and had been shown to induce melanogenesis in S91 melanoma cells at similar potency to that of two commercial αMSH peptides (from Bachem and Sigma). Two B16MCWT-Untag cell lines (B16MCWT-Untag-11 and B16MCWT-Untag-18) were cultured on glass coverslips at 37°C in complete DMEM with 10^{-7} M FITC-αMSH. This concentration of FITC-αMSH was used because 10^{-7} M αMSH is known to bind effectively to MC1R and cause production of cAMP, and because the total amount of FITC-αMSH which had been synthesised by the Department of Chemistry was limited. However, most cells did not demonstrate evidence of FITC-αMSH internalisation, and green fluorescence was observed only in occasional cells in one line (B16MCWT-Untag-18) following the addition of FITC-αMSH for 2 hours (figure 5.6). The B16MCWT-Untag-11 cell line failed to demonstrate any evidence of receptor / ligand internalisation.

Figure 5.6: Internalisation of 10^{-7} M FITC-αMSH in B16MCWT-Untag Transfectants

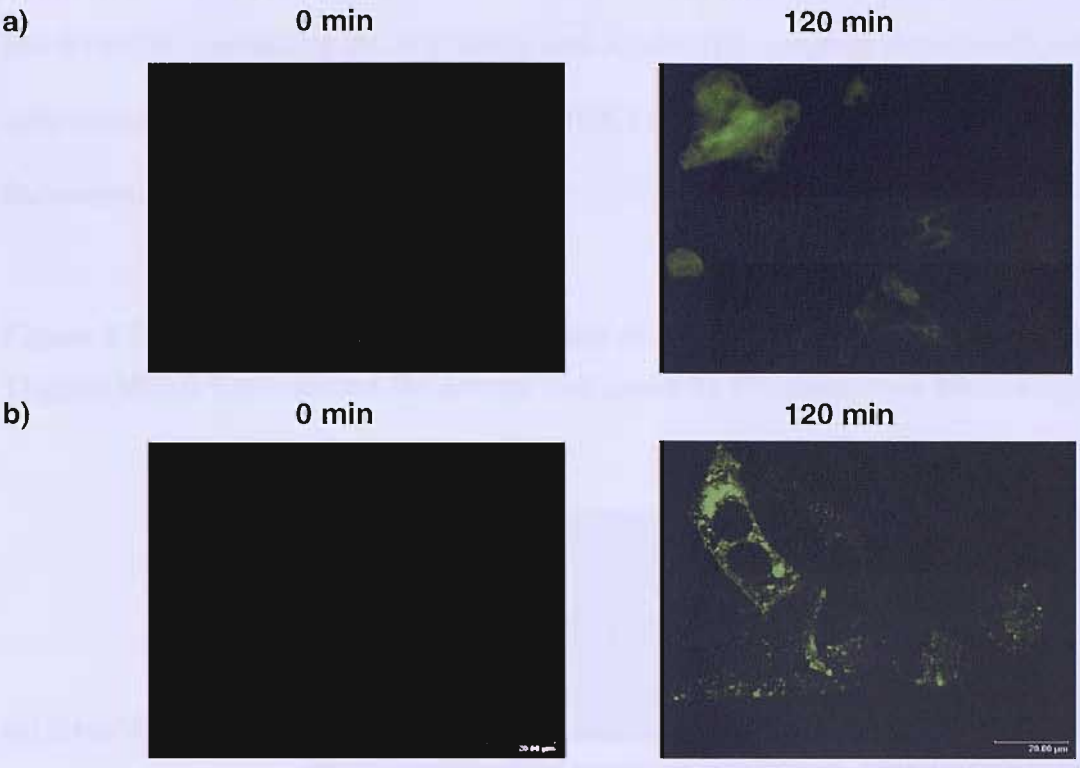

Legend for figure 5.6: B16MCWT-Untag-18 cells were incubated at 37°C with or without 10^{-7} M FITC-αMSH and observed after 120 minutes by a) fluorescence microscopy (x 40) and b) confocal microscopy (x100). Cells treated with FITC-αMSH demonstrated green fluorescence in occasional cells (0.1-0.2% of the population) at 120 minutes.

5.3.5 Internalisation of FITC-αMSH in B16G4F Cell Lines Containing FLAG Tagged MC1R

In a parallel set of experiments, stably transfected B16G4F cells, containing FLAG-tagged human wild-type *MC1R* and separately FLAG-tagged human *MC1R* variants (Arg160Trp and Asp294His), which were previously generated within the department (Robinson and Healy, 2002) were employed to investigate internalisation of MC1R using FITC labelled αMSH. These cell lines had previously demonstrated the ability to bind ligand suggesting that MC1R was present at the cell membrane (Robinson and Healy, 2002). Cells (1×10^5) were cultured overnight on glass coverslips and were incubated with 10^{-7} M FITC-αMSH for 30 minutes and 120 minutes. Overall, little evidence of internalisation was seen in two wild-type MC1R-FLAG cell lines

(B16FWT5 and B16FWT33), and two variant MC1R-FLAG transfectants (B16F160 and B16F294) containing the Arg160Trp and Asp294His receptors respectively, with only occasional cells (approximately 1 per 1000) showing some intracellular green fluorescence at 120 minutes (figure 5.7).

Figure 5.7: Investigating the Internalisation of 10^{-7}M FITC-αMSH within FLAG-Tagged MC1R Transfected Melanoma Cell Lines by Fluorescence Microscopy

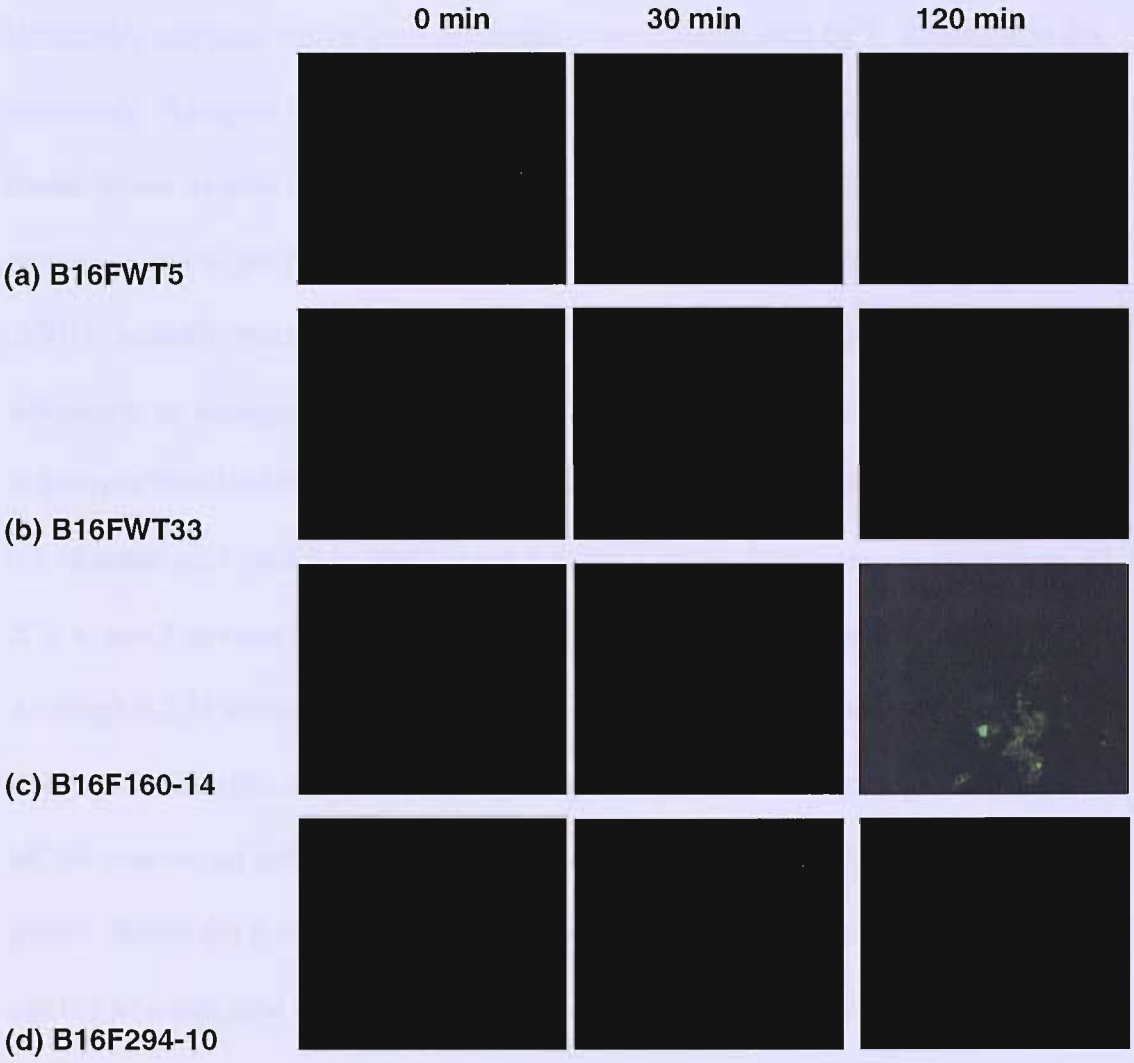

Legend for figure 5.7: No significant internalisation of 10^{-7} M FITC-αMSH was observed at 30 and 120 minutes within the (a) B16FWT5, (b) B16FWT33, (c) B16F160, and (d) B16F294 cell lines.

5.3.6 Investigating the Internalisation of ^{125}I NDP-αMSH by Acid Stripping of Surface Membrane Radiolabelled MC1R

Although the investigations to visualise MC1R internalisation directly using eGFP and indirectly using FITC-αMSH were not successful, investigation of internalisation using transfected lines using a radioligand approach would enable the comparison of internalisation between wild-type and variant MC1R. Therefore, this approach was undertaken using untagged human wild-type and Asp294His variant MC1R transfected HEK294A cell lines which were generated in association with Dr S. Robinson in the laboratory. Receptor internalisation was assessed following removal of the surface bound ligand by acid washing and counting the radioactivity remaining within the remaining cell as per previous reports by Siegrist *et al.*, (1989) and Groarke *et al.*, (2001). Initially, to establish the ligand binding / acid washing technique in the laboratory, an untagged MC1R transfected B16G4F cell line was employed. The viability of the B16MCWT-Untag-30 cell line was assessed following the addition of 0.2 M acetic acid (in 0.5 M NaCl at pH 2.6) for a range of different washing times (0, 1, 2, 3, 4, and 5 minutes) by looking at cell viability using exclusion of trypan blue dye. Although 0.2 M acetic acid was used previously to strip the surface radiolabelled receptors by Siegrist *et al.*, (1989) and Groarke *et al.*, (2001), washing the B16G4F MC1R transfected cells with 0.2 M acetic acid resulted in 100% dead cells at all time points. Hence the B16MCWT-Untag-30 cells were washed with 0.01, 0.02, 0.05, 0.1, and 0.2 M acetic acid for 1 minute and cell viability assessed.

Figure 5.8: Viability of B16MCWT-Untag Transfectants Following Acetic Acid Washing

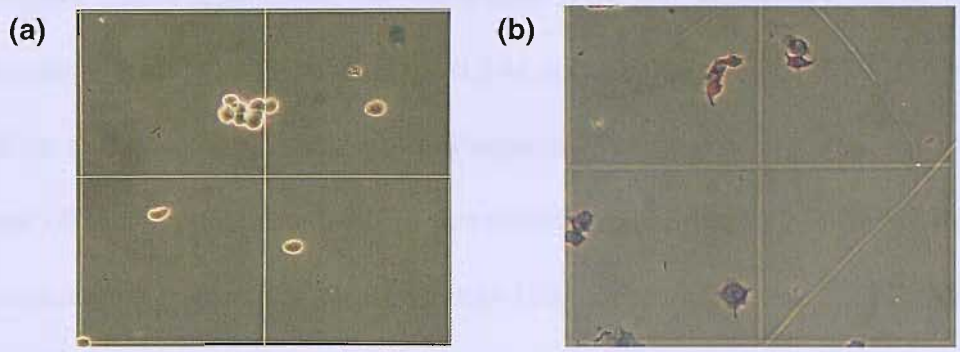

Legend for figure 5.8: The B16MCWT-Untag-30 cells were washed for 1 minute with (a) 0.01 M acetic acid, and (b) 0.2 M acetic acid, resuspended in media and diluted 1:1 with trypan blue and placed on a haemocytometer to be observed under a light microscope. The cells washed with 0.01 M acetic acid remained viable (a), whereas the cells washed with 0.2 M acetic acid were non-viable and stained with trypan blue dye (b).

Acid washing of cells for 1 minute with 0.01 M acetic acid resulted in approximately 98% cell viability (figure 5.8), whereas 0.02 M acetic acid reduced viability to approximately 60%, 0.05 M acetic acid produced 40% viability, and 0.1 M resulted in 30% viable cells. A duplicate set of cells were incubated for 2 hours with ^{125}I NDP-αMSH at 37°C and subsequently washed with acetic acid ranging from 0.01, 0.02, 0.05, 0.1, and 0.2 M for 1 minute and radioactivity was counted in the acid wash and in the remaining cells. The 0.01 M acetic acid washed off 83.87% of the ligand, whereas 0.02 M removed 80.37%, 0.05 M removed 83.35%, 0.1 M removed 84.26%, and 0.2 M removed 82.60%, indicating that the stripping of surface radiolabelled MC1R by acetic acid was similar regardless of cell viability. Furthermore, cells incubated with ^{125}I NDP-αMSH at 37°C and washed with 0.2 M acetic acid for 0, 1, 2, 3, 4, and 5 minutes demonstrated that 0.2 M acetic acid washed off between 76% and 85% of the total bound ^{125}I NDP-αMSH irrespective of washing for 1 to 5 minutes. The B16MCWT-Untag-30 cells (4×10^4) were subsequently incubated with ^{125}I NDP-αMSH for 30, 60

and 120 minutes at 37°C, and exhibited a time dependant increase in ligand binding activity (figure 5.9). Furthermore, following each of these incubabtion times of 30, 60 and 120 minutes with ^{125}I NDP-αMSH the 0.2 M acetic acid stripped 80.7%, 77.7%, and 83.7% of the surface associated radioligand respectively (these percentages are derived from mean CPM from duplicate wells of two separate experiments). Therefore these results combined suggested that approximately 18% of the total bound ^{125}I NDP-αMSH had internalised following 30, 60 and 120 minutes of ligand binding (figure 5.9).

Figure 5.9: Ligand Binding and 0.2 M Acid Striping of Surface Membrane Associated Radiolabelled MC1R in the B16MCWT-Untag-30 Transfectants

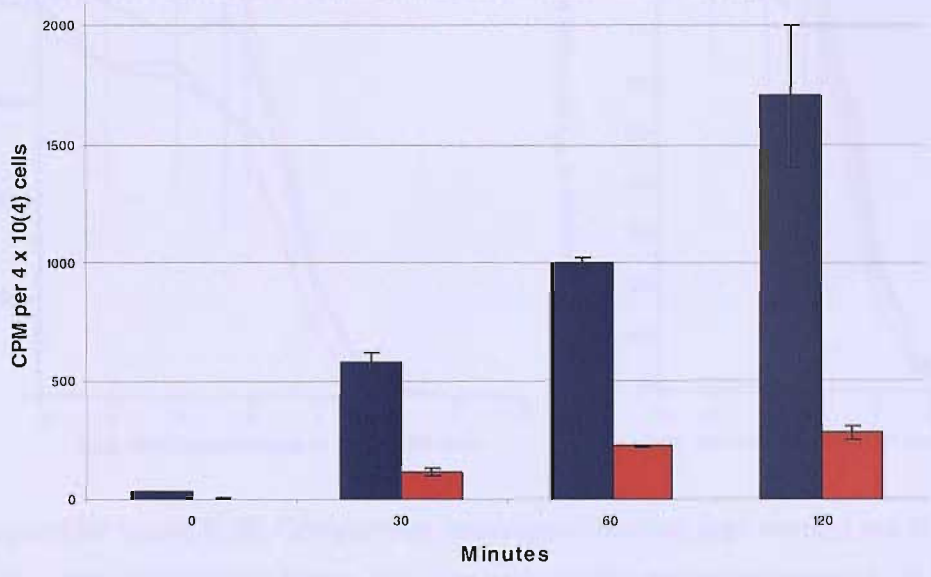

Legend for figure 5.9: The B16MCWT-Untag-30 transfected cells were incubated with radioligand for 0, 30, 60 and 120 minutes and demonstrated a time dependant increase in ^{125}I NDP-αMSH binding (mean counts per minutes shown in blue). 0.2 M acetic acid washes stripped surface ligand, which demonstrated that approximately 18% of the radioligand had internalised at each time point. Data are from duplicate wells of 2 separate experiments.

Following the pilot experiments with the B16G4F MC1R transfected cell line, the radioligand and acetic acid washing experiments were carried out using the HEKMCWT-Untag and HEKMC294-Untag transfectants in order to compare the

ability of wild-type and variant MC1R to internalise. Initially ligand binding showed the presence of cell surface MC1R in these lines (figure 5.10)

Figure 5.10: Ligand Binding of the HEKMCWT-Untag and HEKMC294-Untag Cell Lines

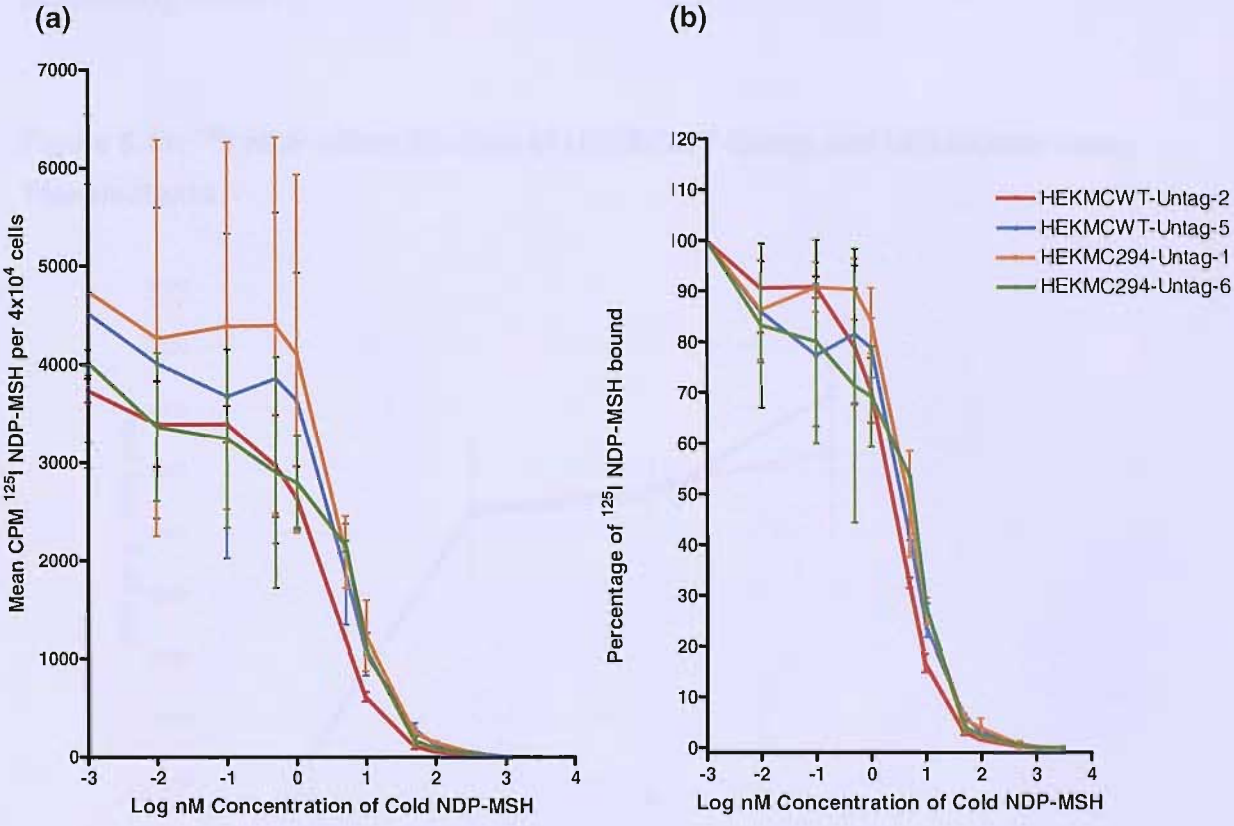

Legend for figure 5.10: Competitive radioligand binding was carried out in HEKMCWT-Untag and HEKMC294-Untag cell lines using a fixed concentration of ^{125}I NDP-MSH and varying concentrations of cold NDP-MSH. (a) Demonstrates the mean CPM of ^{125}I NDP-αMSH binding at varying concentrations of cold NDP-αMSH per $4x10^4$ cells from two wild-type and two variant MC1R transfected cell lines. (b) Demonstrtes the percentage of total ^{125}I NDP-αMSH binding within the same cell lines (normalised to binding at 10^{-12} M cold NDP-αMSH). The data represents the mean and standard deviation of 2 separate experiments.

A time course of ^{125}I NDP-αMSH binding at 0, 30, 60 and 120 minutes in HEKMCWT-Untag-2 cells containing 'untagged' wild-type MC1R, and in the HEKMC294-Untag-6 cell line transfected with 'untagged' Asp294His MC1R showed similar binding in both these lines, with only a slightly higher amount of binding at 2 hours compared to 30 minutes (figure 5.11).

Figure 5.11: ^{125}I NDP-αMSH Binding of HEKMCWT-Untag and HEKMC294-Untag Transfectants

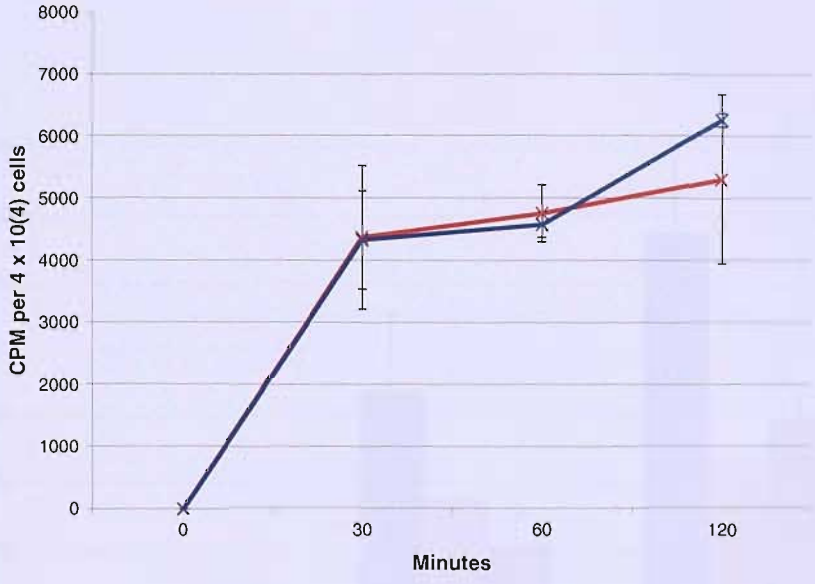

Legend for figure 5.11: Binding of ^{125}I NDP-αMSH to the HEKMCWT-Untag-2 cells (red) and the HEKMC294-Untag-6 cells (blue) at 30, 60 and 120 minutes. The experiment was carried out in duplicate wells on 2 separate occasions.

The HEKMCWT-Untag-2 cells demonstrated internalisation of wild-type MC1R following incubation with ^{125}I NDP-αMSH for 30 minutes and 120 minutes on two separate occasions (figure 5.12) with little difference between 0.1 M and 0.2 M acetic acid washes, where a means of 55.0% and 54.1% ^{125}I NDP-αMSH remained bound after 30 and 120 minutes of ligand binding and 0.1 M or 0.2 M acetic acid washing. The HEKMC294-Untag-6 cell line demonstrated internalisation of Asp294His MC1R also with little variation following acid washing with 0.1 M and 0.2 M acetic acid (figure

5.12). The same cells demonstrated means of 32.1% and 37.0% ^{125}I NDP-αMSH remained bound after 30 and 120 minutes of ligand binding and 0.1 M or 0.2 M acetic acid washing. These results demonstrate that both the wild-type MC1R and the Asp294His variant MC1R internalise to a similar degree, but more importantly the Asp294His variant could internalise despite its inability to signal efficiently.

Figure 5.12: Internalisation of ^{125}I NDP-αMSH in the HEKMCWT-Untag and HEKMC294-Untag Transfectants

(a)

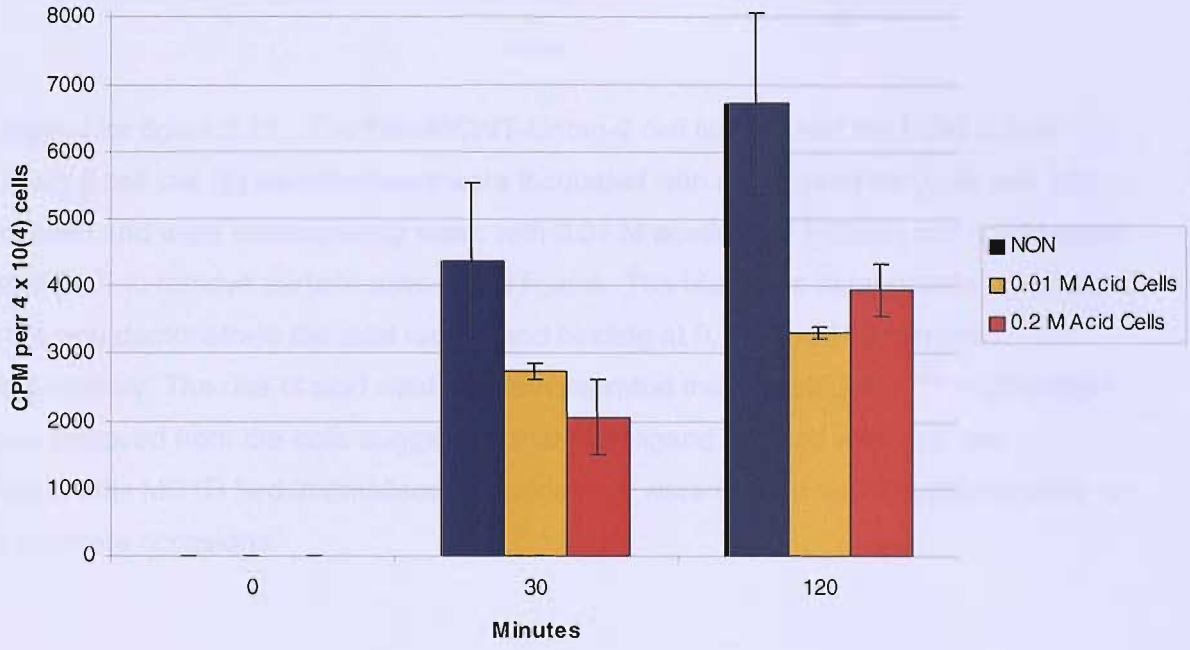

(b)

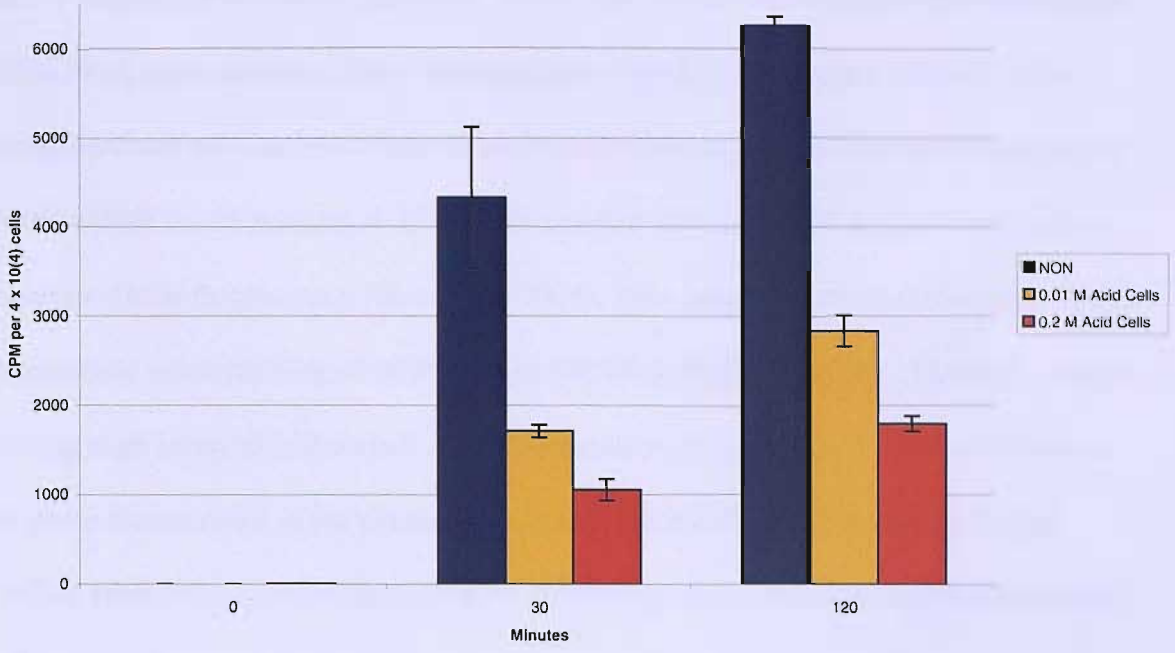

Legend for figure 5.12: The HEKMCWT-Untag-2 cell line (a) and the HEKMC294-Untag-6 cell line (b) demonstrated were incubated with radioligand for 0, 30 and 120 minutes and were subsequently wash with 0.01 M acetic acid (yellow) and 0.2 M acetc acid (red) to remove surface associated ligand. The blue bars demonstrate non treated cells and demonstrate the total radioligand binding at 0, 30 and 120 minutes respectively. The use of acid washing demonstrated that not all of the ^{125}I NDP-αMSH was removed from the cells suggesting that radioligand labelled wild-type and Asp294His MC1R had internalised. Experiments were carried out in duplicate wells on 2 separate occasions.

5.4 Discussion

EGFP tagging of MC4R by Gao *et al.,* (2003) and its subsequent stable transfection into HEK293A cells permitted direct visualisation of the MC4R receptor internalisation using confocal microscopy. Internalisation was demonstrated following the addition of NDP-αMSH for 45 minutes at 37°C, with a partial shift from cell surface fluorescence to intracellular fluorescence (Gao *et al.,* 2003). This approach was therefore undertaken to examine internalisation of eGFP tagged MC1R in HEK293A cells. However, despite having high levels of cell surface MC1R expression (as visualised by the accentuation of green fluorescence at the plasma membrane) the eGFP tagged human wild-type MC1R HEK293A transfectants (HEKMCWT-Ctag) also contained significant amounts of intracellular green fluorescence. Unfortunately this prevented the easy visualisation of receptor internalisation (if it was occurring) in these cell lines. It is possible that some MC1R-eGFP had already internalised or was continuously internalising due to the presence of αMSH or other POMC derived MC1R ligands in the 10% FBS added to the culture medium, but the MC4R-eGFP HEK293A transfectants which were also grown in the presence of 10% FBS did not show evidence of MC4R internalisation in the absence of NDP-αMSH (Gao *et al.,* 2003). However, even when the HEKMCWT-Ctag cells were grown in the presence of 1% FBS, a similar visible pattern of intracellular green fluorescence was observed, and complete absence of FBS from the media resulted in cell death, precluding observations in the absence of FBS. It is also possible that MC1R-eGFP, especially wild-type MC1R-eGFP, may be constitutively activated causing a continual internalisation from the cell membrane in the absence of bound ligand because constitutive activation of MC1R and MC2R has been previously reported (Sanchez-Mas *et al.,* 2004; Swords *et al.,* 2002).

As a second way of investigating for MC1R internalisation, FITC labelled αMSH was used for visualisation of ligand-bound receptor at the plasma membrane and to examine

for internalisation of this receptor in stably transfected B16MCWT-Untag cells (containing untagged wild-type MC1R) and separately in B16G4F cells containing FLAG-tagged wild-type and variant MC1R. FITC-αMSH internalisation was seen in approximately 1 per 1000 cells, suggesting that there was something different about these occasional cells (for example they may have been undergoing necrosis or apoptosis), but also indicating that internalisation was either not occurring in most cells or was not being detected by this approach. In the case of the B16G4F transfectants containing FLAG-tagged wild-type and variant MC1R, it was possible that the absence of intracellular FITC-αMSH was because the N-terminal FLAG tag had interfered with the FITC-αMSH binding, but this seems unlikely as these lines had previously demonstrated their ability to bind radio-labelled ligand (Robinson and Healy, 2002). Admittedly, the concentration of 10^{-7}M FITC-αMSH may have been too low and it may have been necessary to increase the amount of ligand to detect internalisation by this method, but the limited quantity of FITC-αMSH that had been synthesised for this study by the Department of Chemistry in the University of Southampton meant that higher concentrations could not be tested.

The technique of radio-ligand binding / acid washing permitted the indirect detection of ligand internalisation and by inference suggested that variant as well as wild-type MC1R could internalise. Orlow *et al.,* (1990) originally demonstrated that the internal ^{125}I-βMSH binding sites were reduced in numbers in "variant" Cloudman melanoma cells, which differed to "wild-type" Cloudman melanoma cells in their response to βMSH, despite the binding of βMSH at the cell surface being similar in both lines. However, the benefits of the current study were that, 1) the HEK293A transfectants permitted the comparison of wild-type and the Asp294His variant MC1R internalisation while controlling for background genetic variation, 2) the wild-type and variant MC1Rs

had been sequenced and verified as correct prior to transfection into each cell line, and not assumed to be wild-type and variant receptors based on their responses to MSH (Orlow *et al.,* 1990), 3) it is known that the Asp294His MC1R is a non-functional variant which causes red hair and fair skin in humans, so it is of interest to know whether this receptor internalises differently to the wild-type receptor because it may increase the understanding of mechanisms underlying phenotypic differences between wild-type and variant MC1R. The mechanism of acid striping of surface ligand has proved to be a popular method of determining receptor internalisation. Following the initial binding and internalisation event, the surface radio-ligand can be dissociated from its receptor within an acidic environment, which breaks the bonding between the ligand and its receptor. It is proposed that in such a harsh environment most if not all of the ligand is released into the supernatant, with only internal ligand remaining.

Acetic acid stripping of surface bound radio-labelled ligand from MC1R had been employed previously using 0.2 M acetic acid (in 0.5 M NaCl at pH 2.6) by Siegrist *et al.,* (1989) and Groake *et al.,* (2001). In the present study, despite the successful removal of approximately 82% of the surface associated ^{125}I NDP-αMSH from the B16MCWT-Untag cells, which suggested that 18% of the ligand was intracellular, a parallel cell viability investigation revealed that 0.2 M acetic acid resulted in 100% cell death (as shown by trypan blue dye uptake). It was therefore a concern that these necrotic cells with low membrane integrity may not retain all of the internalised ligand. Thus, the same transfectants were subjected to acetic acid ranging from 0.2 M to 0.01 M acid and the percentage of internalised ligand was determined. Most of the B16MCWT-Untag cells remained viable following 1 minute exposure to 0.01 M acetic acid, whereas cells treated with increasing concentrations of acetic acid were less healthy and the majority of the cells were dead following 1 minute of exposure to 0.2 M acetic acid.

However, the remaining radioactivity in the cells, equivalent to internalised ligand, was similar for cells washed with 0.2 M and 0.01 M acetic acid respectively. This suggested that the cell viability did not appear to affect the quantification of internalised ligand, and that the ligand did not leak back out of non-viable cells (at least not during the acid wash procedure).

The radiolabelled ligand binding experiments demonstrated that there was a time dependant increase in total ligand binding activity (after 30, 60, and 120 minutes), but that the proportion of ligand which had internalised was similar at each time point in the same cell line but different for different cell lines. The use of the HEKMCWT-Untag and HEKMC294-Untag stable transfectants, which contained a higher number of surface receptors than the B16MCWT-Ctag cell lines showed that the Asp294His MC1R internalised to a similar degree as the wild-type receptor. Admittedly, it would have been useful to have tested for this in other cell lines, however due to restricted time this could not be performed. Future work could examine whether less of the Asp294His variant MC1R (and other common MC1R variants including Arg151Cys and Arg160Trp) internalise than wild-type receptor in various types of cells which express these receptors (e.g. keratinocytes, monocytes).

Chapter 6

Final Discussion

MC1R is a 7-pass transmembrane GPCR which is expressed by melanocytes, in which it signals via cAMP to activate the synthesis of melanin within melanosomes. A number of polymorphisms within *MC1R* give rise to MC1R variants such as Arg151Cys, Arg160Trp and Asp294His, which can not signal via cAMP. These particular variant receptors have a tendency to induce phaeomelanin production instead of eumelanin via signalling pathways other than cAMP. Furthermore, these MC1R variants are causal of red hair and fair skin and predispose these individuals to skin cancers. The latter is thought to be due mainly to the lack of protective melanins, but additional effects due to non-pigmentation related mechanisms may be involved. Although, it is important to acknowledge that αMSH may be present at the melanosome for functions that occur independently of MC1R. Receptor independent regulation of tyrosinase by αMSH has been suggested, in which αMSH activation of the (6R)-L-erythro-5,6,7,8-tetrahydrobiopterin ($6BH_4$) / tyrosinase inhibitor complex can inhibit tyrosinase activity (Schallreuter *et al.*, 1999, Peters *et al.*, 2000). More recently there was evidence that βMSH may also be present within the melanosome, and that βMSH could interact with a 7-isomer of $6BH_4$ ($7BH_4$) to regulate human melanogenesis Spencer *et al.*, 2005). The accumulation of $7BH_4$ in the epidermis occurs when the pterin-4a-carbinolamine dehydratase (PCD) enzyme is mutated and $7BH_4$ accumulation in the epidermis of vitiligo patients has been found (Schallreuter *et al.*, 1994). Since αMSH, the natural ligand for MC1R, is present within the melanosome (Peters *et al.*, 2000), the question arose of whether the MC1Rs also may be present within this organelle to play a role in melanin synthesis at this site. Therefore, the subcellular location of MC1R was investigated to determine whether or not MC1R can be found at the melanosome. Moreover, the intracellular distribution and characteristics of wild-

type MC1R was compared to that of the red hair / fair skin associated Asp294His MC1R variant.

The generation of wild-type MC1R and Asp294His variant MC1R tagged with eGFP was carried out with the aim of producing a pigment cell model in which the cellular characteristics and the distribution of these receptors could be observed. The direct labelling of MC1R was desirable since all the available antibodies against human MC1R were considered suboptimal for the purpose of investigating the intracellular localisation of MC1R. The benefit of fluorescent protein tagging has been demonstrated in numerous cell systems as a useful tool for directly observing protein localisation (by confocal microscopy) and protein-protein interactions (i.e. by FRET imaging). Moreover, eGFP has been widely used in a number of *in vitro* systems for labelling GPCRs whilst permitting normal receptor ligand interactions and subsequent signalling (Barak *et al.*, 1997; Blondet *et al.*, 2004; Ivic *et al.*, 2002; Rached *et al.*, 2003; Tarasova *et al.*, 1997). Competitive ligand binding demonstrated that the B16MCWT-Ctag transfectants retained their ability to bind NDP-αMSH ligand and in the case of the wild-type, MC1R could also signal via cAMP despite the presence of an eGFP tag at the C-terminus. Secondly, the transfectants containing MC1R tagged at the C-terminus with eGFP allowed visualisation of MC1R-eGFP within the cell by fluorescence microscopy.

Both the B16MCWT-Ctag and the B16MC294-Ctag transfectants exhibited a punctate pattern of green fluorescence upon confocal microscopy, which was comparable if not more specific to the punctate pattern previously observed when a FITC labelled anti-MC1R antibody was used to label MC1R within human hair follicle epithelia, sebocytes, secretory and ductal epithelia of sweat glands, and periadnexal mesenchymal

cells (Böhm *et al.*, 1999). Moreover those researchers observed MC1R staining in interfollicular epidermis in undifferentiated keratinocytes in foetal and adult skin. Separately, the immunofluorescence labelling of αMSH in cultured human melanocytes also produced a punctuate pattern of fluorescence concentrated around the nucleus and at apical tips of bipolar melanocytes, later confirmed by TEM to be at the melanosome (using immunogold labelling) and western blotting (Peters *et al.*, 2000). MC1R expression was confirmed in sebocytes of normal human skin by immunohistochemistry by Böhm *et al.*, (2002) and subsequent immunofluorescent labelling demonstrated a punctuate pattern of labelling throughout the cytoplasm, which appear to be extra nuclear. Interestingly, in primary cutaneous melanoma cells the MC1R labelling appeared to be more focal and less punctate (Böhm *et al.*, 2002). This would suggest that the green fluorescence emitted by the presence of MC1R-eGFP within the B16G4F transfectants showed a pattern of distribution similar to that of MC1R staining in normal skin rather than in the melanoma cells (Böhm *et al.*, 2002). Stander *et al.*, (2002) used an MC1R antibody directed against the amino acids 2–18 of the human MC1R to investigate the expression of MC1R within specimens of normal healthy skin as well as hamartomas, cysts, hyperplasias, and benign or malignant neoplasms with eccrine, apocrine, sebaceous gland, and hair follicles (Stander *et al.*, 2002). They observed that the MC1R expression was similar between the various malformations and neoplasms when compared with normal skin, showing intracytoplasmic granular staining. TEM investigations also showed that MC1R was expressed at the cell surface and also within tubular endosomes within the cytoplasm, the latter suggesting the possibility of receptor internalisation. As expected of these transmembrane receptors, we observed wild-type and Asp294His MC1R-eGFP accentuated at the membrane of stably transfected B16G4F melanoma cell lines, consistent with the previous publications that used an MC1R antibody (above). By contrast, the B16G4F cells that were stably transfected

with the pEGFP-N3 vector (as a control) displayed a mottled and diffuse pattern of green fluorescence throughout the cytoplasm and within cell nuclei, with no evidence of eGFP exposure at the plasma membrane. We therefore assumed that the eGFP did not alter the normal distribution of MC1R, nor cause the aberrant trafficking of this protein. The lack of difference in the intracellular expression between the eGFP tagged wild-type and Asp294His MC1Rs suggested to us that this variant does not alter the receptor localisation, although it is possible that greater numbers of Asp294His receptors reach the cell surface as evidenced by ligand binding which demonstrated higher counts per minute of ^{125}I NDP-αMSH binding at the cell surface of B16G4F transfectants containing the Asp294His MC1R in comparison to wild-type MC1R transfectants (Robinson and Healy, 2002). Beaumont *et al.,* (2005) recently published fluorescence microscopy data of N-terminal eGFP-labelled wild-type and separately the Arg151Cys, Arg160Trp, and Asp294His MC1R variants transiently transfected in metastatic melanoma and HEK293A cells. Their work demonstrated membrane and intracellular distribution of green fluorescence from the eGFP tagged wild-type and variant MC1Rs (Beaumont *et al.,* 2005), which was consistent with that observed in the B16G4F and HEK293A transfectants containing C-terminal eGFP tagged wild-type MC1R and separately Asp294His MC1R within this thesis. Beaumont *et al.,* (2005) also used an immunofluorescently labelled anti-MC1R antibody to double stain the wild-type and variant eGFP-MC1Rs at the plasma membrane of non-permeablised melanoma and HEK293A transfected cells. Beaumont *et al.,* (2005) determined that the eGFP-labelled Arg151Cys and Arg160Trp MC1R variants co-localised differently to the eGFP tagged wild-type and Asp294His MC1R, and recorded an 80-95% reduction in cell surface labelling with these particular variants. It may therefore be possible that the Arg151Cys and Arg160Trp MC1R variants could be retained intracellularly, and lack the capability of recycling back to the plasma membrane following initial internalisation (also

assuming that these receptors are constitutively active, or exogenous αMSH was present in the culture media).

The B16MCWT-Ctag and B16MC294-Ctag transfectants (within this thesis) exhibited co-localisation of green fluorescence with a number of intracellular organelles including ER and golgi apparatus, which was not unexpected since MC1R synthesis and glycosylation events may take place at these sites similar to that of other cellular proteins. However, more interestingly, the wild-type and variant Asp294His MC1R demonstrated co-localisation with gp100 and Trp-1, which are proteins that are abundant in early and late stage melanosomes respectively. Whether the receptor exists following its internalisation from the cell surface, it is also possible, that like other melanosomal proteins (i.e. tyrosinase) which are processed through the ER and golgi to melanosomes, MC1R may traffic similarly to be incorporated into this organelle as well as trafficking via endosomes to the plasma membrane (Stander *et al.*, 2002).

Interestingly, within this study we noticed that MC1R-eGFP co-localised more strongly with the Trp-1 labelling in late melanosomes, which suggested to us that MC1R may be more abundant in later rather than in early melanosomes. Peters *et al.*, (2000) previously described the presence of POMC, the catalytic enzymes PC1 and PC2, and the respective POMC cleavage products ACTH and αMSH within the melanosome, and those authors hypothesised that the αMSH may have pigmentary effects in the absence of MC1R at this site. Later proteomic analysis of early melanosomes identified over 56 proteins that are shared with other organelles including αMSH and 6 melanosome specific proteins (Basrur *et al.*, 2003). This analysis did not identify the presence of MC1R in early melanosomes. It is possible however, that MC1R is preferentially incorporated into late melanosomes. It may also be possible that Basrur *et al.*, (2003)

only observed a small percentage of the total proteins associated with the melanosome. Interestingly, the early melanosomes (stained with an anti-gp100 antibody and alexa fluor 633 secondary antibody) demonstrated greater areas of co-localisation with MC1R-eGFP in both the wild-type and Asp294His variant MC1R-eGFP transfectants following stimulation with IBMX. This may reflect an increase in melanosome numbers following the addition of IBMX, hence causing greater amounts of co-localisation, alternatively it is possible that IBMX could increase MC1R-eGFP internalisation, and this may cause increased co-localisation of melanosomes in close proximity to the receptor. It would be interesting to observe the ratio of spherical early stage melanosomes to ellipsoid melanised late stage melanosomes in melanocytes / melanoma cells following αMSH / IBMX stimulation, which may indicate whether IBMX can induce melanosome maturation and hence a greater co-localisation with MC1R-eGFP. The purification of melanosomes from the B16MCWT-Ctag and B16MC294-Ctag cell lines was attempted by sucrose density ultracentrifugation, however the purity of melanosomes observed by TEM was too low. This was most likely due to the fact that early melanosomes are difficult to enrich from amelanotic cell types due to there lack of dense melanin (personal communication with Professor V. Hearing). Therefore melanosomes were purified from melanotic B16F10 transfectants containing the same wild-type MC1R-eGFP construct. Melanosome yield from these B16F10 transfectants was satisfactory although not 100% pure as observed by TEM analysis, and confocal microscopy confirmed the presence of green fluorescence in the melanosome-enriched fraction. The intensity of green fluorescence was low in the melanosomes compared to that observed in whole cells, possibly due to the presence of melanin within the melanosomes which has a quenching effect by absorbing the excitatory UV wavelength. It has also been shown that the acidic pH of melanosomes has a quenching effect on eGFP (Berens *et al.,* 2005). The quenching effect of *melanin*

on eGFP would have been less likely in whole cells since the MC1R-eGFP was also located at other sites including ER and golgi, which do not contain melanin. The presence of MC1R at the melanosome may be interpreted in a number of ways. Since melanosomes are derived from large vesicles which originate from rough endoplasmic reticulum and small coated vesicles containing tyrosinase from golgi apparatus (Jimbow *et al.,* 1982; Mishima, 1992) it is possible that MC1R being made within the ER and golgi may also be incorporated into early melanosomes. A second possibility is that following ligand binding and receptor activation, MC1R internalisation could allow the receptor to become associated with melanosomes. Melanin synthesized within these organelles is deposited on their internal matrices hence giving rise to stage II melanosomes (Huri *et al.,* 1968; Okazaki *et al.,* 1976). If MC1R is present at the melanosome membrane it is possible that this receptor may play a role in the production of melanin at this site. It would be interesting to investigate the orientation of the receptor at the melanosome surface, which would perhaps elucidate the role of MC1R at this organelle. It may be hypothesised that the N-terminus of the receptor is inward facing in order access the αMSH within the lumen of the melanosome. In this case it may be hypothesised that the role of MC1R at the melanosome would be to signal out into the cytoplasm of the melanocyte in order to increase cAMP signalling from the wild-type receptor / other signalling pathways in the case of the MC1R variants. Alternatively if the N-terminus of MC1R is outward facing, it is possible that αMSH present within the cytoplasm of the melanocyte could bind to the receptor to permit intramelanosomal signalling i.e. to boost the intramelanosomal synthesis and deposition of melanin on the matrices. In this case the role of MC1R at the melanosome could be related to enabling melanosome maturation. Independent of a role for MC1R as a signalling receptor at the melanosome, there are other possibilities that the receptor may be important for anchorage of the melanosome either during the transfer of

melanosomes to keratinocytes. Therefore it may be interesting to examine for co-localisation of MC1R-eGFP with other proteins that are present within the membrane of the melanosome such as myosin Va, Rab27a and melanophilin, which normally play a role in the transportation of melanosomes along microtubules to distal actin rich regions of dendrites extending from the body of melanocyte cells (Bahadoran *et al.*, 2001). Alternatively, the presence of MC1Rs at the surface of the melanosome may even influence where the melanosome traffics within the keratinocyte following transfer i.e. in formation of nuclear caps. Dyneins have been shown to co-localise with focal supranuclear aggregates of melanosomes within keratinocytes (Byers *et al.*, 2003). It would be interesting to carry out melanosome transfer experiments with the aim of investigating co-localisation between dyneins and MC1R-eGFP. Moreover, if human melanocytes were transfected with eGFP tagged MC1R (either by viral vector or perhaps by DNA loaded calcium phosphate nanoparticles) and co-cultured on a monolayer of human keratinocytes it may be possible to observe co-localisation between immunofluorescent labelled dynein and MC1R-eGFP by use of confocal microscopy.

As previously hypothesised, it is possible that the internalisation of MC1R may allow MC1R access to melanosomes or position them in close proximity to enable αMSH binding. Varga *et al.*, (1976b) used FITC labelled βMSH to examine for ligand internalisation in Cloudman S91 cells and demonstrated evidence for the association of FITC-βMSH at the golgi. Together with other researchers (who demonstrated ferritin-labelled βMSH co-localisation at premelanosomes) assumptions were made that the MSH hormone may be exerting its effects in close proximity to premelanosomes (Lerner *et al.*, 1979; Varga *et al.*, 1976b).

The first study to visualise the internalisation of an MCR used confocal microscopy to demonstrate wild-type MC4R-eGFP internalisation in HEK293A cell transfectants following the addition of NDP-αMSH (for up to 45 minutes at 37°C) (Gao et al., 2003). These HEK293A cell transfectants showed a 'chicken wire-like' green fluorescence pattern highlighting MC4R-eGFP at the plasma membrane, and a subsequent time-dependent increase in intracellular green fluorescence observed as a punctuate pattern. This approach was therefore repeated within our internalisation study using HEK293A cells stably transfected with the MC1R-eGFP construct. These cells were used instead of the B16G4F transfectants which had demonstrated significant levels of intracellular green fluorescence when unstimulated suggestive of constitutive activation and internalisation of MC1R-eGFP or possibly that the MC1R-eGFP was being sequestered within the cell. Therefore the HEK293A provided an environment deficient in melanosomes in an attempt to reproduce the pattern of MC4R-eGFP internalisation with the MC1R-eGFP. The HEK293A transfectants containing MC1R-eGFP exhibited a strong membrane accentuation of green fluorescence, however a punctate pattern of intracellular green fluorescence was observed within the cell cytoplasm, consistent with the appearance of the B16G4F transfectants expressing MC1R-eGFP. In order to remove any external sources of αMSH, FBS was omitted from the culture medium, however, the same intracellular pattern of green fluorescence was observed in this system. Interestingly the HEK293A transfectants containing MC4R-eGFP were maintained in 10% FBS (Gao *et al.*, 2003), which suggested two things, either that the characteristics of MC4R-eGFP internalisation were completely different to those of MC1R-eGFP i.e. speed of internalisation, or that the MC1R was constitutively active and MC4R was not. The MC1R-eGFP seemed to internalise similarly in the HEK293A human embryonic kidney cells and the B16G4F melanoma cells despite the obvious cellular differences (absence of melanosomes in the HEK293A cells). The appearance

of intracellular green fluorescence therefore suggested the constitutive activation and internalisation / recycling of MC1R-eGFP and / or continual synthesis and trafficking of receptor through intracellular compartments to the cell surface. Other researchers visualised MC1R within tubular endosomes of human skin cells using immunogold labelling of MC1R with antibodies (Böhm *et al.*, 1999; Stander *et al.*, 2002). There is recent evidence to suggest that both the MC1R and MC2R receptors may be constitutively activated (Sanchez-Mas *et al.*, 2004; Swords *et al.*, 2002) which supports the confocal microscopy work within this thesis, demonstrating an intracellular pattern of MC1R-eGFP green fluorescence. It is unlikely that receptors were only travelling in one direction up to the cell surface as there was no evidence of MC1R-eGFP accumulation at the plasma membrane over time. It was apparent that the HEK293A transfectants presented a higher intensity of surface membrane green fluorescence, suggestive of higher receptor numbers at the plasma membrane. Later evidence demonstrated higher ligand binding counts per minute in the HEK293A transfectants compared to the B16G4F transfectants, consistent with the confocal microscopy observations. As an alternative approach, FITC-labelled αMSH was used to attempt the indirect labelling of MC1R to visualise internalisation of MC1Rs in stably transfected B16G4F cells containing untagged wild-type MC1R, and separately FLAG-tagged wild-type MC1R and three MC1R variants (Arg151Cys, Arg160Trp, Asp294His). The FITC-αMSH possessed a similar activity to commercially acquired αMSH peptides (Sigma and Bachem) however the lack of FITC-αMSH (at 10^{-7} M) labelling at the cell surface and the absence of intracellular staining made further investigation via this method unlikely to be informative. It may be the case that a higher concentration of FITC-αMSH was required to visualise intracellular green fluorescence, however this synthetic compound was in limited supply due to the nature of its synthesis in the Chemistry Department of the University of Southampton.

Historically, ligand binding experiments utilising ^{125}I-βMSH have indirectly demonstrated MSH receptor internalisation with approximately a 60% reduction in surface binding sites, and also the redistribution of ligand binding sites from the cell surface (to intracellular locations) in various murine melanoma cell lines (B16-F1 and Cloudman S91) (Chakraborty *et al.*, 1991; Siegrist *et al.*, 1988; Siegrist *et al.*, 1989). In contrast, human D10 and 205 melanoma cell lines have demonstrated increases in surface binding sites upon MSH stimulation, suggestive of an increase in surface MSH receptors from intracellular stores (Eberle *et al.*, 1993; Siegrist and Eberle 1993). Radio-labelled ligand binding and acetic acid washing (at pH 2.6) of surface associated ligand permitted the indirect quantitation of MC1R internalisation in wild-type MC1R and Asp294His MC1R transfected B16G4F and HEK293A cell lines (the ligand binding / acid washing technique was adapted from other MC1R internalisation studies Siegrist *et al.*, (1989) and Groake *et al.*, (2001). There was a time-dependent increase in total ^{125}I NDP-αMSH ligand binding activity after 30, 60, and 120 minutes, and the percentage ligand internalisation proportionally increased also with time. At 120 minutes the acetic acid removed 82% of the cell associated ^{125}I NDP-αMSH from the B16MCWT-Untag cells inferring that 18% of the ligand had internalized, the remainder being on the surface. Cell viability studies demonstrated that exposure to 0.2 M acetic acid caused 100% cell death (as demonstrated by the uptake of trypan blue dye into dead cells). In order to exclude the possibilities that following exposure to 0.2 M acetic acid the ^{125}I NDP-αMSH could either enter the cells spontaneously or even leak back out if the outer membrane was not intact, a weaker 0.01 M acetic acid wash which did not kill the cells was used to strip surface-associated ligand. B16MCWT-Untag cells that were incubated with ^{125}I NDP-αMSH for 120 minutes and subsequently washed with 0.2 M and 0.01 M acetic acid, demonstrated that 17.4% and 16.1% of the total bound ligand internalised respectively. This demonstrated that despite inducing cell

death when washing with the 0.2 M acetic acid the percentage of total internalised ligand was similar between the two groups (those washed with 0.2 M or 0.01 M acetic acid). HEKMCWT-Untag and HEKMC294-Untag stable transfectants containing untagged wild-type and Asp294His MC1Rs respectively, demonstrated higher external ligand binding sites than the B16G4F transfected cell lines. Orlow *et al.*, (1990) originally demonstrated a reduced number of intracellular ^{125}I-βMSH binding sites in "variant" Cloudman melanoma cells (which differed to "wild-type" Cloudman melanoma cells in their response to MSH), despite there being similar binding sites at the cell surface. By inference these authors suggested that the "variant" MSH receptors (MC1R variants) could not internalise as efficiently as the wild-type MSH receptors. The HEK293A transfectants permitted a superior investigation of wild-type and the Asp294His variant MC1R internalisation by controlling for background genetics, and by specifically comparing the cAMP signalling wild-type MC1R with the non-cAMP signalling Asp294His MC1R (receptor sequences verified prior to transfection). The HEKMCWT-Untag cells demonstrated 54.1% and 55.0% of ligand internalisation following incubation with ^{125}I NDP-αMSH for 30 minutes and 120 minutes. The HEKMC294-Untag cells demonstrated 32.1% and 37.0% receptor internalisation following incubation with ^{125}I NDP-αMSH for 30 minutes and 120 minutes respectively. This suggested that the Asp294His MC1R internalised similarly to the wild-type receptor, inconsistent with the findings by Orlow *et al.*, (1990). Since these findings were based on repeated experiments in two HEK293A transfected cell lines, it would be prudent to examine more cell lines in future work. However this evidence supports the literature in suggesting that the MC1R may internalise to some degree following ligand binding at the cell surface.

The results presented in this thesis provide the basis for future experimental work. To further confirm the presence of MC1R at the melanosome, and to determine its transmembrane positioning at this site, immuno-gold labelling using an eGFP specific antibody and electron microscopy would be helpful. This technique was attempted during this thesis, however repeated attempts by Dr A. Page of the Biomedical Imaging Unit at the University of Southampton were not successful, and future studies might require more robust anti-GFP antibodies. The evidence presented within this thesis suggested the presence of MC1R at the melanosome within melanoma cells. It would therefore be interesting to further investigate for the presence of MC1R at the melanosome of normal human melanocytes. It would be possible to use viral transfection methods to transfect melanocytes with MC1R-eGFP for the visualisation of membrane associated / intracellular MC1R. It would also be important to investigate the orientation of the receptor at the melanosome. Since αMSH is present within the melanosome, it may be hypothesised that the N-terminus of the receptor could be facing into the melanosome in order to signal back out into the cytoplasm. In this case, the effect of MC1R signalling at both the plasma membrane and also at the melanosome membrane would amplify cAMP signalling or other signalling pathways within the cytoplasm. Alternatively if the receptor signals into the melanosome it could be hypothesised that MC1R is involved in the biogenesis / maturation of the melanosome or in melanin production at this site. It would be interesting to investigate whether MC1R has a role to play in the transfer of melanosomes from melanocyte to keratinocyte, and whether the presence of MC1R effects the distribution or final positioning of melanosomes, such as the formation of a nuclear cap. The Arg151Cys, Arg160Trp, Asp294His MC1R variants most commonly associated with red hair, fair skin and increased skin cancer risk could also be investigated to see whether these

receptors are also present at the melanosome and whether they fulfil a similar role to the wild-type receptor at this site.

For future work relating to MC1R internalisation using ^{125}I NDP-αMSH, it would be useful to characterise a greater numbers of clones from the B16G4F and HEK293A transfectants containing untagged wild-type and variant MC1Rs. It would also be interesting to observe other cell types such as murine / human: melanoma cells, melanocytes, and keratinocytes. It would also be prudent to investigate other MC1R variants as well as the Asp294His MC1R variant. Perhaps the MC1R variants of greatest interest are those which predispose to the red hair / fair skin phenotype such as Arg151Cys, Arg160Trp, and Asp294His. This may identify important differences in the internalisation / plasma membrane expression of these variants when compared to the functional wild-type receptor. The main aims of continuing to investigate the molecular and cellular characteristics of MC1Rs (including intracellular localisation and functional capabilities) may help to develop a clearer understanding of how individuals (harbouring MC1R variants) with red hair and fair skin develop skin cancers more readily than individuals with wild-type MC1R pigmentation phenotypes.

Appendix

1.1 Bacterial Growth Media and Solutions

1.1.1 Luria-Bertani (LB) Medium

LB broth (Lennox L broth, Sigma, Poole, UK) was prepared by dissolving 4 g LB broth (dried powder) into 200 ml dH_2O. The medium was autoclaved immediately and stored at 4°C.

1.1.2 LB Agar

LB agar (Lennox L agar, Sigma, Poole, UK) was prepared by mixing 7 g LB agar (dried powder) into 200 ml dH_2O. The agar was allowed to cool and plates were stored inverted at 4°C. These plates were used for the growth and maintenance of *E. coli TOP10.*

1.1.3 LB-Glycerol

LB-Glycerol permitted the long term storage of bacterial suspensions at -70°C. LB media (appendix 1.1.1) was prepared to contain 10% (w/v) glycerol and was sterilised by autoclaving in 10 ml aliquots. The medium was stored at room temperature indefinitely.

1.1.4 Antibiotics

Kanamycin (Sulphate salt, Sigma, Poole, UK) was dissolved in UHQ H_2O to 10 mg/ml. The antibiotic solution was filter sterilised through a 0.22 μm Millipore filter. This was aliquoted and stored at -20°C.

1.1.5 LB agar and Broth with antibiotics

LB agar and media were supplemented with 30 μg/ml kanamycin. Kanamycin (1. d) was added to either LB medium (appendix 1.1.1) or to molten LB agar (appendix 1.1.2) at a final concentration of 30 μg/ml. LB agar plates containing kanamycin were prepared as described above (appendix 1.1.2).

1.2 DNA Gel Electrophoresis

1.2.1 50 x TAE stock solution:

2 M Tris (Sigma, Poole, UK)

50 mM EDTA (Sigma, Poole, UK)

Prepared in dH_2O, pH 8.5

57% (v/v) glacial acetic acid (Sigma, Poole, UK)

1.2.2 Orange G:

50 mg Orange G salt (Sigma, Poole, UK)

12 ml 50 x TAE (appendix 1.2.1)

3.2 ml UHQ H_2O

6g glycerol (Sigma, Poole, UK)

1.3 Buffers used in DNA Extraction / Purification Kits (Qiagen, W. Sussex, UK)

1.3.1 Buffer P1:

50 mM Tris base

3.72 g $Na_2EDTA \cdot 2H_2O$

Prepared into 1 L dH_2O, pH 8.0

Add 100 mg RNase A per Litre (Supplied)

1.3.2 Buffer P2:

200 mM NaOH

Prepared into 950 ml dH_2O

50 ml 20% SDS solution

1.3.3 Buffer EB:

10 mM Tris·Cl

Prepared in dH_2O, pH 8.5

1.3.4 Buffer QBT:

750 mM NaCl

50 mM MOPS (free acid)

Prepared in 800 ml dH_2O, pH 7.0

Add 150 ml isopropanol

15 ml 10% Triton X-100

Make up to 1 L with dH_2O

1.3.5 Buffer QC:

1 M NaCl

50 mM MOPS (free acid)

Prepared in 800 ml dH_2O, pH 7.0

Add 150 ml isopropanol

Make up to 1 L with dH_2O

1.3.6 Buffer QF:

1.25 M NaCl

50 mM Tris base

Prepared into 800 ml dH_2O, pH 8.5

Add 150 ml isopropanol

Make up to 1L with dH_2O

1.3.7 Buffers of Unspecified Content (Qiagen, W. Sussex, UK)

Buffer N3

Wash buffer PE

Buffer PB

Buffer P3

Lysis buffer AL

Wash buffer AW1 (stringent wash buffer, made up as per instructions)

Wash buffer AW2 (ethanol based wash buffer, made up as per instructions)

Elution buffer AE

Buffer QG (for DNA extraction from gel)

1.4 DNA Ligation

1.4.1 10 x Ligase Buffer:

700 mM Tris.HCl pH7.5

70 mM $MgCl_2$

10 mM DTT

1 mM ATP

Prepared in UHQ dH_2O

1.5 Polymerase Chain Reaction

1.5.1 10 x PCR Reaction Buffer:

160 mM $(NH_4)_2SO_4$

670 mM Tris.HCl

Prepared in UHQ dH_2O, pH 8.8 at 25°C

0.1% Tween 20

1.6 DNA Sequencing

1.6.1 Sequencing gel

25 ml 4.8% Acrylamide, 6M Urea Gene PAGE plus gel solution (Amresco, Anachem, Luton, UK)

Add the following and invert to mix:

150 µl 10% APS (Ammonium Persulphate, Sigma, Poole, UK, Prepared in UHQ dH_2O)

15 µl TEMED (Sigma, Poole, UK)

N.B. The addition of APS and TEMED causes the gel to polymerise quickly, therefore the sequencing plates should be are prepared and horizontal (on a level surface) to receive the gel solution. In order to minimise air bubbles, light tapping on the top glass plate helps the gel to travel from the top end to the bottom end of the glass plates. The plates containing gel solution should be left to polymerise at room temperature for approximately 1-2 hours.

1.6.2 TBE Buffer

50 x TBE Buffer (Ameresco, Anachem, Luton, UK)

1.7 Cell Culture Reagents

1.7.1 Complete Dulbecco's Modified Eagle Medium (DMEM):

To 500 ml of DMEM (Cat. No. 21969-035, Gibco-Invitrogen, Paisley, UK) containing: Sodium Pyruvate, Pyroxidine and without L-Glutamine add:

10% EU approved heat inactivated FBS (Gibco-Invitrogen, Paisley, UK)

2 mM L-Glutamine (Gibco-Invitrogen, Paisley, UK)

5 ml (2 μg/ml) Ciprofloxacin (Bayer, Berkshire, UK)

1.7.2 Cell Dissociation Solution (Sigma, Poole, UK):

(1x) Non-enzymatic sterile filtered Cell Dissociation Solution, prepared on HBSS without Calcium and without Magnesium.

1.7.3 Geneticin:

Contains 50 mg/ml active geneticin (Invitrogen, Paisley, UK)

1.7.4 Cell Storage Medium:

EU approved Heat inactivated FBS (Gibco-Invitrogen, Paisley, UK)

10% DMSO (Sigma, Poole, UK)

1.8 Flow Cytometry

1.8.1 FACS Buffer:

0.1% Sodium azide (Sigma, Poole, UK)

1% BSA (Sigma, Poole, UK)

Prepared into 500 ml PBS

1.9 Ligand Binding

1.9.1 Ligand Binding Buffer:

To 500 ml Minimal Essential Medium (Cat. No. 32360-026, Gibco-Invitrogen, Paisley, UK) with Earle's salts, with 25 mM HEPES (pH 7.0), and without L-Glutamine add:

0.2% BSA (Sigma, Poole, UK)

1mM 1, 10-phenanthrolin (Sigma, Poole, UK)

0.5 mg/l leupeptin (Sigma, Poole, UK)

200 mg/l bacitracin (Sigma, Poole, UK)

1.10 Analysis of cAMP by ELISA

1.10.1 Buffer ED2

Contents unspecified (R&D Systems, Abingdon, UK)

1.11 Melanosome Extraction from Cells

1.11.1 Dounce Buffer:

1.5 mM Magnesium Chloride (Sigma, Poole, UK)

5 mM Potassium Chloride (Sigma, Poole, UK)

10 mM HEPES, pH 7.5 (Invitrogen, Paisley, UK)

1.12 Transmission Electron Microscopy Reagents

1.12.1 Primary Fixative contains:

3% glutaraldehyde (Agar Scientific, Stanstead, UK)

4% formaldehyde (Agar Scientific, Stanstead, UK)

Prepared in a 0.1 M PIPES buffer, pH 7.2

1.12.2 Spurr Resin

(Agar Scientific, Stanstead, UK)

1.12.3 Reynolds Lead Stain

Reynold's lead stain: 6 ml ddH2O in glass tube (blue-cap)

0.35 g NaCitrate.2H2O (Sigma, Poole, UK)

0.27 g Pb(NO3)2 (Sigma, Poole, UK)

Vortex for 1 minute

Add 1.6 ml 1M NaOH while vortexing

Add 2 mls ddH2O to 10 ml (may be stored in the dark at 4°C for a maximum of 12 hours)

References

Abdel-Malek, Z., Suzuki, I., Tada, A., Im, S., & Akcali, C. 1999, "The melanocortin-1 receptor and human pigmentation", *Ann.N.Y.Acad.Sci.*, vol. 885, pp. 117-133.

Abdel-Malek, Z., Swope, V. B., Trinkle, L. S., & Nordlund, J. J. 1989, "Stimulation of Cloudman melanoma tyrosinase activity occurs predominantly in G2 phase of the cell cycle", *Exp.Cell Res.*, vol. 180, no. 1, pp. 198-208.

Aberdam, E., Auberger, P., Ortonne, J. P., & Ballotti, R. 2000, "Neprilysin, a novel target for ultraviolet B regulation of melanogenesis via melanocortins", *J.Invest Dermatol.*, vol. 115, no. 3, pp. 381-387.

Aberdam, E., Bertolotto, C., Sviderskaya, E. V., de, T., V, Hemesath, T. J., Fisher, D. E., Bennett, D. C., Ortonne, J. P., & Ballotti, R. 1998, "Involvement of microphthalmia in the inhibition of melanocyte lineage differentiation and of melanogenesis by agouti signal protein", *J.Biol.Chem.*, vol. 273, no. 31, pp. 19560-19565.

Aksan, I. & Goding, C. R. 1998, "Targeting the microphthalmia basic helix-loop-helix-leucine zipper transcription factor to a subset of E-box elements in vitro and in vivo", *Mol.Cell Biol.*, vol. 18, no. 12, pp. 6930-6938.

Al-Obeidi, F., Castrucci, A. M., Hadley, M. E., & Hruby, V. J. 1989, "Potent and prolonged acting cyclic lactam analogues of alpha-melanotropin: design based on molecular dynamics", *J.Med.Chem.*, vol. 32, no. 12, pp. 2555-2561.

Ancans, J. & Thody, A. J. 2000, "Activation of melanogenesis by vacuolar type H(+)-ATPase inhibitors in amelanotic, tyrosinase positive human and mouse melanoma cells", *FEBS Lett.*, vol. 478, no. 1-2, pp. 57-60.

Ancans, J., Tobin, D. J., Hoogduijn, M. J., Smit, N. P., Wakamatsu, K., & Thody, A. J. 2001, "Melanosomal pH controls rate of melanogenesis, eumelanin/phaeomelanin ratio and melanosome maturation in melanocytes and melanoma cells", *Exp.Cell Res.*, vol. 268, no. 1, pp. 26-35.

Ao, Y., Park, H. Y., Olaizola-Horn, S., & Gilchrest, B. A. 1998, "Activation of cAMP-dependent protein kinase is required for optimal alpha-melanocyte-stimulating hormone-induced pigmentation", *Exp.Cell Res.*, vol. 244, no. 1, pp. 117-124.

Archer, C. B. 2004, "Function of the skin", In: Rook's Textbook of Dermatology, 7th edition, Blackwell Science, Burns, T., Breathnach, S., Cox, N., Griffiths, C., eds. vol. 1, chapter 3, pp. 4.1-4.12.

Ashworth, R., Yu, R., Nelson, E. J., Dermer, S., Gershengorn, M. C., & Hinkle, P. M. 1995, "Visualization of the thyrotropin-releasing hormone receptor and its ligand during endocytosis and recycling", *Proc.Natl.Acad.Sci.U.S.A*, vol. 92, no. 2, pp. 512-516.

Au, J. S. & Huang, J. D. 2002, "A tissue-specific exon of myosin Va is responsible for selective cargo binding in melanocytes", *Cell Motil.Cytoskeleton*, vol. 53, no. 2, pp. 89-102.

Bahadoran, P., Aberdam, E., Mantoux, F., Busca, R., Bille, K., Yalman, N., Saint-Basile, G., Casaroli-Marano, R., Ortonne, J. P., & Ballotti, R. 2001, "Rab27a: A key to melanosome transport in human melanocytes", *J.Cell Biol.*, vol. 152, no. 4, pp. 843-850.

Baig, A. H., Swords, F. M., Szaszak, M., King, P. J., Hunyady, L., & Clark, A. J. 2002, "Agonist activated adrenocorticotropin receptor internalizes via a clathrin-mediated G protein receptor kinase dependent mechanism", *Endocr.Res.*, vol. 28, no. 4, pp. 281-289.

Barak, L. S., Ferguson, S. S., Zhang, J., & Caron, M. G. 1997, "A beta-arrestin/green fluorescent protein biosensor for detecting G protein-coupled receptor activation", *J.Biol.Chem.*, vol. 272, no. 44, pp. 27497-27500.

Barral, D. C., Ramalho, J. S., Anders, R., Hume, A. N., Knapton, H. J., Tolmachova, T., Collinson, L. M., Goulding, D., Authi, K. S., & Seabra, M. C. 2002, "Functional redundancy of Rab27 proteins and the pathogenesis of Griscelli syndrome", *J.Clin.Invest*, vol. 110, no. 2, pp. 247-257.

Basrur, V., Yang, F., Kushimoto, T., Higashimoto, Y., Yasumoto, K., Valencia, J., Muller, J., Vieira, W. D., Watabe, H., Shabanowitz, J., Hearing, V. J., Hunt, D. F., & Appella, E. 2003, "Proteomic analysis of early melanosomes: identification of novel melanosomal proteins", *J.Proteome.Res.*, vol. 2, no. 1, pp. 69-79.

Bassi, M. T., Incerti, B., Easty, D. J., Sviderskaya, E. V., & Ballabio, A. 1996, "Cloning of the murine homolog of the ocular albinism type 1 (OA1) gene: sequence, genomic structure, and expression analysis in pigment cells", *Genome Res.*, vol. 6, no. 9, pp. 880-885.

Bassi, M. T., Schiaffino, M. V., Renieri, A., De, N. F., Galli, L., Bruttini, M., Gebbia, M., Bergen, A. A., Lewis, R. A., & Ballabio, A. 1995, "Cloning of the gene for ocular albinism type 1 from the distal short arm of the X chromosome", *Nat.Genet.*, vol. 10, no. 1, pp. 13-19.

Bastiaens, M., ter Huurne, J., Gruis, N., Bergman, W., Westendorp, R., Vermeer, B. J., & Bouwes Bavinck, J. N. 2001a, "The melanocortin-1-receptor gene is the major freckle gene", *Hum.Mol.Genet.*, vol. 10, no. 16, pp. 1701-1708.

Bastiaens, M. T., ter Huurne, J. A., Kielich, C., Gruis, N. A., Westendorp, R. G., Vermeer, B. J., & Bavinck, J. N. 2001b, "Melanocortin-1 receptor gene variants determine the risk of nonmelanoma skin cancer independently of fair skin and red hair", *Am.J.Hum.Genet.*, vol. 68, no. 4, pp. 884-894.

Beaumont, K. A., Newton, R. A., Smit, D. J., Leonard, J. H., Stow, J. L., & Sturm, R. A. 2005, "Altered cell surface expression of human MC1R variant receptor alleles associated with red hair and skin cancer risk", *Hum.Mol.Genet.*, vol. 14, no. 15, pp. 2145-2154.

Becher, E., Mahnke, K., Brzoska, T., Kalden, D. H., Grabbe, S., & Luger, T. A. 1999, "Human peripheral blood-derived dendritic cells express functional melanocortin receptor MC-1R", *Ann.N.Y.Acad.Sci.*, vol. 885, pp. 188-195.

Berens, W., Van Den, B. K., Yoon, T. J., Westbroek, W., Valencia, J. C., Out, C. J., Marie, N. J., Hearing, V. J., & Lambert, J. 2005, "Different approaches for assaying melanosome transfer", *Pigment Cell Res.*, vol. 18, no. 5, pp. 370-381.

Bertolotto, C., Abbe, P., Hemesath, T. J., Bille, K., Fisher, D. E., Ortonne, J. P., & Ballotti, R. 1998, "Microphthalmia gene product as a signal transducer in cAMP-induced differentiation of melanocytes", *J.Cell Biol.*, vol. 142, no. 3, pp. 827-835.

Bertolotto, C., Bille, K., Ortonne, J. P., & Ballotti, R. 1996, "Regulation of tyrosinase gene expression by cAMP in B16 melanoma cells involves two CATGTG motifs surrounding the TATA box: implication of the microphthalmia gene product", *J.Cell Biol.*, vol. 134, no. 3, pp. 747-755.

Bhardwaj, R., Becher, E., Mahnke, K., Hartmeyer, M., Schwarz, T., Scholzen, T., & Luger, T. A. 1997, "Evidence for the differential expression of the functional alpha-melanocyte-stimulating hormone receptor MC-1 on human monocytes", *J.Immunol.*, vol. 158, no. 7, pp. 3378-3384.

Bhardwaj, R. S., Schwarz, A., Becher, E., Mahnke, K., Aragane, Y., Schwarz, T., & Luger, T. A. 1996, "Pro-opiomelanocortin-derived peptides induce IL-10 production in human monocytes", *J.Immunol.*, vol. 156, no. 7, pp. 2517-2521.

Bhatnagar, V., Anjaiah, S., Puri, N., Darshanam, B. N., & Ramaiah, A. 1993, "pH of melanosomes of B 16 murine melanoma is acidic: its physiological importance in the regulation of melanin biosynthesis", *Arch.Biochem.Biophys.*, vol. 307, no. 1, pp. 183-192.

Blondet, A., Doghman, M., Rached, M., Durand, P., Begeot, M., & Naville, D. 2004, "Characterization of cell lines stably expressing human normal or mutated EGFP-tagged MC4R", *J.Biochem.(Tokyo)*, vol. 135, no. 4, pp. 541-546.

Bohm, M., Metze, D., Schulte, U., Becher, E., Luger, T. A., & Brzoska, T. 1999, "Detection of melanocortin-1 receptor antigenicity on human skin cells in culture and in situ", *Exp.Dermatol.*, vol. 8, no. 6, pp. 453-461.

Bohm, M., Schiller, M., Stander, S., Seltmann, H., Li, Z., Brzoska, T., Metze, D., Schioth, H. B., Skottner, A., Seiffert, K., Zouboulis, C. C., & Luger, T. A. 2002, "Evidence for expression of melanocortin-1 receptor in human sebocytes in vitro and in situ", *J.Invest Dermatol.*, vol. 118, no. 3, pp. 533-539.

Boissy, R. E., Sakai, C., Zhao, H., Kobayashi, T., & Hearing, V. J. 1998, "Human tyrosinase related protein-1 (TRP-1) does not function as a DHICA oxidase activity in contrast to murine TRP-1", *Exp.Dermatol.*, vol. 7, no. 4, pp. 198-204.

Boissy, R. E., Zhao, H., Oetting, W. S., Austin, L. M., Wildenberg, S. C., Boissy, Y. L., Zhao, Y., Sturm, R. A., Hearing, V. J., King, R. A., & Nordlund, J. J. 1996, "Mutation in and lack of expression of tyrosinase-related protein-1 (TRP-1) in melanocytes from an individual with brown oculocutaneous albinism: a new subtype of albinism classified as "OCA3"", *Am.J.Hum.Genet.*, vol. 58, no. 6, pp. 1145-1156.

Bondurand, N., Pingault, V., Goerich, D. E., Lemort, N., Sock, E., Caignec, C. L., Wegner, M., & Goossens, M. 2000, "Interaction among SOX10, PAX3 and MITF, three genes altered in Waardenburg syndrome", *Hum.Mol.Genet.*, vol. 9, no. 13, pp. 1907-1917.

Box, N. F., Duffy, D. L., Irving, R. E., Russell, A., Chen, W., Griffyths, L. R., Parsons, P. G., Green, A. C., & Sturm, R. A. 2001, "Melanocortin-1 receptor genotype is a risk factor for basal and squamous cell carcinoma", *J.Invest Dermatol.*, vol. 116, no. 2, pp. 224-229.

Box, N. F., Wyeth, J. R., O'Gorman, L. E., Martin, N. G., & Sturm, R. A. 1997, "Characterization of melanocyte stimulating hormone receptor variant alleles in twins with red hair", *Hum.Mol.Genet.*, vol. 6, no. 11, pp. 1891-1897.

Brannan, C. I., Lyman, S. D., Williams, D. E., Eisenman, J., Anderson, D. M., Cosman, D., Bedell, M. A., Jenkins, N. A., & Copeland, N. G. 1991, "Steel-Dickie mutation encodes a c-kit ligand lacking transmembrane and cytoplasmic domains", *Proc.Natl.Acad.Sci.U.S.A*, vol. 88, no. 11, pp. 4671-4674.

Bultman, S. J., Michaud, E. J., & Woychik, R. P. 1992, "Molecular characterization of the mouse agouti locus", *Cell*, vol. 71, no. 7, pp. 1195-1204.

Busca, R. & Ballotti, R. 2000, "Cyclic AMP a key messenger in the regulation of skin pigmentation", *Pigment Cell Res.*, vol. 13, no. 2, pp. 60-69.

Busca, R., Bertolotto, C., Abbe, P., Englaro, W., Ishizaki, T., Narumiya, S., Boquet, P., Ortonne, J. P., & Ballotti, R. 1998, "Inhibition of Rho is required for cAMP-induced melanoma cell differentiation", *Mol.Biol.Cell*, vol. 9, no. 6, pp. 1367-1378.

Busca, R., Bertolotto, C., Ortonne, J. P., & Ballotti, R. 1996, "Inhibition of the phosphatidylinositol 3-kinase/p70(S6)-kinase pathway induces B16 melanoma cell differentiation", *J.Biol.Chem.*, vol. 271, no. 50, pp. 31824-31830.

Butler, A. A., Kesterson, R. A., Khong, K., Cullen, M. J., Pelleymounter, M. A., Dekoning, J., Baetscher, M., & Cone, R. D. 2000, "A unique metabolic syndrome causes obesity in the melanocortin-3 receptor-deficient mouse", *Endocrinology*, vol. 141, no. 9, pp. 3518-3521.

Byers, H. R., Maheshwary, S., Amodeo, D. M., & Dykstra, S. G. 2003, "Role of cytoplasmic dynein in perinuclear aggregation of phagocytosed melanosomes and supranuclear melanin cap formation in human keratinocytes", *J.Invest Dermatol.*, vol. 121, no. 4, pp. 813-820.

Catania, A., Suffredini, A. F., & Lipton, J. M. 1995, "Endotoxin causes release of alpha-melanocyte-stimulating hormone in normal human subjects", *Neuroimmunomodulation.*, vol. 2, no. 5, pp. 258-262.

Ceriani, G., Diaz, J., Murphree, S., Catania, A., & Lipton, J. M. 1994, "The neuropeptide alpha-melanocyte-stimulating hormone inhibits experimental arthritis in rats", *Neuroimmunomodulation.*, vol. 1, no. 1, pp. 28-32.

Chabot, B., Stephenson, D. A., Chapman, V. M., Besmer, P., & Bernstein, A. 1988, "The proto-oncogene c-kit encoding a transmembrane tyrosine kinase receptor maps to the mouse W locus", *Nature*, vol. 335, no. 6185, pp. 88-89.

Chakraborty, A. K., Orlow, S. J., Bolognia, J. L., & Pawelek, J. M. 1991, "Structural/functional relationships between internal and external MSH receptors: modulation of expression in Cloudman melanoma cells by UVB radiation", *J.Cell Physiol*, vol. 147, no. 1, pp. 1-6.

Chakraborty, A. K., Platt, J. T., Kim, K. K., Kwon, B. S., Bennett, D. C., & Pawelek, J. M. 1996, "Polymerization of 5,6-dihydroxyindole-2-carboxylic acid to melanin by the pmel 17/silver locus protein", *Eur.J.Biochem.*, vol. 236, no. 1, pp. 180-188.

Chalepakis, G., Goulding, M., Read, A., Strachan, T., & Gruss, P. 1994, "Molecular basis of splotch and Waardenburg Pax-3 mutations", *Proc.Natl.Acad.Sci.U.S.A*, vol. 91, no. 9, pp. 3685-3689.

Chalfie, M., Tu, Y., Euskirchen, G., Ward, W. W., & Prasher, D. C. 1994, "Green fluorescent protein as a marker for gene expression", *Science*, vol. 263, no. 5148, pp. 802-805.

Chedekel, M. R., Smith, S. K., Post, P. W., Pokora, A., & Vessell, D. L. 1978, "Photodestruction of pheomelanin: role of oxygen", *Proc.Natl.Acad.Sci.U.S.A*, vol. 75, no. 11, pp. 5395-5399.

Chen, D., Guo, J., Miki, T., Tachibana, M., & Gahl, W. A. 1997, "Molecular cloning and characterization of rab27a and rab27b, novel human rab proteins shared by melanocytes and platelets", *Biochem.Mol.Med.*, vol. 60, no. 1, pp. 27-37.

Chhajlani, V. 1996, "Distribution of cDNA for melanocortin receptor subtypes in human tissues", *Biochem.Mol.Biol.Int.*, vol. 38, no. 1, pp. 73-80.

Chhajlani, V. & Wikberg, J. E. 1992, "Molecular cloning and expression of the human melanocyte stimulating hormone receptor cDNA", *FEBS Lett.*, vol. 309, no. 3, pp. 417-420.

Chretien, M., Benjannet, S., Gossard, F., Gianoulakis, C., Crine, P., Lis, M., & Seidah, N. G. 1979, "From beta-lipotropin to beta-endorphin and 'pro-opio-melanocortin'", *Can.J.Biochem.*, vol. 57, no. 9, pp. 1111-1121.

Chretien, M. & LI, C. H. 1967, "Isolation, purification, and characterization of gamma-lipotropic hormone from sheep pituitary glands", *Can.J.Biochem.*, vol. 45, no. 7, pp. 1163-1174.

Chu, D. H, Haake, A. R., Holbrook, K., Loomis, C. A. 2003, "Structure and development of skin", In: Fitzpatrick's Dermatology in General Medicine, 6th edition, McGraw-Hill medical publishing division, Freedberg, I. M., Eisen, A. Z., Wolff, K., Austen, K. F., Goldsmith, L. A., Katz, S. I., eds. vol. 1, part 2, "Biology and Development of Skin", section 3-6, pp. 58-88.

Cone, R. D., Lu, D., Koppula, S., Vage, D. I., Klungland, H., Boston, B., Chen, W., Orth, D. N., Pouton, C., & Kesterson, R. A. 1996, "The melanocortin receptors: agonists, antagonists, and the hormonal control of pigmentation", *Recent Prog.Horm.Res.*, vol. 51, pp. 287-317.

Cooper, A., Robinson, S. J., Pickard, C., Jackson, C. L., Friedmann, P. S., & Healy, E. 2005, "alpha-melanocyte-stimulating hormone suppresses antigen-induced lymphocyte proliferation in humans independently of melanocortin 1 receptor gene status", *J.Immunol.*, vol. 175, no. 7, pp. 4806-4813.

Copeland, N. G., Gilbert, D. J., Cho, B. C., Donovan, P. J., Jenkins, N. A., Cosman, D., Anderson, D., Lyman, S. D., & Williams, D. E. 1990, "Mast cell growth factor maps near the steel locus on mouse chromosome 10 and is deleted in a number of steel alleles", *Cell*, vol. 63, no. 1, pp. 175-183.

Cormack, B. P., Valdivia, R. H., & Falkow, S. 1996, "FACS-optimized mutants of the green fluorescent protein (GFP)", *Gene*, vol. 173, no. 1 Spec No, pp. 33-38.

Corre, S., Primot, A., Sviderskaya, E., Bennett, D. C., Vaulont, S., Goding, C. R., & Galibert, M. D. 2004, "UV-induced expression of key component of the tanning process, the POMC and MC1R genes, is dependent on the p-38-activated upstream stimulating factor-1 (USF-1)", *J.Biol.Chem.*, vol. 279, no. 49, pp. 51226-51233.

Costin, G. E., Valencia, J. C., Vieira, W. D., Lamoreux, M. L., & Hearing, V. J. 2003, "Tyrosinase processing and intracellular trafficking is disrupted in mouse primary melanocytes carrying the underwhite (uw) mutation. A model for oculocutaneous albinism (OCA) type 4", *J.Cell Sci.*, vol. 116, no. Pt 15, pp. 3203-3212.

d'Addio, M., Pizzigoni, A., Bassi, M. T., Baschirotto, C., Valetti, C., Incerti, B., Clementi, M., De, L. M., Ballabio, A., & Schiaffino, M. V. 2000, "Defective intracellular transport and processing of OA1 is a major cause of ocular albinism type 1", *Hum.Mol.Genet.*, vol. 9, no. 20, pp. 3011-3018.

Diment, S., Eidelman, M., Rodriguez, G. M., & Orlow, S. J. 1995, "Lysosomal hydrolases are present in melanosomes and are elevated in melanizing cells", *J.Biol.Chem.*, vol. 270, no. 9, pp. 4213-4215.

Dorr, R. T., Lines, R., Levine, N., Brooks, C., Xiang, L., Hruby, V. J., & Hadley, M. E. 1996, "Evaluation of melanotan-II, a superpotent cyclic melanotropic peptide in a pilot phase-I clinical study", *Life Sci.*, vol. 58, no. 20, pp. 1777-1784.

Du, J. & Fisher, D. E. 2002, "Identification of Aim-1 as the underwhite mouse mutant and its transcriptional regulation by MITF", *J.Biol.Chem.*, vol. 277, no. 1, pp. 402-406.

Eberle, A. N., Siegrist, W., Bagutti, C., Chluba-De, T. J., Solca, F., Wikberg, J. E., & Chhajlani, V. 1993, "Receptors for melanocyte-stimulating hormone on melanoma cells", *Ann.N.Y.Acad.Sci.*, vol. 680, pp. 320-341.

Eipper, B. A. & Mains, R. E. 1980, "Structure and biosynthesis of pro-adrenocorticotropin/endorphin and related peptides", *Endocr.Rev.*, vol. 1, no. 1, pp. 1-27.

Elias, P. M., Feingold, K. R., Fluhr, J. W. 2003, "Skin as an organ of protection", In: Fitzpatrick's Dermatology in General Medicine, 6th edition, McGraw-Hill medical publishing division, Freedberg, I. M., Eisen, A. Z., Wolff, K., Austen, K. F., Goldsmith, L. A., Katz, S. I., eds. vol. 1, part 2, "Biology and Development of Skin", section 3-9, pp. 107-118.

Englaro, W., Bertolotto, C., Busca, R., Brunet, A., Pages, G., Ortonne, J. P., & Ballotti, R. 1998, "Inhibition of the mitogen-activated protein kinase pathway triggers B16 melanoma cell differentiation", *J.Biol.Chem.*, vol. 273, no. 16, pp. 9966-9970.

Engle, L. J. & Kennett, R. H. 1994, "Cloning, analysis, and chromosomal localization of myoxin (MYH12), the human homologue to the mouse dilute gene", *Genomics*, vol. 19, no. 3, pp. 407-416.

Ferrell, W. R., Lockhart, J. C., Kelso, E. B., Dunning, L., Plevin, R., Meek, S. E., Smith, A. J., Hunter, G. D., McLean, J. S., McGarry, F., Ramage, R., Jiang, L., Kanke, T., & Kawagoe, J. 2003, "Essential role for proteinase-activated receptor-2 in arthritis", *J.Clin.Invest*, vol. 111, no. 1, pp. 35-41.

Fitzpatrick, T. B., & Breathnach, A. S. 1963, "The epidermal-melanin unit system", *Dermatol.Wochenschr.*, May 18, vol. 147, pp. 481-489.

Flanagan, N., Healy, E., Ray, A., Philips, S., Todd, C., Jackson, I. J., Birch-Machin, M. A., & Rees, J. L. 2000, "Pleiotropic effects of the melanocortin 1 receptor (MC1R) gene on human pigmentation", *Hum.Mol.Genet.*, vol. 9, no. 17, pp. 2531-2537.

Fleischman, R. A., Saltman, D. L., Stastny, V., & Zneimer, S. 1991, "Deletion of the c-kit protooncogene in the human developmental defect piebald trait", *Proc.Natl.Acad.Sci.U.S.A*, vol. 88, no. 23, pp. 10885-10889.

Frandberg, P. A., Doufexis, M., Kapas, S., & Chhajlani, V. 2001, "Cysteine residues are involved in structure and function of melanocortin 1 receptor: Substitution of a cysteine residue in transmembrane segment two converts an agonist to antagonist", *Biochem.Biophys.Res.Commun.*, vol. 281, no. 4, pp. 851-857.

Frandberg, P. A., Doufexis, M., Kapas, S., & Chhajlani, V. 1998a, "Human pigmentation phenotype: a point mutation generates nonfunctional MSH receptor", *Biochem.Biophys.Res.Commun.*, vol. 245, no. 2, pp. 490-492.

Frandberg, P. A., Doufexis, M., Kapas, S., & Chhajlani, V. 1998b, "Amino acid residues in third intracellular loop of melanocortin 1 receptor are involved in G-protein coupling", *Biochem.Mol.Biol.Int.*, vol. 46, no. 5, pp. 913-922.

Friedmann, P. S., Wren, F., Buffey, J., & Macneil, S. 1990, "Alpha-MSH causes a small rise in cAMP but has no effect on basal or ultraviolet-stimulated melanogenesis in human melanocytes", *Br.J.Dermatol.*, vol. 123, no. 2, pp. 145-151.

Fukunaga, S., Setoguchi, S., Hirasawa, A., & Tsujimoto, G. 2006, "Monitoring ligand-mediated internalization of G protein-coupled receptor as a novel pharmacological approach", *Life Sci.*

Fuller, B. B., Rungta, D., Iozumi, K., Hoganson, G. E., Corn, T. D., Cao, V. A., Ramadan, S. T., & Owens, K. C. 1993, "Hormonal regulation of melanogenesis in mouse melanoma and in human melanocytes", *Ann.N.Y.Acad.Sci.*, vol. 680, pp. 302-319.

Fuller, B. B. & Viskochil, D. H. 1979, "The role of RNA and protein synthesis in mediating the action of MSH on mouse melanoma cells", *Life Sci.*, vol. 24, no. 26, pp. 2405-2415.

Furumura, M., Potterf, S. B., Toyofuku, K., Matsunaga, J., Muller, J., & Hearing, V. J. 2001, "Involvement of ITF2 in the transcriptional regulation of melanogenic genes", *J.Biol.Chem.*, vol. 276, no. 30, pp. 28147-28154.

Galibert, M. D., Carreira, S., & Goding, C. R. 2001, "The Usf-1 transcription factor is a novel target for the stress-responsive p38 kinase and mediates UV-induced Tyrosinase expression", *EMBO J.*, vol. 20, no. 17, pp. 5022-5031.

Gantz, I. & Fong, T. M. 2003, "The melanocortin system", *Am.J.Physiol Endocrinol.Metab*, vol. 284, no. 3, p. E468-E474.

Gantz, I., Konda, Y., Tashiro, T., Shimoto, Y., Miwa, H., Munzert, G., Watson, S. J., DelValle, J., & Yamada, T. 1993a, "Molecular cloning of a novel melanocortin receptor", *J.Biol.Chem.*, vol. 268, no. 11, pp. 8246-8250.

Gantz, I., Miwa, H., Konda, Y., Shimoto, Y., Tashiro, T., Watson, S. J., DelValle, J., & Yamada, T. 1993b, "Molecular cloning, expression, and gene localization of a fourth melanocortin receptor", *J.Biol.Chem.*, vol. 268, no. 20, pp. 15174-15179.

Gantz, I., Shimoto, Y., Konda, Y., Miwa, H., Dickinson, C. J., & Yamada, T. 1994a, "Molecular cloning, expression, and characterization of a fifth melanocortin receptor", *Biochem.Biophys.Res.Commun.*, vol. 200, no. 3, pp. 1214-1220.

Gantz, I., Yamada, T., Tashiro, T., Konda, Y., Shimoto, Y., Miwa, H., & Trent, J. M. 1994b, "Mapping of the gene encoding the melanocortin-1 (alpha-melanocyte stimulating hormone) receptor (MC1R) to human chromosome 16q24.3 by Fluorescence in situ hybridization", *Genomics*, vol. 19, no. 2, pp. 394-395.

Gao, Z., Lei, D., Welch, J., Le, K., Lin, J., Leng, S., & Duhl, D. 2003, "Agonist-dependent internalization of the human melanocortin-4 receptors in human embryonic kidney 293 cells", *J.Pharmacol.Exp.Ther.*, vol. 307, no. 3, pp. 870-877.

Garcia-Borron, J. C., Sanchez-Laorden, B. L., & Jimenez-Cervates, C. 2005, "Melanocortin-1 receptor structure and functional regulation", *Pigment Cell Res.*, vol. 18, no. 6, pp. 393-410.

Garner, A. & Jay, B. S. 1980, "Macromelanosomes in X-linked ocular albinism", *Histopathology*, vol. 4, no. 3, pp. 243-254.

Geffrotin, C., Crechet, F., Le Roy, P., Le Chalony, C., Leplat, J. J., Iannuccelli, N., Barbosa, A., Renard, C., Gruand, J., Milan, D., Horak, V., Tricaud, Y., Bouet, S., Franck, M., Frelat, G., & Vincent-Naulleau, S. 2004, "Identification of five chromosomal regions involved in predisposition to melanoma by genome-wide scan in the MeLiM swine model", *Int.J.Cancer*, vol. 110, no. 1, pp. 39-50.

Getting, S. J. 2002, "Melanocortin peptides and their receptors: new targets for anti-inflammatory therapy", *Trends Pharmacol.Sci.*, vol. 23, no. 10, pp. 447-449.

Getting, S. J., Christian, H. C., Lam, C. W., Gavins, F. N., Flower, R. J., Schioth, H. B., & Perretti, M. 2003, "Redundancy of a functional melanocortin 1 receptor in the anti-inflammatory actions of melanocortin peptides: studies in the recessive yellow (e/e) mouse suggest an important role for melanocortin 3 receptor", *J.Immunol.*, vol. 170, no. 6, pp. 3323-3330.

Giebel, L. B., Tripathi, R. K., Strunk, K. M., Hanifin, J. M., Jackson, C. E., King, R. A., & Spritz, R. A. 1991, "Tyrosinase gene mutations associated with type IB ("yellow") oculocutaneous albinism", *Am.J.Hum.Genet.*, vol. 48, no. 6, pp. 1159-1167.

Gilardeau, C. & Chretien, M. 1970, "Isolation and characterization of beta-lipolytic hormone from porcine pituitary gland", *Can.J.Biochem.*, vol. 48, no. 9, pp. 1017-1021.

Gilchrest, B. A., Park, H. Y., Eller, M. S., & Yaar, M. 1996, "Mechanisms of ultraviolet light-induced pigmentation", *Photochem.Photobiol.*, vol. 63, no. 1, pp. 1-10.

Gimenez, E., Lavado, A., Giraldo, P., Cozar, P., Jeffery, G., & Montoliu, L. 2004, "A transgenic mouse model with inducible Tyrosinase gene expression using the tetracycline (Tet-on) system allows regulated rescue of abnormal chiasmatic projections found in albinism", *Pigment Cell Res.*, vol. 17, no. 4, pp. 363-370.

Goldstein, A. M., Landi, M. T., Tsang, S., Fraser, M. C., Munroe, D. J., & Tucker, M. A. 2005, "Association of MC1R variants and risk of melanoma in melanoma-prone families with CDKN2A mutations", *Cancer Epidemiol.Biomarkers Prev.*, vol. 14, no. 9, pp. 2208-2212.

Grabbe, S., Steinert, M., Mahnke, K., Schwartz, A., Luger, T. A., & Schwarz, T. 1996, "Dissection of antigenic and irritative effects of epicutaneously applied haptens in mice. Evidence that not the antigenic component but nonspecific proinflammatory effects of haptens determine the concentration-dependent elicitation of allergic contact dermatitis", *J.Clin.Invest*, vol. 98, no. 5, pp. 1158-1164.

Graham, A., Wakamatsu, K., Hunt, G., Ito, S., & Thody, A. J. 1997, "Agouti protein inhibits the production of eumelanin and phaeomelanin in the presence and absence of alpha-melanocyte stimulating hormone", *Pigment Cell Res.*, vol. 10, no. 5, pp. 298-303.

Griscelli, C., Durandy, A., Guy-Grand, D., Daguillard, F., Herzog, C., & Prunieras, M. 1978, "A syndrome associating partial albinism and immunodeficiency", *Am.J.Med.*, vol. 65, no. 4, pp. 691-702.

Groarke, D. A., Drmota, T., Bahia, D. S., Evans, N. A., Wilson, S., & Milligan, G. 2001, "Analysis of the C-terminal tail of the rat thyrotropin-releasing hormone receptor-1 in interactions and cointernalization with beta-arrestin 1-green fluorescent protein", *Mol.Pharmacol.*, vol. 59, no. 2, pp. 375-385.

Halaban, R., Langdon, R., Birchall, N., Cuono, C., Baird, A., Scott, G., Moellmann, G., & McGuire, J. 1988, "Paracrine stimulation of melanocytes by keratinocytes through basic fibroblast growth factor", *Ann.N.Y.Acad.Sci.*, vol. 548, pp. 180-190.

Halaban, R. & Moellmann, G. 1990, "Murine and human b locus pigmentation genes encode a glycoprotein (gp75) with catalase activity", *Proc.Natl.Acad.Sci.U.S.A*, vol. 87, no. 12, pp. 4809-4813.

Halaban, R., Svedine, S., Cheng, E., Smicun, Y., Aron, R., & Hebert, D. N. 2000, "Endoplasmic reticulum retention is a common defect associated with tyrosinase-negative albinism", *Proc.Natl.Acad.Sci.U.S.A*, vol. 97, no. 11, pp. 5889-5894.

Harbour, D. V., Smith, E. M., & Blalock, J. E. 1987, "Novel processing pathway for proopiomelanocortin in lymphocytes: endotoxin induction of a new prohormone-cleaving enzyme", *J.Neurosci.Res.*, vol. 18, no. 1, pp. 95-101.

Harding, R. M., Healy, E., Ray, A. J., Ellis, N. S., Flanagan, N., Todd, C., Dixon, C., Sajantila, A., Jackson, I. J., Birch-MacHin, M. A., & Rees, J. L. 2000, "Evidence for variable selective pressures at MC1R", *Am.J.Hum.Genet.*, vol. 66, no. 4, pp. 1351-1361.

Hashizume, T., Yang, W. H., Clay, C. M., & Nett, T. M. 2001, "Internalization rates of murine and ovine gonadotropin-releasing hormone receptors", *Biol.Reprod.*, vol. 64, no. 3, pp. 898-903.

Healy, E., Flannagan, N., Ray, A., Todd, C., Jackson, I. J., Matthews, J. N., Birch-MacHin, M. A., & Rees, J. L. 2000, "Melanocortin-1-receptor gene and sun sensitivity in individuals without red hair", *Lancet*, vol. 355, no. 9209, pp. 1072-1073.

Healy, E., Jordan, S. A., Budd, P. S., Suffolk, R., Rees, J. L., & Jackson, I. J. 2001, "Functional variation of MC1R alleles from red-haired individuals", *Hum.Mol.Genet.*, vol. 10, no. 21, pp. 2397-2402.

Hiltz, M. E., Catania, A., & Lipton, J. M. 1992, "Alpha-MSH peptides inhibit acute inflammation induced in mice by rIL-1 beta, rIL-6, rTNF-alpha and endogenous pyrogen but not that caused by LTB4, PAF and rIL-8", *Cytokine*, vol. 4, no. 4, pp. 320-328.

Hirobe, T. & Takeuchi, T. 1977, "Induction of melanogenesis in vitro in the epidermal melanoblasts of newborn mouse skin by MSH", *In Vitro*, vol. 13, no. 5, pp. 311-315.

Ho, G. & Mackenzie, R. G. 1999, "Functional characterization of mutations in melanocortin-4 receptor associated with human obesity", *J.Biol.Chem.*, vol. 274, no. 50, pp. 35816-35822.

Hoashi, T., Watabe, H., Muller, J., Yamaguchi, Y., Vieira, W. D., & Hearing, V. J. 2005, "MART-1 is required for the function of the melanosomal matrix protein PMEL17/GP100 and the maturation of melanosomes", *J.Biol.Chem.*, vol. 280, no. 14, pp. 14006-14016.

Hoekstra, H. E., Drumm, K. E., & Nachman, M. W. 2004, "Ecological genetics of adaptive color polymorphism in pocket mice: geographic variation in selected and neutral genes", *Evolution Int.J.Org.Evolution*, vol. 58, no. 6, pp. 1329-1341.

Hoekstra, H. E., Hirschmann, R. J., Bundey, R. A., Insel, P. A., & Crossland, J. P. 2006, "A single amino acid mutation contributes to adaptive beach mouse color pattern", *Science*, vol. 313, no. 5783, pp. 101-104.

Hoekstra, H. E., Krenz, J. G., & Nachman, M. W. 2005, "Local adaptation in the rock pocket mouse (Chaetodipus intermedius): natural selection and phylogenetic history of populations", *Heredity*, vol. 94, no. 2, pp. 217-228.

Holman, C. D. & Armstrong, B. K. 1984, "Pigmentary traits, ethnic origin, benign nevi, and family history as risk factors for cutaneous malignant melanoma", *J.Natl.Cancer Inst.*, vol. 72, no. 2, pp. 257-266.

Hoogduijn, M. J., McGurk, S., Smit, N. P., Nibbering, P. H., Ancans, J., van der, L. A., & Thody, A. J. 2002, "Ligand-dependent activation of the melanocortin 5 receptor: cAMP production and ryanodine receptor-dependent elevations of [Ca(2+)](I)", *Biochem.Biophys.Res.Commun.*, vol. 290, no. 2, pp. 844-850.

Hori, Y., Toda, K., Pathak, M. A., Clark, W. H., Jr., & Fitzpatrick, T. B. 1968, "A fine-structure study of the human epidermal melanosome complex and its acid phosphatase activity", *J.Ultrastruct.Res.*, vol. 25, no. 1, pp. 109-120.

Horvat, R. D., Barisas, B. G., & Roess, D. A. 2001, "Luteinizing hormone receptors are self-associated in slowly diffusing complexes during receptor desensitization", *Mol.Endocrinol.*, vol. 15, no. 4, pp. 534-542.

Hruby, V. J., Lu, D., Sharma, S. D., Castrucci, A. L., Kesterson, R. A., al-Obeidi, F. A., Hadley, M. E., & Cone, R. D. 1995, "Cyclic lactam alpha-melanotropin analogues of Ac-Nle4-cyclo[Asp5, D-Phe7,Lys10] alpha-melanocyte-stimulating hormone-(4-10)-NH2 with bulky aromatic amino acids at position 7 show high antagonist potency and selectivity at specific melanocortin receptors", *J.Med.Chem.*, vol. 38, no. 18, pp. 3454-3461.

Hughes, A. E., Newton, V. E., Liu, X. Z., & Read, A. P. 1994, "A gene for Waardenburg syndrome type 2 maps close to the human homologue of the microphthalmia gene at chromosome 3p12-p14.1", *Nat.Genet.*, vol. 7, no. 4, pp. 509-512.

Hume, A. N., Collinson, L. M., Rapak, A., Gomes, A. Q., Hopkins, C. R., & Seabra, M. C. 2001, "Rab27a regulates the peripheral distribution of melanosomes in melanocytes", *J.Cell Biol.*, vol. 152, no. 4, pp. 795-808.

Hunt, G., Donatien, P. D., Lunec, J., Todd, C., Kyne, S., & Thody, A. J. 1994, "Cultured human melanocytes respond to MSH peptides and ACTH", *Pigment Cell Res.*, vol. 7, no. 4, pp. 217-221.

Hunt, G., Kyne, S., Ito, S., Wakamatsu, K., Todd, C., & Thody, A. 1995, "Eumelanin and phaeomelanin contents of human epidermis and cultured melanocytes", *Pigment Cell Res.*, vol. 8, no. 4, pp. 202-208.

Huszar, D., Lynch, C. A., Fairchild-Huntress, V., Dunmore, J. H., Fang, Q., Berkemeier, L. R., Gu, W., Kesterson, R. A., Boston, B. A., Cone, R. D., Smith, F. J., Campfield, L. A., Burn, P., & Lee, F. 1997, "Targeted disruption of the melanocortin-4 receptor results in obesity in mice", *Cell*, vol. 88, no. 1, pp. 131-141.

Ichii-Jones, F., Lear, J. T., Heagerty, A. H., Smith, A. G., Hutchinson, P. E., Osborne, J., Bowers, B., Jones, P. W., Davies, E., Ollier, W. E., Thomson, W., Yengi, L., Bath, J., Fryer, A. A., & Strange, R. C. 1998, "Susceptibility to melanoma: influence of skin type and polymorphism in the melanocyte stimulating hormone receptor gene", *J.Invest Dermatol.*, vol. 111, no. 2, pp. 218-221.

Ichiyama, T., Sakai, T., Catania, A., Barsh, G. S., Furukawa, S., & Lipton, J. M. 1999, "Inhibition of peripheral NF-kappaB activation by central action of alpha-melanocyte-stimulating hormone", *J.Neuroimmunol.*, vol. 99, no. 2, pp. 211-217.

Incerti, B., Cortese, K., Pizzigoni, A., Surace, E. M., Varani, S., Coppola, M., Jeffery, G., Seeliger, M., Jaissle, G., Bennett, D. C., Marigo, V., Schiaffino, M. V., Tacchetti, C., & Ballabio, A. 2000, "Oa1 knock-out: new insights on the pathogenesis of ocular albinism type 1", *Hum.Mol.Genet.*, vol. 9, no. 19, pp. 2781-2788.

Inouye, S. & Tsuji, F. I. 1994, "Evidence for redox forms of the Aequorea green fluorescent protein", *FEBS Lett.*, vol. 351, no. 2, pp. 211-214.

Ivic, L., Zhang, C., Zhang, X., Yoon, S. O., & Firestein, S. 2002, "Intracellular trafficking of a tagged and functional mammalian olfactory receptor", *J.Neurobiol.*, vol. 50, no. 1, pp. 56-68.

Jackson, I. J. 1997, "Homologous pigmentation mutations in human, mouse and other model organisms", *Hum.Mol.Genet.*, vol. 6, no. 10, pp. 1613-1624.

Jackson, I. J., Chambers, D. M., Tsukamoto, K., Copeland, N. G., Gilbert, D. J., Jenkins, N. A., & Hearing, V. 1992, "A second tyrosinase-related protein, TRP-2, maps to and is mutated at the mouse slaty locus", *EMBO J.*, vol. 11, no. 2, pp. 527-535.

Jimbow, K., Quevedo, W. C., Jr., Fitzpatrick, T. B., & Szabo, G. 1976, "Some aspects of melanin biology: 1950-1975", *J.Invest Dermatol.*, vol. 67, no. 1, pp. 72-89.

Jimbow, K. & Uesugi, T. 1982, "New melanogenesis and photobiological processes in activation and proliferation of precursor melanocytes after UV-exposure: ultrastructural differentiation of precursor melanocytes from Langerhans cells", *J.Invest Dermatol.*, vol. 78, no. 2, pp. 108-115.

Jimenez, M., Kameyama, K., Maloy, W. L., Tomita, Y., & Hearing, V. J. 1988, "Mammalian tyrosinase: biosynthesis, processing, and modulation by melanocyte-stimulating hormone", *Proc.Natl.Acad.Sci.U.S.A*, vol. 85, no. 11, pp. 3830-3834.

Jimenez, M., Maloy, W. L., & Hearing, V. J. 1989, "Specific identification of an authentic clone for mammalian tyrosinase", *J.Biol.Chem.*, vol. 264, no. 6, pp. 3397-3403.

Jimenez-Cervantes, C., Germer, S., Gonzalez, P., Sanchez, J., Sanchez, C. O., & Garcia-Borron, J. C. 2001a, "Thr40 and Met122 are new partial loss-of-function natural mutations of the human melanocortin 1 receptor", *FEBS Lett.*, vol. 508, no. 1, pp. 44-48.

Jimenez-Cervantes, C., Olivares, C., Gonzalez, P., Morandini, R., Ghanem, G., & Garcia-Borron, J. C. 2001b, "The Pro162 variant is a loss-of-function mutation of the human melanocortin 1 receptor gene", *J.Invest Dermatol.*, vol. 117, no. 1, pp. 156-158.

Jimenez-Cervantes, C., Solano, F., Kobayashi, T., Urabe, K., Hearing, V. J., Lozano, J. A., & Garcia-Borron, J. C. 1994, "A new enzymatic function in the melanogenic pathway. The 5,6-dihydroxyindole-2-carboxylic acid oxidase activity of tyrosinase-related protein-1 (TRP1)", *J.Biol.Chem.*, vol. 269, no. 27, pp. 17993-18000.

Kameyama, K., Tanaka, S., Ishida, Y., & Hearing, V. J. 1989, "Interferons modulate the expression of hormone receptors on the surface of murine melanoma cells", *J.Clin.Invest*, vol. 83, no. 1, pp. 213-221.

Kanetsky, P. A., Swoyer, J., Panossian, S., Holmes, R., Guerry, D., & Rebbeck, T. R. 2002, "A polymorphism in the agouti signaling protein gene is associated with human pigmentation", *Am.J.Hum.Genet.*, vol. 70, no. 3, pp. 770-775.

Kennedy, C., ter Huurne, J., Berkhout, M., Gruis, N., Bastiaens, M., Bergman, W., Willemze, R., & Bavinck, J. N. 2001, "Melanocortin 1 receptor (MC1R) gene variants are associated with an increased risk for cutaneous melanoma which is largely independent of skin type and hair color", *J.Invest Dermatol.*, vol. 117, no. 2, pp. 294-300.

Kidson, S. H., Richards, P. D., Rawoot, F., & Kromberg, J. G. 1993, "An ultrastructural study of melanocytes and melanosomes in the skin and hair bulbs of rufous albinos", *Pigment Cell Res.*, vol. 6, no. 4 Pt 1, pp. 209-214.

Kijas, J. M., Moller, M., Plastow, G., & Andersson, L. 2001, "A frameshift mutation in mc1r and a high frequency of somatic reversions cause black spotting in pigs", *Genetics*, vol. 158, no. 2, pp. 779-785.

Kim, J., Lo, L., Dormand, E., & Anderson, D. J. 2003, "SOX10 maintains multipotency and inhibits neuronal differentiation of neural crest stem cells", *Neuron*, vol. 38, no. 1, pp. 17-31.

Kim, K. S., Park, D. H., Wessel, T. C., Song, B., Wagner, J. A., & Joh, T. H. 1993, "A dual role for the cAMP-dependent protein kinase in tyrosine hydroxylase gene expression", *Proc.Natl.Acad.Sci.U.S.A*, vol. 90, no. 8, pp. 3471-3475.

Kimura, K., Hattori, S., Kabuyama, Y., Shizawa, Y., Takayanagi, J., Nakamura, S., Toki, S., Matsuda, Y., Onodera, K., & Fukui, Y. 1994, "Neurite outgrowth of PC12 cells is suppressed by wortmannin, a specific inhibitor of phosphatidylinositol 3-kinase", *J.Biol.Chem.*, vol. 269, no. 29, pp. 18961-18967.

Kimyai-Asadi, A., Jih, M. H., Freedberg, I. M. 2003, "Epidermal cell kinetics, epidermal differentiation, and keratinisation", In: Fitzpatrick's Dermatology in General Medicine, 6th edition, McGraw-Hill medical publishing division, Freedberg, I. M., Eisen, A. Z., Wolff, K., Austen, K. F., Goldsmith, L. A., Katz, S. I., eds. vol. 1, part 2, "Biology and Development of Skin", section 4-7, pp. 88-98.

King, R. A., Creel, D., Cervenka, J., Okoro, A. N., & Witkop, C. J. 1980, "Albinism in Nigeria with delineation of new recessive oculocutaneous type", *Clin.Genet.*, vol. 17, no. 4, pp. 259-270.

King, R. A., Mentink, M. M., & Oetting, W. S. 1991, "Non-random distribution of missense mutations within the human tyrosinase gene in type I (tyrosinase-related) oculocutaneous albinism", *Mol.Biol.Med.*, vol. 8, no. 1, pp. 19-29.

King, R. A., Willaert, R. K., Schmidt, R. M., Pietsch, J., Savage, S., Brott, M. J., Fryer, J. P., Summers, C. G., & Oetting, W. S. 2003, "MC1R mutations modify the classic phenotype of oculocutaneous albinism type 2 (OCA2)", *Am.J.Hum.Genet.*, vol. 73, no. 3, pp. 638-645.

King, R. A. & Witkop, C. J., Jr. 1976, "Hairbulb tyrosinase activity in oculocutaneous albinism", *Nature*, vol. 263, no. 5572, pp. 69-71.

Klungland, H., Vage, D. I., Gomez-Raya, L., Adalsteinsson, S., & Lien, S. 1995, "The role of melanocyte-stimulating hormone (MSH) receptor in bovine coat color determination", *Mamm.Genome*, vol. 6, no. 9, pp. 636-639.

Kobayashi, T., Urabe, K., Orlow, S. J., Higashi, K., Imokawa, G., Kwon, B. S., Potterf, B., & Hearing, V. J. 1994, "The Pmel 17/silver locus protein. Characterization and investigation of its melanogenic function", *J.Biol.Chem.*, vol. 269, no. 46, pp. 29198-29205.

Kobayashi, T., Vieira, W. D., Potterf, B., Sakai, C., Imokawa, G., & Hearing, V. J. 1995, "Modulation of melanogenic protein expression during the switch from eu- to pheomelanogenesis", *J.Cell Sci.*, vol. 108 (Pt 6), pp. 2301-2309.

Kock, A., Schwarz, T., Micksche, M., & Luger, T. A. 1991, "Cytokines and human malignant melanoma. Immuno- and growth-regulatory peptides in melanoma biology", *Cancer Treat.Res.*, vol. 54, pp. 41-66.

Konda, Y., Gantz, I., DelValle, J., Shimoto, Y., Miwa, H., & Yamada, T. 1994, "Interaction of dual intracellular signaling pathways activated by the melanocortin-3 receptor", *J.Biol.Chem.*, vol. 269, no. 18, pp. 13162-13166.

Korner, A. & Pawelek, J. 1982, "Mammalian tyrosinase catalyzes three reactions in the biosynthesis of melanin", *Science*, vol. 217, no. 4565, pp. 1163-1165.

Korner, A. M. & Gettins, P. 1985, "Synthesis in vitro of 5,6-dihydroxyindole-2-carboxylic acid by dopachrome conversion factor from Cloudman S91 melanoma cells", *J.Invest Dermatol.*, vol. 85, no. 3, pp. 229-231.

Krude, H., Biebermann, H., Luck, W., Horn, R., Brabant, G., & Gruters, A. 1998, "Severe early-onset obesity, adrenal insufficiency and red hair pigmentation caused by POMC mutations in humans", *Nat.Genet.*, vol. 19, no. 2, pp. 155-157.

Kwon, B. S., Chintamaneni, C., Kozak, C. A., Copeland, N. G., Gilbert, D. J., Jenkins, N., Barton, D., Francke, U., Kobayashi, Y., & Kim, K. K. 1991, "A melanocyte-specific gene, Pmel 17, maps near the silver coat color locus on mouse chromosome 10 and is in a syntenic region on human chromosome 12", *Proc.Natl.Acad.Sci.U.S.A*, vol. 88, no. 20, pp. 9228-9232.

Kwon, B. S., Halaban, R., Ponnazhagan, S., Kim, K., Chintamaneni, C., Bennett, D., & Pickard, R. T. 1995, "Mouse silver mutation is caused by a single base insertion in the putative cytoplasmic domain of Pmel 17", *Nucleic Acids Res.*, vol. 23, no. 1, pp. 154-158.

Kwon, B. S., Haq, A. K., Pomerantz, S. H., & Halaban, R. 1987, "Isolation and sequence of a cDNA clone for human tyrosinase that maps at the mouse c-albino locus", *Proc.Natl.Acad.Sci.U.S.A*, vol. 84, no. 21, pp. 7473-7477.

Kwon, B. S., Kim, K. K., Halaban, R., & Pickard, R. T. 1994, "Characterization of mouse Pmel 17 gene and silver locus", *Pigment Cell Res.*, vol. 7, no. 6, pp. 394-397.

Lamason, R. L., Mohideen, M. A., Mest, J. R., Wong, A. C., Norton, H. L., Aros, M. C., Jurynec, M. J., Mao, X., Humphreville, V. R., Humbert, J. E., Sinha, S., Moore, J. L., Jagadeeswaran, P., Zhao, W., Ning, G., Makalowska, I., McKeigue, P. M., O'donnell, D., Kittles, R., Parra, E. J., Mangini, N. J., Grunwald, D. J., Shriver, M. D., Canfield, V. A., & Cheng, K. C. 2005, "SLC24A5, a putative cation exchanger, affects pigmentation in zebrafish and humans", *Science*, vol. 310, no. 5755, pp. 1782-1786.

Landi, M. T., Bauer, J., Pfeiffer, R. M., Elder, D. E., Hulley, B., Minghetti, P., Calista, D., Kanetsky, P. A., Pinkel, D., & Bastian, B. C. 2006, "MC1R germline variants confer risk for BRAF-mutant melanoma", *Science*, vol. 313, no. 5786, pp. 521-522.

Landi, M. T., Kanetsky, P. A., Tsang, S., Gold, B., Munroe, D., Rebbeck, T., Swoyer, J., Ter Minassian, M., Hedayati, M., Grossman, L., Goldstein, A. M., Calista, D., & Pfeiffer, R. M. 2005, "MC1R, ASIP, and DNA repair in sporadic and familial melanoma in a Mediterranean population", *J.Natl.Cancer Inst.*, vol. 97, no. 13, pp. 998-1007.

Lee, S. T., Nicholls, R. D., Bundey, S., Laxova, R., Musarella, M., & Spritz, R. A. 1994, "Mutations of the P gene in oculocutaneous albinism, ocular albinism, and Prader-Willi syndrome plus albinism", *N.Engl.J.Med.*, vol. 330, no. 8, pp. 529-534.

Lehman, A. L., Silvers, W. K., Puri, N., Wakamatsu, K., Ito, S., & Brilliant, M. H. 2000, "The underwhite (uw) locus acts autonomously and reduces the production of melanin", *J.Invest Dermatol.*, vol. 115, no. 4, pp. 601-606.

Lerner, A. B. & McGuire, J. S. 1964, "MELANOCYTE-STIMULATING HORMONE AND ADRENOCORTICOTROPHIC HORMONE. THEIR RELATION TO PIGMENTATION", *N.Engl.J.Med.*, vol. 270, pp. 539-546.

Lerner, A. B., Moellmann, G., Varga, J. M., Halaban, R., & Pawelek, J. 1979, "Action of melanocyte-stimulating hormone on pigment cells. In: Cold Spring Harbour Conferences on Cell Proliferation, Cold Spring Harbour Laboratory, New York, Sato, G.H., Pardee, A. B., Sirbascu, D. A., eds., vol. 6, pp. 187-197.

Levine, N., Sheftel, S. N., Eytan, T., Dorr, R. T., Hadley, M. E., Weinrach, J. C., Ertl, G. A., Toth, K., McGee, D. L., & Hruby, V. J. 1991, "Induction of skin tanning by subcutaneous administration of a potent synthetic melanotropin", *JAMA*, vol. 266, no. 19, pp. 2730-2736.

LI, C. H. 1964, "LIPOTROPIN, A NEW ACTIVE PEPTIDE FROM PITUITARY GLANDS", *Nature*, vol. 201, p. 924.

Li, X. D., Ikebe, R., & Ikebe, M. 2005, "Activation of myosin Va function by melanophilin, a specific docking partner of myosin Va", *J.Biol.Chem.*, vol. 280, no. 18, pp. 17815-17822.

Liu, J., Conklin, B. R., Blin, N., Yun, J., & Wess, J. 1995, "Identification of a receptor/G-protein contact site critical for signaling specificity and G-protein activation", *Proc.Natl.Acad.Sci.U.S.A*, vol. 92, no. 25, pp. 11642-11646.

Lu, D., Willard, D., Patel, I. R., Kadwell, S., Overton, L., Kost, T., Luther, M., Chen, W., Woychik, R. P., Wilkison, W. O., & . 1994, "Agouti protein is an antagonist of the melanocyte-stimulating-hormone receptor", *Nature*, vol. 371, no. 6500, pp. 799-802.

Lubrano-Berthelier, C., Durand, E., Dubern, B., Shapiro, A., Dazin, P., Weill, J., Ferron, C., Froguel, P., & Vaisse, C. 2003, "Intracellular retention is a common characteristic of childhood obesity-associated MC4R mutations", *Hum.Mol.Genet.*, vol. 12, no. 2, pp. 145-153.

Luger, T. A., Scholzen, T., & Grabbe, S. 1997, "The role of alpha-melanocyte-stimulating hormone in cutaneous biology", *J.Investig.Dermatol.Symp.Proc.*, vol. 2, no. 1, pp. 87-93.

Lyon, M. F., King, T. R., Gondo, Y., Gardner, J. M., Nakatsu, Y., Eicher, E. M., & Brilliant, M. H. 1992, "Genetic and molecular analysis of recessive alleles at the pink-eyed dilution (p) locus of the mouse", *Proc.Natl.Acad.Sci.U.S.A*, vol. 89, no. 15, pp. 6968-6972.

Mackenzie, M. A., Jordan, S. A., Budd, P. S., & Jackson, I. J. 1997, "Activation of the receptor tyrosine kinase Kit is required for the proliferation of melanoblasts in the mouse embryo", *Dev.Biol.*, vol. 192, no. 1, pp. 99-107.

Mandrika, I., Petrovska, R., & Wikberg, J. 2005, "Melanocortin receptors form constitutive homo- and heterodimers", *Biochem.Biophys.Res.Commun.*, vol. 326, no. 2, pp. 349-354.

Manga, P., Kromberg, J. G., Box, N. F., Sturm, R. A., Jenkins, T., & Ramsay, M. 1997, "Rufous oculocutaneous albinism in southern African Blacks is caused by mutations in the TYRP1 gene", *Am.J.Hum.Genet.*, vol. 61, no. 5, pp. 1095-1101.

Mansky, K. C., Sankar, U., Han, J., & Ostrowski, M. C. 2002, "Microphthalmia transcription factor is a target of the p38 MAPK pathway in response to receptor activator of NF-kappa B ligand signaling", *J.Biol.Chem.*, vol. 277, no. 13, pp. 11077-11083.

Marklund, L., Moller, M. J., Sandberg, K., & Andersson, L. 1996, "A missense mutation in the gene for melanocyte-stimulating hormone receptor (MC1R) is associated with the chestnut coat color in horses", *Mamm.Genome*, vol. 7, no. 12, pp. 895-899.

Marsh, D. J., Hollopeter, G., Huszar, D., Laufer, R., Yagaloff, K. A., Fisher, S. L., Burn, P., & Palmiter, R. D. 1999, "Response of melanocortin-4 receptor-deficient mice to anorectic and orexigenic peptides", *Nat.Genet.*, vol. 21, no. 1, pp. 119-122.

Matsui, Y., Zsebo, K. M., & Hogan, B. L. 1990, "Embryonic expression of a haematopoietic growth factor encoded by the Sl locus and the ligand for c-kit", *Nature*, vol. 347, no. 6294, pp. 667-669.

Maul, G. G. & Brumbaugh, J. A. 1971, "On the possible function of coated vesicles in melanogenesis of the regenerating fowl feather", *J.Cell Biol.*, vol. 48, no. 1, pp. 41-48.

Mayer, T. C. 1973, "The migratory pathway of neural crest cells into the skin of mouse embryos.", *Develop.Biol.*, vol. 34, pp. 39-46.

McArdle, C. A., Franklin, J., Green, L., & Hislop, J. N. 2002, "The gonadotrophin-releasing hormone receptor: signalling, cycling and desensitisation", *Arch.Physiol Biochem.*, vol. 110, no. 1-2, pp. 113-122.

McGrath, J. A., Eady, R. A. J., Pope, F. M. 2004, "Anatomy and organisation of human skin", In: Rook's Textbook of Dermatology, 7th edition, Blackwell Science, Burns, T., Breathnach, S., Cox, N., Griffiths, C., eds. vol. 1, chapter 3, pp. 3.1-3.84.

Millar, S. E., Miller, M. W., Stevens, M. E., & Barsh, G. S. 1995, "Expression and transgenic studies of the mouse agouti gene provide insight into the mechanisms by which mammalian coat color patterns are generated", *Development*, vol. 121, no. 10, pp. 3223-3232.

Miller, C. L., Hruby, V. J., Matsunaga, T. O., & Bickford, P. C. 1993, "alpha-MSH and MCH are functional antagonists in a central nervous system auditory gating paradigm", *Ann.N.Y.Acad.Sci.*, vol. 680, pp. 571-574.

Mishima, Y. 1992, "A post melanosomal era: control of melanogenesis and melanoma growth", *Pigment Cell Res.*, vol. Suppl 2, pp. 3-16.

Mistry, A. M., Swick, A. G., & Romsos, D. R. 1997, "Leptin rapidly lowers food intake and elevates metabolic rates in lean and ob/ob mice", *J.Nutr.*, vol. 127, no. 10, pp. 2065-2072.

Mountjoy, K. G. 1994, "The human melanocyte stimulating hormone receptor has evolved to become "super-sensitive" to melanocortin peptides", *Mol.Cell Endocrinol.*, vol. 102, no. 1-2, pp. R7-11.

Mountjoy, K. G., Kong, P. L., Taylor, J. A., Willard, D. H., & Wilkison, W. O. 2001, "Melanocortin receptor-mediated mobilization of intracellular free calcium in HEK293 cells", *Physiol Genomics*, vol. 5, no. 1, pp. 11-19.

Mountjoy, K. G., Robbins, L. S., Mortrud, M. T., & Cone, R. D. 1992, "The cloning of a family of genes that encode the melanocortin receptors", *Science*, vol. 257, no. 5074, pp. 1248-1251.

Naik, S., Billington, C. K., Pascual, R. M., Deshpande, D. A., Stefano, F. P., Kohout, T. A., Eckman, D. M., Benovic, J. L., & Penn, R. B. 2005, "Regulation of cysteinyl leukotriene type 1 receptor internalization and signaling", *J.Biol.Chem.*, vol. 280, no. 10, pp. 8722-8732.

Naysmith, L., Waterston, K., Ha, T., Flanagan, N., Bisset, Y., Ray, A., Wakamatsu, K., Ito, S., & Rees, J. L. 2004, "Quantitative measures of the effect of the melanocortin 1 receptor on human pigmentary status", *J.Invest Dermatol.*, vol. 122, no. 2, pp. 423-428.

Neumann, A. G., Nagaeva, O., Mandrika, I., Petrovska, R., Muceniece, R., Mincheva-Nilsson, L., & Wikberg, J. E. 2001, "MC(1) receptors are constitutively expressed on leucocyte subpopulations with antigen presenting and cytotoxic functions", *Clin.Exp.Immunol.*, vol. 126, no. 3, pp. 441-446.

Newton, J. M., Cohen-Barak, O., Hagiwara, N., Gardner, J. M., Davisson, M. T., King, R. A., & Brilliant, M. H. 2001, "Mutations in the human orthologue of the mouse underwhite gene (uw) underlie a new form of oculocutaneous albinism, OCA4", *Am.J.Hum.Genet.*, vol. 69, no. 5, pp. 981-988.

Newton, J. M., Orlow, S. J., & Barsh, G. S. 1996, "Isolation and characterization of a mouse homolog of the X-linked ocular albinism (OA1) gene", *Genomics*, vol. 37, no. 2, pp. 219-225.

Newton, J. M., Wilkie, A. L., He, L., Jordan, S. A., Metallinos, D. L., Holmes, N. G., Jackson, I. J., & Barsh, G. S. 2000, "Melanocortin 1 receptor variation in the domestic dog", *Mamm.Genome*, vol. 11, no. 1, pp. 24-30.

Newton, R. A., Smit, S. E., Barnes, C. C., Pedley, J., Parsons, P. G., & Sturm, R. A. 2005, "Activation of the cAMP pathway by variant human MC1R alleles expressed in HEK and in melanoma cells", *Peptides*, vol. 26, no. 10, pp. 1818-1824.

Nishizuka, Y. 1986, "Studies and perspectives of protein kinase C", *Science*, vol. 233, no. 4761, pp. 305-312.

Nocka, K., Majumder, S., Chabot, B., Ray, P., Cervone, M., Bernstein, A., & Besmer, P. 1989, "Expression of c-kit gene products in known cellular targets of W mutations in normal and W mutant mice--evidence for an impaired c-kit kinase in mutant mice", *Genes Dev.*, vol. 3, no. 6, pp. 816-826.

Nystedt, S., Emilsson, K., Wahlestedt, C., & Sundelin, J. 1994, "Molecular cloning of a potential proteinase activated receptor", *Proc.Natl.Acad.Sci.U.S.A*, vol. 91, no. 20, pp. 9208-9212.

Ohta, T. 1995, "Synonymous and nonsynonymous substitutions in mammalian genes and the nearly neutral theory", *J.Mol.Evol.*, vol. 40, no. 1, pp. 56-63.

Okazaki, K., Uzuka, M., Morikawa, F., Toda, K., & Seiji, M. 1976, "Transfer mechanism of melanosomes in epidermal cell culture", *J.Invest Dermatol.*, vol. 67, no. 4, pp. 541-547.

Ollmann, M. M., Wilson, B. D., Yang, Y. K., Kerns, J. A., Chen, Y., Gantz, I., & Barsh, G. S. 1997, "Antagonism of central melanocortin receptors in vitro and in vivo by agouti-related protein", *Science*, vol. 278, no. 5335, pp. 135-138.

Opdecamp, K., Nakayama, A., Nguyen, M. T., Hodgkinson, C. A., Pavan, W. J., & Arnheiter, H. 1997, "Melanocyte development in vivo and in neural crest cell cultures: crucial dependence on the Mitf basic-helix-loop-helix-zipper transcription factor", *Development*, vol. 124, no. 12, pp. 2377-2386.

Orlow, S. J., Boissy, R. E., Moran, D. J., & Pifko-Hirst, S. 1993, "Subcellular distribution of tyrosinase and tyrosinase-related protein-1: implications for melanosomal biogenesis", *J.Invest Dermatol.*, vol. 100, no. 1, pp. 55-64.

Orlow, S. J., Hotchkiss, S., & Pawelek, J. M. 1990, "Internal binding sites for MSH: analyses in wild-type and variant Cloudman melanoma cells", *J.Cell Physiol*, vol. 142, no. 1, pp. 129-136.

Otaki, N. 1970, "Melanosome and lysosome. I. Lysosomal activity in relation to growth of melanoma", *Bull.Tokyo Med.Dent.Univ*, vol. 17, no. 2, pp. 89-102.

Ou, W. J., Cameron, P. H., Thomas, D. Y., & Bergeron, J. J. 1993, "Association of folding intermediates of glycoproteins with calnexin during protein maturation", *Nature*, vol. 364, no. 6440, pp. 771-776.

Owerbach, D., Rutter, W. J., Roberts, J. L., Whitfeld, P., Shine, J., Seeburg, P. H., & Shows, T. B. 1981, "The proopiocortin (adrenocorticotropin/beta-lipoprotein) gene is located on chromosome 2 in humans", *Somatic.Cell Genet.*, vol. 7, no. 3, pp. 359-369.

Ozeki, H., Ito, S., Wakamatsu, K., & Hirobe, T. 1995, "Chemical characterization of hair melanins in various coat-color mutants of mice", *J.Invest Dermatol.*, vol. 105, no. 3, pp. 361-366.

Palmer, J. S., Duffy, D. L., Box, N. F., Aitken, J. F., O'Gorman, L. E., Green, A. C., Hayward, N. K., Martin, N. G., & Sturm, R. A. 2000, "Melanocortin-1 receptor polymorphisms and risk of melanoma: is the association explained solely by pigmentation phenotype?", *Am.J.Hum.Genet.*, vol. 66, no. 1, pp. 176-186.

Palumbo, A., Di, C. A., Gesualdo, I., & Hearing, V. J. 1997, "Subcellular localization and function of melanogenic enzymes in the ink gland of Sepia officinalis", *Biochem.J.*, vol. 323 (Pt 3), pp. 749-756.

Paratore, C., Goerich, D. E., Suter, U., Wegner, M., & Sommer, L. 2001, "Survival and glial fate acquisition of neural crest cells are regulated by an interplay between the transcription factor Sox10 and extrinsic combinatorial signaling", *Development*, vol. 128, no. 20, pp. 3949-3961.

Park, H. Y., Perez, J. M., Laursen, R., Hara, M., & Gilchrest, B. A. 1999, "Protein kinase C-beta activates tyrosinase by phosphorylating serine residues in its cytoplasmic domain", *J.Biol.Chem.*, vol. 274, no. 23, pp. 16470-16478.

Park, H. Y., Wu, H., Killoran, C. E., & Gilchrest, B. A. 2004, "The receptor for activated C-kinase-I (RACK-I) anchors activated PKC-beta on melanosomes", *J.Cell Sci.*, vol. 117, no. Pt 16, pp. 3659-3668.

Peters, E. M., Tobin, D. J., Seidah, N. G., & Schallreuter, K. U. 2000, "Pro-opiomelanocortin-related peptides, prohormone convertases 1 and 2 and the regulatory peptide 7B2 are present in melanosomes of human melanocytes", *J.Invest Dermatol.*, vol. 114, no. 3, pp. 430-437.

Petrou, C., Chen, L., & Tashjian, A. H., Jr. 1997, "A receptor-G protein coupling-independent step in the internalization of the thyrotropin-releasing hormone receptor", *J.Biol.Chem.*, vol. 272, no. 4, pp. 2326-2333.

Pingault, V., Bondurand, N., Kuhlbrodt, K., Goerich, D. E., Prehu, M. O., Puliti, A., Herbarth, B., Hermans-Borgmeyer, I., Legius, E., Matthijs, G., Amiel, J., Lyonnet, S., Ceccherini, I., Romeo, G., Smith, J. C., Read, A. P., Wegner, M., & Goossens, M. 1998, "SOX10 mutations in patients with Waardenburg-Hirschsprung disease", *Nat.Genet.*, vol. 18, no. 2, pp. 171-173.

Pitcher, J., Lohse, M. J., Codina, J., Caron, M. G., & Lefkowitz, R. J. 1992, "Desensitization of the isolated beta 2-adrenergic receptor by beta-adrenergic receptor kinase, cAMP-dependent protein kinase, and protein kinase C occurs via distinct molecular mechanisms", *Biochemistry*, vol. 31, no. 12, pp. 3193-3197.

Prasher, D. C., Eckenrode, V. K., Ward, W. W., Prendergast, F. G., & Cormier, M. J. 1992, "Primary structure of the Aequorea victoria green-fluorescent protein", *Gene*, vol. 111, no. 2, pp. 229-233.

Probst, W. C., Snyder, L. A., Schuster, D. I., Brosius, J., & Sealfon, S. C. 1992, "Sequence alignment of the G-protein coupled receptor superfamily", *DNA Cell Biol.*, vol. 11, no. 1, pp. 1-20.

Prota, G. 1992, "The role of peroxidase in melanogenesis revisited", *Pigment Cell Res.*, vol. Suppl 2, pp. 25-31.

Prota, G., Lamoreux, M. L., Muller, J., Kobayashi, T., Napolitano, A., Vincensi, M. R., Sakai, C., & Hearing, V. J. 1995, "Comparative analysis of melanins and melanosomes produced by various coat color mutants", *Pigment Cell Res.*, vol. 8, no. 3, pp. 153-163.

Prota, G. & Thomson, R. H. 1976, "Melanin pigmentation in mammals", *Endeavour*, vol. 35, no. 224, pp. 32-38.

Prusis, P., Schioth, H. B., Muceniece, R., Herzyk, P., Afshar, M., Hubbard, R. E., & Wikberg, J. E. 1997, "Modeling of the three-dimensional structure of the human melanocortin 1 receptor, using an automated method and docking of a rigid cyclic melanocyte-stimulating hormone core peptide", *J.Mol.Graph.Model.*, vol. 15, no. 5, pp. 307-17, 334.

Puri, N., Gardner, J. M., & Brilliant, M. H. 2000, "Aberrant pH of melanosomes in pink-eyed dilution (p) mutant melanocytes", *J.Invest Dermatol.*, vol. 115, no. 4, pp. 607-613.

Qanbar, R. & Bouvier, M. 2003, "Role of palmitoylation/depalmitoylation reactions in G-protein-coupled receptor function", *Pharmacol.Ther.*, vol. 97, no. 1, pp. 1-33.

Raap, U., Brzoska, T., Sohl, S., Path, G., Emmel, J., Herz, U., Braun, A., Luger, T., & Renz, H. 2003, "Alpha-melanocyte-stimulating hormone inhibits allergic airway inflammation", *J.Immunol.*, vol. 171, no. 1, pp. 353-359.

Rached, M., Buronfosse, A., Durand, P., Begeot, M., & Penhoat, A. 2003, "Stable expression of human melanocortin 3 receptor fused to EGFP in the HEK293 cells", *Biochem.Biophys.Res.Commun.*, vol. 306, no. 1, pp. 208-212.

Rajora, N., Boccoli, G., Catania, A., & Lipton, J. M. 1997, "alpha-MSH modulates experimental inflammatory bowel disease", *Peptides*, vol. 18, no. 3, pp. 381-385.

Ramsay, M., Colman, M. A., Stevens, G., Zwane, E., Kromberg, J., Farrall, M., & Jenkins, T. 1992, "The tyrosinase-positive oculocutaneous albinism locus maps to chromosome 15q11.2-q12", *Am.J.Hum.Genet.*, vol. 51, no. 4, pp. 879-884.

Rana, B. K., Hewett-Emmett, D., Jin, L., Chang, B. H., Sambuughin, N., Lin, M., Watkins, S., Bamshad, M., Jorde, L. B., Ramsay, M., Jenkins, T., & Li, W. H. 1999, "High polymorphism at the human melanocortin 1 receptor locus", *Genetics*, vol. 151, no. 4, pp. 1547-1557.

Rawles, M. E. 1947, "Origin of pigment cells from the neural crest in the mouse embryo.", *Physiol.Zool*, vol. 20, pp. 248-266.

Rees, J. 2006, "Plenty new under the sun", *J.Invest Dermatol.*, vol. 126, no. 8, pp. 1691-1692.

Ringholm, A., Klovins, J., Rudzish, R., Phillips, S., Rees, J. L., Schioth, H. B. 2004, "Pharmacological characterization of loss of function mutations of the melanocortin 1 receptor that are associated with red hair", *J.Invest Dermatol.*, vol. 123, no. 5, pp. 917-923.

Robbins, L. S., Nadeau, J. H., Johnson, K. R., Kelly, M. A., Roselli-Rehfuss, L., Baack, E., Mountjoy, K. G., & Cone, R. D. 1993, "Pigmentation phenotypes of variant extension locus alleles result from point mutations that alter MSH receptor function", *Cell*, vol. 72, no. 6, pp. 827-834.

Robinson, S. J. & Healy, E. 2002, "Human melanocortin 1 receptor (MC1R) gene variants alter melanoma cell growth and adhesion to extracellular matrix", *Oncogene*, vol. 21, no. 52, pp. 8037-8046.

Romero-Graillet, C., Aberdam, E., Biagoli, N., Massabni, W., Ortonne, J. P., & Ballotti, R. 1996, "Ultraviolet B radiation acts through the nitric oxide and cGMP signal transduction pathway to stimulate melanogenesis in human melanocytes", *J.Biol.Chem.*, vol. 271, no. 45, pp. 28052-28056.

Romero-Graillet, C., Aberdam, E., Clement, M., Ortonne, J. P., & Ballotti, R. 1997, "Nitric oxide produced by ultraviolet-irradiated keratinocytes stimulates melanogenesis", *J.Clin.Invest*, vol. 99, no. 4, pp. 635-642.

Rompler, H., Rohland, N., Lalueza-Fox, C., Willerslev, E., Kuznetsova, T., Rabeder, G., Bertranpetit, J., Schoneberg, T., & Hofreiter, M. 2006, "Nuclear gene indicates coat-color polymorphism in mammoths", *Science*, vol. 313, no. 5783, p. 62.

Roselli-Rehfuss, L., Mountjoy, K. G., Robbins, L. S., Mortrud, M. T., Low, M. J., Tatro, J. B., Entwistle, M. L., Simerly, R. B., & Cone, R. D. 1993, "Identification of a receptor for gamma melanotropin and other proopiomelanocortin peptides in the hypothalamus and limbic system", *Proc.Natl.Acad.Sci.U.S.A*, vol. 90, no. 19, pp. 8856-8860.

Rouzaud, F., Costin, G. E., Yamaguchi, Y., Valencia, J. C., Berens, W. F., Chen, K. G., Hoashi, T., Bohm, M., bdel-Malek, Z. A., & Hearing, V. J. 2006, "Regulation of constitutive and UVR-induced skin pigmentation by melanocortin 1 receptor isoforms", *FASEB J.*, vol. 20, no. 11, pp. 1927-1929.

Salazar-Onfray, F., Lopez, M., Lundqvist, A., Aguirre, A., Escobar, A., Serrano, A., Korenblit, C., Petersson, M., Chhajlani, V., Larsson, O., & Kiessling, R. 2002, "Tissue distribution and differential expression of melanocortin 1 receptor, a malignant melanoma marker", *Br.J.Cancer*, vol. 87, no. 4, pp. 414-422.

Sanchez, M. J., Olivares, S. C., Ghanem, G., Haycock, J., Lozano Teruel, J. A., Garcia-Borron, J. C., & Jimenez-Cervantes, C. 2002, "Loss-of-function variants of the human melanocortin-1 receptor gene in melanoma cells define structural determinants of receptor function", *Eur.J.Biochem.*, vol. 269, no. 24, pp. 6133-6141.

Sanchez-Laorden, B. L., Sanchez-Mas, J., Martinez-Alonso, E., Martinez-Menarguez, J. A., Garcia-Borron, J. C., & Jimenez-Cervantes, C. 2006, "Dimerization of the human melanocortin 1 receptor: functional consequences and dominant-negative effects", *J.Invest Dermatol.*, vol. 126, no. 1, pp. 172-181.

Sanchez-Mas, J., Hahmann, C., Gerritsen, I., Garcia-Borron, J. C., & Jimenez-Cervantes, C. 2004, "Agonist-independent, high constitutive activity of the human melanocortin 1 receptor", *Pigment Cell Res.*, vol. 17, no. 4, pp. 386-395.

Satoh, H. & Mori, S. 1997, "Subregional assignment of the proopiomelanocortin gene (POMC) to human chromosome band 2p23.3 by fluorescence in situ hybridization", *Cytogenet.Cell Genet.*, vol. 76, no. 3-4, pp. 221-222.

Schallreuter, K. U., Wood, J. M., Ziegler, I., Leinke, K. R., Pitelkow, M. R., Lindsey, N. J., &Gutlich, M., 1994, "Defective tetrahydrobiopterin and catecholamine biosynthesis in the depigmentation disorder vitiligo", *Biochimica et Biophysica Acta.*, vol. 1226, pp. 181-192.

Schallreuter, K. U., Moore, J., Tobin, D. J., Gibbons, N. J., Marshall, H. S., Jenner, T., Beazley, W. D., & Wood, J. M. 1999, "alpha-MSH can control the essential cofactor 6-tetrahydrobiopterin in melanogenesis", *Ann.N.Y.Acad.Sci.*, vol. 885, pp. 329-341.

Schiaffino, M. V., Bassi, M. T., Galli, L., Renieri, A., Bruttini, M., De, N. F., Bergen, A. A., Charles, S. J., Yates, J. R., Meindl, A., & . 1995, "Analysis of the OA1 gene

reveals mutations in only one-third of patients with X-linked ocular albinism", *Hum.Mol.Genet.*, vol. 4, no. 12, pp. 2319-2325.

Schiaffino, M. V., d'Addio, M., Alloni, A., Baschirotto, C., Valetti, C., Cortese, K., Puri, C., Bassi, M. T., Colla, C., De, L. M., Tacchetti, C., & Ballabio, A. 1999, "Ocular albinism: evidence for a defect in an intracellular signal transduction system", *Nat.Genet.*, vol. 23, no. 1, pp. 108-112.

Schioth, H. B., Chhajlani, V., Muceniece, R., Klusa, V., & Wikberg, J. E. 1996a, "Major pharmacological distinction of the ACTH receptor from other melanocortin receptors", *Life Sci.*, vol. 59, no. 10, pp. 797-801.

Schioth, H. B., Kuusinen, A., Muceniece, R., Szardenings, M., Keinanen, K., & Wikberg, J. E. 1996b, "Expression of functional melanocortin 1 receptors in insect cells", *Biochem.Biophys.Res.Commun.*, vol. 221, no. 3, pp. 807-814.

Schioth, H. B., Muceniece, R., Wikberg, J. E., & Chhajlani, V. 1995, "Characterisation of melanocortin receptor subtypes by radioligand binding analysis", *Eur.J.Pharmacol.*, vol. 288, no. 3, pp. 311-317.

Schioth, H. B., Mutulis, F., Muceniece, R., Prusis, P., & Wikberg, J. E. 1998, "Selective properties of C- and N-terminals and core residues of the melanocyte-stimulating hormone on binding to the human melanocortin receptor subtypes", *Eur.J.Pharmacol.*, vol. 349, no. 2-3, pp. 359-366.

Schioth, H. B., Phillips, S. R., Rudzish, R., Birch-MacHin, M. A., Wikberg, J. E., & Rees, J. L. 1999, "Loss of function mutations of the human melanocortin 1 receptor are common and are associated with red hair", *Biochem.Biophys.Res.Commun.*, vol. 260, no. 2, pp. 488-491.

Scott, A. P., Lowry, P. J., & Van Wimersma Greidanus, T. B. 1976, "Incorporation of 14C-labelled amino acids into corticotrophin-like intermediate lobe peptide and alpha-melanocyte-stimulating hormone by the rat pituitary neurointermediate lobe in vitro, and the identification of four new pars intermedia peptides", *J.Endocrinol.*, vol. 70, no. 2, pp. 197-205.

Scott, M. C., Wakamatsu, K., Ito, S., Kadekaro, A. L., Kobayashi, N., Groden, J., Kavanagh, R., Takakuwa, T., Virador, V., Hearing, V. J., & Abdel-Malek, Z. A. 2002, "Human melanocortin 1 receptor variants, receptor function and melanocyte response to UV radiation", *J.Cell Sci.*, vol. 115, no. Pt 11, pp. 2349-2355.

Seachrist, J. L. & Ferguson, S. S. 2003, "Regulation of G protein-coupled receptor endocytosis and trafficking by Rab GTPases", *Life Sci.*, vol. 74, no. 2-3, pp. 225-235.

Seeley, R. J., van, D. G., Campfield, L. A., Smith, F. J., Burn, P., Nelligan, J. A., Bell, S. M., Baskin, D. G., Woods, S. C., & Schwartz, M. W. 1996, "Intraventricular leptin reduces food intake and body weight of lean rats but not obese Zucker rats", *Horm.Metab Res.*, vol. 28, no. 12, pp. 664-668.

Seiji, M. & Kikuchi, A. 1969, "Acid phosphatase activity in melanosomes", *J.Invest Dermatol.*, vol. 52, no. 2, pp. 212-216.

Shen, B., Rosenberg, B., & Orlow, S. J. 2001, "Intracellular distribution and late endosomal effects of the ocular albinism type 1 gene product: consequences of disease-

causing mutations and implications for melanosome biogenesis", *Traffic.*, vol. 2, no. 3, pp. 202-211.

SHEPARD, T. H., LANDING, B. H., & MASON, D. G. 1959, "Familial Addison's disease; case reports of two sisters with corticoid deficiency unassociated with hypoaldosteronism", *AMA.J.Dis.Child*, vol. 97, no. 2, pp. 154-162.

Shibata, T., Prota, G., & Mishima, Y. 1993, "Non-melanosomal regulatory factors in melanogenesis", *J.Invest Dermatol.*, vol. 100, no. 3, pp. 274S-280S.

Shinyama, H., Masuzaki, H., Fang, H., & Flier, J. S. 2003, "Regulation of melanocortin-4 receptor signaling: agonist-mediated desensitization and internalization", *Endocrinology*, vol. 144, no. 4, pp. 1301-1314.

Siegrist, W., Drozdz, R., Cotti, R., Willard, D. H., Wilkison, W. O., & Eberle, A. N. 1997, "Interactions of alpha-melanotropin and agouti on B16 melanoma cells: evidence for inverse agonism of agouti", *J.Recept.Signal.Transduct.Res.*, vol. 17, no. 1-3, pp. 75-98.

Siegrist, W. & Eberle, A. N. 1993, "Homologous regulation of the MSH receptor in melanoma cells", *J.Recept.Res.*, vol. 13, no. 1-4, pp. 263-281.

Siegrist, W., Oestreicher, M., Stutz, S., Girard, J., & Eberle, A. N. 1988, "Radioreceptor assay for alpha-MSH using mouse B16 melanoma cells+", *J.Recept.Res.*, vol. 8, no. 1-4, pp. 323-343.

Siegrist, W., Solca, F., Stutz, S., Giuffre, L., Carrel, S., Girard, J., & Eberle, A. N. 1989, "Characterization of receptors for alpha-melanocyte-stimulating hormone on human melanoma cells", *Cancer Res.*, vol. 49, no. 22, pp. 6352-6358.

Smit, N. P., Kolb, R. M., Lentjes, E. G., Noz, K. C., van der, M. H., Koerten, H. K., Vermeer, B. J., & Pavel, S. 1998, "Variations in melanin formation by cultured melanocytes from different skin types", *Arch.Dermatol.Res.*, vol. 290, no. 6, pp. 342-349.

Smith, A. G., Box, N. F., Marks, L. H., Chen, W., Smit, D. J., Wyeth, J. R., Huttley, G. A., Easteal, S., & Sturm, R. A. 2001, "The human melanocortin-1 receptor locus: analysis of transcription unit, locus polymorphism and haplotype evolution", *Gene*, vol. 281, no. 1-2, pp. 81-94.

Smith, R., Healy, E., Siddiqui, S., Flanagan, N., Steijlen, P. M., Rosdahl, I., Jacques, J. P., Rogers, S., Turner, R., Jackson, I. J., Birch-MacHin, M. A., & Rees, J. L. 1998, "Melanocortin 1 receptor variants in an Irish population", *J.Invest Dermatol.*, vol. 111, no. 1, pp. 119-122.

Solca, F. F., Chluba-de Tapia, J., Iwata, K., & Eberle, A. N. 1993, "B16-G4F mouse melanoma cells: an MSH receptor-deficient cell clone", *FEBS Lett.*, vol. 322, no. 2, pp. 177-180.

Spencer, J. D., Chavan, B., Marles, L. K., Kauser, S., Rokos, H., & Schalreuter, K. U. 2005, "A novel mechanism in control of human pigmentation by β-melanocyte-stimulating hormone and 7-tetrahydrbiopterin", *J. Endocrinology.*, vol. 187, pp. 293-302.

Stander, S., Bohm, M., Brzoska, T., Zimmer, K. P., Luger, T., & Metze, D. 2002, "Expression of melanocortin-1 receptor in normal, malformed and neoplastic skin glands and hair follicles", *Exp.Dermatol.*, vol. 11, no. 1, pp. 42-51.

Steel, K. P., Davidson, D. R., & Jackson, I. J. 1992, "TRP-2/DT, a new early melanoblast marker, shows that steel growth factor (c-kit ligand) is a survival factor", *Development*, vol. 115, no. 4, pp. 1111-1119.

Steingrimsson, E., Moore, K. J., Lamoreux, M. L., Ferre-D'Amare, A. R., Burley, S. K., Zimring, D. C., Skow, L. C., Hodgkinson, C. A., Arnheiter, H., Copeland, N. G., & . 1994, "Molecular basis of mouse microphthalmia (mi) mutations helps explain their developmental and phenotypic consequences", *Nat.Genet.*, vol. 8, no. 3, pp. 256-263.

Sturm, R. A., Duffy, D. L., Box, N. F., Chen, W., Smit, D. J., Brown, D. L., Stow, J. L., Leonard, J. H., & Martin, N. G. 2003, "The role of melanocortin-1 receptor polymorphism in skin cancer risk phenotypes", *Pigment Cell Res.*, vol. 16, no. 3, pp. 266-272.

Sturm, R. A., Teasdale, R. D., & Box, N. F. 2001, "Human pigmentation genes: identification, structure and consequences of polymorphic variation", *Gene*, vol. 277, no. 1-2, pp. 49-62.

Su, Y. F., Harden, T. K., & Perkins, J. P. 1979, "Isoproterenol-induced desensitization of adenylate cyclase in human astrocytoma cells. Relation of loss of hormonal responsiveness and decrement in beta-adrenergic receptors", *J.Biol.Chem.*, vol. 254, no. 1, pp. 38-41.

Suzuki, I., Cone, R. D., Im, S., Nordlund, J., & Abdel-Malek, Z. A. 1996, "Binding of melanotropic hormones to the melanocortin receptor MC1R on human melanocytes stimulates proliferation and melanogenesis", *Endocrinology*, vol. 137, no. 5, pp. 1627-1633.

Suzuki, I., Tada, A., Ollmann, M. M., Barsh, G. S., Im, S., Lamoreux, M. L., Hearing, V. J., Nordlund, J. J., & bdel-Malek, Z. A. 1997, "Agouti signaling protein inhibits melanogenesis and the response of human melanocytes to alpha-melanotropin", *J.Invest Dermatol.*, vol. 108, no. 6, pp. 838-842.

Swope, V. B., bdel-Malek, Z. A., Sauder, D. N., & Nordlund, J. J. 1989, "A new role for epidermal cell-derived thymocyte activating factor/IL-1 as an antagonist for distinct epidermal cell function", *J.Immunol.*, vol. 142, no. 6, pp. 1943-1949.

Swords, F. M., Baig, A., Malchoff, D. M., Malchoff, C. D., Thorner, M. O., King, P. J., Hunyady, L., & Clark, A. J. 2002, "Impaired desensitization of a mutant adrenocorticotropin receptor associated with apparent constitutive activity", *Mol.Endocrinol.*, vol. 16, no. 12, pp. 2746-2753.

Szabo, G. 1954, "The number of melanocytes in human epidermis", *Br.Med.J.*, vol. 4869, pp. 1016-1017.

Szabo, G., Gerald, A. B., Pathak, M. A., & Fitzpatrick, T. B. 1969, "Racial differences in the fate of melanosomes in human epidermis", *Nature*, vol. 222, no. 198, pp. 1081-1082.

Tachibana, M. 1999, "A cascade of genes related to Waardenburg syndrome", *J.Investig.Dermatol.Symp.Proc.*, vol. 4, no. 2, pp. 126-129.

Tachibana, M., Perez-Jurado, L. A., Nakayama, A., Hodgkinson, C. A., Li, X., Schneider, M., Miki, T., Fex, J., Francke, U., & Arnheiter, H. 1994, "Cloning of MITF, the human homolog of the mouse microphthalmia gene and assignment to chromosome 3p14.1-p12.3", *Hum.Mol.Genet.*, vol. 3, no. 4, pp. 553-557.

Taherzadeh, S., Sharma, S., Chhajlani, V., Gantz, I., Rajora, N., Demitri, M. T., Kelly, L., Zhao, H., Ichiyama, T., Catania, A., & Lipton, J. M. 1999, "alpha-MSH and its receptors in regulation of tumor necrosis factor- alpha production by human monocyte/macrophages", *Am.J.Physiol*, vol. 276, no. 5 Pt 2, p. R1289-R1294.

Takeuchi, S., Suzuki, H., Yabuuchi, M., & Takahashi, S. 1996, "A possible involvement of melanocortin 1-receptor in regulating feather color pigmentation in the chicken", *Biochim.Biophys.Acta*, vol. 1308, no. 2, pp. 164-168.

Takeuchi, S., Zhang, W., Wakamatsu, K., Ito, S., Hearing, V. J., Kraemer, K. H., & Brash, D. E. 2004, "Melanin acts as a potent UVB photosensitizer to cause an atypical mode of cell death in murine skin", *Proc.Natl.Acad.Sci.U.S.A*, vol. 101, no. 42, pp. 15076-15081.

Tan, C. P., McKee, K. K., Weinberg, D. H., Macneil, T., Palyha, O. C., Feighner, S. D., Hreniuk, D. L., Van der Ploeg, L. H., MacNeil, D. J., & Howard, A. D. 1999, "Molecular analysis of a new splice variant of the human melanocortin-1 receptor", *FEBS Lett.*, vol. 451, no. 2, pp. 137-141.

Tarasova, N. I., Stauber, R. H., Choi, J. K., Hudson, E. A., Czerwinski, G., Miller, J. L., Pavlakis, G. N., Michejda, C. J., & Wank, S. A. 1997, "Visualization of G protein-coupled receptor trafficking with the aid of the green fluorescent protein. Endocytosis and recycling of cholecystokinin receptor type A", *J.Biol.Chem.*, vol. 272, no. 23, pp. 14817-14824.

Tassabehji, M., Read, A. P., Newton, V. E., Harris, R., Balling, R., Gruss, P., & Strachan, T. 1992, "Waardenburg's syndrome patients have mutations in the human homologue of the Pax-3 paired box gene", *Nature*, vol. 355, no. 6361, pp. 635-636.

Tatro, J. B., Atkins, M., Mier, J. W., Hardarson, S., Wolfe, H., Smith, T., Entwistle, M. L., & Reichlin, S. 1990, "Melanotropin receptors demonstrated in situ in human melanoma", *J.Clin.Invest*, vol. 85, no. 6, pp. 1825-1832.

Theron, E., Hawkins, K., Bermingham, E., Ricklefs, R. E., & Mundy, N. I. 2001, "The molecular basis of an avian plumage polymorphism in the wild: a melanocortin-1-receptor point mutation is perfectly associated with the melanic plumage morph of the bananaquit, Coereba flaveola", *Curr.Biol.*, vol. 11, no. 8, pp. 550-557.

Thiboutot, D., Sivarajah, A., Gilliland, K., Cong, Z., & Clawson, G. 2000, "The melanocortin 5 receptor is expressed in human sebaceous glands and rat preputial cells", *J.Invest Dermatol.*, vol. 115, no. 4, pp. 614-619.

Thieblemont, N. & Wright, S. D. 1999, "Transport of bacterial lipopolysaccharide to the golgi apparatus", *J.Exp.Med.*, vol. 190, no. 4, pp. 523-534.

Thody, A. J. & Shuster, S. 1973a, "Possible role of MSH in the mammal", *Nature*, vol. 245, no. 5422, pp. 207-209.

Thody, A. J. & Shuster, S. 1973b, "The control of melanocyte-stimulating hormone secretion", *J.Endocrinol.*, vol. 58, no. 2, p. XXXV-XXXVI.

Tolmachova, T., Ramalho, J. S., Anant, J. S., Schultz, R. A., Huxley, C. M., & Seabra, M. C. 1999, "Cloning, mapping and characterization of the human RAB27A gene", *Gene*, vol. 239, no. 1, pp. 109-116.

Toyofuku, K., Wada, I., Valencia, J. C., Kushimoto, T., Ferrans, V. J., & Hearing, V. J. 2001, "Oculocutaneous albinism types 1 and 3 are ER retention diseases: mutation of tyrosinase or Tyrp1 can affect the processing of both mutant and wild-type proteins", *FASEB J.*, vol. 15, no. 12, pp. 2149-2161.

Tripathi, R. K., Hearing, V. J., Urabe, K., Aroca, P., & Spritz, R. A. 1992, "Mutational mapping of the catalytic activities of human tyrosinase", *J.Biol.Chem.*, vol. 267, no. 33, pp. 23707-23712.

Vage, D. I., Klungland, H., Lu, D., & Cone, R. D. 1999, "Molecular and pharmacological characterization of dominant black coat color in sheep", *Mamm.Genome*, vol. 10, no. 1, pp. 39-43.

Vage, D. I., Lu, D., Klungland, H., Lien, S., Adalsteinsson, S., & Cone, R. D. 1997, "A non-epistatic interaction of agouti and extension in the fox, Vulpes vulpes", *Nat.Genet.*, vol. 15, no. 3, pp. 311-315.

Vaisse, C., Clement, K., Guy-Grand, B., & Froguel, P. 1998, "A frameshift mutation in human MC4R is associated with a dominant form of obesity", *Nat.Genet.*, vol. 20, no. 2, pp. 113-114.

Vallet, V. S., Casado, M., Henrion, A. A., Bucchini, D., Raymondjean, M., Kahn, A., & Vaulont, S. 1998, "Differential roles of upstream stimulatory factors 1 and 2 in the transcriptional response of liver genes to glucose", *J.Biol.Chem.*, vol. 273, no. 32, pp. 20175-20179.

Valverde, P., Healy, E., Jackson, I., Rees, J. L., & Thody, A. J. 1995, "Variants of the melanocyte-stimulating hormone receptor gene are associated with red hair and fair skin in humans", *Nat.Genet.*, vol. 11, no. 3, pp. 328-330.

Valverde, P., Healy, E., Sikkink, S., Haldane, F., Thody, A. J., Carothers, A., Jackson, I. J., & Rees, J. L. 1996, "The Asp84Glu variant of the melanocortin 1 receptor (MC1R) is associated with melanoma", *Hum.Mol.Genet.*, vol. 5, no. 10, pp. 1663-1666.

Van der Ploeg, L. H., Martin, W. J., Howard, A. D., Nargund, R. P., Austin, C. P., Guan, X., Drisko, J., Cashen, D., Sebhat, I., Patchett, A. A., Figueroa, D. J., DiLella, A. G., Connolly, B. M., Weinberg, D. H., Tan, C. P., Palyha, O. C., Pong, S. S., Macneil, T., Rosenblum, C., Vongs, A., Tang, R., Yu, H., Sailer, A. W., Fong, T. M., Huang, C., Tota, M. R., Chang, R. S., Stearns, R., Tamvakopoulos, C., Christ, G., Drazen, D. L., Spar, B. D., Nelson, R. J., & MacIntyre, D. E. 2002, "A role for the melanocortin 4 receptor in sexual function", *Proc.Natl.Acad.Sci.U.S.A*, vol. 99, no. 17, pp. 11381-11386.

van der Velden, P. A., Sandkuijl, L. A., Bergman, W., Pavel, S., van Mourik, L., Frants, R. R., & Gruis, N. A. 2001, "Melanocortin-1 receptor variant R151C modifies melanoma risk in Dutch families with melanoma", *Am.J.Hum.Genet.*, vol. 69, no. 4, pp. 774-779.

Vancoillie, G., Lambert, J., Mulder, A., Koerten, H. K., Mommaas, A. M., Van, O. P., & Naeyaert, J. M. 2000, "Kinesin and kinectin can associate with the melanosomal surface and form a link with microtubules in normal human melanocytes", *J.Invest Dermatol.*, vol. 114, no. 3, pp. 421-429.

Varga, J. M., Dipasquale, A., Pawelek, J., McGuire, J. S., & Lerner, A. B. 1974, "Regulation of melanocyte stimulating hormone action at the receptor level: discontinuous binding of hormone to synchronized mouse melanoma cells during the cell cycle", *Proc.Natl.Acad.Sci.U.S.A*, vol. 71, no. 5, pp. 1590-1593.

Varga, J. M., Moellmann, G., Fritsch, P., Godawska, E., & Lerner, A. B. 1976a, "Association of cell surface receptors for melanotropin with the Golgi region in mouse melanoma cells", *Proc.Natl.Acad.Sci.U.S.A*, vol. 73, no. 2, pp. 559-562.

Varga, J. M., Saper, M. A., Lerner, A. B., & Fritsch, P. 1976b, "Nonrandom distribution of receptors for melanocyte-stimulating hormone on the surface of mouse melanoma cells", *J.Supramol.Struct.*, vol. 4, no. 1, pp. 45-49.

Verastegui, C., Bille, K., Ortonne, J. P., & Ballotti, R. 2000, "Regulation of the microphthalmia-associated transcription factor gene by the Waardenburg syndrome type 4 gene, SOX10", *J.Biol.Chem.*, vol. 275, no. 40, pp. 30757-30760.

Vetrini, F., Auricchio, A., Du, J., Angeletti, B., Fisher, D. E., Ballabio, A., & Marigo, V. 2004, "The microphthalmia transcription factor (Mitf) controls expression of the ocular albinism type 1 gene: link between melanin synthesis and melanosome biogenesis", *Mol.Cell Biol.*, vol. 24, no. 15, pp. 6550-6559.

Vinson, G. P., Ho, M. M., Puddefoot, J. R., Teja, R., Barker, S., Kapas, S., & Hinson, J. P. 1995, "Internalisation of the type I angiotensin II receptor (AT1) and angiotensin II function in the rat adrenal zona glomerulosa cell", *Endocr.Res.*, vol. 21, no. 1-2, pp. 211-217.

Voisey, J., Box, N. F., & van Daal, A. 2001, "A polymorphism study of the human Agouti gene and its association with MC1R", *Pigment Cell Res.*, vol. 14, no. 4, pp. 264-267.

Walsh, R. J. 1971, "A distinctive pigment of the skin in New Guinea indigenes", *Ann.Hum.Genet.*, vol. 34, no. 4, pp. 379-388.

Watterson, K. R., Johnston, E., Chalmers, C., Pronin, A., Cook, S. J., Benovic, J. L., & Palmer, T. M. 2002, "Dual regulation of EDG1/S1P(1) receptor phosphorylation and internalization by protein kinase C and G-protein-coupled receptor kinase 2", *J.Biol.Chem.*, vol. 277, no. 8, pp. 5767-5777.

Weber, A., Kapas, S., Hinson, J., Grant, D. B., Grossman, A., & Clark, A. J. 1993, "Functional characterization of the cloned human ACTH receptor: impaired responsiveness of a mutant receptor in familial glucocorticoid deficiency", *Biochem.Biophys.Res.Commun.*, vol. 197, no. 1, pp. 172-178.

Wess, J., Gdula, D., & Brann, M. R. 1991, "Site-directed mutagenesis of the m3 muscarinic receptor: identification of a series of threonine and tyrosine residues involved in agonist but not antagonist binding", *EMBO J.*, vol. 10, no. 12, pp. 3729-3734.

Wikberg, J. E., Muceniece, R., Mandrika, I., Prusis, P., Lindblom, J., Post, C., & Skottner, A. 2000, "New aspects on the melanocortins and their receptors", *Pharmacol.Res.*, vol. 42, no. 5, pp. 393-420.

Williams, D. E., Eisenman, J., Baird, A., Rauch, C., Van Ness, K., March, C. J., Park, L. S., Martin, U., Mochizuki, D. Y., Boswell, H. S., & . 1990, "Identification of a ligand for the c-kit proto-oncogene", *Cell*, vol. 63, no. 1, pp. 167-174.

Wilson, B. D., Ollmann, M. M., Kang, L., Stoffel, M., Bell, G. I., & Barsh, G. S. 1995, "Structure and function of ASP, the human homolog of the mouse agouti gene", *Hum.Mol.Genet.*, vol. 4, no. 2, pp. 223-230.

Wilson, S. M., Yip, R., Swing, D. A., O'Sullivan, T. N., Zhang, Y., Novak, E. K., Swank, R. T., Russell, L. B., Copeland, N. G., & Jenkins, N. A. 2000, "A mutation in Rab27a causes the vesicle transport defects observed in ashen mice", *Proc.Natl.Acad.Sci.U.S.A*, vol. 97, no. 14, pp. 7933-7938.

Wong, G. & Pawelek, J. 1973, "Control of phenotypic expression of cultured melanoma cells by melanocyte stimulating hormones", *Nat.New Biol.*, vol. 241, no. 111, pp. 213-215.

Wong, T. H. & Rees, J. L. 2005, "The relation between melanocortin 1 receptor (MC1R) variation and the generation of phenotypic diversity in the cutaneous response to ultraviolet radiation", *Peptides*, vol. 26, no. 10, pp. 1965-1971.

Wong, W. & Minchin, R. F. 1996, "Binding and internalization of the melanocyte stimulating hormone receptor ligand [Nle4, D-Phe7] alpha-MSH in B16 melanoma cells", *Int.J.Biochem.Cell Biol.*, vol. 28, no. 11, pp. 1223-1232.

Wu, X. S., Tsan, G. L., & Hammer, J. A., III 2005, "Melanophilin and myosin Va track the microtubule plus end on EB1", *J.Cell Biol.*, vol. 171, no. 2, pp. 201-207.

Xia, Y., Wikberg, J. E., & Chhajlani, V. 1995, "Expression of melanocortin 1 receptor in periaqueductal gray matter", *Neuroreport*, vol. 6, no. 16, pp. 2193-2196.

Yamamoto, O. & Bhawan, J. 1994, "Three modes of melanosome transfers in Caucasian facial skin: hypothesis based on an ultrastructural study", *Pigment Cell Res.*, vol. 7, no. 3, pp. 158-169.

Yaswen, L., Diehl, N., Brennan, M. B., & Hochgeschwender, U. 1999, "Obesity in the mouse model of pro-opiomelanocortin deficiency responds to peripheral melanocortin", *Nat.Med.*, vol. 5, no. 9, pp. 1066-1070.

Yohn, J. J., Morelli, J. G., Walchak, S. J., Rundell, K. B., Norris, D. A., & Zamora, M. R. 1993, "Cultured human keratinocytes synthesize and secrete endothelin-1", *J.Invest Dermatol.*, vol. 100, no. 1, pp. 23-26.

Yoon, T. J., Lei, T. C., Yamaguchi, Y., Batzer, J., Wolber, R., & Hearing, V. J. 2003, "Reconstituted 3-dimensional human skin of various ethnic origins as an in vitro model for studies of pigmentation", *Anal.Biochem.*, vol. 318, no. 2, pp. 260-269.

Yu, R. & Hinkle, P. M. 1998, "Signal transduction, desensitization, and recovery of responses to thyrotropin-releasing hormone after inhibition of receptor internalization", *Mol.Endocrinol.*, vol. 12, no. 5, pp. 737-749.

Zabel, B. U., Naylor, S. L., Sakaguchi, A. Y., Bell, G. I., & Shows, T. B. 1983, "High-resolution chromosomal localization of human genes for amylase, proopiomelanocortin, somatostatin, and a DNA fragment (D3S1) by in situ hybridization", *Proc.Natl.Acad.Sci.U.S.A*, vol. 80, no. 22, pp. 6932-6936.

Zhou, B. K., Boissy, R. E., Pifko-Hirst, S., Moran, D. J., & Orlow, S. J. 1993b, "Lysosome-associated membrane protein-1 (LAMP-1) is the melanocyte vesicular membrane glycoprotein band II", *J.Invest Dermatol.*, vol. 100, no. 2, pp. 110-114.

Zhou, B. K., Kobayashi, T., Donatien, P. D., Bennett, D. C., Hearing, V. J., & Orlow, S. J. 1994, "Identification of a melanosomal matrix protein encoded by the murine si (silver) locus using "organelle scanning"", *Proc.Natl.Acad.Sci.U.S.A*, vol. 91, no. 15, pp. 7076-7080.

Zimmerman, J., Winfrey, F., & Good, P. 1981, "Observations on the structure of the eumelanosome matrix in melanosomes of the chick retinal pigment epithelium", *Anat.Rec.*, vol. 200, no. 4, pp. 415-420.